Bioremediation of Toxic Metals for Protecting Human Health and the Ecosystem

Dedicated
To
My parents

We won't have a society if we destroy the environment.

—Margaret Mead (1901-1978)

Örebro Studies in Life Science 15

AMINUR RAHMAN

Bioremediation of Toxic Metals for Protecting Human Health and the Ecosystem

Title: Bioremediation of Toxic Metals for Protecting Human Health and the Ecosystem
Publisher: Örebro University (2016)
www.publications.oru.se

Print: Örebro University, Repro 08/2016

ISSN 1653-3100
ISBN 978-91-7529-146-8

Abstract

Aminur Rahman (2016): Bioremediation of Toxic Metals for Protecting Human Health and the Ecosystem. Örebro Studies in Life Science 15.

Heavy metal pollutants, discharged into the ecosystem as waste by anthropogenic activities, contaminate drinking water for millions of people and animals in many regions of the world. Long term exposure to these metals, leads to several lethal diseases like cancer, keratosis, gangrene, diabetes, cardio-vascular disorders, etc. Therefore, removal of these pollutants from soil, water and environment is of great importance for human welfare. One of the possible eco-friendly solutions to this problem is the use of microorganisms that can accumulate the heavy metals from the contaminated sources, hence reducing the pollutant contents to a safe level.

In this thesis an arsenic resistant bacterium *Lysinibacillus sphaericus* B1-CDA, a chromium resistant bacterium *Enterobacter cloacae* B2-DHA and a nickel resistant bacterium *Lysinibacillus* sp. BA2 were isolated and studied. The minimum inhibitory concentration values of these isolates are 500 mM sodium arsenate, 5.5 mM potassium chromate and 9 mM nickel chloride, respectively. The time of flight-secondary ion mass spectrometry and inductively coupled plasma-mass spectroscopy analyses revealed that after 120 h of exposure, the intracellular accumulation of arsenic in B1-CDA and chromium in B2-DHA were 5.0 mg/g dwt and 320 µg/g dwt of cell biomass, respectively. However, the arsenic and chromium contents in the liquid medium were reduced to 50% and 81%, respectively. The adsorption values of BA2 when exposed to nickel for 6 h were 238.04 mg of Ni(II) per gram of dead biomass indicating BA2 can reduce nickel content in the solution to 53.89%. Scanning electron micrograph depicted the effect of these metals on cellular morphology of the isolates. The genetic composition of B1-CDA and B2-DHA were studied in detail by sequencing of whole genomes. All genes of B1-CDA and B2-DHA predicted to be associated with resistance to heavy metals were annotated.

The findings in this study accentuate the significance of these bacteria in removing toxic metals from the contaminated sources. The genetic mechanisms of these isolates in absorbing and thus removing toxic metals could be used as vehicles to cope with metal toxicity of the contaminated effluents discharged to the nature by industries and other human activities.

Keywords: Heavy Metals, Pollution, Accumulation, Remediation, Human Health, Bacteria, Genome Sequencing, *de novo* Assembly, Gene Prediction.

Aminur Rahman, School of Science and Technology, Örebro University, SE-701 82 Örebro, Sweden, e-mail: aminur.rahman@his.se

LIST OF PAPERS

Paper I
Rahman A, Nahar N, Nawani NN, Jass J, Desale P, Kapadnis BP, Hossain K, Saha AK, Ghosh S, Olsson B, Mandal A (2014) Isolation of a *Lysinibacillus* strain B1-CDA showing potentials for arsenic bioremediation. J. Environ. Sci. and Health, Part A: Hazardous Substances and Environmental Engineering. 49:12, 1349-1360. doi: 10.1080/10934529.2014.928247

Paper II
Rahman A, Nahar N, Nawani NN, Jass J, Hossain K, Saha AK, Ghosh S, Olsson B, Mandal A (2015) Bioremediation of hexavalent chromium (VI) by a soil borne bacterium, *Enterobacter cloacae* B2-DHA. J. Environ. Sci. and Health, Part A: Hazardous Substances and Environmental Engineering. 50:11, 1136-1147. doi: 10.1080/10934529.2015.1047670

Paper III
Desale P., Kashyap D., Nawani N., Nahar N., Rahman A., Kapadnis B. and Mandal A. (2014) Biosorption of Nickel by *Lysinibacillus* sp. BA2 native to bauxite mine. Ecotoxicology and Environmental Safety. 107, 260-268. doi: 10.1016/j.ecoenv.2014.06.009

Paper IV
Rahman A, Nahar N, Nawani NN, Jass J, Ghosh S, Olsson B, Mandal A (2015) Comparative genome analysis of *Lysinibacillus* B1-CDA, a bacterium that accumulates arsenics. Genomics. 106: 384-392. doi: http://dx.doi.org/10.1016/j.ygeno.2015.09.006

Paper V
Rahman A, Nahar N, Olsson B, Jass J, Nawani NN, Ghosh S, Saha AK, Hossain K, Mandal A (2016) Genome analysis of *Enterobacter cloacae* B2-DHA – A bacterium resistant to chromium and/or other heavy metals. Genomics, (Submitted).

PAPERS NOT INCLUDED IN THIS THESIS

1. **Rahman A**, Nahar N, Nawani N, Mandal A (2016) Investigation on arsenic accumulating and transforming bacteria for potential use in bioremediation. Handbook of Metal-microbe interactions and bioremediation: Eds. Surajit Das, Hirak R. Dash. CRC Press, Taylor & Francis.
2. Yewale P., **Rahman A**., Nahar N., Saha A., Jass J., Mandal A. and Nawani N. (2016) Sources of metal pollution, global status and conventional bioremediation practices. Handbook of Metal-microbe interactions and bioremediation: Eds. Surajit Das, Hirak R. Dash. CRC Press, Taylor & Francis.
3. Nawani N, **Rahman A**, Nahar N, Saha A, Kapadnis B, Mandal A (2016) Status of metal pollution in rivers flowing through urban settlements at Pune and its effect on resident microflora. Biologia. 71 (5): doi: 10.1515/biolog-2016-0074.
4. **Rahman A**, Nahar N, Olsson B, Mandal A (2016) Complete genome sequence of Enterobacter cloacae B2-DHA, a chromium resistant bacterium. Genome Announce. 4(3): e00483-16. doi:10.1128/genomeA.00483-16.
5. **Rahman A**, Nahar N, Jass J, Olsson B, Mandal A (2016) Complete genome sequence of *Lysinibacillus sphaericus* B1-CDA, a bacterium that accumulates arsenic. Genome Announc 4(1):e00999-15. doi: 10.1128/genomeA.00999-15.
6. **Rahman A**, Nahar N, Nawani NN, Jass J, Ghosh S, Olsson B, Mandal A (2015) Data in support of the comparative genome analysis of Lysinibacillus B1-CDA, a bacterium that accumulates arsenics. Data in Brief. *5*: 579–585. doi: http://dx.doi.org/10.1016/j.ygeno.2015.09.006
7. Islam MS, Mohanto NC, Karim MR, Aktar S, Hoque MM, Rahman A, Jahan M , Khatun R, Aziz A , Salam KA, Saud ZA, Hossain M, **Rahman A**, Mandal A, Haque A, Miyataka H, Himeno S, Hossain K (2015) Arsenic exposure-related elevation of serum matrix metllaoproteinases- and -9 levels and their associations with circulating markers of cardiovascular diseases. Environmental Health 14:92. doi: 10.1186/s12940-015-0079-7
8. Nahar N, **Rahman A**, Moś M, Warzecha T, Ghosh S, Hossain K, Nawani NN, Mandal A (2014) *In silico* and *in vivo* studies of molecular structures and mechanisms of AtPCS1 protein involved in binding arsenite and/or cadmium in plant cells. *J Mo. Model* 20: 2104. doi: 10.1007/s00894-014-2104-0.

9. Nahar N., **Rahman A.**, Moś M, Warzecha T., Algerin M, Ghosh S., Johnson-Brousseau S. and Mandal A. (2012) *In silico* and *in vivo* studies of an *Arabidopsis thaliana* gene *ACR2* putatively involved in arsenic accumulation in plants. *J. Mol. Model*18:4249–4262, doi: 10.1007/s00894-012-1419-y.

LIST OF PATENTS

1. Nawani N, Desale P, **Rahman A**, Nahar N, Kapadnis B, Mandal A (2015) A novel technology for the removal of metals from aqueous solutions. Indian patent 17/MUM/2015 dated 03/01/2015.

2. Nawani N, Desale P, **Rahman A**, Nahar N, Kapadnis B, Mandal A (2015) A method for removal of metals from aqueous solutions. PCT/IB2016/050358 dated 25/01/2016.

ABBREVIATIONS

ACR2	Arsenic reductase genes
$AgNO_3$	Silver nitrate
As	Arsenic
As^{III}	Arsenite
AsO_2^-	Meta-arsenite
AsO_3^{3-}	Ortho-arsenite
$AsO_4H_2^-$	Arsenate
As^V	Arsenate
Cd	Cadmium
CFU	Colony forming unit
Cr	Chromium
Cr(III)	Trivalent chromium
Cr(VI)	Hexavalent chromium
CrO^-	Chromium oxide
CrO_2^-	Chromium dioxide
dwt	Dry weight
DC	Direct current
ddH_2O	Double deionized water
DMAA	Dimethyl arsenic acid
dNTPs	Deoxy nucleotide triphosphates
E. coli	*Escherichia coli*
EDS	Energy dispersive system
ESEM	Environmental scanning electron microscope
FAO	Food and agricultural organization
$FeCl_3$	Ferric chloride
FIA	Flow injection analysis
GO	Gene ontology
ICP-AES	Inductively coupled plasma atomic emission spectroscopy
ICP-MS	Inductively coupled plasma-mass spectroscopy
LB	Luria-Bertani
LSD	Least significant difference
MIC	Minimum inhibitory concentration
MMAA	Monomethyl arsenic acid
$MnCl_2$	Manganese chloride
Na_2HAsO_4	Sodium arsenate
ND	Nano drop
NEB	New England Bio lab
Ni	Nickel
$NiCl_2$	Nickel chloride
Pb	Lead
PBS	Phosphate buffered saline

RAST	Rapid annotations using subsystems technology
RFW	Reconstructed field water
SEM	Scanning electron microscope
TE	Tris EDTA
TOF-SIMS	Time of flight-secondary ion mass spectrometry
$ZnCl_2$	Zinc chloride

Table of Contents

Introduction

As the society has gradually grown wealthier, this has created more diverse pollutants. Without sweeping action, population growth and urbanization will outperform the reduction of hazardous waste generated from industrial activities. For example, intensive use of agricultural and forest lands continues to emit toxic pollutants to the environment, particularly ground and surface water (FAO, 2014). Hence, the quality of life on Earth is being denigrated while the living standards have surely improved to a great extent at the cost of environmental degradation. The problems associated with contaminated sites are increasingly becoming important in many countries throughout the world. In fact, there are new challenges regarding environmental protection (Duruibe et al., 2007) in the world with increasing globalization, urbanization and industrialization. Consequently, many toxic pollutants like the heavy metals and metalloids are widespread, especially in developing countries. It is indeed a matter of concern as it has direct effect on human and environmental health (Hogan, 2012). In particular, the dangers to human health are associated with continuous exposure to heavy metals such as arsenic, cadmium, chromium, lead, mercury, and nickel among others. These toxic metals, commonly found in soils, sediments and water, are discharged as wastes of industrial, agricultural, and mining activities, and the leading cause of various lethal diseases in both humans and animals (Jaishankar et al., 2014).

Water, a precious natural resource, is the most important element of human life and plays a key role of human civilization. Water pollution in both developing and developed countries has increased due to anthropogenic activities such as electroplating, leather industries, sugar-mills, fertilizer industries, textiles, mining, metallurgical processing and municipal waste generation (Kaewsarn and Yu, 2001; Rahman et al., 2014, 2015a). Most of the animals and plants have 60-65% water in their body and release of toxic metals into water systems due to such anthropogenic activities is of major concern to the health and well-being of humans and animals (Castro-González and Méndez-Armenta, 2008). Thus, the world is heading towards water crises (Rosegrant and Cai, 2001). In the future, most of the social conflicts are going to be water based as predicated by the great scientist Albert Einstein (Giri, 2012). At present, in USA one liter of bottled water costs 1.05-1.18 dollars whereas one liter of milk costs 1.00-1.02 dollars and in the future, pure water will be an expensive and pivotal commodity.

Toxic heavy metals, discharged into the environment as waste either by industries or human activities, contaminate drinking water for millions of people and animals in many regions of the world, particularly South East Asia. At low concentrations, metals can serve as important components in life processes, often serving important functions in enzyme productivity. However, above certain threshold concentrations, these metals can become toxic to many species. Long-term exposure to these toxic substances e.g., to arsenic via drinking water or consuming contaminated foods, leads to several lethal diseases such as cancer, keratosis, gangrene, diabetes and cardiovascular disorders among others (Diaz-Villasenor et al., 2007; Marshall et al., 2007; Chen et al., 2009; Argos et al., 2010; Zhao et al., 2010; Huang et al., 2011; Rossman et al., 2011). For example, Figure 1 depicts manifestation of arsenic poisoning like pigmentation and keratosis. The spotty depigmentation (leucomelanosis) occurs in arsenicosis, diseases caused by long term exposure to arsenics. Simple keratosis usually appears as bilateral thickening of the palms and soles, while in nodular keratosis multiple raised keratotic lesions appear in palm and soles. Moreover, skin lesions pose an important public health problem because advanced forms of keratosis are not only painful, but also the consequent disfigurement can lead to social isolation, particularly in the villages of South East Asian countries (Kadono et al., 2002; Argos et al., 2010). In contrast to cancer caused by arsenic poisoning, which takes decades to develop, the skin lesions are generally developed after 5-10 years of exposure. Ingestion of water contaminated with arsenic leads to weakness, conjunctive congestion, hepatomegaly, portal hypertension, lung disease, poly neuropathy, solid edema of limbs, ischemic heart disease, peripheral vascular disease, hypertension, and anemia in adults (Shi et al., 2004; WHO, 2006; Ahmed et al., 2008).

Figure 1. Effects of long-term exposure of humans to arsenic poisoning through drinking water and consumption of contaminated foods [Pictures (except picture a) were taken from Chuadanga, Bangladesh]. These diseases, also called as "arsenicosis" are the direct evidences of human suffering resulting from arsenic contamination. a, female laborers are working in an arsenic contaminated paddy field. b-e, hyper-melanosis leading to development of cancer. f, hyper- and hypo melanosis with skin cancer.

Although heavy metals are non-biodegradable, they can be transformed through sorption, methylation, and complexation, and changes in valence state (Adeniji, 2004). These transformations affect the mobility and bioavailability of metals. This thesis focuses on remediation of toxic heavy metals (arsenic, chromium and nickel) from the contaminated sources using microorganisms. Furthermore, the mechanisms of arsenic bioremediation in the Gram positive bacterium, *Lysinibacillus sphaericus;* chromium bioremediation in the Gram negative bacterium, *Enterobacter cloacae* and nickel bioremediation in the Gram positive bacterium *Lysinibacillus* sp. BA2 were studied in this thesis. The primary goal of this thesis is to reduce or eliminate heavy metal pollutants from the contaminated sources by using microorganisms, and development of sustainable and cost effective methods for protecting human health and the environment from toxic metal contamination.

Heavy metal and metalloid contaminants

Any metal or metalloid species may be considered as "contaminant" if it occurs where it is unwanted, or in a form or concentration that causes a harmful human or environmental effect (Matschullat, 2000). The most widely distributed heavy metals and metalloids in the environment are arsenic (As), cadmium (Cd), chromium (Cr), lead (Pb), mercury (Hg), and nickel (Ni) among others, and are major pollutants in ground water, industrial effluent and marine water (Hogan, 2012; Rahman et al., 2014). These heavy metals and metalloids are considered to be the most toxic to humans and animals at high concentrations, but are not limited to, neurotoxic and carcinogenic actions (Jomova and Valko, 2011; Tokar et al., 2011). These metals enter into the environment directly via three routes: (i) deposition of atmospheric particulates, (ii) disposal of metal and metalloid enriched sewage effluents, and (iii) by-product from metal mining processes and other processing industries (Shrivastav, 2001). Furthermore, a considerable area of land is contaminated with these metals originating from the use of sludge or municipal compost, pesticides, fertilizers, and emissions from municipal waste products, car exhausts, residues from metalliferous mines, and smelting industries (Hani and Pazira, 2011; Jackson et al., 2012). Therefore, humans are considered the topmost exposure of these toxic metals by directly and/or indirectly consuming of metal contaminated foods and water through the "Plants–Animal –Human" pathway (Figure 2) and thus may pose significant danger to the health of humans, animals and plants (Tchounwou et al., 2012). Rice and wheat are the staple food for over half of the world's population especially in South-Asia (Liu, et al., 2009; Halder et al., 2012). In many countries, these crops are grown extensively in areas where toxic metal contamination is widespread exceeding the safety level. As for example, nearly 30–50% of the cultivated lands in Bangladesh and West Bengal state of India are irrigated with toxic metal contaminated water to grow rice, wheat, vegetables and other crops (Neidhardt et al., 2012; Halder et al., 2012). Rice, vegetables and wheat accumulate high levels of arsenite (AsIII) (Meharg et al., 2004). Also, cadmium and nickel accumulated in the rice crops, vegetables, and fruits grown in highly contaminated areas, which contributes toxicity to the general populations (Nogawa et al., 2004). Moreover, rice straw is used in animal fodders in many countries, including Bangladesh, China, India, United States, and many others (Christopher et al., 2012). The contaminated rice straw may have adverse health effects on cattle and may result in an increased metal exposure in humans via the "Plant–Animal–Human" pathway (Abedin et al., 2002; Rahman et

al., 2009). Consequently, it raises a significant concern on accumulation of toxic metals in meat, dairy products, consumable crops and other vegetables grown in contaminated areas (Arora et al., 2008; Pandey and Pandey, 2009).

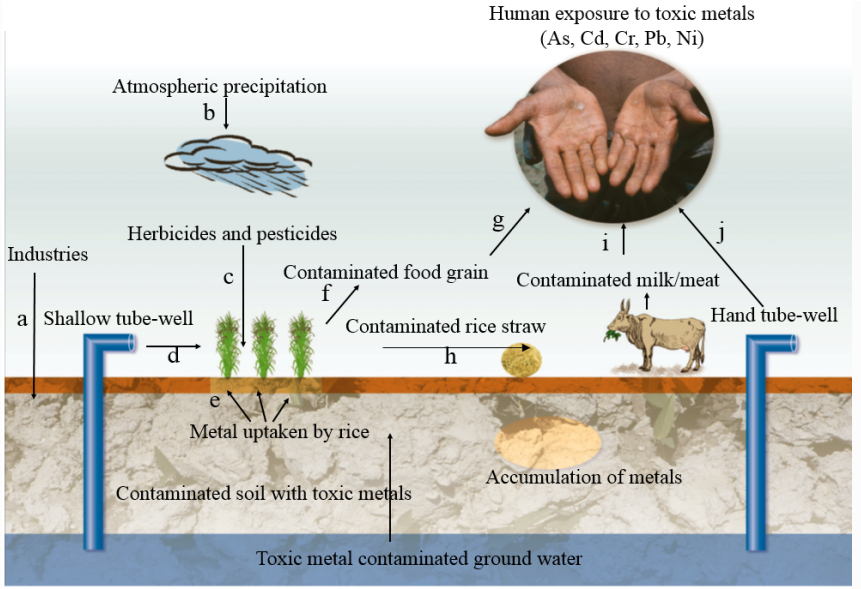

Figure 2. A diagram of toxic metal contamination of the ecosystem responsible for poisoning of human health. Metal poisoning takes place directly through drinking of contaminated water or consumption of contaminated foods and indirectly via meat-milk pathway. a, Exposure of toxic metals to the ecosystem by anthropogenic activities like industries; b, atmospheric precipitation to the surface of the earth; c, using metal containing herbicides and pesticides in agriculture fields; d, irrigation of cultivated crops with toxic metal contaminated ground water; e, uptake and accumulation of metals in plants; f, consumption of metal contaminated foods; g, human exposure to metal toxicity; h, feeding of metal contaminated straw or leaves to cattle; i, consumption of arsenic contaminated milk and meat; j, drinking metal contaminated water pumped up using hand tube-wells.

A number of toxic heavy metals are available in nature. The following describes sequentially the nature, source, uses, and toxicity of arsenic, chromium, and nickel in details:

Forms of arsenic

Arsenic, a chemical element with the symbol of **As** taken from the Latin arsenicum, and atomic number of 33, was discovered in the 13th century by Albertus Magnus. Arsenic is a metalloid having both metal and non-metal properties. It is the most ubiquitous element on earth, and ranks 20th in natural abundance, comprising about 0.00005% of the earth's crust, 14th in water and 12th in the human body (Mandal and Suzuki, 2002). Moreover, arsenic concentration in most rocks ranges from 0.5 to 2.5 mg/kg, though higher concentrations are found in finer grained argillaceous sediments and phosphorites (Mandal and Suzuki, 2002). Steel gray, brittle and crystalline arsenic tarnishes in air and when heated rapidly forms arsenious oxide with the odor of garlic. Arsenic possess atomic weight 74.92 g mol^{-1}, melting point 817°C, boiling point 613°C, specific gravity 5.73, and vapor pressure 1 mm Hg at 372°C, and exists in the –3, 0, +3 and +5 oxidation states (Smedley et al., 2002). The arsenical compounds are separated into two groups: (1) inorganic compounds combined with chlorine, iron, oxygen, sulfur, and (2) organic compounds combined with carbon and other atoms. The various forms of arsenic in the environment include arsenious acids (H_3AsO_3), arsenic acids (H_3AsO_4, $H_2AsO_4^-$, and $HAsO_4^{2-}$), arsenites, arsenates, monomethylarsonic acid (MMAA), dimethylarsonic acid (DMAA), and arsine among others. Arsenic (III) exists as a hard acid and preferentially as complexes with oxides and nitrogen. Conversely, arsenic (V) behaves like a soft acid, forming complexes with sulfides. Trivalent (+3) arsenites include As(OH)3, $As(OH)_4^-$, AsO_2OH^{2-} and AsO_3^{3-} (Mohan and Pittman Jr. 2007) while pentavalent (+5) or arsenate species are (AsO_4^{3-}, $HAsO_4^{2-}$, $H_2AsO_4^-$) oxyanions (Ranjan et al., 2009). Trivalent arsenites predominate in moderately reducing state in anaerobic environments such as groundwater while pentavalent species predominate and are stable in oxygen rich aerobic environments.

Sources of arsenic

Arsenic is found in the earth's crust, rocks, soils, water and air (Reimer et al., 2010; Emsley, 2011). Additionally, inorganic arsenic compounds are found in industry, in building material, and in arsenic-contaminated ground water such as arsenic trioxide (As_2O_3), orpiment (As_2S_3), arsenopyrite (AsFeS) and realgar (As_4S_4) (Smedley and Kinniburgh, 2005). Leaching of arsenic from weathered rocks and soils in groundwater depends on pH, redox conditions, temperature, and solution composition (Matschullat, 2000; Jackson et al., 2012). Arsenic is released by anthropogenic activity from combustion of fossil fuels as well as by natural weathering reactions, biological activity, mining activity, geochemical reactions, and volcanic eruptions (Dogan and Dogan, 2007). It can also be released into the environment

from agricultural and industrial sources, such as fertilizer, pesticide, fungicide, herbicides, and crop desiccants.

Uses of arsenic

Although arsenic has negative impact on human and animal's health, it is utilized in industry to produce semiconductors, and in pharmacy to produce medicines (Stéphane and Gérard, 2010). Despite serious safety concerns, arsenic is often used in minute dosage as a part of homeopathic remedies for digestive disorders, food poisoning, sleep problems (insomnia), allergies, anxiety, depression and obsessive-compulsive disorder. Furthermore, arsenic is used for pigment in paints – especially as a white and green enhancer pigments in white and green paints, respectively (Benner, 2010). In traditional Chinese medicine, arsenic is used (i) to treat psoriasis, syphilis, asthma, joint pain (rheumatism), hemorrhoids, cough, itchiness, and cancer, (ii) to reduce swelling (as an anti-inflammatory agent) and (iii) as a general tonic and pain-killer. Arsenic is used in bronzing, hardening and improving the sphericity of shot (Haynes, 2014). In the agricultural industry, arsenic is widely used in paints, wood preservatives, tanning, fungicides, and semiconductor manufacturing (Rahman et al., 2004). In the defense industry, pure form of arsenic (99.99%) is used to make the gallium arsenide or indium arsenide, which is required for manufacturing of semiconductors. The main use of metallic arsenic is for strengthening the alloys of copper and lead to use in batteries (Benner, 2010). Also, gallium arsenide is used in light-emitting diodes (LEDs) and solar cells, while indium arsenide is used to produce infrared devices, and lasers (Brooks, 2008). Another use of arsenic is as a doping agent in solid state devices such as transistors. In ammunition manufacturing arsenic is used to create harder and rounder bullets. Arsenic-74 an isotope is being used as a way to locate tumors within the body as it produces clearer pictures than that of iodine (Benner, 2010). Other arsenic compounds are applied in glass processing, in chemical industries, or in semiconductor technique with gallium and indium (Garelick et al., 2008). Another use of arsenic is as an anti-friction additive in ball bearings and for hardening of lead and for manufacturing germanium-arsenide-selenide optical materials. Now-a-days most countries, however, have banned arsenic usages in consumer products including pesticides, herbicides and insecticides because of its high toxicity.

Toxicity of arsenic

Constant release of arsenic, a class-1 human carcinogen, into groundwater through natural occurrences or anthropogenic activities contributes to environmental pollution worldwide and is a severe threat for the ecosystem and human health (Rahman et al., 2014). Inorganic arsenic severely impacts human health, causing many cancerous diseases, neurological and vascular disorders, and system-wide organ damage and failure as well as melanosis like hyper- and hypo- pigmentation and cancers of skin, lung and bladder, skin thickening (hyperkeratosis), muscular weakness, loss of appetite, and nausea (Wang et al., 2007; Guha, 2007; Marshall et al., 2007; Kitchin and Wallace, 2008; Argos et al., 2010; Zhao et al., 2012). On the other hand, organic arsenic compounds are found in some foods that are much less toxic than inorganic arsenic (Meharg and Rahman, 2003). Thus far, there is no report on organic arsenic compounds inducing cancerous diseases in human, but recent findings suggest that many food items cultivated in the arsenic contaminated areas also contain inorganic arsenic (Rahman and Hasegawa, 2011). The most potent form of inorganic arsenic is available in drinking water (WHO, 2011). Contamination of soils and groundwater with high concentrations of arsenic is reported in several countries, including Argentina, Bangladesh, Chile, China, India, Japan, Mexico, Mongolia, Nepal, Poland, Sweden, Taiwan, Vietnam and some parts of the United States (Ahmed et al., 2008, EPA 2009; Karim et al., 2013). In particular, the inhabitants of countries in South-East Asia, who live in densely populated and currently the fastest developing regions of the planet, are most exposed to arsenic. The threat of arsenic exposure continues to grow as rapid industrial development in South-East Asia increases industrial emission in addition to natural emission caused by volcanic eruptions and rock erosion. For example, just in Bangladesh and India, approximately 300 million people are exposed to arsenic contamination on a daily basis either through drinking water or by consumption of foods (Huang et al., 2011; Tani et al., 2012).

In Bangladesh, arsenic-rich bedrock of the Brahmaputra river basin contaminates the groundwater as it is pumped up through hundreds of thousands of tube-wells and is consumed by millions of people. The oral intake of more than 100 mg at a time is found to be lethal. The lethal dose of arsenic trioxide is 10-180 mg, and for arsenide is 70-210 mg. Arsenic poisoning through drinking tube-well water has now become a national problem in Bangladesh (Argos et al., 2010). The WHO provisional guideline of

10 ppb (0.01 mg/L) has been adopted as the drinking water standard. However, many countries have retained the earlier WHO guideline of 50 ppb (0.05 mg/L) as their standard or as an interim target including Bangladesh and China. Most recently, according to Bangladesh Bureau of Statistics, approximately 60% of 160 million people (96 million) of the country are affected by arsenic contaminated water (Islam et al., 2015). In these regions, when crops are cultivated on arsenic polluted lands and irrigated with arsenic contaminated groundwater, a very high amount of arsenic accumulates in edible parts of the crops (Wang et al., 2007; Guha, 2007; Zhao et al., 2012). Long-term consumption of these crops, such as rice, wheat and vegetables (Signes-Pastor et al., 2012), leads to potential risk for severe diseases in both human and animals.

In plants, arsenic becomes toxic when combined with sulfhydryl groups in cells. Therefore, the plants that are not resistant to arsenic show symptoms such as decreased plant growth, plasmolysis, necrosis of leaf tips, and decrease in photosynthetic capacity (Thomas et al., 2007; Natarajan et al., 2008). Also, this toxicity in plant cells interrupts ATP production by inhibiting pyruvate dehydrogenase, and competing with phosphate, hence uncoupling oxidative phosphorylation (mitochondrial respiration) and inhibiting energy-linked reduction of NAD^+ (Vigo and Ellzey, 2006). The use of (i) arsenic additives to livestock feed and (ii) contaminated rice straw for many purposes including animal fodder causing adverse health effects in livestock and further introduces arsenic to the human food chain via arsenic-contaminated meat and milk (Datta et al., 2012).

Forms of chromium

Chromium, an element with the symbol **Cr** and atomic number 24, is a steel-gray, lustrous, hard crystalline metal. This element was discovered in 1761 by Johann Gottlob Lehmann. The name chromium is derived from the Greek word χρῶμα, *chrōma*, meaning color, because many of its compounds are colored. The atomic weight, specific gravity, melting point, and boiling point of chromium is 51.99 $g.mol^{-1}$; 7.18 to 7.20; 1857 °C and 2672 °C, respectively (Becquer et al., 2003). It comprises about 0.037 percent of the earth's crust and therefore ranks 21st in relative natural abundance (Shanker et al., 2005; Saha et al., 2011). The concentration of chromium in sea water, soil, and lakes and rivers ranges between 5 to 800 µg/L, 1 to 300 mg/kg, and 26 µg/L to 5.2 mg/L, respectively (Kotaś, and Stasicka, 2000). In the ground water, 30 µg/L of 39 µg/L chromium is present as hexavalent chromium Cr(VI) (Gonzalez, et al., 2005). The producers of

chromium ore are South Africa (44%), India (18%), Kazakhstan (16%), Zimbabwe (5%), Finland (4%), Iran (4%) and Brazil (2%) while the several other countries are producing the rest of about 7% of the world production (Papp, 2002). The stable forms of Cr are the trivalent Cr (III) and the hexavalent Cr (VI) species. Although there are various others valence states of chromium, they are unstable and short lived in biological systems (Zhang et al., 2007). Cr (VI) is considered the most toxic form of Cr, which generally associated with oxygen as chromate (CrO_4^{2-}) or dichromate ($Cr_2O_7^{2-}$) oxyanions (Kotaś and Stasicka, 2000; Kabay et al., 2003). Cr (III) is less mobile and remains bound to organic matter in soil and aquatic environments (Becquer et al., 2003; Chen et al., 2011). The predominate species, are CrO_4^{2-}, $HCrO_4^{2-}$, and $Cr_2O_7^{2-}$.

Sources of chromium

Chromium is released to the environment by natural as well as anthropogenic activities (Alves et al., 2012). It is found in effluents discharged from industries manufacturing electronics, wood preservatives, electroplating, metallurgical, leather tanning materials. Sources of chromium in the environment include airborne emissions from cement dust, contaminated landfill, effluents from chemical plants, asbestos lining erosion, road dust from catalytic converter erosion and asbestos brakes, and tobacco smoke (Ahluwalia and Goyal, 2007). Also, several sources including chrome alloy production, glassmaking, paints/pigments, ceramics manufacturing, production of high-fidelity magnetic audio tapes, textile manufacturing, and welding of alloys or steel are chromium contributors to environmental contamination. (Kotaś and Stasicka, 2000).

Uses of chromium

Chromium has a wide range of uses in metals, chemicals, and refractories industries. Trace amount of trivalent chromium [Cr(III)] may be an essential element in the diet for sugar metabolism in the human body (Cronin, 2004; Bona et al., 2011). In 2014, the European Food Safety Authority demonstrated that Cr(III) has no beneficial effect on healthy people, thus the Board removed it from the list of nutrients and essential elements (Thor et al., 2011; EFSA, 2014). Chromium is primarily used in tannery industries as the chrome liquor in leather processing because it stabilizes the leather by cross-linking the collagen fibers (Brown, 1997). In addition to leather processing, chromium is used in wood preservation, steel production, paints, cement production, chromium/electroplating, metal processing, alloy formation, textiles, ceramics and thermonuclear weapons manufacturing, among others (Hingston et al., 2001; Ortegel et al., 2002; Viti et al., 2003;

Chourey et al., 2006; Sardohan et al., 2010; Wugan and Tao, 2012). Moreover, chromic acid, a powerful oxidizing agent, is used for cleaning laboratory glassware of any trace of organic compounds.

Chromium toxicity

Chromium is well known for its toxic, carcinogenic, and mutagenic effects on humans and other living organisms, hence chromium is classified as a priority pollutant (Avudainayagam et al., 2003). Strong exposure to Cr (VI) may cause epigastria pain, nausea, vomiting, severe diarrhea and cancer in the digestive tract and lungs (Saçmac et al., 2012). Long-time exposure to strong chromate solutions used by electroplating, tanning and chrome-producing manufacturers can lead to allergic, dermatitis and irritant dermatitis, resulting in ulceration of the skin, sometimes referred to as "chrome ulcers" (Basketter et al., 2000; Baselt, 2008). In the soil, chromium is found in two oxidized forms: (i) trivalent chromium Cr (III) and (ii) hexavalent chromium Cr(VI). Several *in vitro* studies demonstrated that high concentrations of chromium in the cell can lead to DNA damage (Shrivastava et al., 2002). Hexavalent chromium Cr (VI), a soluble oxidizing agent, is reduced intracellularly to Cr^{5+} and reacts with nucleic acids and other cellular components to create carcinogenic and mutagenic effects in biological systems (Camargo et al., 2003; Eastmond, et al., 2008). Cr(III) is less toxic than Cr(VI) (Jeyasingh, and Philip, 2005). For example, acute oral toxicity for Cr (III) ranges between 1.5 and 3.3 mg/kg and for Cr(VI) ranges between 50 and 150 μg/kg (Dayan and Paine, 2001). Cr(VI), a strong oxidizing agent, damages the liver, the kidneys and blood cells by oxidation reactions after it reaches to the blood stream resulting in hemolysis, and liver and renal failure. Chromium based compounds are also highly toxic to plants at multiple levels, from reduced yield, through effects on leaf and root growth, to inhibition of enzymatic activities and mutagenesis (Becquer et al., 2003).

Forms of nickel

Nickel, an element with the symbol **Ni** and atomic number 28, was isolated and classified as a chemical element in 1751 by Axel Fredrik Cronstedt, who initially mistook its ore for a copper mineral. Nickel is the 24th most abundant element in the Earth's crust and contributing about 3% of the composition of the earth. Nickel, a silvery-white lustrous metal with a slight golden tinge, is the 5th most abundant element by weight after iron, oxygen, magnesium and silicon. On Earth, native nickel is found in combination with iron, a reflection of those elements' origin as major end products of supernova nucleosynthesis. An iron–nickel mixture is thought to be the Earth's

inner core (Badro et al., 2014). The most prevalent oxidation state of nickel in the environment is Ni (II) (nickel in the +2 valence state). Other valences (-1, +1, +3, and +4) of nickel are also encountered less frequently (Cempel and Nikel, 2006).

Sources of nickel

Nickel occurs naturally in soil, water and sea salts as nitrates, oxides and sulphides (Wuana and Okieimen, 2011). Natural levels of nickel in water range between 3 and 10 mg/L. The economically important source of nickel is the iron ore limonite that contains 1–2% nickel. Among other nickel's ore minerals include garnierite and pentlandite. The wastes from electroplating, nickel-cadmium batteries and metal finishing industries are the sources of nickel in the environment. Major production sites include the Sudbury region in Canada, New Caledonia in the Pacific, and Norilsk in Russia.

Uses of nickel

Nickel is a nutritionally essential trace element for several animal species, microorganisms and plants (Cempel and Nikel, 2006). Nickel has been found to be a required cofactor for enzymes of some microorganisms and plants (Nath, 2000). Nickel and nickel compounds have many industrial and commercial values, and the progress of industrialization has led to increased emission of this pollutant into ecosystems (Cempel and Nikel, 2006). Furthermore, products that plays a major role in our everyday lives such as food preparation equipment, mobile phones, medical equipments, transport, buildings and power generation among others are made from nickel materials. Compared with other materials, nickel and nickel compounds offer better corrosion resistance, toughness, strength at high and low temperatures, and a range of special magnetic and electronic properties (Cunat, 2004). Nickel is, however, mainly used in producing alloys such as stainless steel, batteries including rechargeable nickel-cadmium batteries and nickel-metal hydride batteries used in hybrid vehicles.

Nickel toxicity

Drinking water generally contains nickel at concentration less than 10 µg/L. Assuming a daily intake of 1.5 L of water and a level of 5-10 µg Ni/L, the mean daily intake of nickel from water for adults would be between 7.5 and 15.0 µg (Cempel and Nikel, 2006). Although inhalation exposure in occupational settings is a primary route for nickel-induced toxicity, most nickel enters the body via food and water consumption (ATSDR, 2005). Excessive nickel poisoning causes pulmonary fibrosis, skin dermatitis, vomiting, diarrhea, nausea and neurological disintegration particularly in children (Das et

al., 2008). It is a known immunotoxic, haematotoxic, neurotoxic, reproductive toxic, genotoxic, nephrotoxic, hepatotoxic, pulmonary toxic and carcinogenic agent (Cempel and Nikel, 2006; Das et al., 2008). Nickel exposure causes formation of free radicals in various tissues in both humans and animals leading to various modifications to DNA bases, enhanced lipid peroxidation, and altered calcium and sulfhydryl homeostasis. Acute inhalation of nickel may produce headache, nausea, respiratory disorders and death (Das et al., 2008). The primary route for nickel toxicity is reduction of glutathione and bonding to sulfhydryl groups of proteins (Das et al., 2008).

Removal of heavy metals

To date, many conventional remediation methods have been developed for removing of toxic metals such as electrochemical treatment, ion exchange, solvent extraction, evaporation, reverse osmosis, precipitation, and adsorption on activated coal (Baciocchi et al., 2005; Kim et al., 2006; Kumari et al., 2006; Balasubramanian et al., 2009; Moussavi and Barikbin, 2010; Chowdhury et al., 2015). Nevertheless, most of these methods have disadvantages such as high operational and reagent costs, incomplete metal removal, require technically skilled manpower for operation and a large area of land. Further, these are also inefficient especially when the contamination levels are very low (Camargo et al., 2003; Zafar et al., 2007; Sharma and Sohn, 2009). Alternatively, various cost effective and eco-friendly biological approaches have been considered for bioremediation (Congeevaram et al., 2007). Although the term, "bioremediation" was used over 100 years ago with the opening of the first biological sewage treatment plant in Sussex, UK, in 1891, the effective use of the process is fairly new as validated in a peer-reviewed scientific literature in 1987 (NABIR, 2003).

The process, bioremediation can be divided into two groups: (i) phytoremediation, and (ii) microbial bioremediation. Comparing to the conventional methods phytoremediation is environmentally friendly, cost-effective, and aesthetically pleasing but has some disadvantages such as it relies on natural cycle of plants and therefore takes time for some plants to absorb the of heavy metals, making them a potential risk to the food chain if animals feed upon them. Thus, to remove sufficient amounts of heavy metals with this technique, plants have to be highly time-efficient in metal uptake and translocation into their above ground vegetative parts so more metal can be stored within the plant.

Microbial bioremediation is another alternative strategy with widespread benefits. Often the microorganisms metabolize the chemicals to produce carbon dioxide or methane, water and biomass (Harms et al., 2011; Silar et al., 2011). Alternatively, the contaminants may be enzymatically transformed to metabolites that are less toxic or innocuous (Iwamoto and Nasu, 2001). Microbial bioremediation's ability to destroy the toxins allows for a more environmentally friendly approach to remediation than other strategies, such as landfill and dumping waste in the sea (Vivaldi, 2001). The technique of microbe populations increasing in number while degrading a contaminant, and decreasing prior degradation appears more natural (Vivaldi, 2001). The microbial bioremediation confers *in situ* and *ex situ* process. *In situ* remediation proves to be more cost effective, as no waste is required to be removed off site as it involves treating the contaminated material at the site. The commonly used *in situ* remediation process includes bio-augmentation, biodegradation and biosparging. However, *ex situ* remediation has the benefit of providing preliminary testing of the removal of the waste (Boopathy, 2000) although it involves the removal of the contaminated material to be treated elsewhere. The most commonly recognized applications of *ex situ* remediation are land farming, composting and biopiles (Pavel and Gavrilescu, 2008). The complete destruction of toxic waste in a polluted environment is extremely advantageous.

Fortunately, those microorganisms with ability to affect the reactivity, and mobility of toxic metals and pollutants, can be used to detoxify the metals and prevent further metal contamination. To this end, *Lysinibacillus, Enterobacter, Bacillus*, *Staphylococcus*, *Pseudomonas*, *Citrobacteia*, *Klebsiella*, and *Rhodococcus* are commonly used organisms in bioremediation of arsenic, cadmium, nickel (Megharaj et al., 2003; Camargo et al., 2003; Desai et al., 2008; Rahman et al., 2014; 2015a ; Desale et al., 2014). These processes include bio-augmentation, in which microbes and nutrients are added to the contaminated site, and bio stimulation, in which nutrients and enzymes are added to supplement the intrinsic microbes of the site (Connor et al., 1996). Furthermore, *Alcaligenes, Enterobacter* and *Pseudomonas* have been used in the bioremediation of chromium (Connor et al., 1996; Rahman et al., 2015a). Likewise, organisms like *Escherichia* and *Pseudomonas* have been used in the bioremediation of copper (Connor et al., 1996). It is anticipated that federal, state, and local governments and private industries will annually invest billions of dollars over the next several decades to clean up sites contaminated with hazardous waste (NABIR,

2003). This investment validates the need to further research the utilization of microbial processes to clean up contaminated sites. The strategy of a microbial bioremediation work proposal has been depicted in Figure 3.

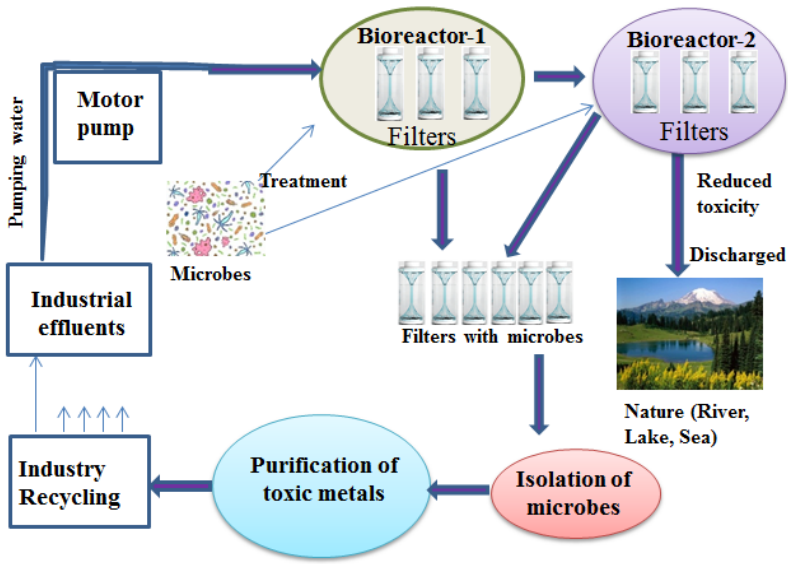

Figure 3. A schematic diagram of the microbial remediation of toxic metals (arsenic, chromium, and/or nickel) disposed as either effluents or solid wastes from the industries or by other anthropogenic activities. Effluents discharged to the drainage or sewage are pumped up and collected in containers (bioreactors). Alternatively, effluents are disposed directly to the bioreactors. Previously investigated and selected bacterial strain/s are applied to the bioreactor 1 for treatment of the effluents. Bacteria absorb and accumulate the toxic metals (arsenic, chromium, and/or nickel) thus reducing the metal content in the effluents. Special filters/membranes installed previously in the bioreactor 1 capture the bacteria after the treatment period is over. Effluent samples from the bioreactors are continuously monitored for the level of toxicity by analyzing toxic metals. This treatment is repeated several times by using bioreactors 2, 3, etc., until the metals are eliminated from the effluents or their content is reduced to a "safe" level. Bacterial cells captured in the filters/membranes are then used as a source for isolation and purification of metals that can be reused by the companies including tannery, nanotech or biotech industries, and fertilizer factories.

Genes involved in metal bioremediation

Bacteria possess many genetic systems for maintaining the resistance against toxic metals or maintaining intracellular homeostasis of metal ions (Chudobova et al., 2015). In bacteria the most well-known genetic mechanisms of metal resistance are the presence of metal binding proteins (Hobman and Crossman 2014) and heavy metal efflux systems (Moraleda-Mun˜oz et al., 2010). There are many bacterial genes that are involved in specific metal binding, transport and resistance. Certain bacteria have evolved the necessary genetic components that confer resistance mechanisms, allowing them to survive and grow in environments containing high levels of arsenic that would be toxic to most other organisms (Rahman et al., 2015b). The arsenic resistance *ars* operon comprising either three (*arsRBC*) (Liao et al., 2011) or five (*arsRDABC*) genes arranged in a single transcriptional unit located on plasmids (Owolabi et al., 1990) or chromosomes (Diorio et al., 1995) conferred a high-level resistance to As in bacteria. ArsB, an integral membrane protein that pumps arsenite out of the cell, is often associated with an ATPase subunit, *arsA* (Achour et al., 2007). The *arsC* gene encodes the enzyme for arsenate reductase, which is responsible for the biotransformation of arsenate [As(V)] to arsenite [As(III)] prior to efflux. *ArsR* is a trans-acting repressor involved in the basal regulation of the *ars* operon, while *arsD* is a second repressor controlling the upper levels of expression of *ars* genes (Silver and Phung, 2005). In addition, several other genes act as arsenic responsive genes like the *arrA* gene for dissimilatory As(V) respiration (DAsR) (Malasarn et al., 2004; Kulp et al., 2007; Song et al., 2009), and the *aoxB* gene for As(III) oxidation (Rhine et al., 2007; Hamamura et al., 2009).

Bacteria have developed coping strategies to survive in chromium toxicity through several mechanisms: (i) the transmembrane efflux of chromate (Ramirez-Diaz et al., 2008) (ii) the chrR transport system (Saier, 2003), (iii) the reduction of chromate (Cervantes and Campos, 2007), (iv) the protection against oxidative stress (Ackerley et al., 2006; Brown et al., 2006; Henne et al., 2009), and (v) the DNA repair systems (Miranda et al., 2005, Chourey et al., 2006). The abilities of microorganisms to survive in presence of chromium and to detoxify chromate require the presence of chromosomal or plasmid encoded genes (Ramirez-Diaz et al., 2008). For example, the chromate efflux system is encoded by the chromium resistance (chr) operon comprising either *chrBAC* (Nies et al., 1990) or *chrBACF* (Branco et al., 2008). The chrA protein belongs to the CHR superfamily of transporters (Diaz-Perez et al., 2007). *ChrA* gene appears to be active in efflux of chromate driven by the membrane potential in a cell (Pimentel et al., 2002). *ChrB* gene encodes a membrane bound protein necessary for the regulation of chromate resistance (Branco et al., 2013). *ChrC* gene encodes a protein

almost similar to iron-containing superoxide dismutase while the *chrE* gene encodes a gene product that is a rhodanese type enzyme and has been detected in *Orthrobacterium tritici* 5bvI1 (Branco et al., 2013). *ChrF* gene encodes a repressor for chromate-dependent induction most probably (Diaz-Perez et al., 2007). *ChrR* catalyzes an initially one-electron shuttle followed by a two-electron transfer to Cr^{6+} (Cheung and Gu, 2007). The *chrB* gene is detected in several microorganisms, such as *Pseudomonas putida*, *Bacillus licheniformis*, *Bacillus cereus*, *Brevibacillus laterosporus*, *Trachelophylum* sp., *Peranema*, and *Adispica* sp. (Kamika et al., 2013). *ChrA1, chrB1* and *chrC* are detected in *Cupriavidus metallidurans* (Juhnke et al., 2002). Also the transfer of chromium resistance determinants are observed between Gram negative and Gram positive bacteria (Abou-Shanab et al., 2007).

Both Gram positive and Gram negative bacteria have developed genetic components that confer resistance mechanisms in presence of nickel (Furuya and Komano, 2003; Rahman et al., 2015b). In bacteria, the *nik* operon comprises of six genes with the first five, *nikABCDE*, encoding components of a typical ATP-dependent transport system (Mulrooney and Hausinger, 2003). NikA characterizes the periplasmic binding protein, *nikB* and *nikC* are similar to integral membrane components of periplasmic permeases, and *nikD* and *nikE* retain typical ATP binding domains that suggest their energy coupling role to the transport process (Navarro et al., 1993). NikR, a protein of the ribbon-helix-helix family of transcription factors, represses expression of the *nikABCDE* operon in the presence of excessive concentrations of intracellular nickel (Chivers and Sauer, 2000).

Aims

The overall aim of my PhD thesis was to develop novel bacterial strains that can remediate toxic metals from the contaminated effluents as well as to develop sustainable and cost effective bioremediation methods for removal of toxic metals and thus protecting human health and environment from these toxic pollutants.

In particular:

Paper I

The main objective of this study was to identify, isolate and characterize novel arsenic resistant bacteria that can be applied for removing arsenic from the contaminated environment to a safe level and thus protecting human health from severe diseases caused by arsenic contamination.

Paper II

The main aim of this study was to identify, isolate and characterize naturally occurring bacterial strain(s) that have potential for reducing chromium concentrations to a safe level in contaminated environments and thus avoiding many lethal diseases caused by chronic chromium poisoning.

Paper III

The main goal of this study was to isolate and study novel nickel resistant bacteria that can be applied for remediation and/or eliminating of nickel from the contaminated industrial effluents and thus avoiding nickel exposure in human and the environment.

Paper IV

The purpose of this study was to investigate the genetic composition of the arsenic resistant bacterium *Lysinibacillus sphaericus* B1-CDA by sequencing of whole genome and annotation of all genes involved in tolerance of this bacterium to arsenic and/or other heavy metals.

Paper V

The aim of this paper was to study the genetic composition of the chromium resistant bacterium *Enterobacter cloacae* B2-DHA by sequencing the whole genome and annotation of all genes involved in tolerance of this bacterium to chromium and/or other heavy metals.

Materials and Methods

Materials

Chemicals used in these studies were analytical standard grade (Merck and Sigma-Aldrich). All solutions were prepared with autoclaved double deionized water (ddH_2O). All the stock solutions were sterilized by syringe filtration (0.2 µm pore-size) and stored at 4°C or -20°C in the dark until further use.

Isolation of strains

For isolation of (i) arsenic resistant bacteria (paper I) the soil samples were collected from a cultivated land in Chuadanga district located in the Southwest region of Bangladesh; (ii) chromium resistant bacteria (paper II) the soil samples were collected from the landfills of leather manufacturing tannery industries located in the Hazaribagh area – a very close vicinity of the capital city Dhaka in Bangladesh; and (iii) nickel resistant bacteria (paper III) the soil samples were collected from near the Bauxite mine at Kolhapur in state of Maharashtra, India. In all cases the samples were collected from the surface at 0-15 cm in depth retained in plastic bags, and kept at 4°C until further uses for either isolation of bacterial, or characterization of the soil.

Metal resistant bacteria were isolated by plating serially diluted soil samples aerobically on the Luria-Bertani (LB) medium supplemented with different concentrations of either arsenic, chromium, or nickel. Following incubation of these plates at 37°C for 48 h, several morphologically different colonies were picked randomly and streak-purified at least twice on the same medium for isolation of the single colonies as described in corresponding papers (papers I, II. and III). The isolated strains were then characterized and identified based on physical, biochemical and 16S rRNA analyses. For each isolate the minimum inhibitory concentrations (MIC) of different metals were determined as described by Mergeay (Mergeay, 1995).

Analyses of metal uptake

The bacterial cultures were prepared for measurement of arsenic and chromium by using Inductively Coupled Plasma-Mass Spectroscopy (ICP-MS) as described previously in papers I and II. Isolates were grown at 37°C in six parallel sets of 50 mL LB broth supplemented with appropriate metals and shaking continuously at 180 rpm. The control samples were treated similarly but without metal exposure. The cell suspensions were centrifuged (10000 rpm for 10 min) and the pellet was washed thrice with deionized

water and dried at 60°C until a constant dry weight was achieved and measured the concentration of metals in cells by using ICP-AES. The concentration of metals was measured in cell free broth by using ICP-MS (Ammann, 2007). As reported in paper III, the bacterial biomass was prepared for measurement of nickel by using anodic stripping voltammetry (ASV: 797 Computrace VA Metrohm, Switzerland). The dead biomass of *Lysinibacillus* sp. BA2 was rolled into beads, which were packed in the glass column to treat effluents having 300 mg/L Ni(II). After every 30 min, eluents were withdrawn to determine residual Ni(II).

TOF-SIMS analysis

In order to verify the intracellular accumulation of metals the bacterial isolates were grown in liquid LB medium supplemented with or without arsenic, or chromium. Cells were collected by centrifugation at 10000 rpm in a micro centrifuge and washed with autoclaved deionised distilled water repeatedly (3-4 times). Cells were then spread out on microscopic slides and analyzed by using a time of flight-secondary ion mass spectrometer (TOF-SIMS) V instrument (ION-TOF, GmbH, Münster, Germany) equipped with a 30 keV Bi_3^+ LMIG analysis gun (Kollmer, 2004; Touboul et al., 2005) with a 512×512 µm raster. Depth profiling of the metal ions inside the cells was performed by using a 0.5 keV Cs^+ sputter gun. Depth profiling and imaging were performed in the burst mode (analyze 30 scans, sputter 0.20 s, pause 6.0 s, to a total of approx. 250 s of sputtering). The Bi3-LMIG was set in the high current bunched mode (negative polarity, analysis area 78×78 µm, mass resolution m/Δm: 6000; focus of the ion beam: 150 nm) with a target current of 0.15 pA while Cs ions were used for sputtering, with a current of 5 nA and with a 250×250 µm raster (Sodhi, 2004). All image analyses were performed using the ION-TOF Surface Lab software (Version 6.1, ION-TOF, GmbH, Münster, Germany) except for image resizing, for publication purposes, which was performed in Adobe Photoshop CS-2 (Adobe Systems Incorporated, San Jose, CA). Each ion image was normalised to the intensity in the brightest pixel.

Genome sequencing

Genomic DNA was extracted from the isolate, *Lysinibacillus sphaericus* B1-CDA using master pure™ Gram positive DNA purification kit (Epicentre, USA) and from the isolate, *E. cloacae* B2-DHA using DNeasy Blood & Tissue Kit (Qiagen, Cat No 69506). The whole genome sequencing of these two strains was performed by Otogenetics Corporation (GA, USA) with the help of HiSeq2500 PE100 read format. Properly paired reads (≥30bp) were extracted from the corrected read pool and the remaining singleton reads

were combined as single-end reads. Both the paired-end and single-end corrected reads were then used in k-mer-based *de novo* assembly employing SOAPDenovo, version 2.04 (Li et al., 2010). The set of scaffolds with largest N50 was identified by evaluating k-mers in the range 29-99. The optimal scaffold sequences were further subjected to gap closing by utilizing the corrected paired-end reads. The resulting scaffolds of length ≥300 bp were chosen as the final assembly. Circular plots of the ordered contigs of B1-CDA and B2-DHA were generated with DNAPlotter (Carver et al., 2009) to predict the graphical map of the genomes.

Gene prediction and annotation of metal resistant genes

The assembled genome sequences were annotated with Rapid Annotations using Subsystems Technology, RAST (Aziz et al., 2008). The RAST analysis pipeline uses the tRNAscan-SE and the GLIMMER algorithm to predict tRNA genes (Lowe and Eddy, 1997) and protein-coding genes (Salzberg et al., 1998), respectively. In addition, an internal script was used for identification of rRNA genes (Aziz et al., 2008). It then infers with putative function(s) of the protein coding genes based on homology to already known protein families in phylogenetic neighbor species. Finally, RAST identifies subsystems represented in the genome, and uses this information to reconstruct the metabolic networks. The GeneMark (Borodovsky et al., 1993) and the FGenesB (Salamov and Solovyev, 2000) algorithms were applied for verification of the RAST results obtained in prediction of protein coding genes. Prediction of rRNA genes was also performed through the RNAmmer prediction server version 1.2. (Lagesen et al., 2007). Annotation of all genes that were predicted to be metal responsive was manually curated with a particular focus on genes responsive to As, Co, Cd, Cr, Ni and Pb. Functional annotation analyses were also carried out by the Blast2GO pipeline (Götz et al., 2008) using all translated protein coding sequences resulting from the GeneMark and/or FgeneB. In Blast2GO the BlastX option was chosen to find the closest homologs in the non-redundant protein databases (nr), followed by employing Gene Ontology (GO) annotation terms (Ashburner et al., 2000) to each gene based on the annotation of its closest homologs. An InterPro scan (Zdobnov and Apweiler, 2001) was then performed through the Blast2GO interface and the InterPro IDs merged with the Blast-derived GO-annotation for obtaining integrated annotation results. The GO annotation of all putative metal responsive genes was manually curated.

Transformation of *ars* genes

The *in silico* results were verified by the *in vitro* laboratory experiments using the mutant strains of *E. coli* carrying deletions of *ars* genes. Two types of mutant strains were used in these experiments: (i) JW3469-1 with deletion of *arsB* and (ii) JW3470-1 with deletion of *arsC* (Baba et al., 2006). RT-PCR was performed to verify whether these strains are indeed knockout mutants with *arsB* and *arsC* genes following the reaction protocol of MasterAmp™ High fidelity RT –PCR kit (Epicentre, USA). Preparation of competent cells of these strains and plasmid transformations were performed as described previously by (Tu et al., 2005). The purified cDNA product obtained from the RT-PCR of B1-CDA strain was ligated into a commercial cloning vector *pGEMT* obtained from Promega. An overnight ligation reaction was set up using ligase enzyme, ligase buffer, cloning vector and PCR product taken in the ratio of (1:3). All the transformed reaction mixtures were plated on LB ampicillin plates at a concentration of 100 µg/ml and incubated overnight at 37°C. Vector-mediated transformation of the genes to the corresponding mutants was confirmed by colony PCR followed by gene sequencing. The sequencing assays were performed with one ABI 3730 instrument (Applied Biosystems) and Big Dye terminator v3.1 Cycle sequencing kit. The purification of the sequencing reactions was performed by Big Dye X terminator purification kit obtained from Applied Biosystems by Life technologies, USA). The expression of *arsB* and *arsC* genes were verified in transgenic *E. coli* strains by performing RT-PCR with the same protocol.

Scanning electron microscopic (SEM) studies

Morphological analysis of all the strains (papers I, II and III) was carried out using the scanning electron microscope (SEM) with an attached X-ray energy dispersive system (EDS). The strains grown in the presence, or absence of either arsenic, chromium, or nickel, were studied under scanning electron microscope (SEM). The bacterial isolates were grown in a nutrient broth at 37°C by shaking on rotary shaker for 48 h. Pellet obtained by centrifugation was first washed twice with sterile deionized water and then twice with Phosphate Buffered Saline (PBS). The cells were chemically fixed at 4°C for 18 h with 1:2 glutaraldehyde: formaldehyde in 1 mL PBS in dark conditions. Dehydration of pellet was carried out by alcohol treatment for 5 min. 10 µL of samples were placed on 1 mm X 1 mm slide. Each slide was transferred to desiccator for moisture absorption. Samples processed were used for SEM-EDS analysis as described in corresponding papers I, II and III.

Statistical analyses

All statistical analyses were performed using standard statistical package Microcal (TM) Origin 6.0 version (http://www.microcal.com/). Parameters one- and two-factor variance analyses were performed using the independent system. The zero or alternative hypotheses were accepted on the basis of the F test at p=0.05 or p=0.01 and marked as */ or **/, respectively. The significance of differentiation in mean values for individual properties was checked using the least significant difference (LSD) test. All analyses were performed in triplicate and the results are presented as mean value with standard deviation.

Results and discussion

Paper I

An arsenic resistant Gram positive bacterium *Lysinibacillus sphaericus* B1-CDA [NCBI database; accession number KF961041] was isolated from the arsenic contaminated cultivated land in the area of Chuadanga district located in the Southwest region of Bangladesh. The minimum inhibitory concentration (MIC) value of the isolate was 500 mM for sodium arsenate ($Na_2HAsO_4.7H_2O$). MIC values of this strain for other toxic pollutants/metals were 6 mM for K_2CrO_4, 5 mM for $FeCl_3$, 3 mM for $MnCl_2$, 2 mM for $ZnCl_2$, 1.5 mM for $NiCl_2$ and 0.3 mM for $AgNO_3$.

Ion imaging of B1-CDA cells, exposed to arsenate, by TOF-SIMS, confirmed accumulation of different species of arsenic in the cells including free form of arsenic (As), meta-arsenite (AsO_2^-), ortho-arsenite (AsO_3^{3-}) and arsenate ($AsO_4H_2^-$). In addition, these cells accumulated arsenite rather than arsenate (Figure 4). Thus, it begs the question, - where did the arsenite come from? In bacterial cells, the As (V) enters inside the cell via phosphate transport systems and it is converted to As (III) by cytoplasmic arsenate reductase (Achour et al., 2007). Similar arsenate reduction has been reported in both prokaryotes such as *Escherichia coli* (DeMel et al., 2004) and eukaryotes such as *Saccharomyces cerevisiae* (Mukhopadhyay et al., 2000) and *Arabidopsis thaliana* (Dhankher et al., 2006; Nahar et al., 2012). These organisms contain arsenic reductase genes (*ACR2*) encoding enzymes required for reduction of arsenate to arsenite within the cell. As the redox reactions are energy giving, reduction of arsenate to arsenite in the cells will produce more energy (Muller et al., 2007). For many bacterial strains the redox energy is essential for their survival under stressful conditions (Anderson and Cook, 2004). The depth profiling revealed distribution of arsenic ions inside of the bacterial cells and further confirmed the results obtained from the ion imaging.

Inductively coupled plasma-mass spectrometry (ICP-MS) analyses revealed 5.0 mg arsenic/g dwt. of bacterial biomass of B1-CDA, when exposed to 50 mM arsenate for 120 h, whereas in the cell free growth medium the arsenic content decreased by 50% (from 50 mM to 25 mM). In control samples (medium not exposed to B1-CDA), any temporal change in the concentration of arsenic was not observed. These results directly suggest that the reduction of arsenic concentration observed in growth medium containing B1-CDA cells was indeed due to the biological activity of this bacterium.

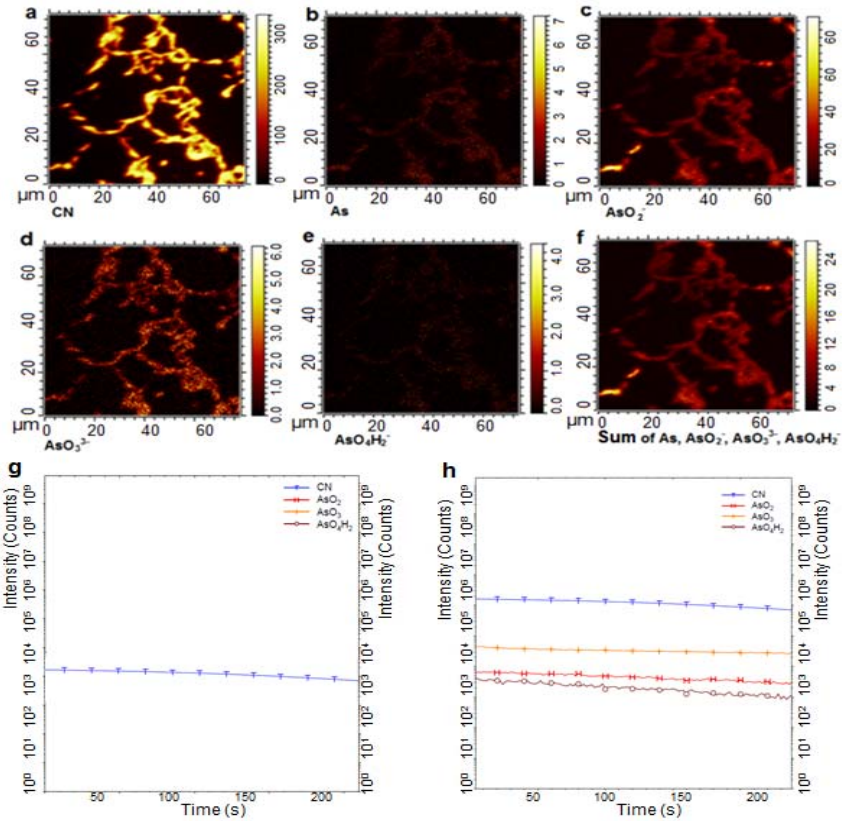

Figure 4. TOF-SMS analysis of arsenic species inside the bacterial cells. a-f, ion imaging. g-h, depth profiling. For TOF-SIMS the bacterial cells were grown overnight in medium containing 50 mM arsenate. The field view of TOF-SIMS was 78×78 μm. All ion images were obtained in high current bunched mode of TOF-SIMS and presented in intensity/unit, whereas depth profiling was performed by using non-interlaced mode of TOF-SIMS and presented in counts/second. a, total protein signals. b, free form of arsenic. c, meta- arsenite ions (AsO_2^-) signal. d, ortho- arsenite ion AsO_3^{3-} signal. e, arsenate (AsO_4H_2) ion signal and f, sum of different types of arsenic. The colored bar represents the intensity of ion imaging. The lower the count, the lower is the intensity. g, depth profiling of bacterial cells grown on medium without arsenate (control). Blue color represents protein signals, whereas dark brown color stands for background activity of arsenic. h, depth profiling of bacterial cells grown on medium containing 50 mM arsenate. Blue color represents protein signals, whereas orange, red and dark brown colors represent meta-arsenite, ortho-arsenite and arsenate, respectively.

"Reconstructed field water" (RFW) was prepared in the laboratory to determine if the B1-CDA strain can reduce and accumulate arsenic in natural conditions. The RFW treated with B1-CDA for 12- h followed by ICP-MS analysis indicated a decline of arsenic by 40% (50 mM to 30 mM) compared to that of 16% (50 mM to 42 mM) reduction in control RFW without treatment with B1-CDA, These results confirm that (i) B1-CDA can decrease arsenic concentration in the RFW, and (ii) the RFW contained other arsenic-accumulating microorganisms derived from the soils collected from the cultivated fields. The results obtained in the experiments with the RFW were a bit different from those obtained with LB medium. Obviously, under natural conditions the biological activity of B1-CDA may vary significantly depending on many environmental factors such as physical and nutritional conditions for bacterial growth, interaction with other microbes existing in nature, and presence of other chemical substances in soils that may interact with arsenic uptake (Chibuike and Obiora 2014; Rahman et al., 2014). In the RFW experiment it was not possible to maintain the physical conditions for the natural growth of the bacteria such as fluctuation in temperature, pH, nutrients and light intensity.

Results from scanning electron microscope (SEM) indicated that B1-CDA formed long chain structures in the presence of arsenic compared to the untreated cells. The long chain like structure of the strain represents mode of response to arsenic stress. The SEM results in presence of arsenic have clearly shown that the elongation of cells and cell aggregation due to arsenic stress (Vijayakumar et al., 2011). In growing cells, biofilm formation or aggregation is a common phenomenon under stress conditions; however, this is unusual for non-growing live cells.

Paper II

A chromium resistant Gram negative bacterium *Enterobacter cloacae* B2-DHA [NCBI database; accession number KF920746] was isolated from the landfills of tannery effluents discharged from leather manufacturing industries located in the Hazaribagh area - a very close vicinity of the capital city Dhaka in Bangladesh. The minimum inhibitory concentration (MIC) value of the isolate was 1000 mg/L potassium chromate (K_2CrO_4) as well as the MIC of this strain was found to be 15 g/L for $Na_2HAsO_4.7H_2O$; 500 mg/L for $FeCl_3$; 400 mg/L for $MnCl_2$; 350 mg/L for $ZnCl_2$; 260 mg/L for $NiCl_2$ and 85 mg/L for $AgNO_3$.

Ion imaging analyses (TOF-SIMS) were performed to verify the presence of chromium inside the cells or absorption to the outside. The TOF-SIMS

analyses confirmed that B2-DHA cells, when exposed to chromium, accumulated the different forms of chromium including chromium oxide (CrO^-) and chromium dioxide (CrO_2^-) inside the cells. In addition, the total protein signals in the cells were also detected by TOF-SIMS. The depth profiling analysis by TOF-SIMS was performed up to 1250 seconds to further confirm the distribution of chromium ions inside the cells. The results demonstrated that the intensity counts for monoxide chromium ions (CrO^-) and dioxide chromium ions (CrO_2^-) were approximately $10^{3.5}$ and $10^{2.8}$, respectively. In the control sample the intensity counts of signal protein were much higher than those observed in samples exposed to chromium. Hence, TOF-SIMS experiment provided both ion images as well as chemical information on the distribution of chromium ions on the outside surface and inside of the bacterial cells.

Inductively coupled plasma mass spectroscopy (ICP -MS) was performed in order to further confirm whether the B2-DHA strain could indeed accumulate chromium inside the cells. This analysis revealed that 320 µg chromium/g dwt of bacterial biomass was accumulated inside the bacterial cells after 120 h of exposure to 100 µg/mL chromium (Figure 5a). The reduction of chromium in liquid growth medium was verified by inductively coupled plasma atomic emission spectroscopy (ICP-AES). This analysis showed that the chromium concentration in the cell free growth medium, after 120 h exposure to B2-DHA, decreased by 81% (from 100 µg/mL to 19 µg/mL) (Figure 5b). Resistance to high concentration of Cr(VI) and high ability for reduction of this toxic metal made this strain a suitable candidate for bioremediation.

Morphological changes of bacteria cultured in the presence (100 µg/mL) or absence (control) of chromium were investigated using an environmental scanning electron microscope (ESEM) with an attached X-ray energy dispersive system (EDS). ESEM-EDS study exhibited a typical cocci shape morphology for B2-DHA control bacteria compared to that of a long chain like formation in chromium-treated bacteria. This is perhaps, a mode of response to metal stress indicating that this strain could accumulate chromium. Furthermore, the ESEM-EDS of the cells grown in presence of chromium revealed that elongation and aggregation of the cells due to the metal stress support the membrane transport process previously reported by Vijayakumar et al. (2011). Rahman et al. (2014) observed a significant elongation of *Lysinibacillus sphaericus* cells when exposed to arsenate, which is consistent with the findings by several other researchers (Nepple et al., 1999; Banerjee et al., 2011; Desale et al., 2014) who reported a similar morphological elongation of bacterial cells exposed to toxic heavy metals including nickel.

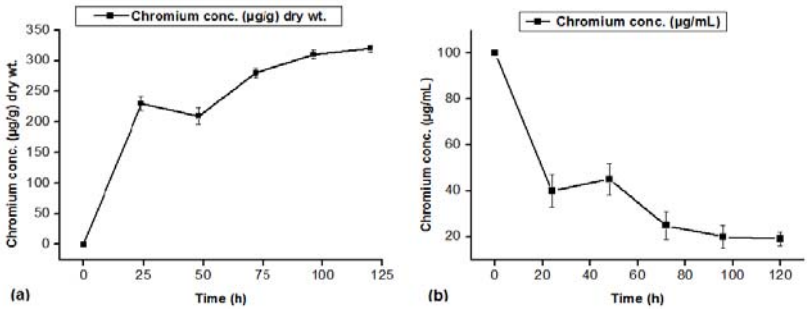

Figure 5. ICP –MS/ICP–AES estimation of Cr(VI) concentration. a, amount of chromium absorbed by the bacterial cells. Error bars denote standard error of mean.*P≤0.05 (one-tailed t-test), significant. b, reduction of chromium by *Enterobacter* sp. B2-DHA in growth medium. Error bars denote standard error of mean. **P≤0.01 (one-tailed t-test), significant.

Paper III

A nickel resistant bacterium was isolated from the Bauxite mine area near Kolhapur in state of Maharashtra, India. Identification of the nickel tolerant isolate was carried out using conventional biochemical tests and by 16S rRNA gene sequence. The isolate showed closest identity (98 percent) with the genus *Lysinibacillus*. Based on biochemical and molecular characteristics, isolate BA2 was identified as *Lysinibacillus* sp. and hereafter is referred as *Lysinibacillus* sp. BA2. *Lysinibacillus* sp. BA2 grows in presence of 9 mM $NiCl_2$.6H2O indicating its tolerance towards nickel. The adsorption of Ni(II) on *Lysinibacillus* sp. BA2 was constant from pH 7.0 to 9.0 due to the precipitation of Ni(II) as nickel hydroxides. The maximum adsorption of Ni(II) ions in the biomass was observed at pH 6.0. Hence other biosorption experiments were performed at this pH. Maximum adsorption of nickel on rubber– wood ash was reported earlier at pH 5.2 (Hasan et al., 2000).

Adsorption of Ni(II) on biomass increased with time and attained saturation after 180 min with rapid biosorption in initial 30 min (Figure 6). The decrease in Ni(II) concentration in aqueous solution was rapid during the first 30 min suggesting that biosorption is a spontaneous process (Chang et al.,1997; Yuan et al., 2009). Several other studies also demonstrated that maximum biosorption was achieved in 30 min (Gabr et al., 2008). The adsorption capacity of dead biomass was higher than that of live biomass due to the surface properties and affinity of adsorbent for adsorbate. Thus, dead

biomass was preferred over live biomass for adsorption of nickel from industrial effluents. The maximum adsorption values obtained were 238.04 mg of Ni(II) per gram of dead biomass and 196.32 mg of Ni(II) per gram of live biomass at the highest initial concentration of Ni(II) tested. The higher adsorption of Ni(II) ions on the dead biomass could be due to larger surface area and several exchangeable binding groups whereas live biomass has smaller surface area giving fewer binding groups on the cell surface (Volesky and May-Phillips, 1995; Salvadori et al., 2013). In both cases, metal binding is independent of the microbial metabolism and depends primarily on the architecture and the chemical composition of microbial cell wall. The metal binding increases based on availabilities of free binding sites and is expected to attain a point where no additional metal can bind on the biomass surface.

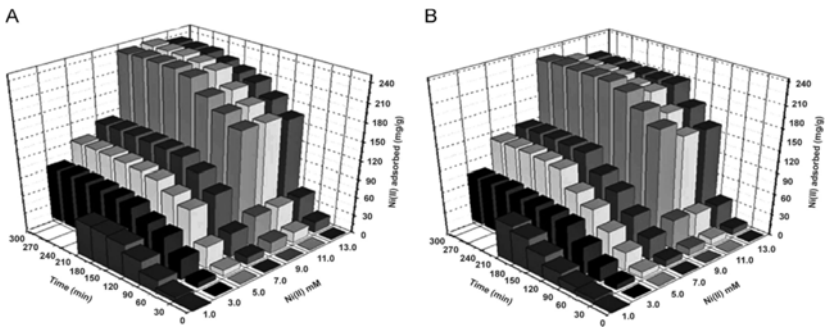

Figure 6. Effect of contact time and initial metal concentrations on biosorption of Ni(II) by the dead biomass (A) and live biomass (B) of *Lysinibacillus* sp. BA2. Biosorption conditions: biomass 1g/L, pH 6.0, and temperature 37°C (Error bar represent means ± SE, $p<0.05$, and N=3).

SEM-EDX analysis for live biomass in presence and absence of Ni(II) confirmed the presence of nickel ions on the live biomass. SEM micrographs recorded the morphological changes before and after biosorption of Ni(II) by live biomass. Cell aggregation and surface modification besides increasing irregularity of cell morphology took place in case of cells suspended in nickel solution (Desale et al., 2014). The EDX spectrum recorded in the examined region of the live biomass confirmed the presence of Ni(II) ions on cell surface. The SEM-EDX of the live biomass also revealed the fact that cells aggregated due to metal stress to support the membrane transport process (Vijayakumar et al., 2011). In growing cells, biofilm formation or aggregation is a common phenomenon under stress conditions; however, this is unusual for non-growing live cells. The FTIR analysis of biomass revealed the presence of carboxyl, hydroxyl and amino groups, which seem responsible for biosorption of Ni(II).

Paper IV

In this study, whole genome sequencing of the arsenic resistant strain *Lysinibacillus sphaericus* B1-CDA was performed by the Illumina sequencer using HiSeq2500 PE100 read format. A total of 11,105,899 pairs of reads was generated by Illumina deep sequencing. Analysis of the raw reads with FastQC showed that the average per base Phred score was ≥32 for all positions and that the mean per sequence Phred score was 38. The overall GC content was 38%. After removal of the TruSeq adaptor sequence (which was found in 13,435 reads, 0.12%) and error correction trimming was done by using the Quake software, 10,940,654 read pairs (98.5%) and 145,888 single end sequences remained for further analysis. Trimming of sequences was performed as part of an important step for improving mapping efficiency. SOAPDenovo was utilized to perform *de novo* assembly optimization with the error corrected reads. The set of scaffold sequences with maximal N50 (507,225 bp) was produced at k-mer 91. The corresponding scaffold sequences were subjected to gap closure using the corrected paired-end reads and the resulting set of scaffolds (≥300 bp) was defined as the final assembly. The final assembly consisted of 31 scaffolds ranging from 314 bp to 1,145,744 bp, resulting a total length of 4,509,276 bp. It contained only 25 bp of unknown nucleotides, i.e. the error rate was less than 1 in 1,000,000.

Rapid annotations using subsystems technology (RAST) server was employed to predict tRNA-, rRNA- and protein coding genes. The search by tRNAscan-SE located 77 tRNA genes in B1-CDA. In an ARAGORN scan, the total number of predicted tRNA genes in B1-CDA was found to be 77, which was similar to that predicted previously in the genome of *L. sphaericus* C3-41 (Hu et al., 2008). The rRNA prediction in RAST revealed 11 rRNA genes, including seven 5S, one 16S and three 23S genes. Due to the surprisingly low number of 16S and 23S genes, RNAmmer scans were performed on the genomes of *L. sphaericus* B1-CDA as well as two other unrelated bacteria (*Enterobacter cloacae* and *Salmonella bongori*). These results confirmed that the *L. sphaericus* B1-CDA genome seems to contain approximately the same number of 5S rRNA genes as the other bacteria do, but substantially fewer 16S and 23S rRNA genes. Previously, Pei et al. (2010) have reported 143 bacterial species containing only a single 16S rRNA, whereas Pei et al. (2009) have shown 184 genomes that had a median of 4.57 23S rRNA genes/ genome (range 1 to 15). Therefore, the lower number of 16S- and 23S rRNA as revealed in this study is not an uncommon feature of bacterial genome.

For prediction of the protein coding genes, RAST uses the GLIMMER algorithm (Salzberg et al., 1998). A total of 4513 protein coding genes were

predicted using GLIMMER algorithm, of which 2671 could be annotated by RAST's automated homology analysis procedure and assigned to functional categories. For confirmation of the number of protein coding genes, the GeneMark and FGenesB algorithms were also applied, yielding 4562 and 4323 genes, respectively. The graphical map of the genome and the locations of all predicted genes are shown in the circular genome plot in Figure 7. It was observed that *L. sphaericus* B1-CDA contains many predicted metal resistant genes, such as those confirming resistance to arsenic, nickel, cobalt, iron, manganese, chromium, cadmium, lead and zinc. The functional annotation carried out by the Blast2GO pipeline also indicated that B1-CDA contains many genes which are responsive to metal ions like arsenic, cobalt, copper, iron, nickel, potassium, manganese and zinc. The annotations by RAST and Blast2GO were found to be in agreement (Table 1).

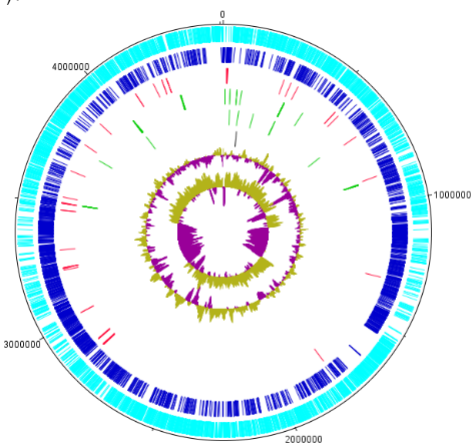

Figure 7. Circular plot of ordered contigs, generated with DNAPlotter. Tracks indicate (from outside inwards) predicted protein coding genes on forward strand (light blue) and reverse strand (dark blue), metalloproetin genes (red) listed in Table 1, tRNA and rRNA genes (both green), origin of replication (black), GC content and GC skew.

The arsenic responsive genes of B1-CDA genome were compared with the genomes of validly named and sequenced species of *Lysinobacter* as well as with other closely related arsenic resistant species by using InterPro (Zdobnov and Apweiler, 2001). There were seven genes of B1-CDA that showed very high similarity with the genes of other *Lysinibacillus* species. The minimum identity level (97%) was observed in the *arsC* gene (arsenic reductase) of *Lysinibacillus fusiformis,* whereas the highest similarity (100%) was observed in the *arsC* gene (arsenate reductase regulatory protein Spx) of *Lysinibacillus sphaericus* C3-41.

Table 1. Metal responsive genes in B1-CDA predicted by RAST and/or Blast2GO.

			Predicted by	
Start (bp)	**End (bp)**	**Predicted function**	**RAST**	**Blast2GO**
16367	18778	Copper ion binding		X
18860	19066	Copper ion transport		X
20450	19497	Cobalt-zinc-cadmium resistance protein CzcD	X	X
20471	20806	Transcriptional regulator, ArsR family	X	
275573	277477	Lead, cadmium, zinc and mercury transporting ATPase	X	X
308097	309131	Toxic anion resistance protein TelA	X	X
342234	343136	Cobalt-zinc-cadmium resistance protein	X	X
539475	540170	Zinc transporter family protein		X
540161	539475	Zinc transporter, ZIP family	X	
562002	562358	Arsenate reductase	X	X
681412	680306	Ferric iron ABC transporter, iron-binding protein	X	
876386	877651	Manganese transport protein MntH	X	X
1328650	1329048	Arsenate reductase family protein	X	X
2839200	2840816	Periplasmic nickel-binding protein NikA	X	
2839200	2840816	Nickel cation transport activity		X
2840888	2841841	Nickel transport system permease protein NikB	X	
2841844	2842653	Nickel transport system permease protein NikC	X	X
2842667	2843437	Nickel transport ATP-binding protein NikD	X	X
2843447	2844253	Nickel transport ATP-binding protein NikE	X	X
2873332	2873748	Arsenate reductase	X	X
2873761	2874819	Arsenical resistance protein ACR3	X	
2873761	2874819	Arsenic resistance protein		X
2875138	2874812	Arsenical resistance operon repressor	X	
3011790	3010906	Cobalt-zinc-cadmium resistance protein	X	
3010906	3011790	Cation transmembrane transporter activity		X
3211275	3211961	Transcriptional regulator, ArsR family	X	
3221732	3220863	Manganese transporter protein SitD	X	
3220863	3221732	Iron ABC transporter		X
3222601	3221729	Manganese transporter protein SitC	X	
3223341	3222613	Manganese ABC transporter, ATP-binding protein SitB	X	X
3224265	3223351	Manganese ABC transporter protein SitA	X	X
3301684	3300737	Zinc metallohydrolase, metallo-beta-lactamase family	X	
3480453	3479848	Manganese superoxide dismutase	X	
3510620	3510192	Zinc uptake regulation protein ZUR	X	
3510192	3510620	Iron family transcriptional regulator		X
3511480	3510617	Zinc ABC transporter protein ZnuB	X	X
3512240	3511494	Zinc ABC transporter, ATP-binding protein ZnuC	X	X
3537560	3536520	Zinc ABC transporter protein ZnuA	X	X
3655964	3655515	Universal stress protein family	X	X
3784105	3784524	Universal stress protein family	X	X
3898460	3899425	Magnesium and cobalt transport protein CorA	X	X
4106518	4105568	Ferrichrome-binding periplasmic protein precursor	X	
4105568	4106518	Ferrichrome ABC transporter substrate binding protein		X
4193280	4194575	Arsenic efflux pump protein	X	X
4233352	4234161	Zinc transporter		X
4254132	4254503	Cadmium efflux system accessory protein	X	
4254484	4256607	Lead, cadmium, zinc and mercury transporting ATPase	X	
4254484	4256607	Cadmium transporter		X

Paper V

In this study I report the entire genetic composition of the bacterium *Enterobacter cloacae* B2-DHA by massive parallel sequencing accomplished with the Illumina HiSeq2500. Illumina deep sequencing analysis revealed a total of 1,756,877,072 bases containing 16,574,312 pairs of reads with an overall GC content of 55% in the genome. After quality trimming error correction followed by removal of the TruSeq adaptor sequence 15,708,650 read pairs (94.78%) and 331,106 single end sequences remained for further analysis. Analysis of the raw reads with FastQC showed that the mean score per base Phred and per sequence Phred was ≥36 and 36, respectively for all positions. The set of scaffold sequences with maximal N50 (492,970 bp) was detected at k-mer 97. The final assembly of 4,218,945 bp was comprised of 13 scaffolds ranging from 72,208 to 777,700 bp.

The goal of gene prediction was to catalogue all the genes encoded within the *E. cloacae* genome to help us to better understand the mechanisms involved in becoming resistant to chromium and other toxic metals. RAST analysis using the GLIMMER algorithm (Salzberg et al., 1998) predicted a total of 3958 protein coding genes of which 3401 could be annotated by RAST's automated homology analysis procedure and assigned to functional categories. For confirmation of the number of protein coding genes, the FGenesB (Salamov and Solovyev, 2000) and the GeneMark (Borodovsky and McIninch, 1993) algorithms were also applied, yielding 3955 and 3764 genes, respectively. It is observed that the strain B2-DHA contains a large number of genes involved in the ion binding, transport, catabolism and efflux of inorganic as well as organic compounds. More specifically, B2-DHA strain contains many predicted specific toxic metal resistant genes, such as arsenic, chromium, cadmium, cobalt, lead and nickel (Table 2) predicted by RAST and/or Blast2GO.

RAST and/or Blast2GO predicted that B2-DHA strain possess many trace elements (manganese, molybdenum and tellurite) binding and/or transporter proteins and several calcium, copper, iron, magnesium, potassium, sodium, and zinc ion binding/transport proteins as well as a total of 104 proteins involved in binding and transport of metal ions (data not shown). Also many other proteins that catalyze binding and transport of the metal ions such as metalloendopeptidase, metalloexopeptidase, metallopeptidase, metallocarboxypeptidase, metalloproteinase, metalloprotease and metallochaperone are present in B2-DHA.

Table 2. Heavy metals responsive proteins in B2-DHA predicted by RAST and/or Blast2GO

			Predicted by	
Start (bp)	**End (bp)**	**Predicted function**	**RAST**	**Blast2GO**
36960	37526	Chromate reductase	X	X
242454	243404	Magnesium and cobalt transport protein CorA	X	X
495488	496147	ArsR family	X	
615926	616912	Cobalt, zinc, magnesium ion binding		X
964298	965137	Nickel, Cobalt cation transporter activity		X
997848	1000430	Copper, lead, cadmium, zinc, mercury transporter	X	X
1100748	1099984	Ferric enterobactin transport protein FepC	X	X
1101770	1100781	Ferric enterobactin transport protein FepG	X	X
1102774	1101770	Ferric enterobactin transport protein FepD	X	X
1105147	1104188	Ferric enterobactin transport protein FepB	X	X
1251060	1252157	Chromate reductase	X	X
1510555	1509272	Ferrous iron transport peroxidase EfeB	X	X
1511686	1510559	Ferrous iron transport periplasmic protein EfeO,	X	
1512560	1511727	Ferrous iron transport permease EfeU	X	X
1703726	1704046	Arsenite resistance operon repressor	X	X
1704087	1705376	Arsenite efflux pump protein	X	X
1705389	1705820	Arsenate reductase	X	X
1834407	1835345	Cobalt-cadmium resistance, Zinc transporter ZitB	X	X
1919484	1921043	Magnesium and cobalt efflux protein CorC	X	
2058555	2059283	Ferric siderophore transport protein TonB	X	
2216754	2216455	Transcriptional regulator, ArsR family	X	
2304506	2303766	Cobalt-zinc-cadmium resistance	X	
2591739	2592824	Cobalt-zinc-cadmium resistance	X	
2592824	2595886	Cobalt-zinc-cadmium resistance protein CzcA	X	
2735411	2736391	Nickel, Cobalt cation transporter activity		X
2810083	2809727	Arsenate reductase	X	X
3168971	3169588	Nickel cation binding		X
3169598	3170242	Nickel cation binding		X
3170821	3171285	Nickel cation binding		X
3171295	3172998	Nickel cation binding		X
3173316	3173618	Nickel cation binding		X
3173629	3174456	Nickel cation binding		X
3170811	3170272	Transport of Nickel and Cobalt	X	
3500732	3499869	Nickel incorporation-associated protein HypB	X	X
3505195	3506904	Nickel cation binding		X
3501086	3500736	Nickel incorporation protein HypA	X	X
3516192	3517214	Nickel/cobalt transporter	X	X
3892272	3892499	Ferrous iron transport protein A	X	X
3892530	3894848	Ferrous iron transport protein B	X	
3951655	3953826	Copper, lead, cadmium, zinc, mercury transporter	X	X
4172744	4173628	Cobalt-zinc-cadmium resistance protein	X	X
4176907	4178211	Arsenic efflux pump protein	X	

This strain owns some metallocenter assembly protein such as HypA, HypB, HypC, HypD, HypE and HypF (data not shown). In addition, B2-DHA strain harbors several polymyxin resistance proteins (PmrM, PmrL, PmrJ and ArnC), multidrug transporter proteins (MdtA, MdtB, MdtC and MdtD), multiple antibiotic resistance proteins (MarA, MarB, MarC and MarR) as well as universal stress proteins (A, B, C, E and G) predicted by RAST and Blast2GO (Table 3).

Table 3. Universal stress proteins, multiple antibiotic resistant proteins, multidrug resistance proteins and polymyxin resistance protein in B2-DHA predicted by RAST and/or Blast2GO

Seq. Name	Start	End	Predicted function
Gene- 1057	1135310	1134879	Universal stress protein G
Gene- 1121	1198337	1199287	Universal stress protein E
Gene- 2184	2325505	2324840	Multiple antibiotic resistance protein MarC
Gene- 2185	2325818	2326195	Multiple antibiotic resistance protein MarR
Gene- 2186	2326216	2326596	Multiple antibiotic resistance protein MarA
Gene- 2187	2326629	2326844	Multiple antibiotic resistance protein MarB
Gene- 2364	2487111	2487539	Universal stress protein C
Gene- 2463	2591265	2590834	Universal stress protein G
Gene- 2531	2669613	2672735	Multidrug resistance MdtB
Gene- 2533	2672736	2675813	Multidrug resistance MdtC
Gene- 2534	2675814	2677229	Multidrug resistance MdtD
Gene- 3334	3544616	3543069	Multidrug resistance MdtB
Gene- 3335	3545805	3544633	Multidrug resistance MdtA
Gene- 3746	3974324	3973941	Polymyxin resistance protein PmrM
Gene- 3747	3974644	3974321	Polymyxin resistance protein PmrL,
Gene- 3749	3977186	3976284	Polymyxin resistance protein PmrJ
Gene- 3751	3980145	3979162	Polymyxin resistance protein ArnC
Gene- 3760	3989137	3988850	Universal stress protein B
Gene- 3761	3989469	3989906	Universal stress protein A

Among several means to protect themselves from adverse environmental stimuli, including exposure to stress factor, cationic antimicrobial peptides, and toxic metals (Olaitan et al., 2014), bacteria has evolved various strategies containing alterations of their lipopolysaccharides (LPSs) in their cell walls. Other strategies comprise the employment of an efflux pump and capsule formation. Thus, the strain B2-DHA, isolated from a highly chromium contaminated tannery industries areas, might have developed similar mechanisms to survive in adverse conditions.

The presence of chromium reductase genes was verified by laboratory based PCR amplification and found B2-DHA strain to harbor *chrR* and *chrA* chromium marker genes. The chrA protein appears to be active in efflux of chromate driven by the membrane potential (Pimentel et al., 2002). The ChrR catalyzes an initially one-electron shuttle followed by a two-electron transfer to Cr^{6+} with the formation of intermediate(s) Cr^{5+} and/or Cr^{4+}before further reduction to Cr^{3+} (Cheung and Gu, 2007), a critical process involved in detoxification of chromium. Therefore, these genetic mechanisms of the isolate could be used to cope with chromium toxicity.

Manuscript in preparation

Expression of *arsB* and *arsC* genes

RT-PCR was performed to see the expression of *ars* genes in bacterial strains. The expression of *arsB* and *arsC* gene in knockout *E. coli* was not observed. The presence of *arsB* and *arsC* genes was confirmed in transgenic *E. coli JW3469-1* and *E. coli JW3470-1* by RT-PCR (data not shown). Gene expression analysis of *arsB* and *arsC* genes showed that the genes are active when exposed to arsenic. The *arsB* and *arsC* genes in transgenic *E. coli JW3469-1 and E. coli JW3470-1* were sequenced and the results were compared with the original sequence of *arsB* and *arsC* by using Blastn tool from NCBI server. Blastn sequence alignment indicated 99% sequence similarity between the clone and the original sequence of *arsB* and *arsC*. These results confirmed that the cloning was successful.

Arsenic resistance analysis

The cells of mutant and transgenic *E. coli* JW3469-1 and/or *E. coli* JW3470-1 strains were grown in LB medium containing 50 mM sodium arsenate over a range of time intervals (24 hrs to 96 hrs). The growth was measured by optical density at 600 nm. Between the mutant and the transgenic strains there was a significant difference in the growth rate of the bacterial cells when grown in the presence of arsenics (data not shown). This difference in the growth rate could be explained due to the presence of *arsB* and/or *arsC* genes in transgenic strains and the lack of these genes in mutant strains. Similar results were reported in bacterial strains deficient in *arsB* gene (Shen et al., 2013) and *arsC* gene (Pandey et al., 2012). From these results, it is evident that the cloning of *arsB* and/or *arsC* gene into transgenic strain was successful and presence of *arsB* and/or *arsC* gene in a bacterial strain renders the organisms tolerance to arsenics (Srivastava et al., 2009; Liao et al., 2011; Sarkar et al., 2012; Sousa et al., 2015).

Analysis of arsenic accumulation

The ICP-MS analysis of arsenic accumulation by mutant and transgenic *E. coli* JW3469-1 and/or *E. coli* JW3470-1 was performed to confirm whether the strains could reduce arsenic content in the LB medium containing 50 mM arsenate. ICP-MS results suggested that the transgenic strain JW3470-1 accumulated higher levels of arsenic from the broth compared to the mutant strain. The maximum difference in accumulation of arsenic was observed at 72 hrs. The transgenic strain JW3470-1 was able to reduce the

arsenic content in the medium from 50 mM to 37 mM. This was due to complementation of *arsC* gene in the transgenic strain. However, the ICP-MS results suggest only a minimal difference in the concentration of arsenic between transgenic and mutant *E. coli JW3469-1*. This is because of arsB is an integral membrane protein that pumps arsenite out of the cell.

Conclusions

Paper I

The results obtained from this study confirm that an arsenic resistant soil borne bacterium, *Lysinibacillus sphaericus* B1-CDA, can grow in presence of 500 mM sodium arsenate. Inductively coupled plasma-mass spectroscopy (ICP-MS) analyses revealed that after 120 h of exposure, the intracellular accumulation of arsenic in B1-CDA was 5.0 mg/g dwt of cell biomass while the arsenic content in the liquid culture medium was reduced to 50%. Hence, the strain has potential for reducing arsenic in the contaminated sources to safe levels. Besides human arsenic poisoning, this discovery will benefit livestock and native animal species. Therefore, the outcome of this research will be vital not only for people, livestock and native animal species in the affected area but also in other countries, which have credible health concerns as a consequence of arsenic-contaminated water and foods.

Paper II

This paper has reported the strain *Enterobacter cloacae* B2-DHA isolated from a landfill containing effluents disposed from leather manufacturing tannery industries. The minimum inhibitory concentration (MIC) values of this isolate is 5.5 mM potassium chromate. Inductively coupled plasma-mass spectroscopy (ICP-MS) analyses revealed that after 120 h of exposure, the intracellular accumulation of chromium in B2-DHA was 320 µg/g dwt of cell biomass while the chromium content in the liquid culture medium was reduced to 81%. Hence, the bacterium has potentials for decreasing chromium concentration to a safe level in the contaminated sources. In the long run, several hundred millions of people worldwide can avoid many lethal diseases caused by chronic chromium poisoning. Hence, the results obtained in this investigation provide us with useful knowledge for the microbial bioremediation of chromium pollution.

Paper III

The results from this study demonstrate biosorption of Ni(II) by Lysinibacillus sp. BA2, which can tolerate nickel up to 9 mM. The adsorption of Ni(II) ions on biomass increased with time and attained saturation after 180 min with rapid adsorption in the initial 30 min. The highest adsorption values obtained were 238.04 mg of Ni(II) per gram of dead biomass and 196.32 mg of Ni(II) per gram of live biomass. The dead biomass of *Lysinibacillus*

sp. BA2 rolled out as beads could serve as an efficient biomatrix for adsorption of nickel. About 54 percent nickel could be removed from the nickel solution in 300 min, indicating the high efficiency of this bio matrix in industrial application. Hence, the dead biomass in the form of beads offers many advantages providing better reusability, high biomass loading and minimal clogging of the flow system over live biomass. The industrial wastewater, however, should be devoid of the solid suspended particles.

Paper IV

The findings of this study highlight the significance of *Lysinibacillus sphaericus* B1-CDA bacterium in removing arsenic and other toxic metals from the contaminated sources. The genetic mechanisms of the isolate could be used to cope with arsenic toxicity. By using RAST and Blast2GO analyses it was found that genes responsive to several metals such as arsenic, nickel, cadmium, iron, manganese, chromium, cadmium, lead, cobalt, zinc, silver and mercury were present in B1-CDA. These genes can be further studied and engineered to other organisms such as plants or yeasts for bioremediation of toxic metals. Furthermore, this study demonstrates that it is possible to speed up molecular biology research by using bioinformatics tools.

Paper V

In this article I described the strain, *Enterobacter cloacae* B2-DHA and it's resistance characteristics to heavy metals including chromium. Moreover, by using RAST and Blast2GO analyses we have predicted the presence of several metal responsive genes in this strain such as arsenic, cadmium, cobalt, iron, lead, manganese, mercury, nickel, silver and zinc. These findings can be employed in bioremediation of these toxic metals in the polluted environments. In a long-term perspective, a large number of people worldwide can avoid many lethal diseases caused by chronic exposure to chromium poisoning.

Future perspectives

Disposal of toxic pollutants through anthropogenic activities leading to large-scale contamination of the ecosystem has raised global awareness on environmental issues in the recent years. The present study focuses on microbial bioremediation of toxic metals to protect both human health and the environment, hence the human wellbeing. The findings of my thesis include an ecofriendly approach for reducing toxic levels of arsenic, chromium and nickel from the contaminated effluents by using three bacterial strains. The toxic metal responsive genes were identified in these bacteria and the function of these genes *arsB, arsC, arsR, chrA, chr*R have been predicted by using molecular and bioinformatics tools. However, to further and better understand the functions of these genes in response to metal bioremediation should be investigated in detail by both practical laboratory experiments and field trials. In the lab experiments mutant strains may be involved to study the mechanisms of metal uptake and accumulation inside the cells. Resulting data obtained from, for example, 3D structures and protein crystallography would give deep insights into how the protein is organized to function. Furthermore, analysis of the data might provide a platform, which can be used as an ecological approach towards remediation of toxic metals from contaminated sites by constructing plant expression vectors or transgenic plants with metal responsive genes. All of these experiments should be validated by field trials.

Future research may also involve development of efficient technology for recovery of the metals absorbed by the strains for recycling.

Acknowledgements

The majority of the experiments and works included in this thesis, financially supported by the Swedish International Development Cooperation Agency (SIDA) (project no. AKT-2010-018), was carried out at the Department of Molecular Biology, School of Bioscience, Systems Biology Research Center, University of Skövde, Sweden, during the years of 2012 through 2016. Some small-scale experiments were also performed at the University of Rajshahi, Bangladesh and D. Y. Patil University in Pune, India. All the administrative works relating my PhD studentship were maintained at the Örebro University. My heartiest thanks go to these universities.

For all of my success, I always give my all praises and thanks to **Allah, the Almighty and the Merciful.** Without His mercy and favor, I cannot succeed in my life at all. I would like to express my appreciation to all people who have supported, helped and encouraged me to complete the PhD work.

In particular,
I would like to express my deepest gratitude to my main supervisor, mentor and teacher, Professor, Dr. Abul Mandal, Head of the Biotechnology, School of Bioscience, Systems Biology Research Center, for accepting me as a PhD student under his guidance at the University of Skövde, Sweden. I remain ever grateful to Dr. Mandal for giving me the opportunity to complete my graduate degrees – a PhD and two MSc. Though I have started PhD research in 2012 but he is my teacher and supervisor since 2009 in different courses, project works and master's thesis. Dr. Mandal taught me how a researcher creates a dynamic and learning environment conducive for conducting successful research. I learned not only science from him but also I learned many things to grow as a good person with a moral discipline.

A special thanks goes to my deputy supervisor, Dr. Jana Jass, Professor in Microbiology, The Life Science Center, School of Science and Technology, Örebro University for giving me an opportunity to work in her laboratory and for her guidance, support and encouragement during my PhD study.

I also thank Dr. Björn Olsson, Associate Professor in Bioinformatics, School of Bioscience, Systems Biology Research Center, University of Skövde for collaboration and acting as my co-supervisor. His creative discussion has always encouraged me to carry out bioinformatics research in combination with molecular biology.

I like to thank Dr. Khaled Hossain, Professor in Biochemistry and Molecular Biology, University of Rajshahi, Bangladesh. He was my first supervisor

when I was working in environmental science and health laboratory in Bangladesh. He played an important role at the very beginning of my scientific carrier.

My special thanks go to Dr. Neelu Nawani, Professor at the Dr. D. Y. Patil University, Pune, India for her collaboration and time in reviewing my manuscripts.

My heartiest thanks go to Professor Dr. Sibdas Ghosh, Dean, School of Arts and Science, Iona College, New Rochelle, New York, USA, for his collaboration and time for advising me to go forward and reviewing my manuscripts.

I would like to thank Dr. Noor Nahar (my PhD colleague) for her guidance in the lab since 2009 to 2014. Under her mentorship I completed one summer project, two master's thesis and part of my PhD thesis. We enjoyed our laboratory work, shared our scientific thoughts and shared our office from the beginning. I also like to thank her son Rafi who has taught me several Swedish words.

My thanks go to Dr. Noél Holmgren, Professor in Ecology who was my PhD mentor. We have discussed the progress of my research and course works every six months. Dr. Holmgren's suggestions regarding professional opportunities really helped me to choose my career path.

In addition, I thank all of my colleagues and teachers at the University of Skövde for their cordial help and support especially, Andreas, Angelica, Mikael, and Zelmina for their kind support in completing my thesis.

Thanks also go to Heléne, Kajsa and Lisa for helping me in fixing laboratory instruments during my PhD studies. A special thank goes to Niklas for helping me to learn Swedish during "fika" time or any other time when we meet.

I appreciate technical help that I received from Jonas Andersson and Alf Svensson. I also appreciate help from Sonja and Marita in printing posters several times. I wish to acknowledge Åsa and Anika, for their help in collecting chemicals and fixing telephone in my office.

I appreciate help from Dr. Than Tin to manage my house in Skövde. I will always be thankful to him for support.

I also wish to express my gratitude to all friends including Abu Bakar, Atiqul, Biprodas, Mosiur, Mahmud, and Shahadat in Skövde who have helped me in various occasions.

I would like to thank my wonderful and supportive family: my beloved wife Tansin Haque. Without her endless support it will never be easy to finish my PhD. Though I did not give her time always but I hope she will be the happiest person to see me successfully completing my PhD. Particularly, in last year of my PhD program her continuous support made my PhD completion very smooth. My cutest son, Abdullah is the most high impact output during my PhD (born 2014). Each day he was the medicine to relief my stress at the end of my work

Last but absolutely not least, I would like to thank my relatives in Bangladesh, my parents, parents-in-law, brother, brother-in-law and others for their moral support. They encourage me always and remember me in their prayer to establish my scientific carrier successfully.

References

Abedin J., Feldman J., Meharg A. (2002): Uptake kinetics of arsenic species in rice plants. *Plant Physiology*. 128, p. 1120-1128.

Abou-Shanab R.A., van Berkum I.P., Angle J.S. (2007): Heavy metal resistance and genotypic analysis of metal resistance genes in gram-positive and gram-negative bacteria present in Ni-rich serpentine soil and in the rhizosphere of Alyssum murale. *Chemosphere*. 68, p. 360 – 367.

Achour A.R., Bauda P., Billard P. (2007): Diversity of arsenite transporter genes from arsenic-resistant soil bacteria. *Res. Microbiol*. 158, p 128–137.

Ackerley D.F., Barak Y., Lynch S.V., Curtin J., Matin A. (2006): Effect of chromate stress on *Escherichia coli* K-12. *J. Bacteriol*. 188(9), p. 3371 - 3381.

Adeniji, A. (2004). Bioremediation of arsenic, chromium, lead and mercury. US Environmental Protection Agency, Office of Solid Waste and Emergency Response. Technology Innovation Office, Washington, DC, USA. P 1 – 43.

Ahluwalia S.S., Goyal D. (2007): Microbial and plant derived biomass for removal of heavy metals from wastewater. *Bioresour. Technol*. 98(12), p. 2243-2257.

Ahmed K., Akhand A.A., Hasan M., Islam M., Hasan A. (2008): Toxicity of arsenic (sodium arsenite) to fresh water spotted snakehead channa punctatus (Bloch) on cellular death and DNA content. *Agric. & Environ. Sci*. 4, p. 18-22.

Alves C.R., de Buzin P.J.W.K., Heck N.C., Schneider I.A.H., (2012): Utilization of ashes obtained from leather shaving incineration as a source of chromium for the production of HC-FeCr alloy. *Minerals Engineering*. 29, p. 124-126.

Ammann A.A. (2007): Inductively coupled plasma mass spectrometry (ICP MS): a versatile tool. *J. Mass Spectrom*. 42, p. 419–427.

Anderson C.R., Cook G.M. (2004): Isolation and characterization of arsenate-reducing bacteria from arsenic contaminated sites in New Zealand. *Curr. Microbiol*. 48, p. 341-347.

Argos M., Kalra T., Rathouz P.J., et al., (2010): Arsenic exposure from drinking water., and all-cause and chronic-disease mortalities in Bangladesh (HEALS): a prospective cohort study. *Lancet*. 376, p. 252–258.

Arora M., Kiran B., Rani S., Rani A., Kaur B., Mittal N. (2008): Heavy metal accumulation in vegetables irrigated with water from different sources. *Food Chemistry*. 111: 811–815, 2008.

Ashburner M., Ball C.A., Blake J.A., et al., (2000): Gene Ontology: tool for the unification of biology. The Gene Ontology Consortium. *Nature Genetics*. 25(1), p. 25–29.

ATSDR (2005): Public health statement-Nickel. Division of toxicology. Agency for Toxic Substances and Disease Registry. CAS # 7440-02-0.

Avudainayagam S., Megharaj M., Owens G., Kookana R.S., Chittleborough D., Naidu R. (2003): Chemistry of chromium in soils with emphasis on tannery waste sites. *Rev. Environ. Contam. Toxicol.* 178, p. 53–91.

Aziz R.K., Bartels D., Best A.A., et al., (2008): The RAST Server: Rapid Annotations using Subsystems Technology. *BMC Genomics*. 9:75.

Baba T., Ara T., Hasegawa M., Takai Y., Okumura Y., Baba M., Datsenko KA., Tomita M., Wanner BL., Mori H. (2006): Construction of Escherichia coli K-12 in-frame, single-gene knockout mutants: the Keio collection. *Mol. Syst. Biol.* 2, p. 1-11.

Baciocchi R., Chiavola A., Gavasci R. (2005): Ion exchange equilibrium of arsenic in the presence of high sulphate and nitrate concentrations. *Water Sci. Technol.: Water Supply*. 5(5), p. 67-74.

Badro J., Côté A.S., Brodholt J.P. (2014): A seismologically consistent compositional model of Earth's core. *PNAS*. 111(21), p. 7542-7545.

Balasubramanian N., Kojima T., Ahmed Basha C., Srinivasakannan C. (2009): Removal of arsenic from aqueous solution using electrocoagulation. *J. Hazard. Mater.* 167, p. 966-969.

Banerjee S., Datta S., Chattyopadhyay D., Sarkar P. (2011): Arsenic accumulating and transforming bacteria isolated from contaminated soil for potential use in bioremediation. *J. Env. Sci. and Health, Part A. 46*, p. 1736–1747.

Baselt R.C. (2008): *Disposition of Toxic Drugs and Chemicals in Man* (8th ed.): Foster City: Biomedical Publications. p. 305–307. ISBN 978-0-9626523-7-0.

Basketter D., Horev L., Slodovnik D., Merimes S., Trattner A., Ingber A. (2000): Investigation of the threshold for allergic reactivity to chromium. *Contact Dermatitis.* 44(2), p. 70–74.

Becquer T., Quantic C., Sicot M., Boudot J.P. (2003): Chromium availability in ultramafic soils from New Caledonia. *Sci. Total. Environ.,* 301, p. 251-261.

Benner S.A. (2010): Comment on "A bacterium that can grow by using arsenic instead of phosphorus". *Science.* 1163:1166.

Bona K.R., Love S., Rhodes Nicholas R., McAdory D., Sinha Sarmistha H., Kern N., Kent J., Strickland J., Wilson A., Beaird J., Ramage J., Rasco Jane F., Vincent John B. (2011): Chromium is not an essential trace element for mammals: Effects of a "low-chromium" diet. *Journal of Biological Inorganic Chemistry.* 16(3), p. 381–390.

Boopathy R. (2000): Factors limiting bioremediation technologies. *Bioresource Technology.* 74, p. 63-67.

Borodovsky M., McIninch J. (1993): GeneMark: parallel gene recognition for both DNA strands. *Comput. Chem.* 17, p. 123-133.

Branco R., Chung A.P., Johnston T., Gurel V., Morais P., Zhitkovich A. (2008): The chromate-inducible *chrBACF* operon from the transposable element Tn*OtChr* confers resistance to chromium(VI) and superoxide. *J. Bacteriol.* 190(21), p. 6996–7003.

Branco R., Morais P. (2013): Identification and characterization of the transcriptional regulator *ChrB* in the chromate resistance determinant of *Ochrobactrum tritici* 5bvl1. *PLoS ONE.* 8: e77987.

Brooks W. E. (2008): Minerals Yearbook. Arsenic [Advance Release]. Reston: U.S. Geological Survey.

Brown, E.M. (1997): A Conformational Study of Collagen as Affected by Tanning Procedures. *Journal of the American Leather Chemists Association.* 92, p. 225–233.

Brown S.D., Thompson M.R., Verberkmoes N.C., Chourey K., Shah M., Zhou J., Hettich R.L., Thompson D.K. (2006): Molecular dynamics of the *Shewanella oneidensis* response to chromate stress. *Mol. Cell. Proteom.* 5, p. 1054 - 1071.

Camargo F.A.O., Bento F.M., Okeke B.C., Frankenberger W.T. (**2003**): Chromate reduction by chromium-resistant bacteria isolated from soils contaminated with dichromate. *J. Environ. Qual.* 32, p. 1228–1233.

Cervantes C., Campos-Garcia J. (2007): Reduction and efflux of chromate by bacteria. In: Nies, D. H., Silver S. (Eds.). *Molecular Microbiology of Heavy Metals.* Springer-Verlag, Berlin. P. 407 - 420.

Carver T., Thomson N., Bleasby A., Berriman M., Parkhill J. (2009): DNAPlotter: circular and linear interactive genome visualization. Bioinformatics (Oxford, England): 25(1), p. 119-120.

Chang J.S., Law R., Chang C.C. (1997): Biosorption of lead, copper and cadmium by biomass of Pseudomonas aeruginosa PU21. *Water Res.* 31, p. 1651–1658.

Castro-González M.I., Méndez-Armenta M. (2008): Heavy metals: Implications associated to fish consumption. *Environmental Toxicology & Pharmacology.* 26, p. 263-271.

Cempel M., Nikel G. (2006): Nickel: A Review of Its Sources and Environmental Toxicology. *Polish J. of Environ. Stud.* 15(3), p. 375-382.

Chen S., Yue Q., Gao B., Li Q., Xu X. (2011): Removal of Cr (VI) from solution using modified corn stalks: Characteristic, equilibrium, kinetic and thermodynamic study. *Chemical Engineering Journal.* 168 (3), p. 1055-1063.

Chen Y., Parvez F., Gamble M., Islam T., Ahmed A., Argos M., Graziano J.H., Ahsan H. (2009): Arsenic exposure at low-to-moderate levels and skin lesions, arsenic metabolism, neurological functions, and biomarkers for respiratory and cardiovascular diseases, Review of recent findings from the health effects of arsenic longitudinal study (HEALS) in Bangladesh. *Toxicol. Appl. Pharmacol.* 239, p. 184–192.

Cheung K.H., Gu J.-D. (2007): Mechanism of hexavalent chromium detoxification by microorganisms and bioremediation application potential: A review. *International Biodeterioration & Biodegradation.* 59: 8–15.

Chibuike G. U., Obiora S. C. (2014): Heavy Metal Polluted Soils: Effect on Plants and Bioremediation Methods: A Review. *Applied and Environmental Soil Science*. 2014, http://dx.doi.org/10.1155/2014/752708

Chivers P.T., Sauer R.T. (2000): Regulation of High Affinity Nickel Uptake in Bacteria. *The journal of biological chemistry*. 275(26), p. 19735–19741.

Chourey K., Thompson M.R., Morrell-Falvey J., VerBerkmoes N.C., Brown S.D., Shah M., Zhou J., Doktycz M., Hettich R.L., Thompson D.K. (2006): Global molecular and morphological effects of 24-hour chromium(vi) exposure on *Shewanella oneidensis* MR-1. *Appl. Environ. Microbiol. 72*, p. 6331–6344.

Chowdhury M., Mostofa M.G., Biswas T.K., Mandal A., Saha A.K. (2015): Characterization of the effluents from leather processing industries. *Environ. Process*. 2, p. 173-187. DOI 1o.1007/s40710-015-0065-7.

Christopher O.A., Haque A.M.M. (2012): Arsenic Contamination in Irrigation Water for Rice Production in Bangladesh: A Review. *Trends in Applied Sciences Res*. 7: 331-349.

Chudobova D., Dostalova S., Nedeckyb B.R., Guran R., Rodrigo M.A.M., Tmejova K., Krizkova S., Zitka O., Adam V., Kizek R. (2015): The effect of metal ions on Staphylococcus aureus revealed by biochemical and mass spectrometric analyses. *Microbiological Research*. 170 p. 147–156.

Congeevaram S., Dhanarani S., Park J., Dexilin M., Thamaraiselvi K. (2007): Biosorption of chromium and nickel by heavy metal resistant fungal and bacterial isolates. *J. Hazard. Mater.* 146, p. 270–277.

Connor D., Landin P., Mellor E., O'Donovan C. *The Microbiology of In Situ Bioremediation*. http://www.cee.vt.edu/program_areas/environmental/teach/gwprimer/biorem.html

Cronin J.R. (2004): The Chromium Controversy. *Alternative and Complementary Therapies*. 10(1), p. 39–42.

Cunat P.-J. (2004): Alloying elements in stainless steel and other chromium-containing alloys. *Euro Inox*. p. 1-24.

Das K.K., Das S.N., Dhundasi S.A. (2008): Nickel, its adverse health effects & oxidative stress. *Indian J. Med. Res.* 128, p. 412–425.

Datta B.K., Bhar M.K., Patra P.H., Majumdar D., Dey R.R., Sarkar S., Chakraborty A.K. (2012). Effect of Environmental Exposure of Arsenic on Cattle and Poultry in Nadia District, West Bengal, India. *Toxicology International*, *19*(1), 59–62.

Dayan A.D., Paine A.J. (2001): Mechanisms of chromium toxicity, carcinogenicity and allergenicity: Review of the literature from 1985 to 2000". *Human & Experimental Toxicology*. 20(9), p. 439–451.

DeMel S., Shi J., Martin P., Rosen B.P., Edwards B.F. (2004): Arginine 60 in the ArsC arsenate reductase of E. coli plasmid R773 determines the chemical nature of the bound As (III) product. *Protein Science*. 13, p. 2330-2340.

Desai J.K., Madamwar D. (2008): Evaluation of in vitro Cr (VI) reduction potential in cytosolic extracts of three indigenous Bacillus sp. isolated from Cr (VI) polluted industrial landfill. *Bioresour. Technol*. 99, p. 6059-6069.

Desale P., Kashyap D., Nawani N., Nahar N., Rahman A., Kapadnis B., Mandal A. (2014): Biosorption of Nickel by Lysinibacillus sp. BA2 native to bauxite mine. *Ecotoxicol. and Environ. Safety*. 107, p. 260-268.

Dhankher O.P., Rosen B.P., McKinney E.C., Meagher R.B. (2006): Hyperaccumulation of arsenic in the shoots of Arabidopsis silenced for arsenate reductase (ACR2): *Proc. Natl. Acad. Sci. USA*. 103, p. 5413–5418.

Diaz-Perez C., Cervantes C., Campos-Garcia J., Julian-Sanchez A., Riveros-Rosas H. (2007): Phylogenetic analysis of the chromate ion transporter (CHR) superfamily. *FEBS J*. 274, p. 6215–6227.

Diaz-Villasenor A., Burns A.L., Hiriart M., Cebrian M.E., Ostrosky-Wegman P. (2007): Arsenic-induced alteration in the expression of genes related to type 2 diabetes mellitus. *Toxicol. Appl. Pharmacol*. 225(2), p. 23-133.

Diorio C., Cai J., Marmor J., Shinder R., DuBow M.S. (1995): An Escherichia coli chromosomal ars operon homolog is functional in arsenic detoxification and is conserved in gram-negative bacteria. *J. Bacteriol*. 177, p. 2050–2056.

Dogan M., Dogan A.U. (2007): Arsenic mineralization, source, distribution, and abundance in the Kutahya region of the Western Anatolia, Turkey. *Environ. Geochem. Health*. 29(2), p. 119-129.

Duruibe J.O., Ogwuegbu M.O.C., Egwurugwu J. N. (2007): Heavy metal pollution and human biotoxic effects. *Int. J. Physical Sci.* 2(5), p. 112-118.

Eastmond D.A., MacGregor J.T, Slesinski R.S. (2008): Trivalent Chromium: Assessing the Genotoxic Risk of an Essential Trace Element and Widely Used Human and Animal Nutritional Supplement. *Critical Reviews in Toxicology*. 38(3), p. 173–190.

Emsley J. (2011): "Arsenic". Nature's Building Blocks: An A-Z Guide to the Elements. Oxford, England, UK: Oxford University Press. p. 47–55.

EPA (Environmental Protection Agency/Naturvårdsverket) (2009): Lägesbeskrivning av efterbehandlingsarbetet i landet 2008. Skrivelse, 2009-02-19, Dnr 642-175-09 Rf

EFSA (2014): European Food Safety Authority. Scientific Opinion on Dietary Reference Values for chromium. *EFSA Journal*. 12(10): doi:10.2903/j.efsa.2014.3845.

FAO (2014) Food and agriculture organization of the United Nations Agriculture's greenhouse gas emissions on the rise. http://www.fao.org/news/story/en/item/216137/icode/ [Retrived on 2016-05-07].

Furuya N., Komano T. (2003): NikAB- or NikB-Dependent Intracellular Recombination between Tandemly Repeated *oriT* Sequences of Plasmid R64 in Plasmid or Single-Stranded Phage Vectors. *J. Bacteriol.* 185(13), p. 3871–3877.

Gabr R.M., Hassan S.H.A., Shoreit A.A.M. (2008): Biosorption of lead and nickel by living and non-living cells of Pseudomonas aeruginosa ASU 6a. *Int. Biodeter. Biodegr.* 62, p. 195–203.

Garelick H., Jones H., Dybowska A., Valsami-Jones E., (2008). Arsenic pollution sources. Rev. Environ. *Contam. Toxicol.* 197, p. 17-60.

Giri A.K. (2012): Removal of arsenic (iii) and chromium (vi) from the water using phytoremediation and bioremediation techniques. PhD dissertation. National Institute of Technology, Rourkela, Odisha, India.

Gonzalez A.R., Ndung'u K., Flegal A.R. (2005): Natural Occurrence of Hexavalent Chromium in the Aromas Red Sands Aquifer, California. *Environmental Science and Technology*. 39(15), p. 5505–5511.

Guha M.D.N., (2007): Arsenic and non-malignant lung diseases. *J. Environ. Sci. Health Part A*. 42, p. 1859-1867.

Götz S., García-Gómez J.M., Terol J., Williams T.D., Nagaraj S.H., Nueda M.J., Robles M., Talón M., Dopazo J., Conesa A. (2008): High-throughput functional annotation and data mining with the Blast2GO suite. *Nucleic Acids Res.* 36, p. 3420-3435.

Halder D., Bhowmick S., Biswas A., Mandal U., Nriagu J., Guha Mazumder D.N., Chatterjee D., Bhattacharya P. (2012): Consumption of brown rice: A potential pathway for arsenic exposure in rural Bengal. *Environmental Science and Technology*, 46, p. 4142 – 4148.

Hamamura N., Macur R.E., Korf S., Ackerman G., Taylor W.P., Kozubal M., Reysenbach A.L., Inskeep W.P. (2009): Linking microbial oxidation of arsenic with detection and phylogenetic analysis of arsenite oxidase genes in diverse geothermal environments. *Environ. Microbiol.* 11, p. 421–431.

Hani A., Pazira E. (2011): Heavy metals assessment and identification of their sources in agricultural soils of Southern Tehran, Iran. *Environ. Monit. Assess.* 176(1-4), p. 677-691.

Harms H., Schlosser D., Wick L.Y. (2011): Untapped potential: exploiting fungi in bioremediation of hazardous chemicals. *Nature Reviews Microbiology*. 9, p. 177-192.

Hasan S., Hashim M.A., Gupta B.S. (2000): Adsorption of Ni (SO4) on Malaysian rubber–wood ash. *Bioresour. Technol.* 72, p. 153–158.

Haynes W.M. (2014): Handbook of chemistry and physics. 94th Edition, CRC press, Taylor & Francis Group. p. 4.5-7. ISBN 978-1-4665-7115-0.

Henne K.L., Nakatsu C.H., Thompson D.K., Konopka A.E. (2009): High-level chromate resistance in *Arthrobacter* sp. strain FB24 requires previously uncharacterized accessory genes. *BMC Microbiol.* 9, p. 199.

Hingston J.A., Collins C.D, Murphy R.J, Lester J.N. (2001): Leaching of chromated copper arsenate wood preservatives: a review". *Environmental Pollution*. 111(1), p. 53–66.

Hobman J.L., Crossman L.C. (2014): Bacterial antimicrobial metal ion resistance. *Journal of Medical Microbiology*, 64, p. 471–497.

Hogan C.M. (2012): *Heavy metal*. In: Encyclopedia of Earth. Eds. Cutler J. Cleveland (Washington, D.C.: Environmental Information Coalition, National Council for Science and the Environment):

Hu X., Fan W., Han B., Liu H., Zheng D., Li Q., Dong W, Yan J., Gao M., Berry C., Yuan Z. (2008): Complete Genome Sequence of the Mosquitocidal Bacterium *Bacillus sphaericus* C3-41 and Comparison with Those of Closely Related Bacillus Species. *J. Bacteriol.* 190(8): 2892–2902.

Huang C.Y., Chu J.S., Pu Y.S., Yang H.Y., Wu C.C., Chung C.J., Hsueh Y.M. (2011): Effect of urinary total arsenic level and estimated glomerular filtration rate on the risk of renal cell carcinoma in a low arsenic exposure area. *J. Urol.* 185, p. 2040-2044.

Islam M.S., Mohanto N.C., Karim M.R., et al, (2015): Arsenic exposure-related elevation of serum matrix metllaoproteinases- and -9 levels and their associations with circulating markers of cardiovascular diseases. *Environ. Health* 14:92. doi: 10.1186/s12940-015-0079-7

Iwamoto T., Nasu M. (2001): Current bioremediation practice and perspective. *J. Biosci. Bioeng.* 32, p. 1-8.

Jaishankar M., Tseten T., Anbalagan N., Mathew B.B., Beeregowda K.N. (2014): Toxicity, mechanism and health effects of some heavy metals. *Interdisciplinary Toxicology.* 7(2): 60–72.

Jackson B.P., Taylor V.F., Punshon T., Cottingham K.L. (2012): Arsenic concentration and speciation in infant formulas and first foods. *Pure Appl. Chem.*, 84(2), p. 215-223.

Jeyasingh J., Philip L. (2005): Bioremediation of chromium contaminated soil: optimization of operating parameters under laboratory conditions. *J. Hazard. Mater. 118*, p. 113-120.

Jomova K., Valko M. (2011): Advances in metal-induced oxidative stress and human disease. *Toxicology.* 283, p. 65–87.

Juhnke S., Peittsh N., Hubener N., Grobe C., Nies D.H. (2002): New genes involved in chromate resistance in Rastolania metallidurans strain CH34. *Arch. Microbiol.* 179, p. 15 - 25.

Kabay N., Arda M., Saha B., Streat M. (2003): Removal of Cr(VI) by solvent impregnated resins (SIR) containing aliquat 336. *Reactive and Functional polymers*. 54(1), p. 103-115.

Kadono T., Inaoka T., Murayama N., et al., (2002): Skin manifestations of arsenicosis in two villages in Bangladesh. *Internat. J. Dermatol*. 41(12), p. 841–846.

Kaewsarn P., Yu Q. (2001): Cadmium (II) removal from aqueous solutions by pre-treated biomass of marine alga *Padina* sp. *Environ. Pollut*. 112, p. 209-213.

Kamika I., Momba M. (2013): Assessing the resistance and bioremediation ability of selected bacterial and protozoan species to heavy metals in metal-rich industrial wastewater. *BMC Microbiol*. 13: 28.

Karim M.R., Rahman M., Islam K., et al., (2013): Increases in oxidized low-density lipoprotein and other inflammatory and adhesion molecules with a concomitant decrease in high-density lipoprotein in the individuals exposed to arsenic in Bangladesh. *Toxicological sciences. doi:10.1093/toxsci/kft130*

Kim D.H., Kim K.W., Cho J. (2006): Removal and transport mechanisms of arsenics in UF and NF membrane processes, *J. Water Health*. 4(2), p. 215-223.

Kitchin K.T., Wallace K. (2008): The role of protein binding of trivalent arsenicals in arsenic carcinogenesis and toxicity. *J. Inorg. Biochem*. 102, p. 532-539.

Kollmer F. (2004): Cluster primary ion bombardment of organic materials. *Appl. Surface. Sci*. 231-232, p. 153-158.

Kotaś J., Stasicka Z. (2000): Chromium occurrence in the environment and methods of its speciation. *Environmental Pollution*. 107(3): p. 263–283.

Krumsiek J., Arnold R., Rattei T. (2007): Gepard: A rapid and sensitive tool for creating dot plots on genome scale. *Bioinformatics*. 23(8), p. 1026-1028.

Kulp T.R., Han S., Saltikov C.W., Lanoil B.D., Zargar K., Oremland R.S. (2007): Effects of imposed salinity gradients on dissimilatory arsenate reduction, sulfate reduction, and other microbial processes in sediments from two California soda lakes. *Appl. Environ. Microbiol*. 73, p. 5130–5137.

Kumari P., Sharma P., Srivastava S., Srivastava M.M. (2006): Biosorption studies on shelled *Moringa oleifera* Lamarck seed powder: removal and recovery of arsenic from aqueous system. *Int. J. Miner. Process*. 78, p. 131-139.

Lagesen K., Hallin P., Rødland E.A., Stærfeldt H.H., Rognes T., Ussery D.W. (2007): RNAmmer: consistent and rapid annotation of ribosomal RNA genes. *Nucleic Acids Research*. 35(9), p. 3100–3108.

Li R., Zhu H., Ruan J., Qian W., Fang X., Shi Z., Li Y., Li S., Shan G., Kristiansen K., Li S., Yang H., Wang J., Wang J. (2010): De novo assembly of human genomes with massively parallel short read sequencing. *Genome Res*. 20(2), p. 265-272.

Liu W.X., Liu J.W., Wu M.Z., Li Y., Zhao Y., Li S.R. (2009): Accumulation and Translocation of Toxic Heavy Metals in Winter Wheat (*Triticum aestivum* L.) Growing in Agricultural Soil of Zhengzhou, China. *Bulletin of Environ. Contam. and Toxicol*. 82(3) p. 343–347

Liao V.H.C., Chu Y.J., Su Y.C., Hsiao S.Y., Wei C.C., Liu C.W., Liao C.M., Shen W.C., Chang F.J. (2011): Arsenite-oxidizing and arsenate-reducing bacteria associated with arsenic-rich groundwater in Taiwan. *J. Contam. Hydrol.* 123, p. 20-29.

Lowe T.M., Eddy S.R. (1997): tRNAscan-SE: a program for improved detection of transfer RNA genes in genomic sequence. *Nucleic Acids Res.* 25(5), p. 955-964.

Malasarn D., Saltikov C.W., Campbell K.M., Santini J.M., Hering J.G., Newman D.K. (2004): arrA is a reliable marker for As(V) respiration. *Science*. 306, p. 455.

Mandal B.K., Suzuki K.T. (2002): Arsenic round the world: a review. *Talanta*, 58(1), p. 201–235. doi: 10.1016/S0039-9140(02)00268-0

Marshall G., Ferreccio C., Yuan Y., Bates M.N., Steinmaus C., Selvin S., Liaw J., Smith A.H. (2007): Fifty-year study of lung and bladder cancer mortality in Chile related to arsenic in drinking water. *J. Natl. Cancer Inst*. 99, p. 920–928.

Matschullat J. (2000): Arsenic in the geosphere – a review. *Sci. Total Environ.* 249, p. 297-312.

Megharaj M., Avudainayagam S., Naidu R. (2003): Toxicity of hexavalent chromium and its reduction by bacteria isolated from soil contaminated with tannery waste. *Curr. Microbiol. 47*, p. 51-54.

Meharg A.A. (2004): Arsenic in rice – understanding a new disaster for South-East Asia. *Trends in Plant Science*. 9, p. 415–417.

Meharg A.A., Rahman M.M. (2003): Arsenic contamination of Bangladesh paddy field soils: implications for rice contribution to arsenic consumption. *Environ. Sci. Technol.* 37, p. 229– 34.

Mergeay M. (1995): Heavy metal resistances in microbial ecosystems. In, *Akkermans ADL., an Elsas JD*., de Bruijn FJ (eds) Molecular microbial ecology manual. Dordrecht, Kluwer Academic Publishers. 6 .1.7/1–6.1.7/17.

Miranda A.T., González M.V., González E.G., Vargas E., Campos-García J., Cervantes C. (2005): Involvement of DNA helicases in chromate resistance by *Pseudomonas aeruginosa* PAO1. *Mutat. Res.* 578, p. 202 - 209. doi:10.1016/j.mrfmmm.2005.05.018

Mohan D., Pittman Jr. C. (2007): Arsenic removal from water/wastewater using adsorbents-A critical review. *J. Hazard. Mater.* 142, p. 1-53.

Moraleda-Mun˜oz A., Pe´rez J., Extremera A.L., Mun˜oz-Dorado J. (2010): Differential Regulation of Six Heavy metal efflux systems in the response of *Myxococcus xanthus* to copper. *App. and Environ. Microbiol.* 76(18), p. 6069–6076.

Moussavi G., Barikbin B. (2010): Biosorption of chromium (VI) from industrial wastewater onto *Pistachio* hull waste biomass. *Chemical Engineering Journal*, 162(3), p. 893-900.

Mukhopadhyay R., Shi J., Rosen B.P. (2000): Purification and characterization of Acr2p., the Saccharomyces cerevisiae arsenate reductase. *J. Biol. Chem. 275*, p. 21149-21157.

Muller D., Médigue C., Koechler S., Barbe V., Barakat M., Talla E., et al. (2007): A tale of two oxidation states, bacterial colonization of arsenic-rich environments. *Plos Genet. 3*, p. 518-530.

Mulrooney S.B., Hausinger R.P. (2003): Nickel uptake and utilization by microorganisms. *FEMS Microbiology Reviews*. 27, p. 239-261.

Nahar N., Rahman A., Moś M., Warzecha T., Algerin M., Ghosh S., Johnson-Brousseau S., Mandal A. (2012): In silico and in vivo studies of an Arabidopsis thaliana gene, ACR2, putatively involved in arsenic accumulation in plants. *J. Mol. Model. 18*, p. 4249–4262.

Natarajan S., Stamps R.H., Saha U.K., Ma L.Q. (2008): Phytofiltration of arsenic- contaminated groundwater using *Pteris Vittata* L.: Effect of plant density and nitrogen and phosphorus Levels. *Int. J. Phytoremed.* 10, p. 222-235.

Nath R. (2000) Health and Disease Role of Micronutrients and Trace Elements. A.P.H Publishing Corporation, New Delhi-110002, ISBN 81-7648-125-4.

NABIR (2003): Natural and Accelerated Bioremediation Research Program, Office of Biological and Environmental Research, Office of Science, U.S. Department of Energy. What is bioremediation? p. 9.

Nies A., Nies D.H., Silver S. (1990) Nucleotide sequence and expression of a plasmid encoded chromate resistance determinant from *Alcaligens eutrophus*. *J. Biol. Chem.* 265: 5648–5653.

Navarro C., Wu L.-F., Mandrand-Berthelot M.A. (1993): The *nik* operon of *Escherichia coli* encodes a periplasmic binding-protein-dependent transport system for nickel. *Molecular Microbiol.* 9, p. 1181–1191.

Nepple B.B., Flynn I., Bachofen R. (1999): Morphological changes in phototrophic bacteria induced bymetalloid oxyanions. *Microbiol. Res. 154(2)*, p. 191–198.

Nogawa K., Kobayashi E., Okubo Y., Suwazono Y. (2004): Environmental cadmium exposure, adverse effects, and preventative measures in Japan. *Biometals.* 17(5), p. 581–587.

Neidhardt S.N., Tang X., Guo H., Stuben D. (2012): Impact of irrigation with high arsenic burden groundwater on the soil-plant system: result from a case study in the Inner Mongolia, China. *Environ. Pollution.* 163, p. 8-13.

Olaitan A.O., Morand S., Rolain J.M. (2014) Mechanisms of polymyxin resistance: acquired and intrinsic resistance in bacteria. A review article. *Frontiers in microbiology. 5*(643), 1-18. doi:10.3389/fmicb.2014.00643

Ortegel J.W., Staren E.D., Faber L.P., Warren W.H., Braun D.P. (2002): Modulation of tumor-infiltrating lymphocyte cytolytic activity against human non-small cell lung cancer. *Lung Cancer*. 36, p. 17-25.

Owolabi J.B., Rosen B.P. (1990): Differential mRNA stability controls relative gene expression within the plasmid-encoded arsenical resistance operon. *J. Bacteriol*. 172, p. 2367–2371.

Pandey S, Rai R, Rai L.C (2012): Proteomics combines morphological, physiological and biochemical attributes to unravel the survival strategy of Anabaena sp. PCC7120 under arsenic stress. *J. Proteomics*. 75, p. 921-937.

Pandey J., Pandey U. (2009): Accumulation of heavy metals in dietary vegetables and cultivated soil horizon in organic farming system in relation to atmospheric deposition in a seasonally dry tropical region of India. *Environ. Monitoring and Assesst*. 148, p. 61-74.

Papp J.F. "Mineral Yearbook 2002: Chromium". United States Geological Survey. Retrieved 2009-02-16.

Pavel L.V., Gavrilescu M (2008) Overview of *ex situ* decontamination techniques for soil cleanup. *Environ. Eng. and Management J*. 7(6), p. 815-834.

Pei A., Nossa C.W., Chokshi P., Blaser M.J., Yang L., Rosmarin D.M., Pei Z. (2009): Diversity of 23S rRNA Genes within Individual Prokaryotic Genomes. *PLoS ONE*. 4(5), p. 5437.

Pei A.Y., Oberdorf W.E., Nossa C.W., Agarwal A., Chokshi P., Gerz E.A., Jin Z., Lee P., Yang L., Poles M., Brown S.M., Sotero S., DeSantis T., Brodie E., Nelson K., Pei Z. (2010): Diversity of 16S rRNA Genes within Individual Prokaryotic Genomes. *Appl. & Environ. Microbiol*. 76(12), p. 3886–3897.

Pimentel B.E., Sa´nchez R.M., Cervantes C. (2002) Effux of chromate by Pseudomonas aeruginosa cells expressing the ChrA protein. *FEMS Microbiology Letters*. 212: 249-254.

Rahman A., Nahar N., Nawani N.N., Jass J., Desale P., Kapadnis B.P., Hossain K., Saha A.K., Ghosh S., Olsson B., Mandal A. (2014): Isolation of a *Lysinibacillus* strain B1-CDA showing potentials for arsenic bioremediation. *J. Environ. Sci. and Health, Part A. 49*, p. 1349–1360.

Rahman A., Nahar N., Nawani N.N, Jass J, Hossain K, Saha AK, Ghosh S, Olsson B, Mandal A (2015a) Bioremediation of hexavalent chromium (VI)

by a soil borne bacterium, *Enterobacter cloacae* B2-DHA. *J. Environ. Sci. and Health, Part A*: 50:11, 1136-1147.

Rahman A., Nahar N., Nawani N.N, Jass J, Ghosh S, Olsson B, Mandal A (2015b) Comparative genome analysis of *Lysinibacillus* B1-CDA, a bacterium that accumulates arsenics. Genomics. 106: 384-392.

Rahman, FA; Allan, DL; Rosen, CJ; Sadowsky, MJ (2004). "Arsenic availability from chromated copper arsenate (CCA)-treated wood". *Journal of environmental quality*. 33(1): 173–80. doi:10.2134/jeq2004.0173.

Rahman M.M., Owens G., Naidu R. (2009): Arsenic levels in rice grain and assessment of daily dietary intake of arsenic from rice in arsenic-contaminated regions of Bangladesh-implications to groundwater irrigation. *Environ. Geochem. and Health*. 1: 179-187.

Rahman M.A., Hasegawa H. (2011): High levels of inorganic arsenic in rice in areas where arsenic-contaminated water is used for irrigation and cooking. *Sci. of the Total Environ*. 409(22), p. 4645–4655.

Ramirez-Diaz M., Diaz-Perez C., Vargas E., Riveros-Rosas H., Campos-Garcia J., Cervantes C. (2008): Mechanisms of bacterial resistance to chromium compounds. *Biometals*. 21, p. 321–332.

Ranjan D., Talat M.H., Hasan S.H. (2009): Biosorption of arsenic from aqueous solution using agricultural residue 'rice polish'. *J. Hazard. Mater.* 166, p. 1050-1059.

Reimer K.J., Koch I., Cullen W.R. (2010): Organoarsenicals. Distribution and transformation in the environment. *Metal ions in life sciences*. 7, p. 165–229.

Rhine E.D., Ní Chadhain S.M., Zylstra G.J., Young L.Y. (2007): The arsenite oxidase genes (aroAB) in novel chemoautotrophic arsenite oxidizers. *Biochem. Biophys. Res. Commun.* 354, p. 662–667.

Rosegrant M.W., Cai X. (2001): Water scarcity and food security: alternative futures for the 21st century. *Water Sci. Technol.* 43(4), p. 61-70.

Rossman T.G., Klein C.B. (2011): Genetic and epigenetic effects of environmental arsenicals. Metallomics: *Integrated biometal science*. 3, p. 1135–1141.

Saçmac S., Kartal S., Yilmaz Y., Saçmac M., Soykan C. (2012): A new chelating resin: Synthesis, characterization and application for speciation of chromium (III)/ (VI) species. *Chemical Engineering Journal*. 181-182, p. 746-753.

Saha R., Nandi R., Saha B. (2011): Sources and toxicity of hexavalent chromium. *J. of Coordination Chemistry*. 64(10), p. 1782-1806.

Saier M.H. Jr. (2003): Tracing pathways of transport protein evolution. *Mol. Microbiol.* 48, p. 1145 - 1156. doi:10.1046/j.1365-2958.2003.03499.x.

Salamov A.A., Solovyev V.V. (2000): Ab initio gene finding in Drosophila genomic DNA. *Genome Res*. 10, p. 516–522.

Salvadori M.R., Lepre L.F., Ando R.A., Ollerdo Nascimento C.A., Corrêa B. (2013): Biosynthesis and uptake of copper nanoparticles by dead biomass of Hypocrea lixii isolated from the metal mine in the Brazilian Amazon Region. *PLoS One*. 25, p. 80519.

Salzberg S.L., Delcher A.L., Kasif S., White O. (1998): Microbial gene identification using interpolated Markov models. *Nucleic acids Res*. 26(2), p. 544–548

Sardohan T., Kir E., Gulec A., Cengeloglu Y. (2010): Removal of Cr (III) and Cr (VI) through the plasama modified and unmodified ion-exchange membrane. *Separation and Purification Technology*. 74, p. 14-20.

Sarkar S., Basu B., Kundu C.K., Patra P.K. (2012): Deficit irrigation: An option to mitigate arsenic load of rice grain in West Bengal, India. *Agriculture, Ecosystems & Environment*. 146, p. 147-152.

Shanker A.K., Cerventes C., Loza-Tavera H., Avudainayagam S. (2005): Chromium toxicity in plants. *Environmental international*. 31, p. 739-753.

Sharma V.K., Sohn M. (2009): Aquatic arsenic: toxicity, speciation, transformations, and remediation. *Environ Int*. 35, p. 743-759.

Shen Z., Han J., Sahin O., Zhang Q. (2013): The contribution of arsB to arsenic resistance in Campylobacter jejuni. *PLoS ONE*. 8(3): e58894.

Shi H., Shi X., Liu K.J. (2004): Oxidative mechanism of arsenic toxicity and carcinogenesis. *Molecular and Cellular Biochemistry*. 255(1-2), p. 67–78.

Shrivastav R. (2001) Atmospheric heavy metal pollution. Development of chronological records and geochemical monitoring. 6(4): p. 62-68.

Shrivastava R., Upreti R.K., Seth P.K., Chaturvedi U.C. (2002): Effects of chromium on the immune system-A mini review. *FEMS Immunology and Medical Microbiology*. 34, p. 1-7.

Signes-Pastor A.J., Al-Rmalli S.W., Jenkins R.O., Carbonell-Barrachina A.A., Haris P.I. (2012): Arsenic bioaccessibility in cooked rice as affected by arsenic in cooking water. *J. Food Sci.* 77, p. 201-206.

Silar P., Dairou J., Cocaign A., Busi F., Rodrigues-Lima F., Dupret J.M. (2011): Fungi as a promising tool for bioremediation of soils contaminated with aromatic amines, a major class of pollutants. *Nature Reviews Microbiology*. 9(6), p. 477.

Silver S., Phung L.T. (2005): Genes and enzymes involved in bacterial oxidation and reduction of inorganic arsenic. *Appl. Environ. Microbiol.* 71, p. 599-608.

Smedley P.L., Kinniburgh D.G. (2005): Sources and behavior of arsenic in natural water. Chapter 1 in United Nations Synthesis Report on Arsenic in Drinking Water.

Smedley P.L., Nicolli H.B., Macdonald D.M.J., Barros A.J., Tullio J.O. (2002): Hydrogeochemistry of arsenic and other inorganic constituents in groundwaters from La Pampa, Argentina. *Appl. Geochem.* 17 (3), p. 259-284.

Sodhi R.N.S. (2004): Time-of-flight secondary ion mass spectrometry (TOF-SIMS), versatility in chemical and imaging surface analysis. *Analyst. 129*, p. 483-487.

Song B., Chyun E., Jaffé P.R., Ward B.B. (2009): Molecular methods to detect and monitor dissimilatory arsenate-respiring bacteria (DARB) in sediments. *FEMS Microbiol. Ecol.* 68, p. 108–117.

Sousa T., Branco R., Piedade A.P., Morais P.V. (2015): Hyper Accumulation of Arsenic in Mutants of Ochrobactrum tritici Silenced for Arsenite Efflux Pumps. *PLoS ONE*. 10(7): e0131317.

Srivastava S., Srivastava A.K., Suprasanna P., D'souza S.F. (2009): Comparative biochemical and transcriptional profiling of two contrasting varieties of *Brassica juncea* L. in response to arsenic exposure reveals mechanisms of stress perception and tolerance. *J. Experimental Botany*. 60, p. 3419-3431.

Stéphane G., Gérard J. (2010). "*Arsenic – based drugs: from Fowler's solution to modern anticancer chemotherapy*". Topics in Organometallic Chemistry. Topics in Organometallic Chemistry **32**: 1–20. ISBN 978-3-642-13184-4.

Tani M., Jahiruddin M., Egashira K., Kurosawa K., Moslehuddin A.Z.M., Rahman M.Z. (2012): Dietary intake of arsenic by households in Marua village in Jessore. *J. Environ. & Nat. Res*.**5**, 283-288.

Tchounwou, P. B., Yedjou, C. G., Patlolla, A. K., & Sutton, D. J. (2012). Heavy Metals Toxicity and the Environment. *EXS*, *101*, 133–164. http://doi.org/10.1007/978-3-7643-8340-4_6.

Thomas S.Y., Choong T.G., Robiah Y., Gregory K.F.L., Azni I. (2007): Arsenic toxicity, health hazards and removal techniques from water: an overview. *Desalination.* 217, p. 139-166.

Thor M.Y., Harnack L., King D., Jasthi B., Pettit J. (2011): Evaluation of the comprehensiveness and reliability of the chromium composition of foods in the literature. *J Food Compost Anal.* 24(8), p. 1147–1152.

Tokar E.J., Benbrahim-Tallaa L., Waalkes M.P. (2011): Metal ions in human cancer development. *Metal Ions on Life Science.* 8, p. 375-401.

Touboul D., Kollmer F., Niehuis E., Brunelle A., Laprevote O. (2005): Improvement of biological time-of-flight-secondary ion mass spectrometry imaging with a bismuth cluster ion source. J. Am. Chem. Soc. *16. P.* 1608-1618.

Tu Z., He G., Li K.X., Chen M.J., Chang J., Chen L., Yao Q., Liu D.P., Ye H., Shi J., Wu X. (2005): An improved system for competent cell preparation and high efficiency plasmid transformation using different *Escherichia coli* strains. *Electronic Journal of Biotechnology*. 8:1.

Vigo J.B., Ellzey J.T. (2006): Effects of Arsenic Toxicity at the Cellular Level: A Review. *Texas Journal of Microscopy.* 37(2), p. 45-49.

Vijayakumar G., Tamilarasan R., Dharmendra M.K. (2011): Removal of Cd2þ ions from aqueous solution using live and dead Bacillus subtilis. *Eng. Res. Bull.* 15, p. 18–24.

Viti C., Pace A., Giovannetti L. (2003): Characterization of Cr(VI)-resistant bacteria isolated from chromium-contaminated soil by tannery activity. *Curr. Microbiol.* 46, p. 1–5.

Vivaldi M. (2001): Bioremediation. An overview. *Pure and Applied Chemistry*. 73, p. 1163-1172.

Volesky B., May-Phillips H., (1995): Biosorption of heavy metals by saccharomyces cerevisiae. Appl. Microbiol. Biotechnol. 42, p. 797–806.

Wang T.C., Jan K.Y., Wang A.S., Gurr J.R. (2007): Trivalent arsenicals include lipid peroxidation, protein carbonylation, and oxidative DNA damage in human urothelial cells. *Mutat. Res*. 615, p. 75-86.

WHO. (2006): Detection, management and surveillance of arsenicosis in South-East Asia region. The regional and national workshops in Bangladesh, India and Thailand. *WHO Technical Report Publication.* **30,** 1-38

WHO (2011): Arsenic in Drinking-water. Background document for development of WHO Guidelines for Drinking-water Quality. WHO/SDE/WSH/03.04/75/Rev/1.

Wuana R.A., Okieimen F.E. (2011): Heavy metals in contaminated soils: a review of sources, chemistry, risks and best available strategies for remediation. ISRN Ecology, 2011. P. 1-20.

Wugan L., Tao L. (2012): The use of chromium minerals in the 4th-3rd century BC China. A preliminary study of a bronze. *J. of Raman Spectroscopy*. 43(2), p. 303-306.

Yuan H.P., Zhang J.H., Lu Z.M., Min H., Wu C. (2009): Studies on biosorption equilibrium and kinetics of Cd2þ by Streptomyces sp. K33 and HL-12. *J. Hazard. Mater.* 164, p. 423–431.

Zafar S., Aqil F., Ahmad I. (2007): Metal tolerance and biosorption potential of filamentous fungi isolated from metal contaminated agricultural soil. *Bioresour. Technol.* 98, p. 2557–2561.

Zdobnov E.M., Apweiler R. (2001): InterProScan—an integration platform for the signature-recognition methods in InterPro. *Bioinformatics*. 17(9), p. 847–848.

Zhang X.H., Liu J., Huang H.T., Chen J., Zhu Y.N., Wang D.Q. (2007) Chromium accumulation by the hyper accumulator plant *Leersia hexandra* Swartz. *Chemosphere*. 67: 1138–1143.

Zhao F.J., McGrath S.P., Meharg A. (2010): Arsenic as a food chain contaminant, mechanisms of plant uptake and metabolism and mitigation strategies. *Annu. Rev. Plant Biol.* 61, p. 535–559.

Zhao Y., Toselli P., Li W. (2012): Microtubules as a critical target for arsenic toxicity in lung cells *in Vitro* and *in Vivo*. *Int. J. of Environ. Res. and Public Health*. 9(2), p. 474-495.

Journal of Environmental Science and Health, Part A (2014) **49**, 1349–1360

ISSN: 1093-4529 (Print); 1532-4117 (Online)
DOI: 10.1080/10934529.2014.928247

Taylor & Francis
Taylor & Francis Group

PAPER I

Isolation and characterization of a *Lysinibacillus* strain B1-CDA showing potential for bioremediation of arsenics from contaminated water

AMINUR RAHMAN[1,3], NOOR NAHAR[1], NEELU N. NAWANI[2], JANA JASS[3], PRITHVIRAJ DESALE[2], BALU P. KAPADNIS[4], KHALED HOSSAIN[5], ANANDA K. SAHA[6], SIBDAS GHOSH[7], BJÖRN OLSSON[1] and ABUL MANDAL[1]

[1]*Systems Biology Research Center, School of Bioscience, University of Skövde, Skövde, Sweden*
[2]*Dr. D. Y. Patil Biotechnology and Bioinformatics Institute, Dr. D. Y. Patil Vidyapeeth, Tathawade, Pune, India*
[3]*The Life Science Center, School of Science and Technology, Örebro University, Örebro, Sweden*
[4]*Department of Microbiology, University of Pune, Pune, India*
[5]*Department of Biochemistry and Molecular Biology, University of Rajshahi, Rajshahi, Bangladesh*
[6]*Department of Zoology, University of Rajshahi, Rajshahi, Bangladesh*
[7]*School of Arts and Science, Iona College, New Rochelle, New York, USA*

The main objective of this study was to identify and isolate arsenic resistant bacteria that can be used for removing arsenic from the contaminated environment. Here we report a soil borne bacterium, B1-CDA that can serve this purpose. B1-CDA was isolated from the soil of a cultivated land in Chuadanga district located in the southwest region of Bangladesh. The morphological, biochemical and 16S rRNA analysis suggested that the isolate belongs to *Lysinibacillus sphaericus*. The minimum inhibitory concentration (MIC) value of the isolate is 500 mM (As) as arsenate. TOF-SIMS and ICP-MS analysis confirmed intracellular accumulation and removal of arsenics. Arsenic accumulation in cells amounted to 5.0 mg g^{-1} of the cells dry biomass and thus reduced the arsenic concentration in the contaminated liquid medium by as much as 50%. These results indicate that B1-CDA has the potential for remediation of arsenic from the contaminated water. We believe the benefits of implementing this bacterium to efficiently reduce arsenic exposure will not only help to remove one aspect of human arsenic poisoning but will also benefit livestock and native animal species. Therefore, the outcome of this research will be highly significant for people in the affected area and also for human populations in other countries that have credible health concerns as a consequence of arsenic-contaminated water.

Keywords: Pollution, toxic metals, arsenics, bioremediation, bacteria, bioaccumulation.

Introduction

Toxic pollutants, including heavy metals, discharged into the environment as waste either by industries or other human activities, contaminate drinking water for millions of people and animals in many regions of the world, particularly South East Asia. In addition, these toxic metals are accumulated in human foods and animal fodder indirectly through irrigation of cultivated crops with the contaminated water. Long term exposure to these toxic substances, for example, to arsenic via drinking water or contaminated foods, leads to several lethal diseases such as cancer, keratosis, gangrene, diabetes and cardio-vascular disorders among others.[1–5]

Recently, the arsenic problem has been considered as a severe threat to mankind in many countries of the world, particularly in the South Asian regions. For example, in Bangladesh, arsenic-rich bedrock of the Brahmaputra river basin contaminates the groundwater as it is pumped up through hundreds of thousands of tube-wells and is consumed by millions of people.[6] Arsenic poisoning through drinking tube-well water has now become a national problem in this country.[3] The World Health Organization [7] describes arsenic contamination of water supplies in this region as "the largest poisoning of a population in human history."

The most common inorganic forms of arsenic in the environment are pentavalent arsenate As (V) and trivalent

Address correspondence to Abul Mandal, System Biology Research Center, School of Bioscience, University of Skövde, P. O. Box 408, SE-541 28 Skövde, Sweden; E-mail: abul.mandal@his.se
Received March 6, 2014.
Color versions of one or more of the figures in this article can be found online at www.tandfonline.com/lesa.

arsenite As (III). Both of these two forms are toxic for human and the ecosystem but As (III) is more toxic than As (V).[8] Therefore, removal of arsenic contamination from soil, water and environment is of great importance for human welfare.

Metal pollutants, particularly those existing as basic elements, cannot be degraded like other organic contaminants. Until today, many conventional physicochemical methods have been developed for removing toxic arsenic substances from the contaminated sources. Examples of these methods are ion exchange, electrochemical treatment, evaporation, reverse osmosis, precipitation, adsorption on activated coal and many others. Nevertheless, most of the methods are inefficient and very expensive especially for metals at low concentration or in large solution volume.[9,10] Furthermore, these chemicals may result in development of many harmful by-products. Therefore, less expensive and an eco-friendly biological approaches should be considered as alternative methods for remediation of arsenics.[11] In the recent years, bioremediation of heavy metals using microorganisms has received a great deal of attention due to its advantages over the conventional methods.[12]

A number of microorganisms have been reported to resist/tolerate arsenic by utilizing periplasmic biosorption, intracellular bioaccumulation, and/or biotransformation to a less toxic speciation state through direct enzymatic reaction, including *Proteobacterium, Firmicutes, Kocuria* - sp.,[13] *Stenotrophomonas, Alcaligenes, Herminnimonas* - sp.,[14] *Lactobacillus* - sp.,[15] *Rhodococcus, Achromobacter, Aliihoeflea -sp*,[16] *Bacillus* - sp.,[17] *Lysinibacillus* - sp.,[18] *Pseudomonas* - sp.[19] etc. Most of them have been isolated from soil, industrial sewage, evaporation ponds, or discharged water, or purchased from culture collection centers.

Our research group has focused on developing a sustainable bioremediation method for removal of arsenics from water, including drinking and irrigation water, cultivated lands, rivers and ponds, using microorganisms such as bacteria occurring naturally in the polluted regions. We believe that specific microorganisms such as the bacterial species selected here for their tolerance to arsenics, and isolated from the affected regions can be put through a cutting edge and yet comparatively inexpensive technique called "directed evolution."[20–22] For removal or reduction of toxic pollutants, the concept of directed evolution can be described as proliferating isolated bacteria after natural selection.

In this technique, bacteria are not genetically altered and can be compared to how humans have historically selected for and thus directed the evolution of many food crops, domesticated animals, baking yeast strains, bacterial strains (dairy, alcoholic products, pest control, bioremediation), and fungi (cultured food, pest control, bioremediation). This method simply increases the rate of evolutionary change for human purposes. Directed evolution, in this work, has simply selected for the bacterial individuals in the isolated strains that are best at remediating pollutants and allowed only these to further proliferate. Hence, these organisms evolve to cope with particular environmental stress.

Over the past decade we have collected water and soil samples from many regions of South Asia, particularly Bangladesh and India, where arsenic contaminated groundwater is frequently used for both consumption and for irrigation of cultivated crops and causing severe diseases in humans and animals as described here. The samples were used for both determination of arsenic content and identification and isolation of novel microorganisms that can be applied for directed evolution. Until today, our collection consists of several hundred bacterial strains isolated from the arsenic contaminated environment.

Among the microbial collection, we have recently identified and characterized a soil-borne bacterium B1-CDA, collected from the arsenic contaminated cultivated land in Chuadanga district in the southwest region of Bangladesh. This strain can survive and grow on medium containing up to 500 mM sodium arsenate ($Na_2HAsO_4.7H_2O$). Here we report the results obtained from characterization (morphological, biochemical, 16S rRNA etc.) and evaluation of this strain to be utilized as a potential candidate for eliminating or significantly reducing arsenics in the contaminated source.

Materials and methods

Collection and analysis of soil samples

Soil samples were collected from a cultivated land in Chuadanga district of Bangladesh, where soil, sediment, and ground water have been contaminated with arsenics for many years. The soil surface at 0–15 cm in depth was collected, retained in plastic bags and kept at 4°C until further analysis. These samples were used for both bacterial isolation and reconstruction of field water (RFW). The pH of collected soil samples was determined by shaking 5 g of soil in 50 mL of distilled water for 1 h followed by measuring pH with a 2210 pH meter (Hanna Instruments, Carrollton, TX, USA).

To determine the arsenic, sodium and potassium content, 5 g of the collected sample was air dried and mixed with 2 mL of HNO_3 (65%, Merck, Darmstadt, Germany) and 6 mL of HCl (37%, Merck). The mixture was heated to 70°C for 1 h, and then diluted with 10 mL of deionized water. The acid-digested solution was filtered to remove residual particulates. Arsenic, sodium and potassium concentration was determined by inductively coupled plasma atomic emission spectroscopy (ICP-AES) method. Concentration of chloride and phosphate was estimated by spectrophotometric analysis methods. Measurement of nitrate was performed in a solution with KCl followed by

flow injection analysis (FIA). The samples were digested based on heat block digestion. All soil sample analyses were performed at Eurofins Environment Testing Sweden AB (Lidköping, Sweden).

Chemicals and bacterial enrichment

Chemicals used in this experiment were analytical standard grade (Merck and Sigma-Aldrich). All solutions were prepared with autoclaved double deionized water (ddH_2O). All the stock solutions were sterilized by syringe filtration (0.2 μm pore-size) and stored at 4°C in the dark until further use. The bacteria culture media were autoclaved at 120°C for 15 min. For isolation of arsenic resistant bacteria, soil samples were serially diluted in sterile distilled water and plated aerobically in the modified Luria–Bertani (LB) medium containing peptone 10 g L^{-1}, sodium chloride 5 g L^{-1}, yeast extracts 5 g L^{-1}, D (+) glucose 1 g/L (Merck) and 10 mM sodium arsenate $Na_2HAsO_4.7H_2O$ (Sigma Cat. No. S9663). Plates were incubated at 37°C for 48 h. Several morphologically different colonies were selected randomly and sub-cultured in the same medium to purify the colonies. Colonies showing resistance to arsenate was selected for further screening processes. Eight arsenic-resistant strains were isolated. Only strain B1-CDA was selected for the rest of this study because of its best performance in growth and tolerance to arsenic.

Morphological and biochemical test

The colony morphology of the purified bacterial strains grown on medium containing arsenate was observed and recorded. Gram-staining and cellular morphology of the strains were studied based on both light- and electron microscopy.[23] Biochemical tests including motility, mannitol test, indole production, H_2S production, catalase test, oxidase test, urease test, carbohydrate (glucose, lactose, sucrose, Rhamnose) fermentation, citrate utilization, hydrolysis of casein etc. were performed to facilitate the identification of the bacterium following Bergey's Manual of Systematic Bacteriology.[24] Scanning electron microscopic (SEM) studies were performed on the bacterial isolate grown in the presence and absence of arsenic.

16S *rRNA sequencing*

Genomic DNA was isolated following the standard protocol Master pure Gram positive DNA purification kit (Epicentre, Madison, WI, USA) as per the specifications of the manufacturer. For PCR amplification of the nearly full-length 16S rRNA domain, *Bacteria* specific universal primers 8F (5-AGAGTTTGATCCTGGCTCAG-3) and 1492R (5-TACGGTTACCTTGTTACGACTT-3) were used. PCR reaction mixtures contained deoxynucleotide triphosphates (dNTPs) at 50 μmol each, primers at 2.5 pmol each, 1.5 U Taq DNA polymerase in 1× buffer, 10 ng of DNA template, 2.5 mM $MgCl_2$ in a 50 μL reaction. The thermal cycling programme included initial denaturation at 94°C for 5 min, followed by 30 cycles of denaturation at 94°C for 1 min, primer annealing at 55°C for 1 min and primer extension at 72°C for 1.5 min. This was followed by a final extension step at 72°C for 10 min and tubes were cooled to 4°C. The amplified PCR products were visualized in agarose-gel electrophoresis, and the DNA fragment was purified from the gel using Agarose gel DNA Purification Spin Kit (Cat. No. MB511, Mumbai, Maharashtra, India). DNA sequencing reaction of PCR amplicon was carried out using BDT v3.1 Cycle sequencing kit (Austin, TX, USA) on ABI 3730xl Genetic Analyzer (Pleasanton, CA, USA) with same primers: 8F and 1492R. A similarity search for the nucleotide sequence of 16S rRNA of the test isolate was carried out using the NCBI nucleotide BLAST (http://blast.ncbi.nlm.nih.gov/). The 16S rRNA sequence was submitted to NCBI GenBank for registration.

Evolutionary relationship of taxa

The evolutionary history was inferred using the neighbor-joining method.[25] The percentage of replicate trees in which the associated taxa clustered together in the bootstrap test (500 replicates) was shown next to the branches.[26] The evolutionary distances were computed using the Kimura 2-parameter method [27] and these were in the units of the number of base substitutions per site. The analysis involved 23 nucleotide sequences. Codon positions included were 1st+2nd+3rd+Noncoding. All positions with less than 95% site coverage were eliminated. This means that fewer than 5% alignment gaps, missing data, and ambiguous bases were allowed at any position. There were a total of 1123 positions in the final data set. Evolutionary analyses were conducted in MEGA6.[28]

Effect of pH and temperature

The influences of pH and temperature on bacterial growth were assessed on LB medium without arsenic. Autoclaved culture media with pH 5.0, 6.0, 7.0, 8.0 and 9.0 were used to test the effect of pH on bacterial growth. The inoculum of B1-CDA strain was 1% of the total volume. The logarithmic-phase cultures of bacterial isolates prepared in LB broth were incubated for 24 h at 37°C with continuous shaking at 180 rpm. The growth of bacteria was measured every 2 h using optical density measurement at 600 nm by Genesys 20 visible spectrophotometer (Thermo Scientific, Madison, WI, USA). For evaluation of the effect of temperature on bacterial growth, the incubation temperature was set up at 25, 30, 37 and 40°C. Similarly, the inoculum of B1-CDA strain was prepared from the logarithmic-phase

cultured in LB broth and incubated for 24 h with shaking at 180 rpm. The growth of bacterial cells was evaluated by measuring optical density of medium at regular intervals of 2 h at 600 nm. All experiments were carried out in triplicates. For the rest of this study, the strain B1-CDA was grown on media with pH 7 maintaining culture temperature at 37°C.

Minimum inhibitory concentration (MIC) of arsenate

The MIC of arsenate of B1-CDA isolate was determined as reported by Mergeay.[29] Minimal salts broth [30] was used to determine the MIC for arsenate. The broth with minimal salts was supplemented with different concentrations (300 mM, 400 mM, 500 mM, 600 mM and 700 mM) of As (V). One percent inoculum of B1-CDA was added to these media in 50-mL Falcon tubes. Bacteria cultured in minimal medium without As (V) were used as control. All tubes were incubated at 37°C with shaking at 180 rpm for 48–96 h. Optical density measurements for estimation of cell growth were carried out at 600 nm by using Genesys 20 visible spectrophotometer (Thermoscientific). Cell count was determined on Luria agar plates supplemented with or without 500 mM sodium arsenate. Besides sodium arsenate, the MIC of bacterial isolate was checked for other heavy metals like K_2CrO_4, $FeCl_3$, $MnCl_2$, $ZnCl_2$, $NiCl_2$ and $AgNO_3$ at different concentrations.

Inductively coupled plasma-mass spectroscopy (ICP-MS) analyses

The bacterial cultures were prepared for measurement of arsenic using ICP-MS. The 18 h old culture of B1-CDA ($OD_{600} = 0.1$) was used to prepare cell suspension as inoculum. The final concentration of inoculum was kept to 1% for all samples. The number of cells exposed in each case ranged from 60,000 to 70,000. Cells were grown in six parallel sets of 50 mL LB broth containing 50 mM sodium arsenate with continuous shaking at 37°C and 180 rpm. Each set was containing four conical flasks. B1-CDA cells were grown similarly but without sodium arsenate and used as controls. The cells were harvested by centrifugation (10000 rpm for 10 min). The amount of arsenic in the cell free broth was measured using ICP-MS. The cell free broth was filtered through 0.2 μm filter and acidified to pH 2.0 with suprapure nitric acid (30%, Merck). This was used for the analysis of total arsenic.

For determination of arsenic in cells, the pellet was washed thrice with deionized water and dried at 50°C until a constant dry weight was achieved. Where entire contents of flask were harvested, the cell dry weight was recorded. Cells were digested with suprapure nitric acid (30%, Merck) according to ratio of 7.5 mL nitric acid per g dry biomass using microwave digestion. The samples were brought to a constant volume prior to determination of arsenic contents. Measurement of arsenics was also carried out similarly in control experiments, i.e., media containing arsenate but not exposed to B1-CDA and in media devoid of arsenic but treated with B1-CDA. All analyses were carried out as mentioned above after filtration of the cell digest through a 0.2 μm filter.

TOF-SIMS analysis

Bacterial samples were grown in liquid LB medium supplied without or with 50 mM arsenate. Cells were collected by repeated (3–4 times) centrifugation at 10,000 rpm in a micro centrifuge and washing with autoclaved deionised distilled water. Cells were then deposited and spread out on microscopic slides and analyzed by using a Time of Flight-Secondary Ion Mass Spectrometry (TOF-SIMS) V instrument (ION-TOF GmbH, Münster, Germany) equipped with a 30 keV Bi_3^+ LMIG analysis gun [31,32] with a 512 × 512 μm raster. Depth profiling of the arsenic ions inside the cells was performed by using a 0.5 keV Cs^+ sputter gun. Depth profiling and imaging were performed in the burst mode (analyze 30 scans, sputter 0.20 s, pause 6.0 s, to a total of approx. 250 s of sputtering). The Bi3-LMIG was set in the high current bunched mode (negative polarity, analysis area 78 × 78 μm, mass resolution m/Δm: 6000; focus of the ion beam: 150 nm) [33] with a target current of 0.15 pA, while Cs ions were used for sputtering, with a current of 5 nA and with a 250 × 250 μm raster.

All image analyses were performed using the ION-TOF Surface Lab software (Version 6.1, ION-TOF GmbH) except for image resizing, for publication purposes, which was done in Adobe Photoshop CS-2 (Adobe Systems Incorporated, San Jose, CA, USA). Each ion image is normalised to the intensity in the brightest pixel. This intensity value is assigned to the colour value of 256. Zero intensity is assigned to the colour value 0. All other intensities are assigned accordingly using a linear relationship.

Reconstruction of field water (RFW)

Five grams of soil were mixed with one liter of autoclaved tap water by shaking at 250 rpm for 24 h. The mixture was then allowed to sediment. The supernatant was collected by pipetting. The minimum amount (1%) of peptone was added in the RFW as a source of nutrient of bacteria to grow them properly. For arsenic exposure, 50 mL of RFW containing 50 mM arsenate was mixed with 50 μL of B1-CDA grown for 18 h on Luria-Broth. The number of cells exposed in each case ranged from 45,000 to 50,000. Cells were grown in three parallel sets, with B1-CDA, without B1-CDA and autoclaved RFW containing 50 mM sodium arsenate. Bacterial cells were grown up to 120 h by continuous shaking at 37°C and 180 rpm. Samples were taken at every 24 h, and the bacterial cells were

separated by centrifugation at 10,000 rpm for 15 min. Samples without exposure to B1-CDA were treated similarly and used as controls. After centrifugation every sample was stored at 4°C.

Statistical analysis

All analyses were performed in triplicates, and results are presented in mean value with standard deviation.

Results and discussion

Sample collection and analysis

Soil containing heavy metals are potential sources for identifying toxic-metal-tolerant bacteria. For isolation of arsenic resistant bacterial strains, we have collected soil samples from arsenic contaminated cultivated land in the area of Chuadanga district located in the south-west region of Bangladesh. The pH of the soil samples was found to be 7.2 (±0.3). Some selected physicochemical characteristics of soil samples were ascertained. Total arsenic content of the soil was 5.63 (±0.03) mg kg^{-1} of soil. Chloride content of the soil was estimated to be 5.1 (±0.20) mg kg^{-1}. The Sodium and potassium contents were 7.4 (±0.03) mg kg^{-1} and 3.4 (±0.03) mg kg^{-1}, respectively, whereas phosphate and nitrate contents were 0.75 (±0.02) mg kg^{-1} and 0.35 (±0.03) mg kg^{-1}, respectively.

Identification and characterization of bacterial strain

The preliminary characterization of the strain B1-CDA was performed on the basis of colonial morphology, cellular morphology and gram staining characteristics. The colonial morphology of the strain was circular and convex. The strain was microscopically studied and cellular morphology such as shape and gram reactions were observed during gram staining. Cellular shape of the strain was found to be rodlike and the isolate was Gram positive. Biochemical characterization was performed in terms of carbohydrate utilization (starch, sucrose, maltose, lactose, citrate, etc.), and production of enzymes such as catalase, oxidase, urease, etc. Table 1 shows the results of various biochemical tests of the isolate. Biochemical characterization indicated that B1-CDA belongs to the genus *Lycinibacillus*. The 16S rRNA sequence was submitted to NCBI databank for registration and the bacteria was classified according to its similarity to sequences in the GenBank database. The accession number of the isolate is KF961041. The BLASTN search of the 16S rRNA gene sequence (1,308 bp) of B1-CDA strain showed that it belonged to the genus Lysinibacillus and possessed 99% similarity with that of *Lysinibacillus sphaericus* (Fig. 1).

Temperature is one of the major environmental factors that affect bacterial growth.[34] The B1-CDA isolate could grow at 20, 30, 37 and 45°C, but the optimum growth was achieved at 37°C. pH is the another factor that plays a major role in growth and metal accumulation properties of the bacterial strains.[35] The B1-CDA isolate could grow at pH ranging from 5 to 9 but the optimum pH for growth was found at pH 7.0 (data not shown).

Table 1. The morphological and biochemical characteristics of strain B1-CDA.

Characteristic	Strain B1-CDA
Gram reaction	+
Shape	Rod
Color	Yellowish
Motility	+
Catalase	+
Oxidase	+
Citrate utilization	+
Hydrolysis of casein	+
Motility	+
Optimum pH	7
Optimum temperature	37°C
Glucose fermentation	-
Lactose fermentation	-
Sucrose fermentation	-
Maltose fermentation	-
Rhamnose fermentation	-
Mannitol fermentation	-
Indole production	-
Urea test	+
H_2S production	-

Arsenic resistance of B1-CDA

Cell growth was measured by considering the optical density of the culture grown with or without exposure to 50 mM arsenate. The results presented in Figure 2a indicate that after 120 h of growth in medium with or without arsenate the bacteria do not exhibit any difference in optical density (OD).

To verify if the B1-CDA strain was indeed resistant to arsenic, we performed viable cell count experiments. For this, the B1-CDA cells were grown first in a liquid medium containing 50 mM arsenate for up to 120 h and then the cells were transferred onto solid medium fortified with or without arsenate. Samples were taken every 24 h and the colony forming units (CFU) were determined. The results show that the number of cells on the plates containing no arsenate increased rapidly up to 72 h (approximately 1.0×10^{14} CFU) and then decreased drastically (approximately 1.0×10^{7} CFU) until 96 h of growth (Fig. 2b).

However, when the cells were plated on arsenic containing medium, the cell count increased gradually up to 120 h (approximately 1.0×10^{11} CFU), confirming that this strain was resistant to arsenate. The higher cell counts on Luria agar without arsenate could be because of the

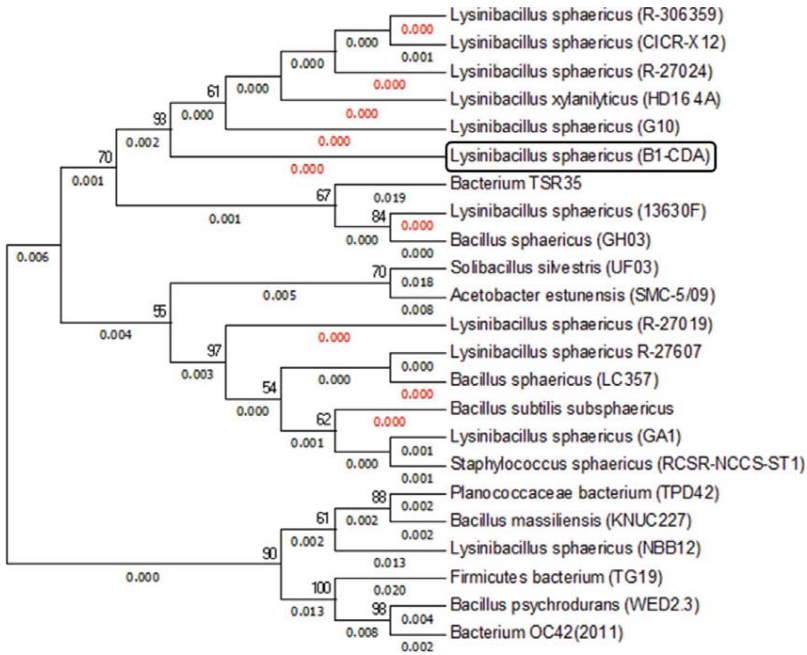

Fig. 1. Neighbour-joining tree based on 16S rRNA gene sequences showing the phylogenetic relationship of the isolated strain B1-CDA compared with species belonging to the Lysinibacillus. The analysis included data from 1123 positions in the final dataset. The bootstrap values (expressed as percentages of 500 replicates) above 50% are shown at the branch points.

reversible dormancy of the cells due to removal of the stress factor (arsenic) from the growth medium. These results suggest that the bacterium was able to grow well in presence of arsenics. Similar results on the use of arsenic by the bacterial cells were also reported by Wolfe-Simon et al.[36] These authors claimed that phosphorous can be substituted by arsenics in the growth medium, although they observed higher cell counts in presence of phosphate (approximately 5.0×10^8 CFU) than that found in the presence of arsenate (approximately 5.0×10^7 CFU). Subsequently, several disagreements to this discovery have been reported recently.[37]

Tolerance of B1-CDA to other metals

To verify if the B1-CDA isolate was also tolerant to other toxic metals we exposed the cells to K_2CrO_4, $FeCl_3$, $MnCl_2$, $ZnCl_2$, $NiCl_2$ and $AgNO_3$ at different concentrations in L. broth medium containing minimum salt concentration. The MIC of these metals was found to be 6 mM for K_2CrO_4, 5 mM for $FeCl_3$, 3 mM for $MnCl_2$, 2 mM for $ZnCl_2$, 1.5 mM for $NiCl_2$ and 0.3 mM for $AgNO_3$.

TOF-SIMS analyses

Ion imaging and depth profiling based on Time of Flight-Secondary Ion Mass Spectrometry (TOF-SIMS) was performed to determine whether the bacterium B1-CDA absorbs and/or accumulates arsenics inside the cells. This analysis relies on the use of a pulsed ion beam to ionize surface molecules that later can be studied by a mass spectrometer. By combining the pulsed ion beam with another ion beam in direct current (DC) mode, depth profiles are obtained as a result of consecutive removal of surface layers. Hence, TOF-SIMS can be used for obtaining both ion images as well as chemical information on the distribution of ions from the surface and downwards into the sample.

With the help of ion imaging we have found that B1-CDA cells, when exposed to arsenate, uptake and accumulate different forms of arsenics inside the cells, such as free form of arsenic (As), meta-arsenite (AsO_2^-), ortho-arsenite (AsO_3^{3-}) and arsenate ($AsO_4H_2^-$) (Fig. 3b-e). In addition, the total protein signals in the cells are also detected by TOF-SIMS (Fig. 3a). The total arsenics encountered inside the cells are shown in Figure 3f.

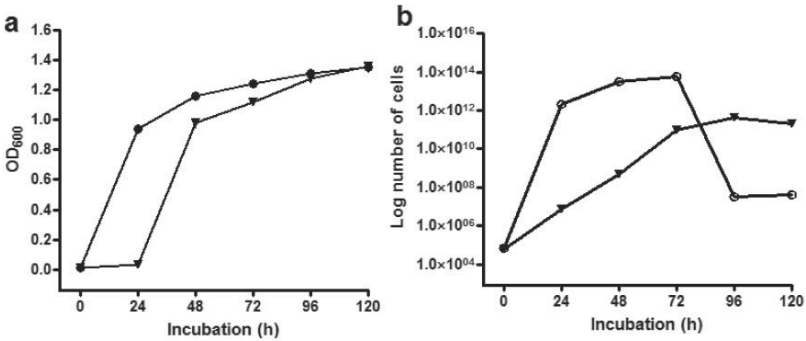

Fig. 2. Study of arsenic resistance of B1-CDA by measuring optical density and colony forming units (CFU). a, represents optical density, where the symbols ▼ and • indicate the OD_{600} obtained with cells exposed to arsenics and without any exposure (control), respectively. b, represents cell counts, where the symbols ▼ and O indicate the number of CFU of bacterial cells exposed to arsenics and without any exposure (control), respectively.

Similarly, B1-CDA cells grown in absence of arsenate were studied by TOF-SIMS and used as a control. In these cells, we could not detect any arsenic ions, therefore data for this study are not shown. The intensity of arsenate ions inside the cells was much lower than the intensity of other arsenic ions although the cells have been previously exposed to arsenate.

These results show that the bacterium, B1-CDA, prefers to accumulate arsenite rather than arsenate inside the cells. The obvious question was where did the arsenite come from? In bacterial cells, the As (V) enters inside the cell via phosphate transport systems and within the bacterial cells, cytoplasmic arsenate reductase transforms As (V) to As (III).[38] Similar arsenate reduction has been reported in both prokaryotes such as *Escherichia coli* [39] and eukaryotes such as *Saccharomyces cerevisiae* [40] and *Arabidopsis thaliana*.[41,42] These organisms contain arsenic reductase genes (*ACR2*) encoding enzymes required for reduction of arsenate to arsenite within the cell. Although for a living cell, arsenite is more toxic than arsenate,[43,44] the advantage of this type reduction could be different in different organisms. For example, the plant cell can sequester arsenite but not arsenate in the vacuoles to avoid arsenic toxicity. Many bacterial strains reduce arsenate to arsenite to produce energy for surviving under stress conditions.[45] As the redox reactions are energy giving, reduction of arsenate to arsenite in the cells will produce more energy.[44]

To further verify the presence of arsenite species inside the cells we have performed depth profiling analyses by TOF-SIMS. This analysis, also known as "sputtering," relies on gradual measurement of arsenic at the different depth of the bacterial cell layers. Sputtering was made up to 250 s and these results are presented in Figs. 3g and 3h. These figures demonstrate that the intensity counts for arsenate ions ($AsO_4H_2^-$) were much lower ($10^{2.7}$) than those obtained for arsenite ions ($10^{2.8}$ for AsO_2^- and $10^{3.6}$ for AsO_3^{3-}). Furthermore, the intensity levels remained constant throughout the sputtering time (0–250 s).

The depth profiling further confirms the results obtained in the ion imaging, indicating comparatively higher amounts of arsenics inside the cells. Reduction of arsenate and oxidation of arsenite under the aerobic conditions has been previously described by several researchers both in eukaryotes [41,42] and in prokaryotes.[46,47] As mentioned earlier, in plants the arsenate reductase gene (*ACR2*) converts arsenate to arsenite inside the cells, facilitating sequestration of arsenite in the vacuoles. Therefore, plants can be used for removal of arsenics from the environment, particularly from the contaminated soil. Importantly, as our isolate B1-CDA exhibits a very high resistance to arsenic, its oxidation/reduction characteristics are therefore significantly beneficial for remediation of arsenics from the contaminated water and/or soils in the affected regions. Appropriate application of this bacterium may maintain the biogeochemical cycles of arsenics in the nature.

Arsenic accumulation analyzed by ICP-MS

To further confirm if the B1-CDA strain can indeed accumulate arsenics inside the cells we performed ICP-MS analyses. This analysis revealed that the amount of arsenics, inside the bacterial cells after 120 h of exposure to 50 mM arsenate resulted in 5.0 mg g^{-1} dry weight of bacterial biomass (Fig. 4a). If this is the case, theoretically equal amounts of arsenics should be decreased from the growth medium. For verification, we also performed ICP-MS (Fig. 4b). The results demonstrate that the concentration of arsenate in the cell free growth medium, after 96 h and 120 h exposure, decreased from 50 mM to 25 mM (50%) (Fig. 4b).

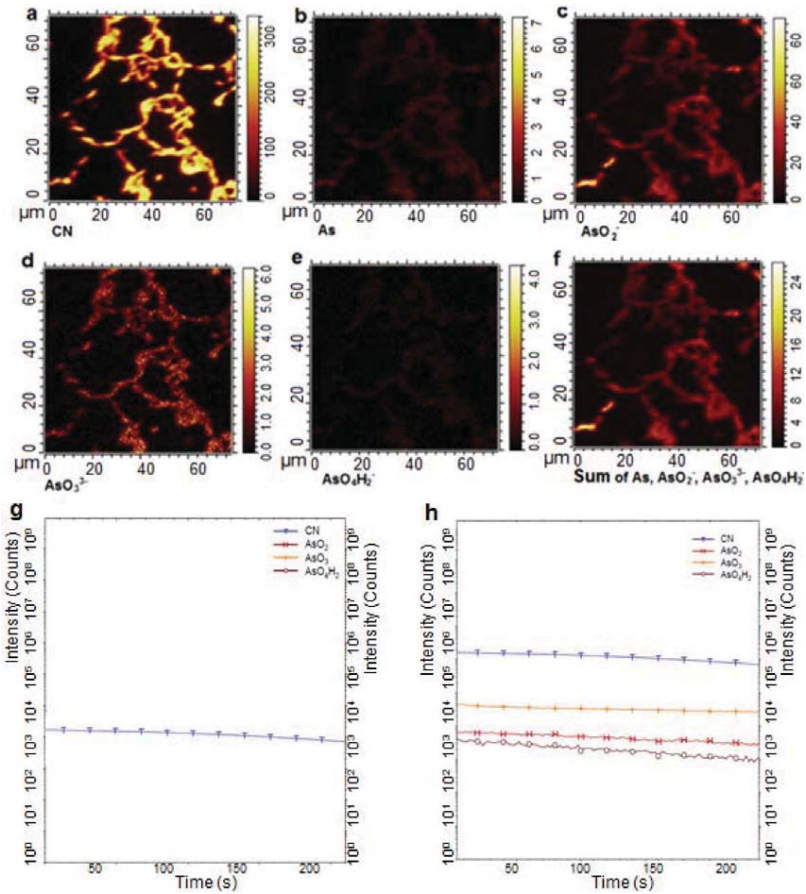

Fig. 3. Analysis of arsenic species inside the bacterial cells by using TOF-SIMS. a-f, ion imaging. g-h, depth profiling. a, total protein signals. b, free form of arsenic. c, meta- arsenite ions (AsO_2^-) signal. d, ortho- arsenite ion AsO_3^{3-} signal. e, arsenate (AsO_4H_2) ion signal and f, sum of different types of arsenics. The scale represents the intensity of ion imaging. g, depth profiling of bacterial cells grown on medium without arsenate (control). Blue color represents protein signals, whereas dark brown color stands for background activity of arsenics. h, depth profiling of bacterial cells grown on medium containing arsenate. Blue, orange, red and dark brown colors represent protein signals, meta-arsenite, ortho-arsenite and arsenate, respectively.

These results showed that after 24 h of exposure to B1-CDA the concentration of arsenic in the liquid medium decreased from 50 mM to 27 mM but after 48 h the reduction rate was a bit lower. This is because of bacterial efflux of arsenic to medium. Almost similar pattern of arsenic accumulation was observed also in the bacterial dry biomass. These results remain in agreement with those reported previously by Banerjee et al.[48] These researchers have shown that accumulation of arsenic in bacterial cells decreased after 48 h but it increased after 72 h. These results indicate that theoretically under laboratory conditions two independent exposures will be required for reducing arsenics in the growth medium to a safe level. In control samples (medium not exposed to B1-CDA), we did not observe any temporal change in the concentration of arsenic. These results directly suggest

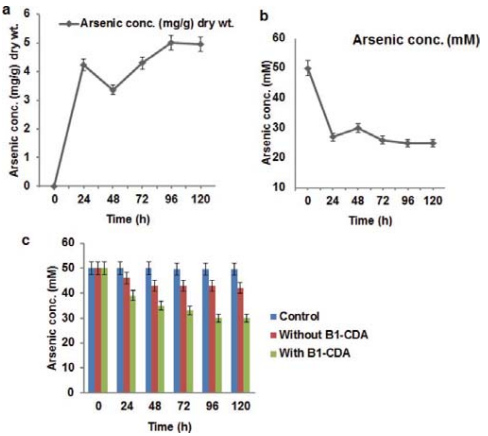

Fig. 4. Estimation of arsenics inside the bacterial cells, in growth medium and reconstructed field water (RFW). a, arsenic accumulated inside the cells. b, arsenic in the cell free growth medium. c, amount of total arsenic in RFW. Blue, red and green bars represent the amount of total arsenic in autoclaved RFW without exposure to B1-CDA (control), the amount of total arsenic in non-autoclaved RFW without exposure to B1-CDA and the amount of total arsenic in non-autoclaved RFW exposed to B1-CDA, respectively.

that the reduction of arsenic concentration we observed in growth medium treated with B1-CDA is indeed due to the biological activity of this bacterium.

Analyses of reconstructed field water (RFW)

In order to determine whether the B1-CDA strain can also take up and accumulate arsenics from natural conditions, we attempted to create "reconstructed field water" (RFW) in the laboratory as described in the Methods. Soil samples collected from the arsenic contaminated regions in Bangladesh were mixed with autoclaved tap water by shaking at 250 rpm for 24 h. The mixture was allowed to sediment and the supernatant (RFW) was collected and supplemented with (50 mM) or without arsenate. The RFW was then exposed to B1-CDA for 120 h and arsenic concentrations were analyzed by using Inductively Coupled Plasma-Mass Spectrometry (ICP-MS).

Autoclaved RFW supplemented with 50 mM arsenate was used as control and analyzed similarly by ICP-MS. The results of this analysis are presented in Figure 4c. The results reveal that the concentration of arsenic in the RFW treated with B1-CDA decreased from 50 mM to 30 mM (40%), whereas in RFW without treatment with B1-CDA decreased from 50 mM to 42 mM (16%). These results confirm that (i) B1-CDA can also decrease arsenic concentration in the RFW, and (ii) the RFW contained other arsenic-accumulating microorganisms derived from field soils (bacterial growth was observed in the RFW even in the absence of B1-CDA, data not shown). In the control samples (autoclaved RFW without exposure to B1-CDA) we did not see any temporal change in arsenic concentration.

To further confirm the ability of B1-CDA, the autoclaved RFW containing 50 mM sodium arsenate was treated similarly with B1-CDA. This experiment revealed that the concentration of arsenic in RFW reduced from 50 mM to 37 mM (26%, data not shown). The results obtained in the experiments with the RFW are a bit different from those we obtained with LB medium. Obviously, under natural conditions the biological activity of B1-CDA bacterium may vary significantly depending on many environmental factors such as physical and nutritional conditions for bacterial growth, interaction with other microbes existing in nature, presence of other chemical substances in soils that may interact with arsenic uptake, etc. In the RFW experiment, it was not possible to maintain the physical conditions for the bacterial growth in nature such as fluctuation in temperature, pH, nutrients and light intensity etc. In spite of this, we can confirm that the bacterium B1-CDA has proven its capability for removing arsenics from liquid sources such as the RFW or LB medium. These features make B1-CDA a potential candidate for remediation of arsenics from contaminated waters.

While several researchers have reported bacterial strains that are resistant to arsenics [36,45,49–53] none have demonstrated to date that their strains can accumulate arsenics inside the cells at high levels (5.0 mg g^{-1} dwt. of cell biomass) as reported here with strain B1-CDA. This bacterium is therefore unique and this is the first report that a soil borne *Lysinibacillus*-like strain from South East Asia can be used for the elimination of arsenics from contaminated sources, specifically waters. Moreover, very high accumulation of arsenics inside the bacterial cells will open up a new era for purification of arsenics from these bacteria and its recycling by the biotech and nanotech industries.

We are currently unable to explain how the bacterial cells avoid arsenic toxicity. One exciting hypothesis is the incorporation of arsenic into their proteins and DNA as well as other metabolic activities.[54] This hypothesis remains in partial agreement with those reported previously [36] where the authors claimed that arsenics taken up by the bacterial cells can substitute phosphorous in their metabolic processes. Arsenic-resistant strains also utilize arsenic in their metabolism, either as a means of generating energy through chemoautotrophic arsenite oxidation [55] or using arsenate as a terminal electron acceptor in an aerobic respiration.[56] These microbes are widely distributed in the environment and heavy metal contaminated

soil and water are the potential sources of heavy metal-resistant bacteria.[12]

Scanning electron microscopic (SEM) studies

Scanning electron microscopic (SEM) studies were performed on the bacterial isolate grown in the presence and absence of arsenic. SEM images are shown in Fig. 5. Results indicated that B1-CDA formed long chains in the presence of arsenic compared to the untreated cells (Figs. 5a, 5b). The long chainlike structure represents the mode of response to arsenic stress. These changes in morphological structure might be a possible strategy for cells to accumulate metals inside the cells indicating that the strain B1-CDA could accumulate arsenic and contribute to bioremediation of this toxic metal. Several researchers have shown the bacterial elongation in presence of toxic heavy metals.[13]

In conclusion, the results from these studies confirm that the bacterial strain B1-CDA isolated from a cultivated but arsenic contaminated land in the southwest region of Bangladesh has potential for reducing arsenics in the contaminated sources to safe levels. Therefore, the socio-economic impact of our research will be highly significant for these countries especially in the developing world where impoverished families and villages are most impacted. Hence our discovery should be considered to be the most vital to the *national strategies for accelerated poverty reduction*. Besides human arsenic poisoning, our discovery will also benefit livestock and native animal species. Therefore, the outcome of this research will be vital not only for people in the affected area but also for human populations in other countries which have credible health concerns as a consequence of arsenic-contaminated water and foods.

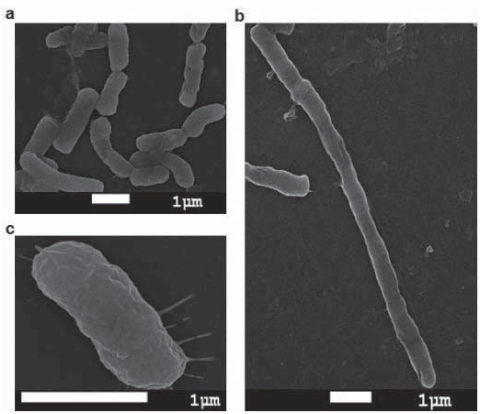

Fig. 5. Scanning electron micrograph representing effect of metals on cellular morphology of the isolates a, strain B1-CDA in absence of arsenic, magnification 6000×. b, strain B1-CDA in presence of 50 mM arsenate, magnification 6000×. c, B1-CDA in presence of arsenate magnifications 20,000×.

Acknowledgment

We acknowledge the Swedish South Asian Studies Network (SASNET) in Lund for delivering us information on South Asian research.

Funding

This research has been funded mainly by the Swedish International Development Cooperation Agency (SIDA, grant no. AKT-2010-018) and partly by the Swedish Research Council for Environment, Agricultural Sciences and Spatial Planning (FORMAS, grant no. 229-2007-217). A small grant from the Nilsson-Ehle (The Royal Physiographic Society in Lund) foundation in Sweden is also acknowledged.

References

[1] Marshall, G.; Ferreccio, C.; Yuan, Y.; Bates, M.N.; Steinmaus, C.; Selvin, S.; Liaw, J.; Smith, A.H. Fifty-year study of lung and bladder cancer mortality in Chile related to arsenic in drinking water. J. Natl. Cancer Inst. **2007**, *99*, 920–928.

[2] Chen, Y.; Parvez, F.; Gamble, M.; Islam, T.; Ahmed, A.; Argos, M.; Graziano, J.H.; Ahsan, H. Arsenic exposure at low-to-moderate levels and skin lesions, arsenic metabolism, neurological functions, and biomarkers for respiratory and cardiovascular diseases, Review of recent findings from the health effects of arsenic longitudinal study (HEALS) in Bangladesh. Toxicol. Appl. Pharmacol. **2009**, *239*, 184–192.

[3] Argos, M.; Kalra, T.; Rathouz, P.J.; Chen, Y.; Pierce, B.; Parvez, F.; Islam, T.; Ahmed, A.; Rakibuz-Zaman, M.; Hasan, R.; Sarwar, G.; Slavkovich, V.; van Geen, A.; Graziano, J.; Ahsan, H. Arsenic exposure from drinking water.; and all-cause and chronic-disease mortalities in Bangladesh (HEALS): a prospective cohort study. Lancet **2010**, *376*, 252–258.

[4] Zhao, F.J.; McGrath, S.P.; Meharg, A. Arsenic as a food chain contaminant, mechanisms of plant uptake and metabolism and mitigation strategies. Annu. Rev. Plant Biol. **2010**, *61*, 535–559.

[5] Huang, C.Y.; Chu, J.S.; Pu, Y.S.; Yang, H.Y.; Wu, C.C.; Chung, C.J.; Hsueh,Y.M. Effect of urinary total arsenic level and estimated glomerular filtration rate on the risk of renal cell carcinoma in a low arsenic exposure area. J. Urol. **2011**, *185*, 2040–2044.

[6] Tani, M.; Jahiruddin, M.; Egashira, K.; Kurosawa, K.; Moslehuddin, A.Z.M.; Rahman, M.Z. Dietary intake of arsenic by households in Marua village in Jessore. J. Environ. Nat. Res. **2012**, *5*, 283–288.

[7] World Health Organization (WHO). Detection, management and surveillance of arsenicosis in South-East Asia region. Cause D., ed.; World Health Organization Technical Publication: New Delhi, India, 2006; 1–38.

[8] Oremland, R.S.; Stolz, J.F. The ecology of arsenic. Science **2003**, *300*, 939–944.

[9] Chaalal, O.; Zekri, A.Y.; Islam, R. Uptake of heavy metals by microorganisms, an experimental approach. Energy Sour. **2005**, *27*, 87–100.

[10] Zafar, S.; Aqil, F.; Ahmad, I. Metal tolerance and biosorption potential of filamentous fungi isolated from metal contaminated agricultural soil. Bioresour. Technol. **2007**, *98*, 2557–2561.

[11] Congeevaram, S.; Dhanarani, S.; Park, J.; Dexilin, M.; Thamaraiselvi, K. Biosorption of chromium and nickel by heavy metal resistant fungal and bacterial isolates. J. Hazard. Mater. **2007**, *146*, 270–277.

[12] Clausen, C.A. Isolating metal-tolerant bacteria capable of removing copper, chromium, and arsenic from treated wood. Waste Manage. Res. **2000**, *18*, 264–268.

[13] Banerjee, S.; Datta, S.; Chattyopadhyay, D.; Sarkar, P. Arsenic accumulating and transforming bacteria isolated from contaminated soil for potential use in bioremediation. J. Environ. Sci. Health Pt. A **2011**, *46*, 1736–1747.

[14] Bahar, M.M.; Megharaj, M.; Naidu, R. Arsenic bioremediation potential of a new arsenite-oxidizing bacterium Stenotrophomonas sp. MM-7 isolated from soil. Biodegradation **2012**, *23*, 803–812.

[15] Halttunen, T.; Finell, M.; Salminen, S. Arsenic removal by native and chemically modified lactic acid bacteria. Int. J. Food Microbiol. **2007**, *120*, 173–178.

[16] Corsini, A.; Zaccheo, P.; Muyzer, G.; Andreoni, V.; Cavalca, L. Arsenic transforming abilities of groundwater bacteria and the-combined use of Aliihoeflea sp. strain 2WW and goethite inmetalloid removal. J. Hazard. Mater. **2014**, *269*, 89–97.

[17] Mondal, P.; Majumder, C.B.; Mohanty, B. Growth of three bacteria in arsenic solution and their application for arsenic removal from wastewater. J. Basic Microbiol. (Short Communication) **2008**, *48*, 521–525.

[18] Lozano, L.C.; Dussa´n, J. Metal tolerance and larvicidal activity of Lysinibacillus sphaericus. World J. Microbiol. Biotechnol. **2013**, *29*, 1383–1389.

[19] Kao, A.C.; Chu, Y.J.; Hsu, F.L.; Liao, H.V.C. Removal of arsenic from groundwater by using a native isolated arsenite-oxidizing bacterium. J. Contaminant. Hydrology. **2013**, *155*, 1–8.

[20] de Crécy, E.; Metzgar, D.; Allen, C.; Pénicaud, M.; Lyons, B.; Hansen, C.J.; de Crécy-Lagard, V. Development of a novel continuous culture device for experimental evolution of bacterial populations. Appl. Microbiol. Biotechnol. **2007**, *77*, 489–496.

[21] de Crécy, E.; Jaronski, S.; Lyons, B.; Lyouns, T.J.; Keyhani, N.O. Directed evolution of a filamentous fungus for thermo tolerance. BMC Biotechnol. **2009**, *9*, 74.

[22] Singh, A.; Kuhad, R.C.; Ward, O.P. *Advances in Applied Bioremediation*, 1st Ed.; Springer: New York, 2009.

[23] Eichorst, S.A.; Breznak, J.A.; Schmidt, T.M. Isolation and characterization of soil bacteria that define Terriglobus gen. nov. in the Phylum Acidobacteria. Appl. Environ. Microbiol. **2007**, *73*, 2708–2717.

[24] Krieg, N.R. *Bergey's Manual of Systematic Bacteriology*, Vol. 1; Williams and Wilkins: Baltimore, MD, 1984.

[25] Saitou, N.; Nei, M. The neighbor-joining method, A new method for reconstructing phylogenetic trees. Mol. Biol. Evol. **1987**, *4*, 406–425.

[26] Felsenstein, J. Confidence limits on phylogenies, An approach using the bootstrap. Evolution **1985**, *39*, 783–791.

[27] Kimura, M. A simple method for estimating evolutionary rate of base substitutions through comparative studies of nucleotide sequences. J. Mol. Evol. **1980**, *16*, 111–120.

[28] Tamura, K.; Stecher, G.; Peterson, D.; Filipski, A.; Kumar, S. MEGA6, Molecular Evolutionary Genetics Analysis version 6.0. Mol. Biol. Evol. **2013**, *30*, 2725–2729.

[29] Mergeay, M. Heavy metal resistances in microbial ecosystems. In *Molecular Microbial Ecology Manual*; Akkermans, A.D.L., Elsas, J.D., de Bruijn, F.J., Eds.; Kluwer Academic Publishers: Dordrecht, 1995; 6.1.7/1–6.1.7/17.

[30] Villegas-Torres, M.F.; Bedoya-Reina, O.C.; Salazar, C.; Vives-Florez, M.J.; Dussan, J. Horizontal arsC gene transfer among microorganisms isolated from arsenic polluted soil. Intl. Biodeterior. Biodegrad. **2011**, *65*,147–152.

[31] Kollmer, F. Cluster primary ion bombardment of organic materials. Appl. Surface. Sci. **2004**, *231–232*, 153–158.

[32] Touboul, D.; Kollmer, F.; Niehuis, E.; Brunelle, A.; Laprevote, O. Improvement of biological time-of-flight-secondary ion mass spectrometry imaging with a bismuth cluster ion source. J. Am. Chem. Soc. **2005**, *16*, 1608–1618.

[33] Sodhi, R.N.S. Time-of-flight secondary ion mass spectrometry (TOF-SIMS), versatility in chemical and imaging surface analysis. Analyst **2004**, *129*, 483–487.

[34] Bhakoo, M.; Herbert, R.A. The effects of temperature on the fatty acid and phospholipid composition of four obligately psychrophilic Vibro spp. Arch. Microbiol. **1979**, *121*, 121–127.

[35] Doenmez, G.; Aksu, Z. Bioaccumulation of copper (II) and Nickel (II) by the non-adapted and adapted growing Candida sp. Water Res. **2001**, *35*, 1425–1434.

[36] Wolfe-Simon, F.; Blum, J.S.; Kulp, T.R.; Gordon, G.W.; Hoeft, S.E.; Pett-Ridge, J.; Stolz, J.F.; Webb, S.M.; Weber, P.K.; Davies, P.C.; Anbar, A.D.; Oremland, R.S. A bacterium that can grow by using arsenic instead of phosphorus. Science **2011**, *332*, 1163–1166.

[37] Hayden, E.C. Open research casts doubt on arsenic life. Nat. News **2011**. doi:10.1038/news.2011.469.

[38] Achour, A.R.; Bauda, P.; Billard, P. Diversity of arsenite transporter genes from arsenic-resistant soil bacteria. Res. Microbiol. **2007**, *158*, 128–137.

[39] DeMel, S.; Shi, J.; Martin, P.; Rosen, B.P.; Edwards, B.F. Arginine 60 in the ArsC arsenate reductase of *E. coli* plasmid R773 determines the chemical nature of the bound As (III) product. Prot. Sci. **2004**, *13*, 2330–2340.

[40] Mukhopadhyay, R.; Shi, J.; Rosen, B.P. Purification and characterization of Acr2p.; the Saccharomyces cerevisiae arsenate reductase. J. Biol. Chem. **2000**, *275*, 21149–21157.

[41] Dhankher, O.P.; Rosen, B.P.; McKinney, E.C.; Meagher, R.B. Hyperaccumulation of arsenic in the shoots of Arabidopsis silenced for arsenate reductase (ACR2). Proc. Natl. Acad. Sci. USA **2006**, *103*, 5413–5418.

[42] Nahar, N.; Rahman, A.; Moś, M.; Warzecha, T.; Algerin, M.; Ghosh, S.; Johnson-Brousseau, S.; Mandal, A. In silico and in vivo studies of an Arabidopsis thaliana gene, ACR2, putatively involved in arsenic accumulation in plants. J. Mol. Model. **2012**, *18*, 4249–4262.

[43] Hughes, M.F. Arsenic toxicity and mechanisms of action. Toxicology **2002**, *133*, 1–16.

[44] Muller, D.; Médigue, C.; Koechler, S.; Barbe, V.; Barakat, M.; Talla, E.; et al. A tale of two oxidation states, bacterial colonization of arsenic-rich environments. Plos Genet. **2007**, *3*, 518–530.

[45] Anderson, C.R.; Cook, G.M. Isolation and characterization of arsenate-reducing bacteria from arsenic contaminated sites in New Zealand. Curr. Microbiol. **2004**, *48*, 341–347.

[46] Jones, C.A.; Langner, H.W.; Anderson, K.; McDermott, T.R.; Inskeep, W.P. Rates of microbially mediated arsenate reduction and solubilization. Sci. Soc. Am. J. **2000**, *64*, 600–608.

[47] Macur, R.E.; Wheeler, J.T.; McDermott, T.R.; Inskeep, W.P. Microbial populations associated with the reduction and enhanced mobilization of arsenic in mine tailing. Environ. Sci. Technol. **2001**, *35*, 3676–3682.

[48] Banerjee, S.; Majumdar, J.; Samal, A.C.; Bhattachariya, P.; Santra, S.C. Biotransformation and bioaccumulation of arsenic by *Brevibacillus brevis* isolated from arsenic contaminated region of West Bengal. J. Environ. Sci. Toxicol. Food Technol. **2013**, *3*, 1–10.

[49] Jackson, C.R.; Jackson, E.F.; Dugas, S.L.; Gamble, K.; Williams, S.E. Microbial transformations of arsenite and arsenate in natural environments. Recent Res. Dev. Microbiol. **2003**, *7*, 103–118.
[50] Escalante, G.; Campos, V.L.; Valenzuela, C.; Yañez, J.; Zaror, C.; Mondaca, M.A. Arsenic resistant bacteria isolated from arsenic contaminated river in the Atacama Desert (Chile). Bull. Environ. Contam. Toxicol. **2009**, *83*, 657–661.
[51] Kaushik, P.; Rawat, N.; Mathur, M.; Raghuvanshi, P.; Bhatnagar, P.; Swarnkar, H.; Flora, S. Arsenic hyper-tolerance in four Microbacterium species isolated from soil contaminated with textile effluent. Toxicol. Int. **2012**, *19*, 188–194.
[52] Raja, C.E.; Omine, K. Arsenic, boron and salt resistant Bacillus safensis MS11 isolated from Mongolia desert soil. Afri. J. Biotechnol. **2012**, *11*, 2267–2275.
[53] Shakya, S.; Pradhan, B.; Smith, L.; Shrestha, S.; Tuladhar, S. Isolation and characterization of aerobic culturable arsenic-resistant bacteria from surface water and ground water of Rautahat District, Nepal. J. Environ. Manag. **2012**, *95*, 250–255.
[54] Mukhopadhyay, R.; Rosen, B.P.; Phung, L.T.; Silver, S. Microbial arsenic, from geocycles to genes and enzymes. FEMS Microbiol. Rev. **2002**, *26*, 311–325.
[55] Santini, J.M.; Sly, L.I.; Schnagl, R.D.; Macy, J.M. A new chemolithoautotrophic arsenite-oxidizing bacterium isolated from a gold mine, Phylogenetic.; physiological and preliminary biochemical studies. Appl. Environ. Microbiol. **2000**, *66*, 92–97.
[56] Stolz, J.F.; Oremland, R.S. Bacterial respiration of arsenic and selenium. FEMS Microbiol. Rev. **1999**, *23*, 615–627.

Journal of Environmental Science and Health, Part A (2015) **50**, 1136–1147

ISSN: 1093-4529 (Print); 1532-4117 (Online)
DOI: 10.1080/10934529.2015.1047670

Taylor & Francis
Taylor & Francis Group

Bioremediation of hexavalent chromium (VI) by a soil-borne bacterium, *Enterobacter cloacae* B2-DHA

AMINUR RAHMAN[1,2], NOOR NAHAR[1], NEELU N. NAWANI[3], JANA JASS[2], KHALED HOSSAIN[4], ZAHANGIR ALAM SAUD[4], ANANDA K. SAHA[5], SIBDAS GHOSH[6], BJÖRN OLSSON[1] and ABUL MANDAL[1]

[1]*Systems Biology Research Center, School of Bioscience, University of Skövde, Skövde, Sweden*
[2]*The Life Science Center, School of Science and Technology, Örebro University, Örebro, Sweden*
[3]*Dr. D. Y. Patil Biotechnology and Bioinformatics Institute, Tathawade, Pune, India*
[4]*Department of Biochemistry & Molecular Biology, University of Rajshahi, Rajshahi, Bangladesh*
[5]*Department of Zoology, University of Rajshahi, Rajshahi, Bangladesh*
[6]*School of Arts and Science, Iona College, New Rochelle, New York, USA*

Chromium and chromium containing compounds are discharged into the nature as waste from anthropogenic activities, such as industries, agriculture, forest farming, mining and metallurgy. Continued disposal of these compounds to the environment leads to development of various lethal diseases in both humans and animals. In this paper, we report a soil borne bacterium, B2-DHA that can be used as a vehicle to effectively remove chromium from the contaminated sources. B2-DHA is resistant to chromium with a MIC value of 1000 $\mu g\ mL^{-1}$ potassium chromate. The bacterium has been identified as a Gram negative, *Enterobacter cloacae* based on biochemical characteristics and 16S rRNA gene analysis. TOF-SIMS and ICP-MS analyses confirmed intracellular accumulation of chromium and thus its removal from the contaminated liquid medium. Chromium accumulation in cells was 320 $\mu g/g$ of cells dry biomass after 120-h exposure, and thus it reduced the chromium concentration in the liquid medium by as much as 81%. Environmental scanning electron micrograph revealed the effect of metals on cellular morphology of the isolates. Altogether, our results indicate that B2-DHA has the potential to reduce chromium significantly to safe levels from the contaminated environments and suggest the potential use of this bacterium in reducing human exposure to chromium, hence avoiding poisoning.

Keywords: Bioremediation, chromium, *Enterobacter cloacae*, human health, soil borne bacterium, tannery effluents.

Introduction

There are high chromium contaminations spreading through soil and water by industrial activities, in particular, the use of chrome liquor in leather processing. In addition to leather processing, chromium is widely used in wood preservation, steel production, chromium/electroplating, metal processing, alloy formation, textiles, ceramics and thermonuclear weapons manufacturing, among others.[1–3] Also, several agronomic practices including the use of organic biomass, like sewage sludge or fertilizers based on leather that contain varying degrees of chromium, are the contributors to environment contamination. For example, there are about 185 leather processing industries in Bangladesh discharging solid and liquid wastes without proper treatment directly into the environments including river and natural canals.[4]

Chromium is one of the major sources of environmental pollution and is well known for its toxic, carcinogenic, and mutagenic effects on humans and other living organisms, hence chromium is classified as a priority pollutant.[5] Trace amount of chromium is an essential element in the diet, because it regulates the glucose metabolism in the human body.[6] Chromium is commonly present in the soil in two oxidized forms: (i) trivalent chromium Cr(III) and (ii) hexavalent chromium Cr(VI). Cr(III) is less mobile, hence less toxic,[7] whereas Cr(VI) is a soluble oxidizing agent that is easily reduced intracellularly to Cr^{5+} and reacts with nucleic acids and other cellular components to create carcinogenic and mutagenic effects in biological systems.[8] Therefore, bioremediation of Cr(VI) is essential to protect human health and the environment.

Address correspondence to Abul Mandal, System Biology Research Center, School of Bioscience, University of Skövde, P. O. Box 408, Skövde SE-541 28, Sweden; E-mail: abul.mandal@his.se
Received February 26, 2015.
Color versions for one or more of the figures in the article can be found online at www.tandfonline.com/lesa.

Many metal pollutants including chromium cannot be degraded like organic contaminants. To date, many conventional physicochemical methods have been developed for removing toxic CrO_4^{2-} such as ion exchange, electrochemical treatment, evaporation, reverse osmosis, precipitation, and adsorption on activated coal. Nevertheless, most of these methods are inefficient and very expensive especially when the contamination levels are very low.[8,9] Alternatively, various cost effective and eco-friendly biological approaches have been considered for bioremediation.[10] To that effect, a number of microorganisms have been reported to resist Cr(VI) by periplasmic biosorption, intracellular bioaccumulation, and/or biotransformation to a less toxic speciation state through direct enzymatic reaction, including *Pseudomonas* sp.[11] *Enterobacter aerogenes*,[12] *Enterobacter cloacae*,[13–16] *Microbacterium*,[17] *Desulfovibrio*,[18] *Escherichia coli*,[19] *Shewanella alga*,[20] *Bacillus* sp.[8] and several other bacterial species.[21] Although, most of these microbes have been isolated from tannery sludge, industrial sewage, evaporation ponds, or discharged water, or were purchased from culture collections, the availability of high Cr(VI)-reducing organisms is an essential prerequisite for the efficient bioremediation of chromate-containing industrial waste water.

Over the past decade we have collected water and soil samples from many regions of South Asia, particularly Bangladesh and India, where metal including chromium, arsenic contaminated ground water is frequently used for both consumption and for irrigation of cultivated crops.[22–24]

The purpose of this study was to identify, isolate and characterize naturally occurring bacterial strain(s) that can grow on chromium contaminated soil or water and can also accumulate chromium in the cells thus reducing the level of this toxic metal in the contaminated source to a safe level. Until today, we have collected several hundred bacterial strains isolated from the chromium contaminated environment. Among this collection, we have recently identified and characterized a soil-borne bacterium B2-DHA that can survive and grow on medium containing up to 1000 $\mu g\ mL^{-1}$ potassium chromate and thereby reducing chromium contents in the contaminated source by 81%.

In this study we have used several modern techniques to localize chromium in the bacterial cells qualitatively and quantitatively. Dynamic time of flight secondary ion mass spectrometry (TOF-SIMS) imaging and depth profiling [25] have been employed to follow the distribution of chromium ion and its products within the cells.[26] Inductively coupled plasma - mass spectrometry (ICP-MS), the fastest growing trace element technique has been used to measure the amount of chromium in the dry bacterial cells. The concentration of chromium in the cell-free broth has been measured by using the inductively coupled plasma - atomic emission spectroscopy (ICP-AES).

We also report the results obtained from morphological, biochemical, and 16S rRNA characterization of the bacterium. Investigation of this strain to be utilized as a potential candidate for eliminating or significantly reducing chromium level in the contaminated source has been made. Hence, the results obtained in this investigation provide us with useful knowledge for the microbial bioremediation of chromium pollution.

Materials and methods

Collection of soil samples

Soil samples were collected from the landfills of leather manufacturing tannery industries in Bangladesh. These are located in the Hazaribagh tannery areas, a very close vicinity of the capital city Dhaka, where the tannery wastes have been disposed for many years. The soil surface at 0–15 cm in depth was collected, retained in plastic bags and kept at 4°C until further analysis including bacterial isolation.

Analysis of soil samples

The pH of soil samples was determined by shaking 5 g of soil in 50 mL of distilled water for one hour by using pH meter (pH meter 2210 Hanna Instruments, Carrollton, TX, USA). To determine the concentrations of different metals such as chromium, arsenic, sodium, potassium, chloride, phosphate, and nitrate, 5 g of the soil sample was air dried and mixed with 2 mL of HNO_3 (65%, Merck, Darmstadt, Germany) and 6 mL of HCl (37%, Merck, Darmstadt, Germany). The mixture was heated at 70°C for 1 h, and then diluted with 10 mL of deionized water. The acid-digested solution was filtered to remove residual particulates. Concentration of chromium, arsenic, sodium and potassium was determined by inductively coupled plasma atomic emission spectroscopy (ICP-AES).[27] However, concentrations of chloride and phosphate were determined by spectrophotometric analysis,[28] whereas nitrate was measured in a solution with KCl followed by flow injection analysis (FIA).[29] All samples were digested based on heat block digestion and analyzed by Eurofins Environment Testing Sweden AB (Lidköping, Sweden).

Chemicals and bacterial enrichment

Chemicals used in this experiment were analytical standard grade (Merck, Darmstadt, Germany and Sigma-Aldrich, St. Louis, MO, USA). All solutions were prepared with autoclaved double deionized water (ddH_2O), sterilized by syringe filtration (0.2-μm pore-size) and stored at 4°C in the dark until further use. The media for bacterial culture were autoclaved at 120°C for 15 min.

For isolation of chromium-resistant bacteria, the soil sample was serially diluted in sterile distilled water and plated aerobically in the modified Luria–Bertani (LB) medium containing peptone 10 g L^{-1}, sodium chloride 5 g L^{-1}, yeast extracts 5 g L^{-1}, D (+) glucose 1 g L^{-1} (Merck) supplemented with 50, 100, 150 or 200 μg mL^{-1} potassium chromate K_2CrO_4 (Sigma). Following incubation of these plates at 37°C for 48 h, several morphologically different colonies were picked randomly and streak-purified at least twice on the same medium for isolation of the single colonies. A number of colonies showing resistance to chromium were selected for further screening. Subsequently, only one strain B2-DHA was used for further studies because it demonstrated the best growth in presence of and resistance to chromium. Purified single colonies were inoculated in LB broth, cultured for 24 to 48 h and stored in 25% glycerol at −80°C for further analyses.

Effects of pH and temperature

The influences of pH and temperature on bacterial growth were assessed using LB medium. Autoclaved culture media at pH 5.0, 6.0, 7.0, 8.0 or 9.0 were used to test the effect of pH on bacterial growth. The inoculum of B2-DHA strain was 1% of the total volume of culture and incubated under continuous shaking at 180 rpm for 24 h. The bacterial growth was measured every 2 h using optical density measurement at 600 nm by Genesys 20 visible spectrophotometer (Thermo Scientific, Madison, WI, USA). For evaluation of the effect of temperature on bacterial growth, the cultures were incubated at 25, 30, 37 or 40°C. Similarly, the inoculum of B2-DHA strain was prepared from the logarithmic-phase cultures in LB broth without supplementation of chromium and incubated for 24 h with shaking at 180 rpm. The growth of bacterial cells was evaluated by measuring optical density of medium at regular intervals of 2 h at 600 nm. All experiments were carried out in triplicates. For the rest of this study, the strain B2-DHA was grown on media with pH 7 and culture temperature at 37°C due to the optimum growth at these conditions.

Minimum inhibitory concentration (MIC) of chromate and other heavy metals

The MIC of chromium for B2-DHA isolate was determined as reported by Mergeay.[30] Minimal salt broth[31] supplemented with different concentrations (600 μg mL^{-1}, 800 μg mL^{-1}, 1000 μg mL^{-1} and 1200 μg mL^{-1}) of Cr(VI) was used to determine the MIC for chromium. One percent inoculum of B2-DHA was added to the media in 50-mL falcon tubes. Bacteria cultured in minimal medium without Cr(VI) were used as controls. All tubes were incubated at 37°C with shaking at 180 rpm for 48–96 h. Optical density measurements for estimation of cell growth were carried out at 600 nm by using Genesys 20 visible spectrophotometer. Besides potassium chromate, the MIC of the bacterial isolate was checked for other heavy metals such as sodium arsenate (Na_2HAsO_4), ferric chloride ($FeCl_3$), manganese chloride ($MnCl_2$), zinc chloride ($ZnCl_2$), nickel chloride ($NiCl_2$) and silver nitrate ($AgNO_3$) at different concentrations.

Morphological and biochemical analyses

The colony morphology of the purified bacterial strains grown on medium containing potassium chromate was evaluated. Gram-staining and cellular morphology of the strain (data not shown) were studied based on both light- and electron microscopy (Carl Zeiss Inc. Thornwood, NY, USA).[32] Negative staining was performed to determine the production of a polysaccharide capsule by bacterial strains. A bacterial colony was mixed up in a drop of India ink on a slide and successively observed with the light microscope. Biochemical tests including motility, mannitol test, indole production, H_2S production, catalase test, oxidase test, urease test, carbohydrate (glucose, lactose, sucrose and rhamnose) fermentation, citrate utilization, hydrolysis of casein etc. were performed to facilitate the identification of the bacterium following *Bergey's Manual of Systematic Bacteriology*.[33]

The morphological analysis of strain B2-DHA was carried out by the Environmental Scanning Electron Microscope (ESEM) (Model: FEI-Quanta 200, Hillsboro, OR, USA) with an attached X-ray energy dispersive system (EDS). Bacterial culture was inoculated in a nutrient broth supplemented with 100 μg mL^{-1} of Cr(VI) kept at 37°C on rotator shaker at 150 rpm. Control incubations were carried out under the same conditions in the absence of Cr (VI). After 48 h of incubation 30 mL from each was centrifuged at 5000 rpm for 15 min to remove excess of liquid media. Pellets obtained were washed twice with sterile deionized water and further, the pellets were twice washed with phosphate-buffered saline (PBS). The cells were chemically fixed at 4°C for 18 h with 2% glutraldehyde: formaldehyde in 1 mL PBS (1:2 glutraldehyde: formaldehyde) in a dark conditions. After 18 h of incubation each sample was centrifuged at 5000 rpm for 15 min. Dehydration of pellet was carried out by a series of alcohol treatments (40, 60, 80, 90, and 100%) for 5 min, respectively. Then, 10 μL of sample was transferred to a 1 mm × 1 mm slide. Slides were transferred to a desiccator for moisture absorption. Samples processed were taken for ESEM-EDS analysis at IIT, Powai, Mumbai, India.

16S rRNA sequencing

Genomic DNA was isolated using DNeasy Blood and Tissue Kit (Qiagen, Germany, Cat. No. 69504) as per

manufacturer. For PCR amplification of the nearly full-length 16S rRNA domain, *Bacteria* specific universal primers 8F (5-AGAGTTTGATCCTGGCTCAG-3) and 1492R (5-TACGGTTACCTTGTTACGACTT-3) were used in PCR reaction mixtures containing deoxynucleotide triphosphates (dNTPs) at 50 μmol each, primers at 2.5 pmol each, 1.5 U Taq DNA polymerase in 1× buffer, 50 ng of DNA template, 2.5 mM $MgCl_2$ in a 50-μL reaction.

The thermal cycling program included initial denaturation at 95°C for 5 min, followed by 34 cycles of denaturation at 95°C for 45 sec, primer annealing at 55°C for 1 min and primer extension at 72°C for 1.5 min. This was followed by a final extension step at 72°C for 10 min and the samples were cooled to 4°C. The amplified PCR products were visualized by agarose-gel electrophoresis and the DNA fragment was purified using QIAquick Gel Extraction Kit (Qiagen). DNA sequencing reaction of PCR amplicon was carried out using BDT v3.1 Cycle sequencing kit (Austin, TX, USA) on ABI 3730×l Genetic Analyzer with same primers: 8F and 1492R. A similarity search for the nucleotide sequence of 16S rRNA of the test isolate was carried out using the NCBI nucleotide BLAST (http://blast.ncbi.nlm.nih.gov/). The 16S rRNA sequence was submitted to NCBI GenBank for registration.

Evolutionary relationship of taxa

The evolutionary history was revealed using the Neighbor-Joining method.[34] The percentage of replicate trees in which the associated taxa clustered together in the bootstrap test (500 replicates) was shown next to the branches.[35] The evolutionary distances were computed using the Kimura 2-parameter method [36] and these were in the units of the number of base substitutions per site. The analysis involved 23 nucleotide sequences. Codon positions included were 1st+2nd+3rd+Noncoding. All positions with less than 95% site coverage were eliminated. This means that fewer than 5% alignment gaps, missing data, and ambiguous bases were allowed at any position. There were a total of 1227 positions in the final data set. Evolutionary analyses were conducted in MEGA6.[37]

Analysis of chromium contents in liquid medium by ICP-AES

The capacity of B2-DHA strain to decrease the chromium contents in the liquid medium was determined by the inductively coupled plasma atomic emission spectroscopy (ICP-AES).[27] The strain B2-DHA was grown in 50-mL LB medium supplemented with 100 μg mL^{-1} of chromium and incubated at 37°C with shaking at 180 rpm for 5 days. The B2-DHA cells grown similarly but without potassium chromate were used as controls. Five sets of experiments were performed with three replicates along with controls. The cell free medium was collected by centrifugation (10,000 rpm for 10 min) using a Sorvall rotor (Sorvall Super T21, Thermo Scientific). The cell free broth was filtered through a 0.2-μm filter and acidified to pH 2.0 with 30% suprapure nitric acid (Merck). The acidified cell-free broth was analyzed for total chromium content by using ICP-AES.[27]

Analysis of chromium contents in the bacterial cells by ICP-MS

The bioaccumulation of chromium was determined in the B2-DHA strain grown in 50 mL LB medium supplemented with 100 μg mL^{-1} of chromium and incubated at 37°C for 5 days. After incubation, samples were collected and centrifuged at 10,000 rpm for 10 min at Sorvall rotor (Sorvall Super T21, Thermo Scientific). The pellet was washed with 0.9 % saline twice and air-dried until a constant dry weight was achieved. The entire contents of the flask were harvested and the dry weight of the cells was recorded. Cells were digested with 30% suprapure nitric acid (Merck, Germany) according to ratio of 7.5 mL nitric acid per g dry biomass using microwave digestion. The samples were brought to a constant volume prior to determination of chromium contents. Measurement of chromium was also carried out similarly in the control experiments using media containing chromium but not exposed to B2-DHA and in media devoid of chromium but treated with B2-DHA. All analyses were carried out after filtration of the cell digest through a 0.2-μm filter. The chromium present in the dried pellets was determined by the inductively coupled plasma mass spectroscopy (ICP -MS).[38]

Confirmation of chromium ions in the bacterial cells by TOF-SIMS

Bacterial samples were grown in liquid medium supplied without or with 100 μg mL^{-1} chromium to perform the TOF-SIMS ion imaging analyses. This technique uses a focused, primary ion beam to bombard a solid sample in ultrahigh vacuum, producing secondary ions from the sample surface. Cells were collected by repeated (3 times) centrifugation at 10,000 rpm for 15 min in a microcentrifuge and washing with autoclaved deionized distilled water. Cells were then deposited and spread out on microscopic slides and analyzed using TOF-SIMS Version 6.1 instrument (ION-TOF, GmbH, Münster, Germany) equipped with a 30 keV Bi_3^+ LMIG analysis gun[39,40] with a 512 × 512 μm raster. Electron bombardment (20 eV) was used to minimize charge built-up at the surface.

Depth profiling of the chromium ions inside the cells was performed by using a 0.5 keV Cs^+ sputter gun. Depth profiling and imaging were performed in the burst mode (analyse 30 scans, sputter 0.20 s, pause 6.0 s, to

a total of approx. 250 s of sputtering). Desorbed secondary ions were accelerated to 2 keV, mass analysed in the flight tube, and post-accelerated to 10 keV before detection. The Bi3-LMIG was set in the high current bunched mode (negative polarity, analysis area 47 × 47 μm, mass resolution m Δm^{-1}: 6000; focus of the ion beam: 150 nm)[41] with a target current of 0.15 pA, while Cs ions were used for sputtering, with a current of 5 nA and with a 250 × 250 μm raster.

All image analyses were performed using the ION-TOF Surface Lab software (Version 6.1, ION-TOF, GmbH, Münster, Germany) except for image resizing, for publication purposes, which was done in Adobe Photoshop CS-2 (Adobe Systems Incorporated, San Jose, CA, USA). Each ion image was normalized to the intensity of the brightest pixel ranging color values of 0 (zero intensity) to 256 (brightest intensity). All other intensities are assigned accordingly using a linear relationship.

Statistical analyses

Statistical analyses were performed using standard statistical package Microcal (TM) Origin 6.0 version (http://www.microcal.com/). For the examined parameters one- and two-factor variance analyses using the independent system were done. The zero or alternative hypotheses were accepted on the basis of the *F*-test at $p = 0.05$ or $p = 0.01$ and marked as */ or **/, respectively. The significance of differentiation in mean values for individual properties was checked using the least significant difference (LSD) test. All analyses were performed in triplicate, and the results are presented as mean value with standard deviation.

Results and discussion

Isolation of toxic-metal-resistant bacteria from soils contaminated with tannery effluents—Soil characteristics

Soils containing heavy metals are potential sources for identifying toxic-metal-resistant bacteria. In this study, we have isolated chromium-resistant bacterial strains from soil samples collected from the landfills comprised of tannery effluents discharged from leather manufacturing industries located in the Hazaribagh area in Bangladesh. The pH of the soil samples was recorded to be neutral, 7.1 (± 0.3). Distribution of soil metals was found to be as follows: (i) 15.4 (± 0.06) μg chromium/g soil d.wt., (ii) 7.52 (± 0.02) μg arsenic/g soil d. wt., (iii) 4.1 (± 0.30) μg chloride/g soil d.wt., (iv) 6.4 (± 0.04) μg sodium/g soil d.wt., (v) 4.4 (± 0.05) μg potassium/g soil d.wt (vi) 0.85 (± 0.03) μg phosphate/g d.wt., and (vii) 0.32 (± 0.02) μg nitrate/g soil d.wt.

Characterization and identification of the soil-borne B2-DHA

Characterization of the strain B2-DHA was performed on the basis of colonial morphology, cellular morphology and Gram staining properties. The colonial morphology of the strain appeared to be circular and convex, whereas cellular shape of the strain was found to be cocci-like and the isolate was Gram negative and motile in character. Biochemical characterization of the isolate was performed in terms of carbohydrate utilization such as the strain showed positive in glucose, lactose, sucrose fermentation. On the other hand the strain showed negative in indole-, urea-, capsule- and hydrogen sulfide production. Moreover, B2-DHA was positive in the catalase test and negative in the oxidase test. The data revealed that B2-DHA belongs to the genus *Enterobacteria*. The BLASTN search of the 16S rRNA gene sequence (1227 bp) of the isolate (accession number KF920746) showed 97% similarity with that of *Enterobacteria cloacae* (Fig. 1) confirming further that the B2-DHA strain belongs to the genus *Enterobacteria*. This is consistent with previously reported studies on chromate reduction by *Enterobacter cloacae*.[13–16,42–44]

Effect of temperature and pH on bacterial growth

Both temperature and pH in combination play a major role in growth of the bacterial strains.[45,46] Although the B2-DHA isolate was able to grow at 20, 30, 37 and 45°C but the optimum growth (estimated based on optical density) was observed at 37°C (data not shown). Similarly, the isolate could grow at pH ranging from 5 to 9 but the optimum growth was found at pH 7.0 (data not shown). Thus, all subsequent experiments were conducted at 37°C in media with pH 7.0. These data are consistent with previously reported[13] optimum pH and temperature for *Enterobacter cloacae* ranging from 7.0–8.0 and 30–37°C, respectively. Wang et al.[43] reported that reduction of Cr (VI) by *E. cloacae* occurred at pH 6.5 to 8.5 and it was strongly inhibited at pH 5.0. In fact, this strain depicted poor growth at temperature below 25°C and at pH of 5 or less compare to that of a faster growth at temperature ranging between at 28 and 40°C and resistance at pH up to 9. In addition, Cr(VI) could be desorbed from soil at a faster rate at elevated pH values.[47]

Minimum inhibitory concentration (MIC) of chromate

The strain *E. cloacae* B2-DHA exhibited a MIC higher than 1000 μg mL^{-1} of K_2CrO_4 which is an indication that this strain is resistant to very high concentrations of chromate than that reported previously by Komori et al.,[13] Yamamoto et al.,[14] Clark,[15] Rege et al.[16] and Cervantes et al.[44] Although the resistance parameter is not absolute; it is correlated to the growth medium. The MIC obtained in rich media is usually two to five times higher

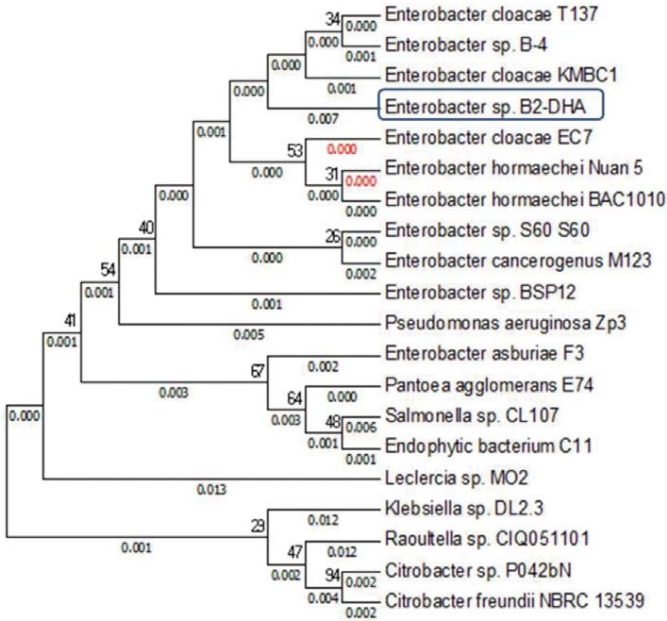

Fig. 1. Neighbour-joining tree based on 16S rRNA gene sequences showing the phylogenetic relationship of the isolated strain B2-DHA in comparison with species belonging to the *Enterobacter* sp. The analysis included data from 1227 positions in the final dataset. The bootstrap values (expressed as percentages of 500 replicates) above 50% are shown at the branch points.

than those obtained in TRIS minimal medium.[30] This is due to that heavy metals can complex with certain components in the media, especially organic substances and phosphate. Thus, it is important to employ an appropriate strategy to select potential bacterial strains for remediation of Cr(VI) fromcontaminated environments. This cannot only be based on the capability of a strain to grow in the presence of high levels of chromate, but it must also include the test of chromate reduction. It is also important to bear in mind that the strain is able to catalyze the reduction of Cr(VI) into the much less toxic and mobile Cr(III), since the chromate resistance and the chromate reduction may be unrelated processes.[48]

Resistance of B2-DHA to chromium

Chromium resistance of B2-DHA was estimated based on bacterial growth detected by optical density with or without exposure to 1000 μg mL^{-1} potassium chromate. The results indicated that after 48 h of incubation the bacterial growth was highest in the control medium whereas the bacterial growth in medium containing chromium was gradually increasing and after 120 h of incubation the growth was highest (Fig. 2a).

To verify if the B2-DHA strain was indeed resistant to chromium, we performed a viable cell count experiments where the cells were grown first in liquid medium containing 1000 μg mL^{-1} chromium for up to 120 h and then transferred onto solid medium fortified with or without chromium. Samples were taken every 24 h and the colony forming units (CFU) were counted. The results showed that the number of cells on the plates without chromium increased rapidly up to 72 h (approximately 2.56×10^{10} CFU) and then decreased drastically (approximately 1.9×10^{9} CFU) up to 96 h of growth (Fig. 2b). The number of CFU in the chromium free plates decreased after 96 h of growth because the nutrients in the medium were already utilized in maximum after 72 h of culture (highest cell count). The bacteria continued to grow but without adequate nutrient supply required for their survival.[49]

However, when the cells were plated on chromium containing medium, they continued to grow gradually up to 120 h (approximately 2.49×10^{10} CFU). The explanation for this is that in the presence of chromium

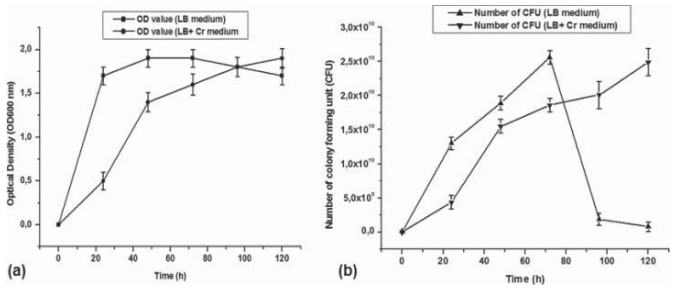

Fig. 2. Study of chromium resistance of B2-DHA by measuring optical density and colony forming units (CFU): (a) represents optical density obtained with cells exposed to chromium and without any exposure to chromium (control). Error bars denote standard error of mean. $P > 0.05$ (Two-tailed *t*-test), not significant. (b) represents cell counts. The number of CFU of bacterial cells, exposed to chromium and without exposure to chromium (control). Error bars denote standard error of mean.* $P \leq 0.05$ (two-tailed *t*-test), significant.

the cells grew slowly (after 72 h of growth the CFU was approximately 1.7×10^{10}) resulting comparatively less utilization of nutrients in the medium. Therefore, the cells in this medium could grow further having adequate nutrient supply. The capacity of this strain to grow in the presence of chromium confirms that it is highly resistant to this toxic metal.

Resistance of B2-DHA to other metals

To verify that the B2-DHA isolate was also resistant to other toxic metals, the growth of this bacterium was monitored in presence of metals like $Na_2HAsO_4.7H_2O$, $FeCl_3$, $MnCl_2$, $ZnCl_2$, $NiCl_2$ and $AgNO_3$ at different concentrations in LB broth. The MIC of these metals was found to be 15 g L^{-1} for $Na_2HAsO_4{\cdot}7H_2O$, 500 mg L^{-1} for $FeCl_3$, 400 mg L^{-1} for $MnCl_2$, 350 mg L^{-1} for $ZnCl_2$, 260 mg L^{-1} for $NiCl_2$ and 85 mg L^{-1} for $AgNO_3$.

ICP –MS and ICP-AES Analysis of Cr(VI)

To confirm if the B2-DHA strain can indeed accumulate chromium inside the cells as performed by inductively coupled plasma mass spectroscopy (ICP-MS). This analysis revealed that the amount of chromium inside the bacterial cells after 120 h of exposure to 100 μg mL^{-1} chromium resulted in 320 μg g^{-1} d.wt. of bacterial biomass (Fig. 3a). If this is the case, theoretically equal amounts of chromium should be decreased from the growth medium exposed to the B2-DHA isolate. We verified this by performing inductively coupled plasma atomic emission spectroscopy (ICP-AES) and found that the chromium concentration in the cell free growth medium, after 120 h exposure, decreased from 100 μg mL^{-1} to 19 μg mL^{-1} (81%) (Fig. 3b). In control samples (medium without exposure to B2-DHA), we did not observe any temporal changes in the concentration of chromium.

The rates of chromate reduction by the B2-DHA isolate were comparable to those of other chromate-resistant

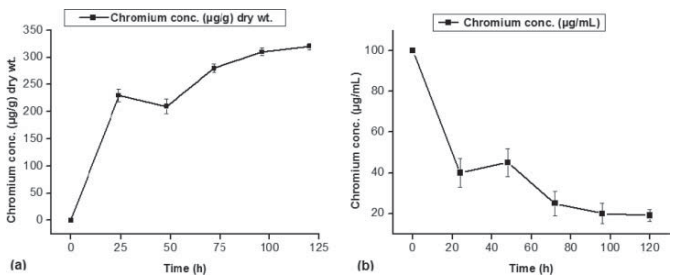

Fig. 3. Estimation of Cr(VI) concentration: (a) amount of chromium absorbed by the bacterial cells. Error bars denote standard error of mean.* $P \leq 0.05$ (one-tailed *t*-test), significant. (b) reduction of chromium by *Enterobacter* sp. B2-DHA in growth medium. Error bars denote standard error of mean. ** $P \leq 0.01$ (one-tailed *t*-test), significant.

bacterial strains as previously reported by many researchers,[21,50–52] who demonstrated that several chromium-reducing bacteria with biotransformation potential and can reduce the different amount of chromium in the medium. Wang and Xiao[50] observed that the rate of Cr(VI) reduction by *Bacillus* sp. increased with initial Cr (VI) concentrations ranging from 20 to 70 mg L^{-1} and decreased at higher concentrations. Thacker et al.[21] reported a Gram negative strain of *Brucella* sp., which has a potential to decrease chromium in the contaminated sources. These authors demonstrated that increasing concentrations of Cr(VI) in the medium lowered the bacterial growth. But the decrease in the growth rate could not be correlated directly with the amount of Cr(VI) reduced. Resistance to high concentration of Cr(VI) and high ability for reduction of this toxic metal make the strain a suitable candidate for bioremediation.

Desai et al.[52] reported three efficient Cr(VI) reducing bacterial strains, Bacillus cereus, Bacillus fusiformis and Bacillus sphaericus, isolated from Cr(VI) polluted landfills and characterized for in vitro Cr(VI) reduction. These researchers showed that the suspended cultures of all Bacillus sp. exhibited more than 85% reduction when exposed to 1000 μM Cr(VI). Megharaj et al.[51] reported two bacterial strains, *Arthrobacter* sp. and a *Bacillus* sp., isolated from soils contaminated a longer term with tannery wastes and their resistance abilities to hexavalent chromium [Cr(VI)] as well as their reducing capabilities of Cr(VI) to Cr(III), a detoxification process in cell suspensions and cell extracts. Overall results of these experiments indicated that *Arthrobacter* sp. could reduce chromate to 60% after 72 h when Cr(VI) concentration is 50 μg mL^{-1} in the medium, whereas *Bacillus* sp. was able to reduce chromate 60% after 72 h when grown in presence of 20 μg Cr(VI) mL^{-1} in the medium. At higher concentration of Cr(VI) *Arthrobacter* sp. was distinctly superior to the *Bacillus* sp. in terms of their Cr(VI)-reducing ability and resistance to Cr(VI). However, both bacteria can reduce 100% chromium from the medium by 72 h when the chromium concentration is very less ranging from 5 to 10 μg mL^{-1}. Our data similar to those previously reported suggest that the reduction of chromium concentration in the growth medium treated with B2-DHA is due to the biological activity of this bacterium.

TOF-SIMS analyses of chromium

To further verify the presence of chromium inside the cells or absorption to the outside we performed ion imaging analyses by TOF-SIMS. Ion imaging analyses by TOF-SIMS based on time of flight-secondary ion mass spectrometry was performed to determine whether the bacterium B2-DHA absorbs and/or accumulates chromium inside the cells. This analysis relies on the use of a pulsed ion beam to ionize surface molecules that later can be studied by a mass spectrometer. With the help of ion imaging we have found that B2-DHA cells, when exposed to chromium, uptake and accumulate the different forms of chromium inside the cells, such as chromium oxide (CrO^-) and chromium dioxide (CrO_2^-) (Fig. 4b–c). In addition, the total protein signals in the cells are also detected by TOF-SIMS (Fig. 4a). On the other hand, the ion imaging analyses by TOF-SIMS of the control B2-DHA cells grown in absence of chromium had no detectable chromium ions (CrO^- or CrO_2^-) (Fig. 4d). Surprisingly, the intensity of chromium ion (CrO^-) inside the cells was much lower than the intensity of other chromium ion (CrO_2^-). These results show that the bacterium, B2-DHA, prefers to accumulate chromium inside the cells.

To further confirm the distribution of chromium ions inside the cells we have performed depth profiling analyses by TOF-SIMS. This analysis, also known as "sputtering," relies on gradual measurement of chromium at the different depth of the bacterial cell layers. Sputtering was done up to 1250 sec and these results demonstrated that the intensity counts for chromium ions (CrO^-) were approximately $10^{3.5}$ and the intensity counts for chromium ions (CrO_2^-) were approximately $10^{2.8}$ (Fig. 4e). Furthermore, sputtering was made up to 1000 seconds for the control sample and the results indicated that the intensity levels remained very low throughout the sputtering time (from 0–1000 sec), which can be attributed to the background activity of chromium (Fig. 4f).

The intensity counts of signal protein are much higher in the control sample than that observed in chromium exposed sample (Figs. 4e–f). By combining the pulsed ion beam with another ion beam in direct current (DC) mode, depth profiles were obtained as a result of consecutive removal of surface layers. The depth profiling further confirmed the results obtained by ion imaging indicating comparatively higher amounts of chromium inside the cells. Importantly, as our isolate B2-DHA exhibited a very high resistance to chromium, its oxidation/reduction characteristics are therefore significantly beneficial for remediation of chromium from the contaminated water and/or soils in the affected regions. Hence, TOF-SIMS can be used for obtaining both ion images as well as chemical information on the distribution of chromium ions from the surface and downwards into the sample. Rahman et al.[24] practiced same technique to profile arsenics in bacterial cells. Appropriate application of this bacterium may maintain the biogeochemical cycles of chromium in the nature.

ESEM-EDS analysis

Morphologic changes in bacteria cultured in medium with (100 μg mL^{-1}) or without chromium (control) were investigated using environmental scanning electron microscopic (ESEM) with an attached X-ray energy dispersive

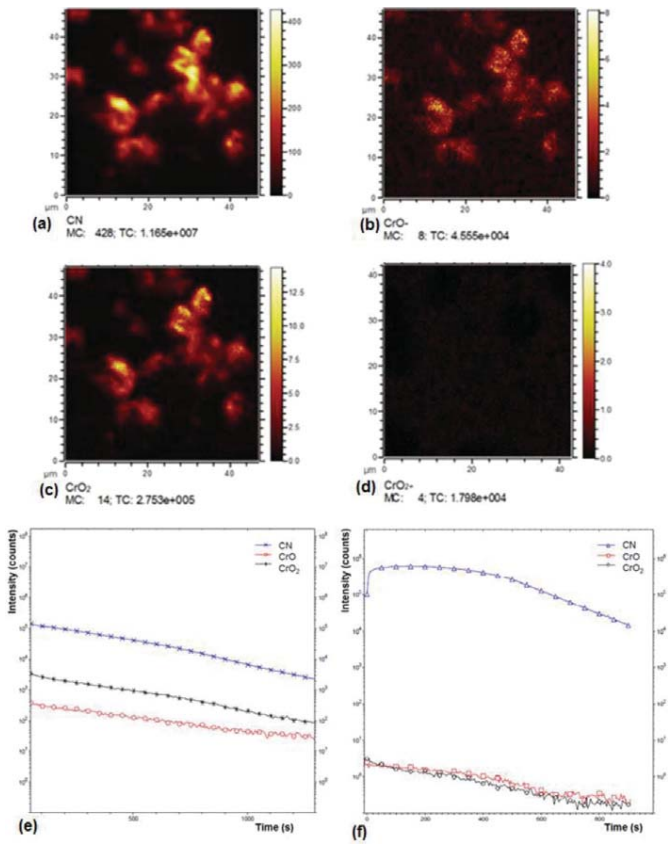

Fig. 4. Ion imaging and depth profiling of chromium species inside the bacterial cells by using TOF-SIMS: (a) total protein signals; (b) chromium oxide; (c) chromium dioxide; and, (d) bacterium was grown in absence of Cr(VI) and considered as control. The colored scale represents the intensity of ion imaging; (e) depth profiling of bacterial cells grown in presence of chromium. Blue, red and black colours represent protein signals, chromium (II) oxide and chromium dioxide, respectively; (f) depth profiling of bacterial cells grown in absence of chromium (control). Blue color represents protein signals, whereas red and black colours stand for background activity of chromium.

system (EDS). ESEM images were taken at 12000× magnification. The results are presented in Figure 5. Results indicated that B2-DHA control bacteria exhibited a typical cocci shape, whereas the chromium-treated bacteria formed long chains compared to the untreated cells (Figs. 5a–b).

Cell aggregation and surface modification besides increasing irregularity of cell morphology took place in case of cells suspended in chromium solution. The long chainlike structures represent mode of response to metal stress. These changes in morphological structure might be a possible strategy for cells to accumulate metals inside the cells indicating that the strain B2-DHA could accumulate chromium and contribute to bioremediation of this toxic metal. The EDS spectrum recorded in the examined region of the cells confirmed the presence of chromium ions on cell surface with respect to control (Figs. 5c–d). The signals for C, N, and O may originate from biomolecules present on the surface of biomass.

The ESEM-EDS of the cells grown in presence of chromium clearly revealed that the elongation of cells and cell aggregation due to the metal stress support the membrane

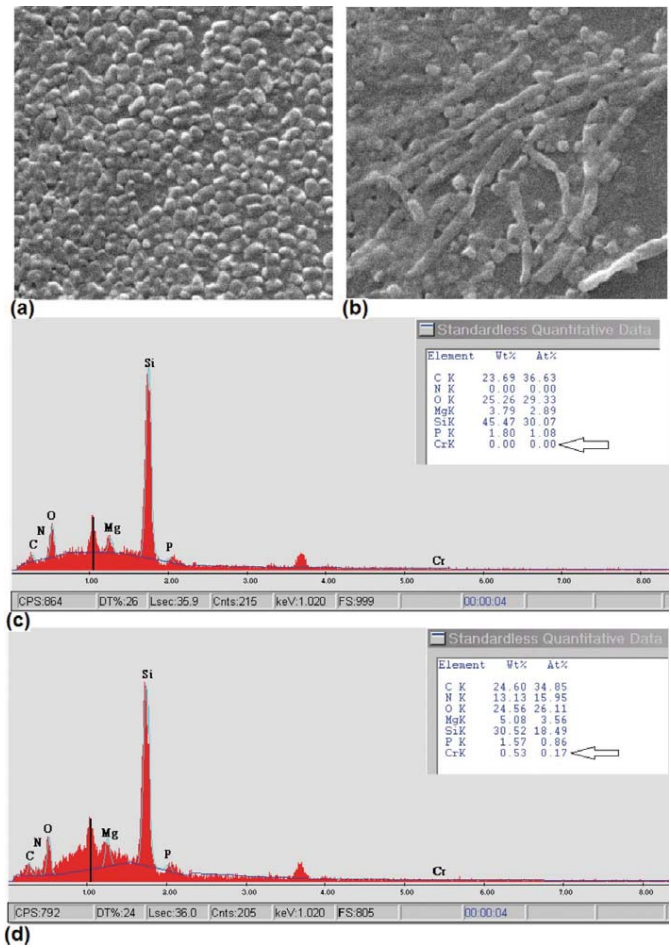

Fig. 5. Effect of metals on cellular morphology of the isolates studied by environmental scanning electron micrograph (ESEM): (a) strain B2-DHA in absence of chromium, magnification 12,000×; (b) strain B2-DHA in presence of 100 μg mL^{-1} chromium, magnification 12,000×; (c) corresponding X-ray energy dispersive system (EDS) spectra in absence of Cr(VI); and, (d) EDS spectra in presence of Cr(VI).

transport process.[53] In growing cells, biofilm formation or aggregation is a common phenomenon under stress conditions; however, this is unusual for non-growing live cells. Rahman et al.[24] reported a significant elongation of bacteria when studying the effects of arsenate on the *Lysinibacillus sphaericus*. Also Desale et al.[54] reported morphological changes of bacteria when studying the effects of nickel on *Lysinibacillus sp*. Several other researchers have shown the bacterial elongation in presence of toxic heavy metals.[55,56]

Conclusions

In this article we report that the *Enterobacter cloacae* strain B2-DHA isolated from a landfill containing effluents disposed from leather manufacturing tannery industries has potentials for decreasing chromium concentration to a safe level in the contaminated environment. In a longer perspective, several hundred millions of people worldwide can avoid many lethal diseases caused by chronic chromium poisoning. Consequently, our findings will

contribute to a significant positive impact on the socioeconomic status of the people particularly in the developing world. The continuation of this research is vital not only for people in the affected area but also for populations in other countries that have credible health concerns as a consequence of chromium contaminated water and foods.

Funding

This research has been funded mainly by the Swedish International Development Cooperation Agency (SIDA, Grant no. AKT-2010-018) and partly by the Swedish Research Council for Environment, Agricultural Sciences and Spatial Planning (FORMAS, Grant no. 229-2007-217). A grant from the Nilsson-Ehle (The Royal Physiographic Society in Lund) Foundation in Sweden is also acknowledged.

References

[1] Ortegel, J.W.; Staren, E.D.; Faber, L.P.; Warren, W.H.; Braun, D.P. Modulation of tumor-infiltrating lymphocyte cytolytic activity against human non-small cell lung cancer. Lung Cancer **2002**, *36*, 17–25.

[2] Viti, C.; Pace, A.; Giovannetti, L. Characterization of Cr(VI)-resistant bacteria isolated from chromium-contaminated soil by tannery activity. Curr. Microbiol. **2003**, *46*, 1–5.

[3] Chourey, K.; Thompson, M.R.; Morrell-Falvey, J.; VerBerkmoes, N.C.; Brown, S.D.; Shah, M.; Zhou, J.; Doktycz, M.; Hettich, R. L.; Thompson, D.K. Global molecular and morphological effects of 24-hour chromium(vi) exposure on *Shewanella oneidensis* MR-1. Appl. Environ. Microbiol. **2006**, *72*, 6331–6344.

[4] The Guardian, Sunday 7 July 2013. Available at http://www.theguardian.com/world/2013/jul/07/bangladesh-tanneries-human-rights-violations (accessed Nov 2013).

[5] Avudainayagam, S.; Megharaj, M.; Owens, G.; Kookana, R.S.; Chittleborough, D.; Naidu, R. Chemistry of chromium in soils with emphasis on tannery waste sites. Rev. Environ. Contam. Toxicol. **2003**, *178*, 53–91.

[6] Offenbacher, E.G.; Pi-Sunyer, F.X. Chromium in human nutrition. Ann. Rev. Nutr. **1988**, *8*, 543–563.

[7] Jeyasingh, J.; Philip, L. Bioremediation of chromium contaminated soil: optimization of operating parameters under laboratory conditions. J. Hazard. Mater. **2005**, *118*, 113–120.

[8] Camargo, F.A.O.; Bento, F.M.; Okeke, B.C.; Frankenberger, W. T. Chromate reduction by chromium-resistant bacteria isolated from soils contaminated with dichromate. J. Environ. Qual. **2003**, *32*, 1228–1233.

[9] Zafar, S.; Aqil, F.; Ahmad, I. Metal tolerance and biosorption potential of filamentous fungi isolated from metal contaminated agricultural soil. Bioresour. Technol. **2007**, *98*, 2557–2561.

[10] Congeevaram, S.; Dhanarani, S.; Park, J.; Dexilin, M.; Thamaraiselvi, K. Biosorption of chromium and nickel by heavy metal resistant fungal and bacterial isolates. J. Hazard. Mater. **2007**, *146*, 270–277.

[11] Alvarez, A.H.; Moreno-Sanchez, R.; Cervantes, C. Chromate efflux by means of the chrA chromate resistance protein from *Pseudomonas aeruginosa*. J. Bacteriol. **1999**, *181*, 7398–7400.

[12] Panda, J.; Sarkar, P. Bioremediation of chromium by novel strains Enterobacter aerogenes T2 and Acinetobacter sp. PD 12 S2. Environ. Sci. Pollut. Res. Int. **2012**, *19*, 1809–1817.

[13] Komori, K.; Rivas, A.; Toda, K.; Ohtake, H. A method for removal of toxic chromium using dialysis-sac cultures of a chromate reducing strain of Enterobacter cloacae. Appl. Microbiol. Biotechnol. **1990**, *33*, 117–119.

[14] Yamamoto, K.; Kato, J.; Yamo, T.; Ohtake, J. Kinetics and modeling of hexavalent chromium reduction in *Enterobacter cloacae*. Biotechnol. Bioeng. **1993**, *41*, 129–133.

[15] Clark, D.P. Chromate reductase activity of *Enterobacter aerogenes* is induced by nitrite. FEMS Microbiol. Lett. **1994**, *122*, 233–238.

[16] Rege, M.A.; Peterson, J.N.; Johnstone, D.L.; Turick, C.E.; Yonge, D.R.; Apel, W.A. Bacterial reduction of hexavalent chromium by Enterobacter cloacae strain HO1 grown on sucrose. Biotechnol. Lett. **1997**, *19*, 691–694.

[17] Pattanapipitpaisal, P.; Brown, N.L.; Macaskie, L.E. Chromate reduction and 16S rRNA identification of bacteria isolated from a Cr(VI)-contaminated site. Appl. Microbiol. Biotechnol. **2001**, *57*, 257–261.

[18] Michel, C.; Brugma, M.; Aubert, C.; Bernadac, A.; Bruschi, M. Enzymatic reduction of chromate: Comparative studies using sulfate-reducing bacteria. Appl. Microbiol. Biotechnol. **2001**, *55*, 95–100.

[19] Shen, H.; Wang, Y. Characterization of enzymatic reduction of hexavalent chromium by *Escherichia coli* ATCC 33456. Appl. Environ. Microbiol. **1993**, *59*, 3771–3777.

[20] Guha, H.; Jayachandran, K.; Maurrasse, F. Kinetics of chromium (VI) reduction by a type strain *Shewanella alga* under different growth conditions. Environ. Pollut. **2001**, *115*, 209–218.

[21] Thacker, U.; Parikh, R.; Shouche, Y.; Madamwar, D. Reduction of chromate by cell-free extract of Brucella sp. isolated from Cr(VI) contaminated sites. Bioresour. Technol. **2007**, *98*, 1541–1547.

[22] de Crécy, E.; Metzgar, D.; Allen, C.; Pénicaud, M.; Lyons, B.; Hansen, C.J.; de Crécy-Lagard, V. Development of a novel continuous culture device for experimental evolution of bacterial populations. Appl. Microbiol. Biotechnol. **2007**, *77*, 489–496.

[23] de Crécy, E.; Jaronski, S.; Lyons, B.; Lyouns, T.J.; Keyhani, N.O. Directed evolution of a filamentous fungus for thermo tolerance. BMC Biotechnol. **2009**, *9*, 74.

[24] Rahman, A.; Nahar, N.; Nawani, N.N.; Jass, J.; Desale, P.; Kapadnis, B.P.; Hossain, K.; Saha, A.K.; Ghosh, S.; Olsson, B.; Mandal, A. Isolation of a *Lysinibacillus* strain B1-CDA showing potentials for arsenic bioremediation. J. Environ. Sci. Health Pt. A **2014**, *49*, 1349–1360.

[25] Vickerman, J.C.; Briggs, D. *TOF-SIMS Surface Analysis by Mass Spectrometry*. IM Publications and Surface Spectra Limited: West Sussex, 2001.

[26] Norrman, K.; Krebs, F.C. Lifetimes of organic photovoltaics: Using TOF-SIMS and $_{18}O^2$ isotopic labelling to characterise chemical degradation mechanisms. Sol. Energy Mater. Sol. Cells **2006**, *90*, 213–227.

[27] Stefánsson, A.; Gunnarsson, I.; Giroud, N. New methods for the direct determination of dissolved inorganic, organic and total carbon in natural waters by Reagent-Free Ion Chromatography and inductively coupled plasma atomic emission spectrometry. Anal. Chim. Acta **2007**, *582*, 69–74.

[28] Schwedt, G. *The Essential Guide to Analytical Chemistry*. (Brooks Haderlie, trans.). Wiley: Chichester, UK. (Original Work Published 1943), 1997; 16–17.

[29] Xu, W.; Sandford, R.; Worsfold, P.; Carlton, A.; Hanrahan, G. Flow Injection Techniques in Aquatic Environmental Analysis: Recent Applications and Technological Advances. Critical Reviews in Analytical Chemistry. **2005**, *35*, 237–246.

[30] Mergeay, M. Heavy metal resistances in microbial ecosystems. In *Molecular Microbial Ecology Manual*, A.D.L. Akkermans, J.D. Elsas, F.J. de Bruin, Eds.; Kluwer Academic Publishers: Dordrecht, 1995; 6.1.7/1–6.1.7/17.
[31] Villegas-Torres, M.F.; Bedoya-Reina, O.C.; Salazar, C.; Vives-Florez, M.J.; Dussan, J. Horizontal arsC gene transfer among microorganisms isolated from arsenic polluted soil. Int. Biodeter. Biodegradat. **2011**, *65*, 147–152.
[32] Eichorst, S.A.; Breznak, J.A.; Schmidt, T.M. Isolation and characterization of soil bacteria that define Terriglobus gen. nov., in the Phylum Acidobacteria. Appl. Environ. Microbiol. **2007**, *73*, 2708–2717.
[33] Krieg, N.R. *Bergey's manual of systematic bacteriology*, vol. 1, G. Garrity, D.R. Boone, R.W. Castenholz, Eds.; Williams and Wilkins: Baltimore, MD, 1984; 722.
[34] Saitou, N.; Nei, M. The neighbor-joining method: A new method for reconstructing phylogenetic trees. Mol. Biol. Evol. **1987**, *4*, 406–425.
[35] Felsenstein, J. Confidence limits on phylogenies: An approach using the bootstrap. Evolution **1985**, *39*, 783–791.
[36] Kimura, M. A simple method for estimating evolutionary rate of base substitutions through comparative studies of nucleotide sequences. J. Mol. Evol. **1980**, *16*, 111–120.
[37] Tamura, K.; Stecher, G.; Peterson, D.; Filipski, A.; Kumar, S. MEGA6: Molecular Evolutionary Genetics Analysis version 6.0. Mol. Biol. Evol. **2013**, *30*, 2725–2729.
[38] Ammann, A.A. Inductively coupled plasma mass spectrometry (ICP MS): A versatile tool. J. Mass Spectrom. **2007**, *42*, 419–427.
[39] Kollmer, F. Cluster primary ion bombardment of organic materials. Appl. Surf. Sci. **2004**, *231–232*, 153–158.
[40] Touboul, D.; Kollmer, F.; Niehuis, E.; Brunelle, A.; Laprevote, O. Improvement of biological time-of-flight-secondary ion mass spectrometry imaging with a bismuth cluster ion source. J. Am. Chem. Soc. **2005**, *16*, 1608–1618.
[41] Sodhi, R.N.S. Time-of-flight secondary ion mass spectrometry (TOF-SIMS): versatility in chemical and imaging surface analysis. Analyst **2004**, *129*, 483–487.
[42] Wang, P.C.; Mori, T.; Komori, K; Sasatsu, M; Toda, K.; Ohtake, H. Isolation and characterization of an Enterobacter cloacae strain that redqces hexavalent chromium under anaerobic conditions. Appl. Environ. Microbiol. **1989**, *55*, 1665–1669.
[43] Wang, P.C.; Mori, T.; Toda, K.; Ohtake, H. Membrane associated chromate reductase activity from *Enterobacter cloacae*. J. Bacteriol. **1990**, *172*, 1670–1672.
[44] Cervantes, C.; Campos-Garcia, J.; Devars, S.; Gutieŕrez-Corona, F.; Loza-Tavera, H.; Torres Guzmań, J.C.; Moreno-Saǹchez, R. Interactions of chromium with microorganisms and plants. FEMS Microbiol. Rev. **2001**, *25*, 333–347.
[45] Kirchman, D.L.; Malmstrom, R.R.; Cottrell, M.T. Control of bacterial growth by temperature and organic matter in the Western Arctic. Deep-Sea Res. II. **2005**, *52*, 3386–3395.
[46] Doenmez, G.; Aksu, Z. Bioaccumulation of copper (II) and Nickel (II) by the non-adapted and adapted growing Candida sp. Water Res. **2001**, *35*, 1425–1434.
[47] Weng, C.H.; Huang, C.P.; Sanders, P.F. Transport of Cr(VI) in soils contaminated with chromite ore processing residue (COPR). Pract. Period. Hazard. Toxic Radioact. Waste Manage. **2002**, *6*, 6–13.
[48] Bopp, L.H.; Ehrlich, H.L. Chromate resistance and reduction in *Pseudomonas florescens* strain LB300. Arch. Microbiol. **1988**, *150*, 426–431.
[49] Novick, A. Growth of bacteria. Ann. Rev. Microbiol. **1955**, *9*, 97–110.
[50] Wang, Y.T.; Xiao, C. Factors affecting hexavalent chromium reduction in pure cultures of bacteria. Water Res. **1995**, *29*, 2467–2474.
[51] Megharaj, M.; Avudainayagam, S.; Naidu, R. Toxicity of hexavalent chromium and its reduction by bacteria isolated from soil contaminated with tannery waste. Curr. Microbiol. **2003**, *47*, 51–54.
[52] Desai, C.; Jain, K.; Madamwar, D. Evaluation of in vitro Cr(VI) reduction potential in cytosolic extracts of three indigenous Bacillus sp. isolated from Cr(VI) polluted industrial landfill. Bioresour. Technol. **2008**, *99*, 6059–6069.
[53] Vijayakumar, G.; Tamilarasan, R.; Dharmendra, M. K. Removal of Cd2Þ ions from aqueous solution using live and dead *Bacillus subtilis*. Eng. Res. Bull. **2011**, *15*, 18–24.
[54] Desale, P.; Kashyap, D.; Nawani, N.; Nahar, N.; Rahman, A.; Kapadnis, B.; Mandal, A. Biosorption of nickel by *Lysinibacillus* sp. BA2 native to bauxite mine. Ecotoxicol. Environ. Saf. **2014**, *107*. 260–268.
[55] Nepple, B.B.; Flynn, I. Bachofen. Morphological changes in phototrophic bacteria induced bymetalloid oxyanions. Microbiol. Res. **1999**, *154*, 191–198.
[56] Banerjee, S.; Datta, S.; Chattyopadhyay, D.; Sarkar, P. Arsenic accumulating and transforming bacteria isolated from contaminated soil for potential use in bioremediation. J. Environ. Sci. Health Pt. A **2011**, *46*, 1736–1747.

Ecotoxicology and Environmental Safety 107 (2014) 260–268

Contents lists available at ScienceDirect

Ecotoxicology and Environmental Safety

journal homepage: www.elsevier.com/locate/ecoenv

Biosorption of nickel by *Lysinibacillus* sp. BA2 native to bauxite mine

Desale Prithviraj [a], Kashyap Deboleena [a], Nawani Neelu [a,*], Nahar Noor [c], Rahman Aminur [c], Kapadnis Balasaheb [b], Mandal Abul [c]

[a] Dr. D. Y. Patil Biotechnology and Bioinformatics Institute, Dr. D. Y. Patil Vidyapeeth, Pune 411033, India
[b] Department of Microbiology, University of Pune, Pune 411007, India
[c] School of Bioscience, University of Skövde, PO Box 408, 541 28 Skövde, Sweden

ARTICLE INFO

Article history:
Received 1 March 2014
Received in revised form
2 June 2014
Accepted 9 June 2014

Keywords:
Lysinibacillus sp. BA2
Heavy metals
Biosorption
Adsorption isotherm

ABSTRACT

The current scenario of environmental pollution urges the need for an effective solution for toxic heavy metal removal from industrial wastewater. Bioremediation is the most cost effective process employed by the use of microbes especially bacteria resistant to toxic metals. In this study, *Lysinibacillus* sp. BA2, a nickel tolerant strain isolated from bauxite mine was used for the biosorption of Ni(II). *Lysinibacillus* sp. BA2 biomass had isoelectric point (pI) of 3.3. The maximum negative zeta potential value (−39.45) was obtained at pH 6.0 which was highly favourable for Ni(II) biosorption. 238.04 mg of Ni(II) adsorbed on one gram of dead biomass and 196.32 mg adsorbed on one gram of live biomass. The adsorption of Ni(II) on biomass increased with time and attained saturation after 180 min with rapid biosorption in initial 30 min. The Langmuir and Freundlich isotherms could fit well for biosorption of Ni(II) by dead biomass while Langmuir isotherm provided a better fit for live biomass based on correlation coefficient values. The kinetic studies of Ni(II) removal, using dead and live biomass was well explained by second-order kinetic model. Ni(II) adsorption on live biomass was confirmed by SEM-EDX where cell aggregation and increasing irregularity of cell morphology was observed even though cells were in non-growing state. The FTIR analysis of biomass revealed the presence of carboxyl, hydroxyl and amino groups, which seem responsible for biosorption of Ni(II). The beads made using dead biomass of *Lysinibacillus* sp. BA2 could efficiently remove Ni(II) from effluent solutions. These microbial cells can substitute expensive methods for treating nickel contaminated industrial wastewaters.

1. Introduction

Heavy metal pollution is a result of increase in anthropogenic and industrial activities like electroplating, fertilizer manufacturing, battery manufacturing, textiles, paper mills, mining and metallurgic processing. Discharge of untreated industrial wastes is a major global concern. Heavy metals in waste severely affect the health and natural life leading to an ecological imbalance (Boopathy, 2000). Chemical methods of wastewater treatment and recycling are extensively reviewed (Gupta et al., 2012) and studies on biological methods are ongoing to choose the best possible treatment technologies for effective application.

Nickel occurs naturally in water, soil and sea salts as sulphides, nitrates and oxides (Boyle and Robinson, 1988). Natural levels of nickel in water range between 3 and 10 μg/L. The wastes from electroplating, nickel-cadmium batteries and metal finishing industries contain nickel. Nickel poisoning causes pulmonary fibrosis, skin dermatitis, vomiting, diarrhoea, nausea and neurological disintegration particularly in children (Das et al., 2008). The best solution to prevent metal poisoning is to treat industrial effluents prior to their discharge in the environment. Bioremediation technologies offer viable, economical, eco-friendly and efficient techniques over conventional methods of metal removal (Puranik and Paknikar, 1999). Bioremediation techniques using inexpensive adsorbents from industrial wastes were successful in treatment of wastewaters (Jain et al., 2004). A comparison of adsorbents particularly those from wastes suggests these materials to be promising in removal of dyes, strengthening the promise of low-cost treatment technologies (Jain et al., 2003). A variety of adsorbents were reported to remove dyes like chrysoidine Y, Amaranth, erythrosine, reactofix golden yellow 3 RFN, carmoisine A, Brilliant Blue FCF and several others (Mittal et al., 2005; Gupta et al., 2006a, 2006b; Gupta et al., 2007a, 2007b; Gupta et al., 2009; Mittal et al., 2010). Similarly, metals like lead and zinc can be adsorbed on carbon nanotubes (Gupta and Sharma, 2003; Gupta et al., 2011; Saleh and Gupta, 2012).

* Corresponding author.
E-mail address: neelunawani@yahoo.com (N. Neelu).

http://dx.doi.org/10.1016/j.ecoenv.2014.06.009
0147-6513/

Biomass of fungi, yeast and bacteria also exhibit metal removal ability (Volesky and May-Phillips, 1995; Hu et al., 2007). *Oedogonium hatei* biomass could adsorb nickel ions with 70 percent recovery indicating the efficiency of biomass in removal of pollutants from wastes (Gupta et al., 2010). Microbes bind metals on the cell surface, accumulate them intracellularly (Chang et al., 1997), or produce chelators that sequester metals from the environment (Gadd, 1988; Wang and Chen, 2006). The first cellular structure that encounters the soluble metal ions in aqueous environment is the cell wall. A microbial cell wall is well-defined polymeric matrix composed of polysaccharides, proteins, lipids, with functional groups such as hydroxyls, carboxyls, amides, amines, imidazole, phosphate that are mainly responsible for adsorption of metal ions. Adsorption of metal ions on cell wall occurs passively with non-metabolic mechanisms like complexation, chelation, coordination, ion exchange, precipitation and reduction (Wang and Chen, 2006). Dead biomass is most valuable for adsorption of metal ions from the aqueous regenerated and systems, as the cells are unaffected by toxic wastes, they require no supply of nutrients and can be reused. Hence, biosorption of metals by dead biomass becomes a promising technique of metal removal (Macek and Mackova, 2011). Fitting the experimental data with Langmuir and Freundlich isotherm models often describes the adsorption equilibrium of the biosorption process Gadd, 1988. In addition, the pseudo first order and second order kinetic studies describe the rate of metal uptake by adsorbent at the solid–liquid interface. Therefore, it is important to predict the rate at which the metal is removed from aqueous solution in order to design appropriate treatment plants based on biosorption technology.

The present study, demonstrates nickel remediation ability of *Lysinibacillus* sp. BA2 isolated from bauxite mine. This paper describes the removal of Ni(II) by adsorbents (live and dead biomass) at variable pH values, initial metal concentration, increasing concentration of metal and contact time. The adsorption data for both adsorbents were analysed using different isotherm models such as Langmuir and Freundlich. The kinetic models are proposed to study rate of adsorption of Ni(II) by the adsorbents for futuristic use in industrial effluent treatments.

2. Materials and methods

2.1. Materials

All the chemicals used in this study were of the highest analytical grade available. Ni(II) solution was prepared by dissolving nickel chloride hexahydrate ($NiCl_2 \cdot 6H_2O$, Hi-media, Mumbai, India) in deionised water.

2.2. Isolation and identification of nickel tolerant bacteria

The soil sample near Bauxite mine at Kolhapur in state of Maharashtra, India was collected at six inches depth from surface. 0.1 g soil was suspended in 10.0 ml water and 0.1 ml of suspension was plated on Luria agar (LA, Hi-media, Mumbai, India) supplemented with 3.0, 5.0, 7.0, 9.0, 10.0, 15.0, 25.0, 50.0 mM $NiCl_2 \cdot 6H_2O$ and incubated at 37 °C for 48 h. Identification of the nickel tolerant isolate was carried out using conventional biochemical tests and by 16S rDNA sequencing as described by Nawani et al. (2002).

2.3. Preparation of Lysinibacillus sp. BA2 biomass as adsorbent

Lysinibacillus sp. BA2 was inoculated in Luria broth (LB medium) and agitated on rotary shaker (150 rpm) at 37 °C for 48 h. The cells were harvested by centrifugation at 10,000*g* for 15 min. The resultant pellet was washed thrice with deionised water, part of the pellet was autoclaved at 121 °C for 15 min, and dried at 70 °C for 12 h to obtain dead biomass and rest of the untreated pellet was used directly as live biomass.

2.4. Analysis of nickel uptake

Anodic Stripping Voltammetry (ASV) was used for analysis of Ni(II) ions (ASV: 797 Computrace VA Metrohm, Switzerland). Before analysis, every experimental sample was filtered through a 0.22 μ filter, adjusted to pH 2.0 with 30 percent concentrated HNO_3 and appropriately diluted with deionised water. The nickel standard solution (SRL, Sisco Research Laboratory, Mumbai, India) was used for the calibration of the method.

2.5. Biosorption experiments using Lysinibacillus sp. BA2

Adsorption of Ni(II) ions by live and dead biomass was carried out between pH 3.0 and 9.0 at interval of 1.0 unit. Aliquots were removed after 24 h for analysis of residual Ni(II) ions and zeta potential measurements. The zeta potential was measured using Zeta metre (ZetaCAD-DC, USA). The contact time giving maximum adsorption of Ni(II) ions on biomass was determined by incubating biomass with Ni (II) (1.0–9.0 mM) and aliquots were removed after every 30 min till 300 min to determine residual Ni(II) ions. Maximum concentration of Ni(II) that could be adsorbed on the biomass was determined by gradually increasing Ni(II) from 1.0 mM to 9.0 mM in the same tube. All experiments were carried out in aqueous Ni (II) solution at pH 6.0 (optimum pH for maximum Ni(II) ion adsorption) using 1 g/L of the adsorbent and agitated on a rotary shaker (150 rpm) at 37 °C. To determine minimum contact time for adsorption equilibrium, the adsorbents were suspended in 300 mg/L Ni(II) solution. After every 30 min, samples were withdrawn for analysing residual Ni(II) ions. Fourier transform infrared spectroscopy (FTIR; Model FT/IR-4200 TypeA) was used to determine the functional groups on cell surface involved in Ni(II) adsorption. The morphology of live biomass in aqueous metal solution was analysed by scanning electron microscopy-energy dispersive X-ray (SEM-EDX; Model – JSM-7600F).

The Ni(II) concentration retained on the adsorbents of *Lysinibacillus* sp. BA2 isolate was calculated by mass balance equation (Bhatti et al., 2007).

$$q_e = (C_o - C_e)V/M \quad (1)$$

where *qe* represents the amount of metal retained (mg Ni(II)/g adsorbent), *Co* and *Ce* are initial metal concentration in the solution and equilibrium concentration of the metal (mg/L), respectively, *V* is volume of the solution (L) and *M* is mass of the adsorbent (g).

2.6. Dead biomass entrapped biomatrix for removal of nickel

Nickel adsorption mechanism, kinetic studies, physical and chemical characteristics of *Lysinibacillus* sp. BA2 could allow the use of this biomass for removal of nickel from industrial wastewater. Dead biomass is preferred over live biomass for adsorption of nickel from industrial effluents, as subsequent discharge of treated effluents does not pose a threat of introducing living cells in the environment. The dead biomass of *Lysinibacillus* sp. BA2 was rolled into beads, which were packed in the glass column and were used to treat effluents having 300 mg/L Ni(II). After every 30 min, eluents were withdrawn to determine residual Ni(II).

3. Results and discussion

3.1. Identification of heavy metal resistant bacteria

Table 1 describes the morphological and biochemical characteristics of strain BA2 isolated from bauxite mine. 16S rDNA gene sequence of isolate BA2 shows closest identity (98 percent) with the genus *Lysinibacillus* (Fig. 1). Based on biochemical and molecular characteristics, isolate BA2 was identified as *Lysinibacillus* and hereafter is referred as *Lysinibacillus* sp. BA2. *Lysinibacillus* sp. BA2 grows in presence of 9 mM $NiCl_2 \cdot 6H_2O$ indicating its tolerance towards nickel. Accordingly, it was promising candidate for bioremediation of nickel from industrial effluents.

3.2. Nickel biosorption ability of Lysinibacillus sp. BA2

3.2.1. Effect of pH on biosorption of Ni(II) ions and zeta potential

Increase in pH from 2.0 to 6.0 increased adsorption of Ni(II) on dead biomass from 18.65 to 193.65 mg/g and on live biomass from 12.36 to 156.32 mg/g. Increase in adsorption of Ni(II) with pH can be attributed to the competition between protons and metal ions for binding to cellular functional groups and to a decrease in positive surface charge (Kadirvelu and Namasivayam, 2003). Increase in pH

exposes several ligands and functional groups, which enhances the binding of positive metal ions on the negatively charged surface of the biomass. This is also seen for non-cellular adsorbents where cadmium adsorption on activated charcoal increased with increasing pH which is similar to the adsorption of nickel on microbial biomass reported here (Fouladi et al., 2009). The adsorption of Ni(II) on *Lysinibacillus* sp. BA2 was constant from pH 7.0 to 9.0 due to the precipitation of Ni(II) as nickel hydroxides. The maximum adsorption of Ni(II) ions on the biomass was observed at pH 6.0 hence other biosorption experiments were performed at this pH. Maximum adsorption of nickel on rubber–wood ash was reported earlier at pH 5.2 (Hasan et al., 2000).

The biosorption of heavy metals due to the influence of pH affects the metal-binding functional groups as well as the surface charge on the biomass. The electrical potential on the surface of a particle is used to predict optimum pH levels, protonation and deprotonation by zeta potential analysis. As the effect of pH on the biosorption of Ni(II) by live and dead biomass had similar pattern, further study for the determination of the zeta potential was carried out using live biomass. The increase in pH increased the negative charge on the biomass, thus Ni(II) adsorbed on negatively charged sites (Babel and Opiso, 2007). As shown in Fig. 2, Ni (II) adsorption on the biomass increased with pH from 3.5 to 6.0–6.5. The isoelectric point (pI) of *Lysinibacillus* sp. BA2 was 3.3 at which the surface carries no net electrical charge. The maximum zeta

Table 1
Morphological and biochemical characteristics of nickel tolerant bacterium *Lysinibacillus* sp. BA2.

Tests	Isolate BA2
Cell shape	Long rods
Endospore	Centrally located
Gram's reaction	Gram positive
Motility	Motile
Cell wall amino acid	
Aspartate	+
Lysine	+
Indole test	−
Methyl orange test	−
Voges Proskauer test	−
Citrate utilisation	−
Casein hydrolysis	−
Gelatin hydrolysis	+
Starch hydrolysis	−
Urea hydrolysis	−
Nitrate reduction	+
H2S production	−
Catalase test	+
Oxidase test	+

Negative (−) and positive (+).

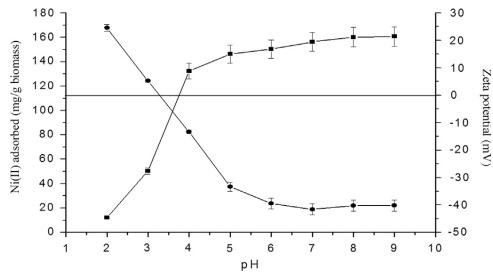

Fig. 2. Adsorption of Ni(II) (■) and zetapotential (●) of *Lysinibacillus* sp. BA2 biomass at different pH values. Biosorption conditions: initial Ni(II) concentration in solution 531.28 mg/L, contact time 24 h, biomass 1 g/L, temperature 37 °C. (Error bar represents means ± SE, $p < 0.05$, and $n = 3$).

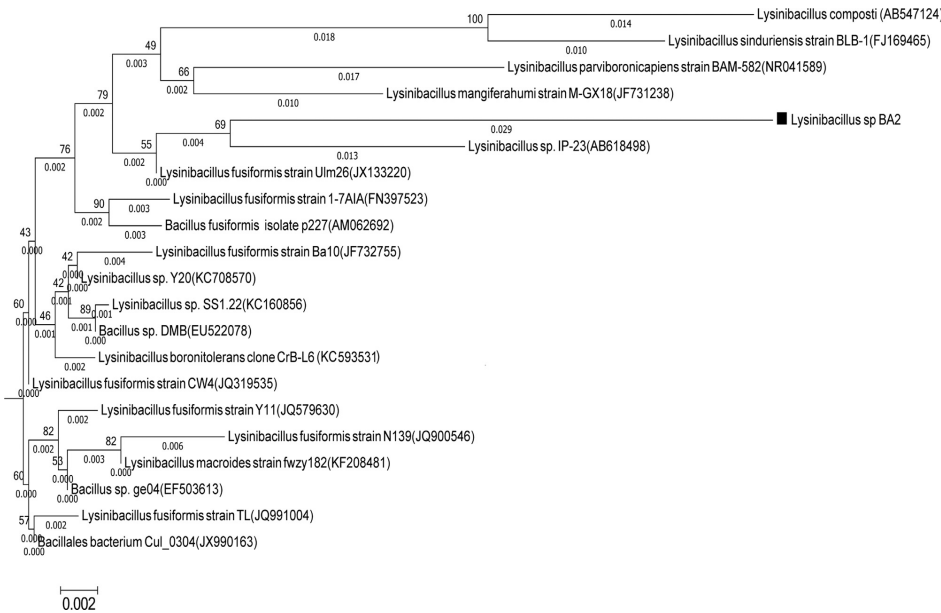

Fig. 1. Phylogenetic tree of the members of the genus *Lysinibacillus* sp. BA2 and representatives of some other taxa based on 16 S rRNA gene sequence comparisons.

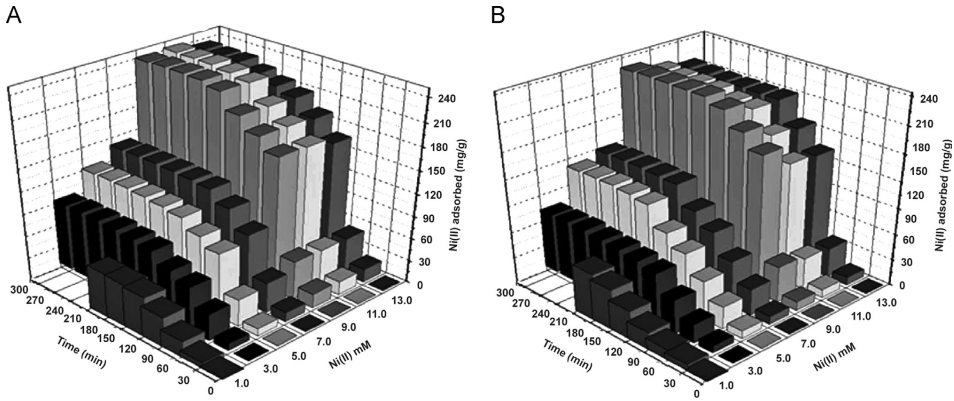

Fig. 3. Effect of contact time and initial metal concentrations on biosorption of Ni(II) by the dead biomass (A) and live biomass (B) of *Lysinibacillus* sp. BA2. Biosorption conditions: biomass 1 g/L, pH 6.0, temperature 37 °C. (Error bar represent means ± SE, $p < 0.05$, and $N=3$).

potential value (zP = −39.45) was obtained at pH 6.0 which corresponds to the maximum adsorption of Ni(II). Binding of Ni (II) increased in the range of pH 3.0–6.0, indicating that the protonation/deprotonation of functional groups within this range plays an important role in the biosorption process. The removal of protons from the surface of the biosorbents relates to the deprotonation constants. Hence, the electrostatic interaction between the positively charged metal ions and biomass typically depends on the increase in negatively charged functional groups on the biomass (Borrok et al., 2004).

3.2.2. *Effect of initial Ni(II) concentration on biomass*

The adsorption of Ni(II) on biomass increased with time and attained saturation after 180 min (Fig. 3). The adsorption capacity of dead biomass was more than live biomass due to the surface properties and affinity of adsorbent for adsorbate. The maximum adsorption values obtained were 238.04 mg of Ni(II) per gram of dead biomass and 196.32 mg of Ni(II) per gram of live biomass at the highest initial concentration of Ni(II) tested here. The higher adsorption of Ni(II) ions on the dead biomass could be due to larger surface area and several exchangeable binding groups whereas live biomass has smaller surface area giving fewer binding groups on the cell surface (Volesky and May-Phillips, 1995; Salvadori et al., 2013). In both cases, metal binding is independent of the microbial metabolism and depends primarily on the architecture and the chemical composition of microbial cell wall. The metal binding increase until binding sites are free and is expected to attain a point where no additional metal can bind on the biomass surface.

3.2.3. *Adsorption isotherms*

The gradual increase in initial Ni(II) concentration increased the removal of Ni(II) ions per unit mass of the biomass (Figs. 3 and 4A). 238.04 mg of Ni(II) adsorbed on one gram of dead biomass and 151.51 mg adsorbed on one gram of live biomass. The validation of experimental data by fitting them to different adsorption isotherm models is an important step to determine the suitable model (Lu et al., 2006). In order to find appropriate fit for present study, equations of Langmuir (Langmuir, 1918) and Freundlich (Freundlich, 1906) adsorption models were considered.

The Langmuir adsorption isotherm assumes monolayer surface coverage and no interaction between adsorbed species. The Langmuir isotherm equation is

$$q_e = q_{\max} K_L C_e / (1 + K_L C_e) \quad (2)$$

where, *KL* (L/g) is Langmuir adsorption constant and related to the affinity of the binding sites (Li et al., 2010). Values of Langmuir parameters *KL* (L/g) and *q*cal (mg/g) were calculated from the slope and intercept of the linear plot of *Ce*/*qe* against *Ce* as shown in Fig. 4B. The ratio of residual metal ions to adsorbed ions (*Ce*/*qe*) depends on the affinity of binding sites, which represent the adsorption constant for Langmuir model. The average value of *Ce*/*qe* (litre of metal solution per gram of adsorbed metal on biomass) for live biomass was highest (1.49 L/g) than dead biomass (0.88 L/g) which implies that the adsorbed Ni(II) ions cannot interact with the neighbouring molecules in case of live biomass (Table 2).

The Freundlich adsorption isotherm is an empirical equation, which assumes a heterogeneous biosorption system. The Freundlich adsorption isotherm represents the relationship between the amounts of Ni(II) adsorbed per unit mass of adsorbent. The general Freundlich adsorption isotherm equation which was used for validation is as follows:

$$q_e = K_F C_e^{\,1/n} \quad (3)$$

The Logarithmic form of Eq. (3) becomes

$$\log q_e = \log K_F + 1/n \log C \quad (4)$$

where, *KF* (L/g) and *n* is an empirical parameter representing the steepness of the isotherm and *qe* (mg/g) is the adsorption density. The *KF* and *n* values are calculated by plotting log *Ce* versus log *qe* (Fig. 4C). A favourable adsorption tends to have the constant *n* between 1 and 10. The *n* values obtained for Ni(II) adsorption by dead biomass and live biomass of *Lysinibacillus* sp. BA2 were 3.43 and 3.41, respectively, which indicate that the binding sites on dead biomass and live biomass are diverse in number (Delle, 2001). The Freundlich isotherm models suggest that Ni(II) ion adsorption by dead biomass represented heterogeneous surface adsorption, while monolayer adsorption happens in case of live biomass according to the correlation coefficient (R^2) values (Table 2). These results confirm that Ni(II) adsorption on the dead biomass could be due to heterogeneous surface binding, which

PAPER III

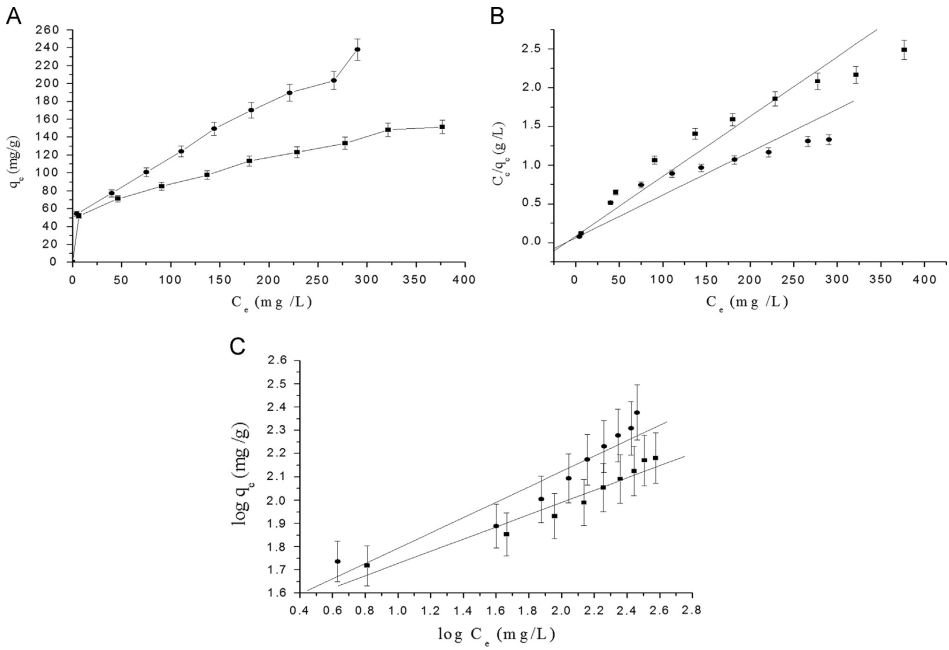

Fig. 4. Effect of gradual increasing metal concentration on biosorption of Ni(II) by dead biomass (•) and live biomass (■) of *Lysinibacillus* sp. BA2 (A). Biosorption conditions: biomass 1 g/L, pH 6.0, and temperature 37 °C; Langmuir adsorption isotherm (B); and Freundlich adsorption isotherm (C). Symbols indicate experimental data and lines indicate kinetic prediction (Error bar represent means ± SE, $p < 0.05$, and $n=3$).

Table 2
Adsorption isotherm constants and correlation coefficients of Ni^{2+} adsorption on dead and live biomass of *Lysinibacillus* sp. BA2. Comparison between the adsorption rate constants and correlation coefficients associated with pseudo-first-order and pseudo-second-order rate equations for the adsorption of Ni^{2+} by dead and live biomass of *Lysinibacillus* sp. BA2.

Biomass	**Biomass**		**Langmuir**			**Freundlich**		
	***q*exp (mg/g)**	***q*cal (mg/g)**	***KL* (L/g)**	***RL***	R^2	***n***	***KF* (L/g)**	R^2
Dead	238.04	180.5	0.0881	0.0210	0.951	3.437	29.10	0.974
Live	151.51	129.7	0.0905	0.0204	0.977	3.410	29.15	0.967
Biomass	**Initial Ni^{2+} ions**	**Pseudo first order kinetics**				**Pseudo second order kinetics**		
	(mg/L)	***q*exp (mg/g)**	***q*cal (mg/g)**	***k*ad (min^{-1})**	R^2	***q*cal (mg/g)**	***k*ad (g/mg/min)**	R^2
Dead	300	134.12	234.81	0.0189	−0.972	140.25	0.000171	0.982
Live	300	113.21	206.53	0.0178	−0.99	137.17	0.000109	0.966

was in accordance with previous reports (King et al., 2007; Li et al., 2010). In this study, the autoclaved biomass could adsorb more Ni(II), which could be due to increase in surface area. The difference in biosorption capacity can be attributed to change in chemical composition and metal binding affinity of the microbial cell wall due to pre-treatment (Gadd, 1988).

3.2.4. Kinetic studies for biosorption of nickel

The time-course equilibrium studies for the adsorption of Ni(II) on dead biomass and live biomass of *Lysinibacillus* sp. BA2 are as shown in Fig. 5. 134.12 mg of Ni(II) ions per gram of dead biomass (Fig. 5A) and 113.21 mg Ni(II) ions per gram of live biomass (Fig. 5B) could be adsorbed. The decrease in Ni(II) concentration in aqueous solution was rapid during first 30 min suggesting that biosorption is a spontaneous process (Chang et al., 1997; Yuan et al., 2009). Several other studies show that maximum biosorption is achieved in 30 min (Gabr et al., 2008).

In order to investigate the rate of reaction and adsorption capacity of adsorbent, pseudo-first-order (Fig. 5C) and pseudo-second-order (Fig. 5D) were applied to represent the kinetics of Ni(II) adsorption on dead biomass and live biomass of *Lysinibacillus* sp. BA2.

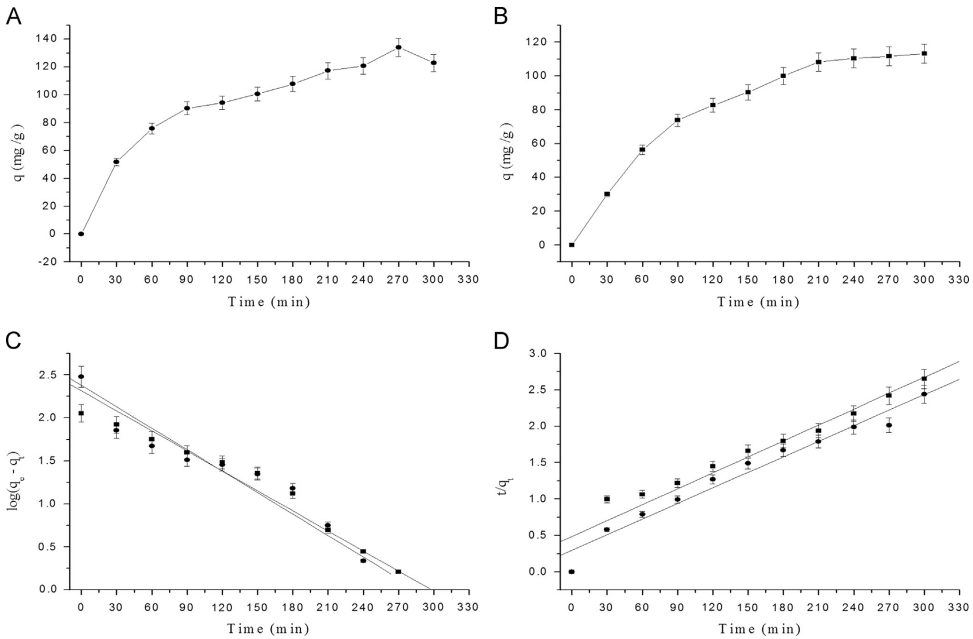

Fig. 5. Time course studies of Ni(II) adsorption onto the live biomass (A) and dead biomass (B) of *Lysinibacillus* sp. BA2; pseudo-first-order (C); and pseudo-second order (D) plots in the presence of (300 mg/L) Ni(II). Symbols indicate experimental data and lines indicate kinetic prediction (Error bar represent means ± SE, $p < 0.05$, and $n = 3$).

The pseudo-first-order rate equation is given as (Ho and McKay, 1999a)

$$\log\ (q_e - q_t) = \log\ q_e - (k_{ad}/2.303)\, t \quad (5)$$

where, *k*ad (min^{-1}) is the rate constant of pseudo-first-order adsorption process. Values of *k*ad were calculated from the plots of log ($qe - qt$) versus time (t) represented in Table 2.

The pseudo-second-order equation (Ho and McKay, 1999b; Malik, 2004) is expressed as

$$t/q_t = 1/kq_e^2 + (1/q_e)\, t \quad (6)$$

where *k*ad (g/mg/min) is the rate constant of pseudo-second-order kinetics. The values of *qe* and *k*ad were determined from the slope and intercept of the linear plot of t/q versus t, respectively represented in Table 2. The correlation coefficients for the pseudo-first-order kinetic constants (−0.972 for dead and −0.990 for live indicating 97–99 percent negative correlation between the adsorbate and adsorbent) were lower than the pseudo-second-order kinetic model (0.982 for dead and 0.966 for live) suggesting the pseudo-second-order kinetic model fitted the biosorption data. This indicates that the adsorption of metal ions on the dead biomass and live biomass could be a chemisorption-mediated process. A similar result was obtained for adsorption of cadmium on dead and live biomass of *Bacillus subtilis* (Vijayakumar et al., 2011).

3.3. SEM-EDX analysis

SEM-EDX for live biomass in presence and absence of Ni(II) confirmed the presence of nickel ions on the live biomass. SEM micrographs recorded before and after biosorption of Ni(II) by live biomass are shown in Fig. 6A and B–C, respectively. Cell aggregation and surface modification besides increasing irregularity of cell morphology took place in case of cells suspended in nickel solution. The EDX spectrum recorded in the examined region of the live biomass confirmed the presence of Ni(II) ions on cell surface (Fig. 6D–G). The signals for C, N, and O may originate from biomolecules present on the surface of biomass. The SEM-EDX of the live biomass also revealed the fact that cells aggregated due to metal stress cells to support the membrane transport process (Vijayakumar et al., 2011). In growing cells, biofilm formation or aggregation is a common phenomenon under stress conditions; however, this is unusual for non-growing live cells.

3.4. FT-IR analysis

FT-IR analyses with biomass treated with ionic solution of Ni(II) revealed considerable changes in the functional group responsible for binding of Ni(II) ions (Fig. 7A and B). The absorption peak for O–H shifted from 3733.02 cm^{-1} to 3723.48 cm^{-1}. There were clear disappearances in intensity of the bands at 3067.52 cm^{-1} (indicative of =C–H), 1328.47 cm^{-1} (indicative of C–N), 937.17 cm^{-1} (indicative of =C–H) and 648.84 cm^{-1} (indicative of C–Cl) were seen. Large shifts were observed in intensity of the bands at 2109.83 cm^{-1}(indicative of –C=C), 1230.28 cm^{-1} (indicative of C–O) and 1162.20 cm^{-1} (indicative of C–N). A large shift of C–O could be stretching of the C–O in polysaccharides (Aravindhan et al., 2004). It seems the C–O bond is mainly responsible for metal binding as the oxygen is most electronegative. The FT-IR spectra of biomass in the presence and absence of Ni(II) revealed that anion–cation interactions could be due to polyfunctional metal-binding capabilities of the biomass (Anand et al.,

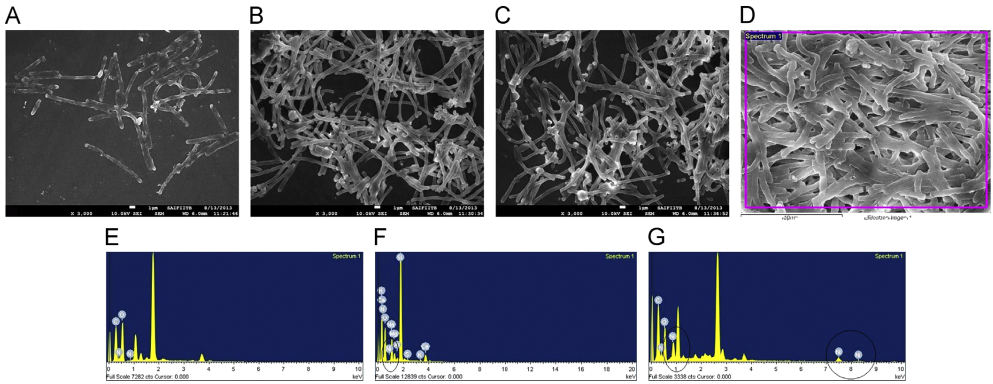

Fig.6. SEM micrograph of Ni(II) biosorption by live biomass of *Lysinibacillus* sp. BA2 in the absence of Ni(II) (A); presence of Ni(II) (B–D) and corresponding EDX spectra in the absence of Ni(II) (E) and in presence of Ni(II) (F and G).

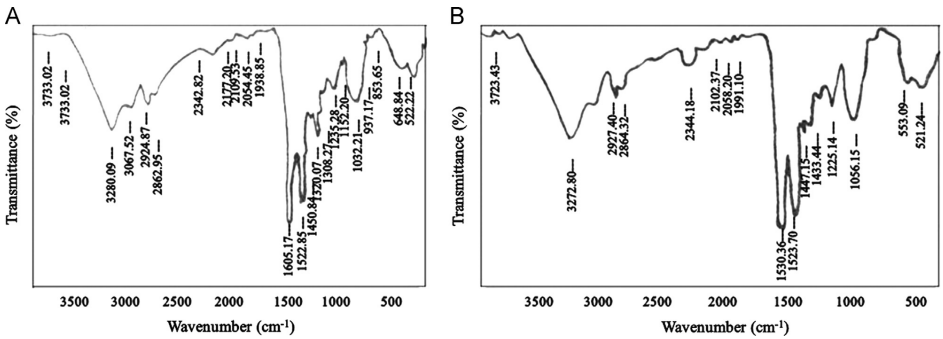

Fig. 7. FTIR of the biomass of *Lysinibacillus* sp. BA2 in the absence of Ni(II) (A) and presence of Ni(II) (B).

2006). The analysis of FTIR spectra gives the idea of the presence of functional groups on the bacterial cell surface able to bind with metal ions.

3.5. Commercial application of biosorption technique

Batch analysis of the eluents showed decrease in Ni(II) concentration with respect to time (data not shown). The biomass was rolled into beads to treat Ni(II) containing solutions (Fig. 8). 53.89 Percent nickel could be removed from the nickel solution in 300 min, indicating the efficiency of this biomatrix in industrial application. Hence, the dead biomass in the form of beads offers many advantages providing better reusability, high biomass loading and minimal clogging of the flow system over live biomass. The industrial wastewater, however, should be devoid of the solid suspended particles.

4. Conclusion

The present study demonstrates biosorption of Ni(II) by *Lysinibacillus* sp. BA2. The strain can tolerate nickel upto 9 mM. Increase in pH increased the adsorption of nickel indicating the exposure of negative charges on biomass surface to be favourable for biosorption. The isoelectric point (pI) of *Lysinibacillus* sp. BA2 was 3.3 and maximum zeta potential value (zP= −39.45) was obtained at pH 6.0 which corresponds to the maximum adsorption of Ni(II). The adsorption of Ni(II) ions on biomass increased with time and attained saturation after 180 min with rapid adsorption in the initial 30 min. The highest adsorption values obtained were 238.04 mg of Ni(II) per gram of dead biomass and 196.32 mg of Ni(II) per gram of live biomass. The dead biomass of *Lysinibacillus* sp. BA2 obeyed Langmuir and Freundlich isotherm whereas live biomass obeyed Langmuir isotherm. The adsorption of nickel by live biomass and dead biomass of *Lysinibacillus* sp. BA2 follows pseudo-second-order rate equation suggesting the process of chemical adsorption. The FTIR analysis suggests the participation of carboxylate, hydroxyl and amide groups in adsorption. The dead biomass of *Lysinibacillus* sp. BA2 rolled out as beads could serve as an efficient biomatrix for adsorption of nickel hence it can be used for treatment of nickel containing industrial effluents. To exert a pull on the usage of biosorption technology, mathematical modelling and some strategies have to be developed so that the biomatrix can be regenerated and the metal recovered can be reused.

Fig. 8. Fixed bead column packed derived from the dead biomass for biosorption of Ni(II).

Acknowledgments

The authors are grateful for funding from the Swedish International Development Cooperation Agency (SIDA), (Grant no. AKT-2010-018), Sweden.

References

Anand, P., Isar, J., Saran, S., Saxena, R.K., 2006. Bioaccumulation of copper by *Trichoderma viride*. Bioresour. Technol. 91, 1018–1025.
Aravindhan, R., Madhan, B., Rao, J.R., Nair, B.U., Ramasami, T., 2004. Bioaccumulation of chromium from tannery wastewater: an approach for chrome recovery and reuse. Environ. Sci. Technol. 38, 300–306.
Babel, S., Opiso, E.M., 2007. Removal of Cr from synthetic wastewater by sorption into volcanic ash soil. Int. J. Eng. Sci. Technol. 4, 99–107.
Bhatti, H.N., Mumtaz, M.A., Hanif, Nadeem, R., 2007. Removal of Zn(II) ions from aqueous solution using *Moringa oleifera* lam.(Horseradish tree) biomass. Process Biochem. 42, 547–553.
Boopathy, R., 2000. Factors limiting bioremediation technologies. Bioresour. Technol. 74, 63–67.
Borrok, D., Fein, J.B., Kulpa, C.F., 2004. Proton and Cd adsorption onto natural bacterial consortia: testing universal adsorption behavior. Geochim. Cosmochim. Acta 68, 3231–3238.
Boyle, R.W., Robinson, H.A. 1988. Nickel and its role in biology, In: Sigel, Sigel and Dekker, (Eds.), Nickel in the Natural Environment 23, 123–164.
Chang, J.S., Law, R., Chang, Chung-Cheng, C., 1997. Biosorption of lead, copper and cadmium by biomass of *Pseudomonas aeruginosa* PU21. Water Res. 31, 1651–1658.
Das, K.K., Das, S.N., Dhundasi, S., 2008. Nickel, its adverse health effects & oxidative stress. Indian J. Med. Res. 128, 412–425.
Delle, S.A., 2001. Factors affecting sorption of organic compounds in natural sorbents, water systems and sorption coefficients for selected pollutants: a review. J. Phys. Chem. Ref. Data 30, 187–439.
Fouladi, T.A., Kaghazchi, T., Soleimani, M., 2009. Adsorption of cadmium from aqueous solutions on sulfurized activated carbon prepared from nut shells. J. Hazard. Mater. 165, 1159–1164.
Freundlich, H., 1906. Über die and adsorption in lösungen.Z. J. Phys. Chem. 57, 385–470.
Gabr, R.M., Hassan, S.H.A., Shoreit, A.A.M., 2008. Biosorption of lead and nickel by living and non-living cells of *Pseudomonas aeruginosa* ASU 6a. Int. Biodeter. Biodegr. 62, 195–203.
Gadd, G.M., 1988. Accumulation of metals by microorganisms and algae. Biotechnology, 6(b). VCH, Weinheim, Germany, pp. 401–403.
Gupta, V.K., Agarwal, S., Tawfik, A., Saleh, 2011. Synthesis and characterization of alumina-coated carbon nanotubes and their application for lead removal. J. Hazard. Mater. 185, 17–23.
Gupta, V.K., Ali, I., Saini, V.K., 2007a. Defluoridation of wastewaters using waste carbon slurry. Water Res. 41, 3307–3316.
Gupta, V.K., Ali, I., Saleh, T.A., Nayak, A., Agarwal, S., 2012. Chemical treatment technologies for waste-water recycling—an overview. RSC Adv. 2, 6380–6388.
Gupta, V.K., Jain, R., Varshney, S., 2007b. Removal of reactofix golden yellow 3 RFN from aqueous solution using wheat husk – an agricultural waste. J. Hazard. Mater. 142, 443–448.
Gupta, V.K., Mittal, A., Kurup, L., Mittal, J., 2006a. Adsorption of a hazardous dye, erythrosine, over hen feathers. J. Colloid Interface Sci. 304, 52–57.
Gupta, V.K., Rastogi, A., Nayak, A., 2010. Biosorption of nickel onto treated alga (Oedogonium hatei): Application of isotherm and kinetic models. J. Colloid Interface Sci. 342, 533–539.
Gupta, V.K., Sharma, S., 2003. Removal of zinc from aqueous solutions using Bagasse fly ash – a low cost adsorbent. Ind. Eng. Chem. Res. 42, 6619–6624.
Gupta, V.K., Mittal, A., Krishnan, L., Mittal, J., 2006b. Adsorption treatment and recovery of the hazardous dye, Brilliant Blue FCF, over bottom ash and de-oiled soya. J. Colloid Interface Sci. 293, 16–26.
Gupta, V.K., Mittal, A., Malviya, A., Mittal, J., 2009. Adsorption of carmoisine A from wastewater using waste materials – bottom ash and deoiled soya. J. Colloid Interface Sci. 335, 24–33.
Hasan, S., Mohd, Ali, Hashim, Gupta, B.S., 2000. Adsorption of Ni(SO4) on Malaysian rubber–wood ash. Bioresour. Technol. 72, 153–158.
Ho, Y., McKay, G., 1999b. Pseudo-second order model for sorption processes. Process Biochem. 34, 451–465.
Ho, Y., McKay, G., 1999a. Comparitive sorption kinetic studies of dye and aromatic compounds onto fly ash. J. Environ. Sci. Health 34, 1179–1204.
Hu, Q., Qi, H., BaiZ., Dou, M., Zeng, J., Zhang, F., Zhang, H., 2007. Biosorption of cadmium by a Cd^{2+} hyper resistant *Bacillus cereus* strain HQ-1 newly isolated from a lead and zinc mine. World J. Microbial. Biotechnol. 23, 971–976.
Jain, A.K., Gupta, V.K., Bhatnagar, A., Suhas, 2003. A comparative study of adsorbents prepared from industrial wastes for removal of dyes. Separ. Sci. Technol. 38, 463–481.
Jain, A.K., Gupta, V.K., Jain, S., Suhas, 2004. Removal of chlorophenols using industrial wastes. Environ. Sci. Technol. 38, 1195–1200.
Kadirvelu, K., Namasivayam, C., 2003. Activated carbon from coconut coirpith as metal adsorbent: adsorption of Cd (II) from aqueous solutions. Adv. Environ. Res. 7, 471–478.
King, P., Rakesh, N., Beenalahari, S., PrasannaKumar, Y., Prasad, V., 2007. Removal of lead from aqueous solution using *Syzgium cumini* L: equilibrium and kinetic studies. J. Hazard. Mater. 142, 340–347.
Langmuir, L., 1918. The adsorption of gases on plane surfaces of glass, mica and platinum. J. Am. Chem. Soc. 40, 1361–1403.
Li, H., Lin, Y., Gaun, W., Chang, J., Xu, L., Guo, J., Wei, G., 2010. Biotransformation of Zn(II) by live and dead cells of *Streptomyces ciscaucasicus* strain CCNWHX 72-14. J. Hazard. Mater 179, 151–159.
Lu, W.B., Shi, J.J., Wang, C.H., 2006. Biosorption of lead, copper and cadmium by an indigenous isolate *Enterobacter* sp. J1 possessing high heavy-metal resistance. J. Hazard. Mater. 134, 80–86.

PAPER III

Macek, T., Mackova, M., 2011. Potential of biosorption technology. In: Kotrba, P., Mackova, T., Macek, T. (Eds.), Microbial Biosorption of Metals. Springer, Netherlands, pp. 7–17.
Malik, A., 2004. Metal bioremediation through growing cells. Environ. Int. 30, 261–278.
Mittal, A., Kurup (Krishnan), L., Gupta, V.K., 2005. Use of waste materials – bottom ash and de-oiled soya, as potential adsorbents for the removal of Amaranth from aqueous solutions. J. Hazard. Mater. 117, 171–178.
Mittal, A., Mittal, J., Malviya, A., Gupta, V.K., 2010. Removal and recovery of Chrysoidine Y from aqueous solutions by waste materials. J. Colloid Interface Sci. 344, 497–507.
Nawani, N.N., Kapadnis, B.P., Das, A.D., Rao, A.R., Mahajan, S.K., 2002. Purification and characterization of a thermophilic and acidophilic chitinase from *Microbispora* sp. V2. J. Appl. Microbiol. 93, 965–975.
Puranik, P., Paknikar, K., 1999. Bioadsorption of lead, cadmium, and zinc by Citrobacter stain MCM B-181: characterisation studies. Biotechnol. Prog. 15, 228–237.
Saleh, T.A., Gupta, V.K., 2012. Column with CNT/magnesium oxide composite for lead(II) removal from water. Environ. Sci. Pollut. Res. Int. 19, 1224–1228.
Salvadori, M.R., Lepre, L.F., Ando, R.A., Oller do Nascimento, C.A., Corrêa, B., 2013. Biosynthesis and uptake of copper nanoparticles by dead biomass of *Hypocrea lixii* isolated from the metal mine in the Brazilian Amazon Region. PLoS One 25, e80519.
Vijayakumar, G., Tamilarasan, R., Dharmendra, M.K., 2011. Removal of Cd^{2+} ions from aqueous solution using live and dead *Bacillus subtilis*. Eng. Res. Bull. 15, 18–24.
Volesky, B., May-Phillips, H., 1995. Biosorption of heavy metals by *saccharomyces cerevisiae*. Appl. Microbiol. Biotechnol. 42, 797–806.
Wang, J., Chen, C., 2006. Biosorption of heavy metals by *Saccharomyces cerevisiae*: a review. Biotechnol. Adv. 24, 427–451.
Yuan, H.P., Zhang, J.H., Lu, Z.M., Min, H., Wu, C., 2009. Studies on biosorption equilibrium and kinetics of Cd2þ by *Streptomyces* sp. K33 and HL-12. J. Hazard. Mater. 164, 423–431.

Genomics 106 (2015) 384–392

Contents lists available at ScienceDirect

Genomics

journal homepage: www.elsevier.com/locate/ygeno

Comparative genome analysis of *Lysinibacillus* B1-CDA, a bacterium that accumulates arsenics

Aminur Rahman [a,c], Noor Nahar [a], Neelu N. Nawani [b], Jana Jass [c], Sibdas Ghosh [d], Björn Olsson [a,1], Abul Mandal [a,*,1]

[a] Systems Biology Research Center, School of Bioscience, University of Skövde, P.O. Box 408, SE-541 28 Skövde, Sweden
[b] Dr. D. Y. Patil Biotechnology and Bioinformatics Institute, Dr. D. Y. Patil Vidyapeeth, Tathawade, Pune, 411033, India
[c] The Life Science Center, School of Science and Technology, Örebro University, SE-701 82 Örebro, Sweden
[d] School of Arts and Science, Iona College, New Rochelle, NY 10801, USA

ARTICLE INFO

Article history:
Received 11 May 2015
Received in revised form 29 July 2015
Accepted 15 September 2015
Available online 24 September 2015

Keywords:
Toxic metals
Bioremediation
Lysinibacillus sphaericus B1-CDA
Genome sequencing
de novo assembly
Gene prediction

ABSTRACT

Previously, we reported an arsenic resistant bacterium *Lysinibacillus sphaericus* B1-CDA, isolated from an arsenic contaminated lands. Here, we have investigated its genetic composition and evolutionary history by using massively parallel sequencing and comparative analysis with other known Lysinibacillus genomes. Assembly of the sequencing reads revealed a genome of ~4.5 Mb in size encompassing ~80% of the chromosomal DNA. We found that the set of ordered contigs contains abundant regions of similarity with other Lysinibacillus genomes and clearly identifiable genome rearrangements. Furthermore, all genes of B1-CDA that were predicted be involved in its resistance to arsenic and/or other heavy metals were annotated. The presence of arsenic responsive genes was verified by PCR *in vitro* conditions. The findings of this study highlight the significance of this bacterium in removing arsenics and other toxic metals from the contaminated sources. The genetic mechanisms of the isolate could be used to cope with arsenic toxicity.

1. Introduction

Worldwide various anthropogenic activities such as mining, chemical industries, use of arsenic-based pesticides, and natural occurrences continue to cause major environmental and health problems by releasing heavy metals into the soil and water alike [1], and exposing millions of people directly or indirectly to toxic metals including arsenic (As). Long-term exposure to As leads to skin diseases, such as hyper- and hypo-pigmentation, hyperkeratosis and melanosis, as well as gangrene, skin cancer, lung cancer and bladder cancer [2]. Poisoning occurs from drinking of contaminated water and/or consuming crops cultivated by irrigation with As-contaminated groundwater [3–5]. Studies by the Food and Agricultural Organization of the United Nations (FAO) indicate that arsenic is accumulated in different parts of the cultivated crops, such as the grain and straw of rice, a major staple food [6]. It is therefore important that we develop efficient, yet affordable, technologies to clean arsenic from soil and water.

Remediation of toxic metal using microbes has been shown to be more proficient than physical and chemical methods [7]. In fact, bacteria have developed several metabolic processes and strategies to transform As, including respiratory arsenate reduction, cytoplasmic arsenate reduction and arsenite methylation [8]. Furthermore, certain bacteria have evolved the necessary genetic components that confer resistance mechanisms, allowing them to survive and grow in environments containing levels of As that would be toxic to most other organisms. The high-level resistance to As in bacteria is conferred by the arsenical resistance (ars) operon comprising either three (*arsRBC*) [9] or five (*arsRDABC*) genes arranged in a single transcriptional unit located on plasmids [10] or chromosomes [11]. ArsB, an integral membrane protein that pumps arsenite out of the cell, is often associated with an ATPase subunit, arsA [12]. The *arsC* gene encodes the enzyme for arsenate reductase, which is responsible for the biotransformation of arsenate [As(V)] to arsenite [As(III)] prior to efflux. ArsR is a trans-acting repressor involved in the basal regulation of the ars operon, while arsD is a second repressor controlling the upper levels of expression of ars genes [13]. Several researchers have studied As transformation mechanisms using genetic markers such as *arsB* and *arsC* genes in the ars operon for arsenic resistance [12,14], the arrA gene for dissimilatory As(V) respiration (DAsR) [15–17], and the aoxB gene for As(III) oxidation [18,19]. Moreover, some studies detected that in spite of clear evidence of the As-transforming activity by microorganisms, no amplicon for arsenite oxidase (aoxB) or As(V) respiratory reductase (arrA) was attained using the reported polymerase chain reaction (PCR) primers and protocols [17,20,21]. Here we report a bacterial strain, *Lysinibacillus*

* Corresponding author.
E-mail address: abul.mandal@his.se (A. Mandal).
[1] Authors have the equal contribution.

http://dx.doi.org/10.1016/j.ygeno.2015.09.006
0888-7543/

Table 1
Summary of the genome with nucleotide content and gene count levels.

Attribute	Value	% of total
Genome size (bp)	4,509,276	100.00
DNA GC content (bp)	1,690,719	37.49
DNA coding region (bp)	3,911,574	86.75
Number of replicons	1	
Extrachromosomal	0	
Total genes	4601	100.00
rRNA genes	11	0.24
tRNA genes	77	1.67
Protein coding genes	4513	98.09
Genes assigned to RAST functional categories	2671	58.05
Genes assigned Gene Ontology terms by Blast2GO	3050	66.29

sphaericus B1-CDA as potential candidate for heavy metal bioremediation. This bacterial strain was isolated from cultivated land in the Chuadanga district of Bangladesh, where soil, sediment, and ground water have been contaminated with arsenics for many years.

In this study, we provide *in vitro* findings of potential arsenic responsive genes in B1-CDA and summarize a set of phenotype features for *L. sphaericus* B1-CDA, together with a description and annotation of its genome sequence. To improve our understanding of genes involved in metal binding activity and reduction of metal by the B1-CDA strain, we performed massively parallel genome sequencing to investigate the metal responsive genes, predicted by RAST and/or Blast2GO. Employing comparative analyses with other available *Lysinibacillus* genome sequences, we investigated genetic composition and evolutionary history of strain B1-CDA and characterized the genetic differences among the various lineages to understand the evolutionary processes involved in shaping the genomes of these bacteria.

2. Methods

2.1. Strain isolation

The soil samples were collected from cultivated land in the Chuadanga district of Bangladesh, a highly arsenic-contaminated region located in the south-west region of this country. The soil was collected from the surface at 0–15 cm in depth, retained in plastic bags and kept at 4 °C until further analysis. Isolation of bacteria from the collected soil, the characterization of the soil samples and the content of metal ions has been described previously [22]. Previously, we have reported that the strain *L. sphaericus* B1-CDA is highly resistant to arsenic and it accumulates arsenic inside the cells [22].

2.2. Genomic DNA extraction and electrophoresis

Genomic DNA was extracted from the isolate, B1-CDA using Master pure™ Gram positive DNA purification kit (Epicenter, USA) with a minor modification. Bacteria were cultured in Luria Bertani (LB) medium and pellets were collected from 1.0 ml of bacterial cultures by

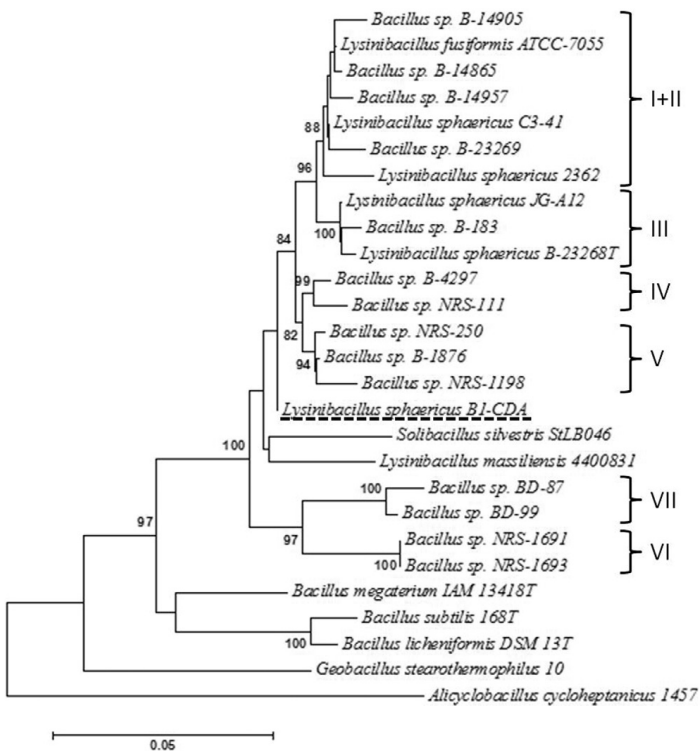

Fig. 1. Phylogenetic tree depicting the position of *Lysinibacillus sphaericus* B1-CDA relative to the available type strains and other non-assigned species within the family *Bacillae*. The percentage of replicate trees in which the associated taxa clustered together in the bootstrap test (500 replicates) is shown next to the branches.

centrifugation at 8000 rpm for 10 min. The pellets were resuspended in TE buffer (10 mM Tris–HCl, 1 mM EDTA [pH 8.0]) containing lysozyme (50 mg/ml) and RNase (50 mg/ml) and incubated at 37 °C for 2 h. The suspension was then mixed with proteinase K (50 μg/μl) and the cells were lysed following incubation at 65–70 °C for 15 min. Protein precipitation solution was added to remove the proteins, and the DNA was precipitated with isopropanol and washed with 70% ethanol. The DNA was resuspended in TE buffer and quantified by Nanodrop® ND-1000 Spectrophotometer (Saveen Werner, USA).

Agarose gel electrophoresis was performed based on the established protocol [23]. The gel was prepared with 0.8% agarose in 1× TAE buffer. The *Saccharomyces cerevisiae* chromosomal DNA (Bio-Rad, USA) was used as the size standard to estimate the molecular weight of the *L. sphaericus* B1-CDA chromosome.

2.3. Primer design and PCR amplification of arsenic-responsive genes

Primers were designed based on the multiple sequence alignment of target genes in a variety of arsenic resistant bacilli. Sequences of the *arsR* gene from 25 *Bacillus* species were randomly selected from GenBank. The multiple sequences of the *arsR* genes were aligned by ClustalW [24] in order to find the longest region of conserved homology. Seven bacterial strains exhibiting highest homology to the conserved region with each other were chosen for designing PCR primers. Two degenerate primer pairs were used to amplify the As marker genes *arsB* [12] and *arsC* [14]. Primers for the *acr3* gene were designed by using the Primer3Plus web tool [25]. PCR amplification of arsenic-related marker genes was performed by using bacterial genomic DNA as a template. All PCR reaction mixtures contained approximately 50 ng DNA template, 1× PCR buffer, 0.2 mM of each deoxyribonucleoside triphosphate, 0.5 mM of each primer and 1 U Taq DNA polymerase in 50 μl volume. Amplifications were performed in a piko thermal cycler (Finzymes). Cycling conditions for all PCRs consisted of 5 min of denaturation at 95 °C followed by 34 cycles of 1 min of denaturation at 95 °C, 45 s of annealing at 57.7 °C and primer extension at 72 °C for 1 min of each Kb product size. This was followed by a final extension reaction at 72 °C for 10–15 min. PCR products were purified with a QIAquick gel extraction kit (Qiagen, Cat No. 28706).

2.4. Genome sequencing

Sequencing of the genomic DNA of *L. sphaericus* B1-CDA was performed by the Otogenetics Corporation (GA, USA). Purified 0.5–1 μg of genomic DNA sample was sheared into smaller fragments with a Covaris E210 ultrasonicator. Genomic DNA library was constructed by using the NEB library preparation kit (New England Biolabs) for the Illumina sequencer with a single sequencing index and sequencing was performed with the help of HiSeq2500 PE100 read format. Properly paired reads (≥30 bp) were extracted from the corrected read pool and the remaining singleton reads were combined as single-end reads. Both corrected paired-end and single-end reads were used in the subsequent de novo assembly.

2.5. Genome assembly

The genome assembly started with Illumina 100-bp paired-end reads of genomic DNA with insert length 300 bp. The read quality was checked by using FastQC, version 1.10.1 [26]. The raw reads were quality trimmed and corrected using Quake version 0.3.4 [27]. Properly paired reads of length ≥30 bp were selected from the pool of corrected reads and the remaining singleton reads were considered as single-end reads. Both the paired-end and single-end corrected reads were then used in k-mer-based de novo assembly employing SOAPDenovo, version 2.04 [28]. The set of scaffolds with largest N50 was identified by evaluating k-mers in the range 29–99. The optimal scaffold sequences were further subjected to gap closing by utilizing the corrected paired-end reads. The resulting scaffolds of length ≥300 bp were chosen as the final assembly. The scaffolds were ordered by finding the location of the best Blastn hit for each scaffold on the reference genome *L. sphaericus* C3-41. A total of 31 scaffolds were used for prediction of the genome size and it was performed by following the Mauve Contigs Mover (http://darlinglab.org/mauve/user-guide/reordering.html).

2.6. Phylogenetic inference of Lysinibacillus sp.

In this study, a phylogenetic tree was inferred from the 16S rRNA genes of B1-CDA and other related bacteria [29] by using the Neighbor–Joining method [30] presented in the MEGA6 software [31]. The analysis involved nucleotide sequences from 27 bacteria in the *Bacillaceae* family. The evolutionary distances were computed using the Kimura 2-parameter method [32] in the units of the number of base substitutions per site, including all codon positions (1st, 2nd, 3rd and noncoding). Positions with <95% site coverage were eliminated, thereby allowing fewer than 5% alignment gaps, missing data, and ambiguous bases at any position. There were a total of 1227 positions in the final dataset.

2.7. Comparative analysis with other Lysinibacillus genomes

To study genome rearrangements in *Lysinibacillus* and related bacteria, the progressive MAUVE algorithm in the MAUVE genome alignment software version 2.3.1 [33] was employed. The main purpose of using this method was to compare the possible rearrangements that may occur in *L. sphaericus* B1-CDA [GenBank accession number SAMN04097202 http://www.ncbi.nlm.nih.gov/biosample/4097202], *L. sphaericus* OT4b.31 [accession number AQPX00000000] and *L. sphaericus* C3-41 [accession number CP000817.1]. A nucleotide-based dot plot analysis was performed with the Gepard software [34] to compare the 4.09 Mbp chromosomal scaffolds of *L. sphaericus* B1-CDA with the 4.6 Mbp chromosome of *L. sphaericus* C3-41 and the genome rearrangements were studied.

2.8. Gene prediction and annotation of metal resistant genes

Circular plot of ordered contigs of B1-CDA was generated with DNAPlotter [35] to predict the graphical map of the genome. The assembled genome sequence was annotated with Rapid Annotations using Subsystems Technology, RAST [36]. The RAST analysis pipeline uses the tRNAscan-SE to predict tRNA genes [37] and the GLIMMER algorithm to predict protein-coding genes [38]. In addition, it uses an internal script for identification of rRNA genes [36]. It then infers putative function(s) of the protein coding genes based on homology to already known protein families in phylogenetic neighbor species. Finally, RAST identifies subsystems represented in the genome, and uses this information to reconstruct the metabolic networks. The GeneMark [39] and the FGenesB [40] algorithms were applied for verification of the RAST results obtained in prediction of protein coding genes. Prediction of rRNA genes was also done through the RNAmmer prediction server version 1.2. [41]. Annotation of all genes that were predicted to be metal responsive was manually curated, with a particular focus on genes responsive to As. Functional annotation analysis was also carried out by the Blast2GO pipeline [42] using all translated protein coding sequences resulting from the GeneMark. In Blast2GO the BlastX option

Fig. 2. (A) Nucleotide-based alignment of a 4.5 Mbp chromosomal assembly of *L. sphaericus B1-CDA* (upper) to a 4.6 Mbp chromosome of *L. sphaericus* C3-41 (middle) and 4.09 Mbp chromosome of *L. sphaericus* OT4b.31 (lower). A total of 27 homologous blocks are shown as identically colored regions and linked across the sequences. Regions that are inverted relative to *L. sphaericus* B1-CDA are shifted to the right of center axis of the sequence. (B) Dot plot of nucleotide sequences of *L. sphaericus B1-CDA* (*x*-axis) and *L. sphaericus* C3-41 (*y*-axis). Aligned segments are represented as dots, with regions of conservation appearing as lines.

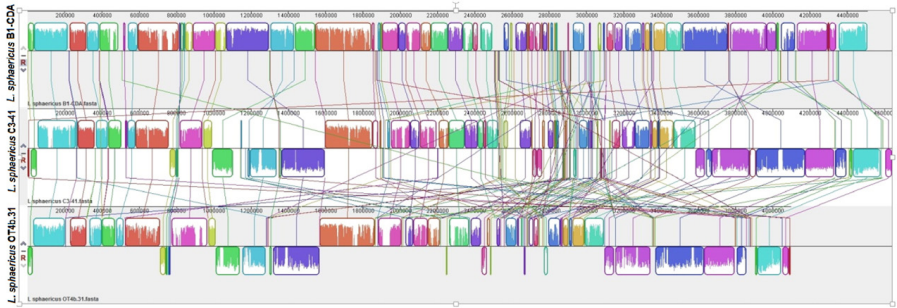
L. sphaericus B1-CDA
L. sphaericus C3-41
L. sphaericus OT4b.31

A

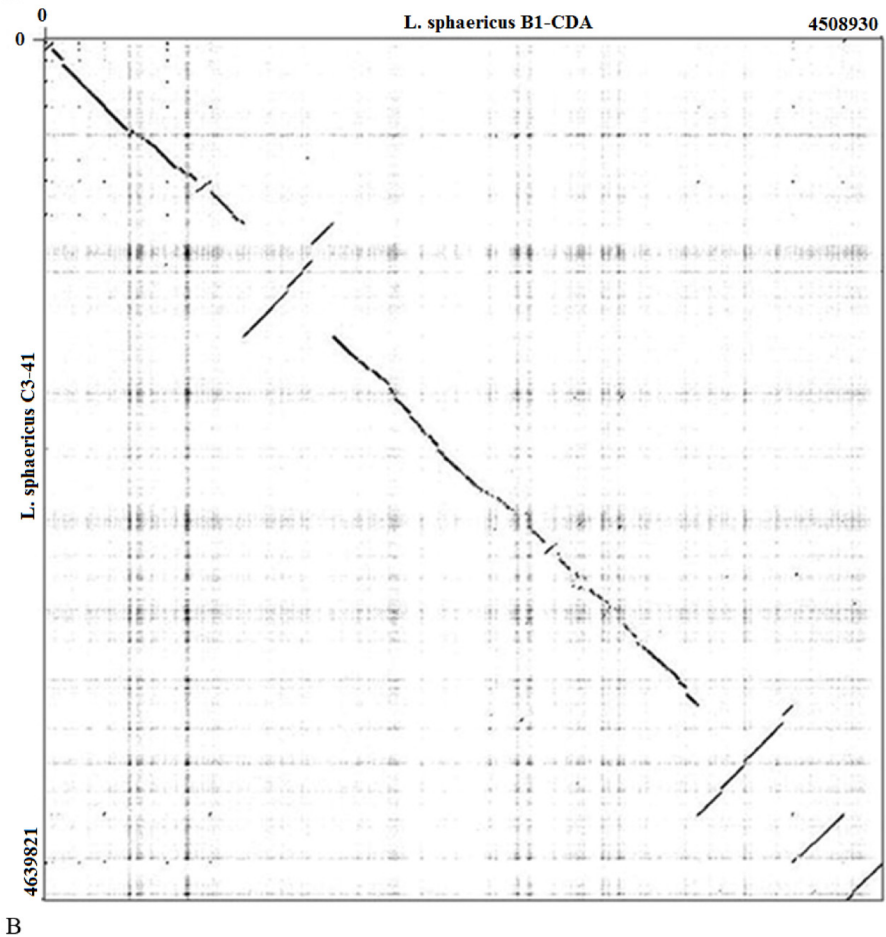
0
L. sphaericus B1-CDA
4508930
0
L. sphaericus C3-41
4639821

B

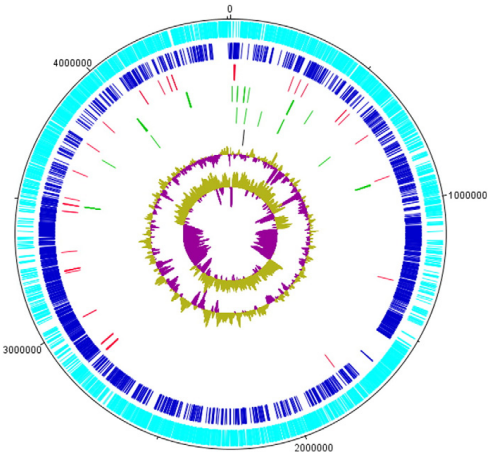

Fig. 3. Circular plot of ordered contigs, generated with DNAPlotter. Tracks indicate (from outside inwards) predicted protein coding genes on forward strand (light blue) and reverse strand (dark blue), metalloprotein genes (red) listed in Table 2, tRNA and rRNA genes (both green), origin of replication (black), GC content and GC skew.

was chosen to find the closest homologs in the non-redundant protein databases (nr), followed by employing Gene Ontology (GO) annotation terms [43] to each gene based on the annotation of its closest homologs. An InterPro scan [44] was then performed through the Blast2GO interface and the InterPro IDs merged with the Blast-derived GO-annotation for obtaining integrated annotation results. The GO annotation of all putative metal responsive genes was manually curated.

3. Results and discussion

3.1. Detection of arsenic marker genes

Several studies have used genetic markers to study As transformation mechanisms [9,12,14–19]. In this study, we present a genetic mechanism for As resistance and As transformation in the bacterial isolates. This mechanism was examined via PCR amplification of As responsive genes. The strain B1-CDA was found to harbor *acr3*, *arsR*, *arsB* and *arsC* arsenic marker genes (Supplementary Fig. 1). The *arsC* gene consists enzyme for arsenate reductase, which is responsible for the biotransformation of arsenate [As(V)] to arsenite [As(III)] prior to efflux. ArsB, an integral membrane protein that pumps arsenite out of the cell, is often associated with an ATPase subunit, arsA [12]. It is hypothesized that the *arsB*/*acr3* genes are the primary determinants in arsenite resistance [12]. These genetic mechanisms of the isolate could be used to cope with arsenic toxicity. Such mechanisms could comprise arsenite methylation that results in volatile products which having very less toxicity that escape from the cells [45].

3.2. Sequencing and de novo genome assembly

A total of 11,105,899 pairs of reads were generated by Illumina deep sequencing. Analysis of the raw reads with FastQC showed that the average per base Phred score was ≥32 for all positions and that the mean per sequence Phred score was 38. The overall GC content was 38%. After removal of the TruSeq adaptor sequence (which was found in 13,435 reads, 0.12%) and error correction and trimming done by using the Quake software, 10,940,654 read pairs (98.5%) and 145,888 single end sequences remained for further analysis. Trimming was performed as the trimming of sequences is an important step for improving mapping efficiency. SOAPDenovo was utilized to perform de novo assembly optimization with the error corrected reads. The set of scaffold sequences with maximal N50 (507,225 bp) was produced at k-mer 91. The corresponding scaffold sequences were subjected to gap closure using the corrected paired-end reads and the resulting set of scaffolds (≥300 bp) was defined as the final assembly. The final assembly consists of 31 scaffolds, with lengths ranging from 314 bp to 1,145,744 bp, resulting a total length of 4,509,276 bp. It contained only 25 bp of unknown nucleotides, i.e. the error rate was less than 1 in 1,000,000. The summary of the genome with nucleotide content and gene count levels is described in Table 1.

3.3. Phylogenetic analysis

Peña-Montenegro and Dussán [29] evaluated phylogenetic tree with native *Bacillaceae* isolates along with *L. sphaericus* OT4b.31, a heavy metal tolerant bacterium. Strains of *L. sphaericus* can be divided into seven DNA similarity subgroups (I–VII), with a clear separation between the groups I–V and groups VI–VII [29,46]. Phylogenetic analysis based on 16S ribosomal RNA gene sequences did not place our strain *L. sphaericus* B1-CDA into any of the existing DNA similarity groups (Fig. 1). The placement of *L. sphaericus* B1-CDA in the phylogeny does, however, indicate higher similarity to groups I–V than to groups VI–VII. In agreement with earlier studies [29,46] *Bacillus silvestris* was also placed between groups I–V and groups VI–VII. This indicated that B1-CDA could also belong to *B. silvestris* but based on the branch lengths it was confirmed that B1-CDA belongs to the species *L. sphaericus* rather than *B. silvestris*.

3.4. Comparative genome analysis

Using the Gepard dot plot software [34] and progressiveMauve from the Mauve software [33], we compared the chromosomal assembly of B1-CDA with that of the *L. sphaericus* C3-41 and *L. sphaericus OT4B.31*. The alignment of B1-CDA, *L. sphaericus* C3-41 and *L. sphaericus* OT4B.31 showing the same chromosomal rearrangement but B1-CDA consists mostly the inversions with *L. sphaericus* C3-41 and *L. sphaericus* OT4B.31 (Fig. 2A). The chromosomal alignments of *L. sphaericus* C3-41 and *L. sphaericus* OT4B.31 are about to be identical (Fig. 2A). The dot plot was performed with B1-CDA and *L. sphaericus* C3-41 since *L. sphaericus* OT4B.31 and *L. sphaericus* C3-41 were similar. The dot plot shows that the genome rearrangements consist mostly of inversions (Fig. 2B). There are large segments of high similarity when most parts of the two chromosomes are mapped onto each other. However, a region comprising around 3 Mbp in the C3-41 chromosome and the contigs 15 to 19 in the B1-CDA chromosomal scaffold were somewhat scattered in the dot plot, revealing lower similarity levels and different syntenial relationships to the reference sequence.

3.5. Gene predictions

Prediction of tRNA-, rRNA- and protein coding genes was performed through the RAST server. The graphical map of the genome and the locations of all predicted genes are shown in the circular genome plot in Fig. 3. The search by tRNAscan-SE (which is the first step in the RAST pipeline) located 77 tRNA genes. A confirmatory scan with the algorithm ARAGORN [47] predicted the identical number, and all predictions overlapped in location, although with slight variation regarding the start or end point for a few genes. The predictions included tRNAs for 19 amino acids, ranging in number from one gene for the cysteine tRNA to six genes for the arginine and glutamic acid tRNAs. The only tRNA gene missing in these predictions was for the amino acid serine. However, three pseudo-tRNA genes were predicted, and two of these contained anticodons for serine. In an ARAGORN scan the total number

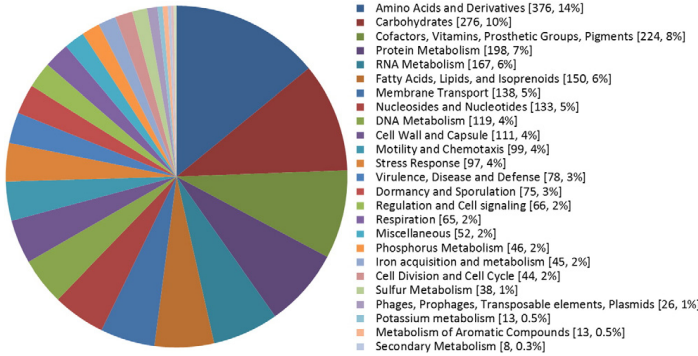

Fig. 4. RAST analysis of genes connected to subsystems and their distribution in different functional categories.

Table 2
Metal responsive genes in B1-CDA predicted by RAST and/or Blast2GO.

Start (bp)	End (bp)	Predicted function	Predicted by	
			RAST	Blast2GO
16,367	18,778	Copper ion binding		X
18,860	19,066	Copper ion transport		X
20,450	19,497	Cobalt–zinc–cadmium resistance protein CzcD	X	X
20,471	20,806	Transcriptional regulator, ArsR family	X	
275,573	277,477	Lead, cadmium, zinc and mercury transporting ATPase	X	X
308,097	309,131	Toxic anion resistance protein TelA	X	X
342,234	343,136	Cobalt-zinc-cadmium resistance protein	X	X
539,475	540,170	Zinc transporter family protein		X
540,161	539,475	Zinc transporter, ZIP family	X	
562,002	562,358	Arsenate reductase	X	X
681,412	680,306	Ferric iron ABC transporter, iron-binding protein	X	
876,386	877,651	Manganese transport protein MntH	X	X
1,328,650	1,329,048	Arsenate reductase family protein	X	X
2,839,200	2,840,816	Periplasmic nickel-binding protein NikA	X	
2,839,200	2,840,816	Nickel cation transport activity		X
2,840,888	2,841,841	Nickel transport system permease protein NikB	X	
2,841,844	2,842,653	Nickel transport system permease protein NikC	X	X
2,842,667	2,843,437	Nickel transport ATP-binding protein NikD	X	X
2,843,447	2,844,253	Nickel transport ATP-binding protein NikE	X	X
2,873,332	2,873,748	Arsenate reductase	X	X
2,873,761	2,874,819	Arsenical resistance protein ACR3	X	
2,873,761	2,874,819	Arsenic resistance protein		X
2,875,138	2,874,812	Arsenical resistance operon repressor	X	
3,011,790	3,010,906	Cobalt–zinc–cadmium resistance protein	X	
3,010,906	3,011,790	Cation transmembrane transporter activity		X
3,211,275	3,211,961	Transcriptional regulator, ArsR family	X	
3,221,732	3,220,863	Manganese transporter, inner membrane permease protein SitD	X	
3,220,863	3,221,732	Iron ABC transporter		X
3,222,601	3,221,729	Manganese transporter, inner membrane permease protein SitC	X	
3,223,341	3,222,613	Manganese ABC transporter, ATP-binding protein SitB	X	X
3,224,265	3,223,351	Manganese ABC transporter, periplasmic-binding protein SitA	X	X
3,301,684	3,300,737	Zinc metallohydrolase, metallo-β-lactamase family	X	
3,480,453	3,479,848	Manganese superoxide dismutase	X	
3,510,620	3,510,192	Zinc uptake regulation protein ZUR	X	
3,510,192	3,510,620	Iron family transcriptional regulator		X
3,511,480	3,510,617	Zinc ABC transporter, inner membrane permease protein ZnuB	X	X
3,512,240	3,511,494	Zinc ABC transporter, ATP-binding protein ZnuC	X	X
3,537,560	3,536,520	Zinc ABC transporter, periplasmic-binding protein ZnuA	X	X
3,655,964	3,655,515	Universal stress protein family	X	X
3,784,105	3,784,524	Universal stress protein family	X	X
3,898,460	3,899,425	Magnesium and cobalt transport protein CorA	X	X
4,106,518	4,105,568	Ferrichrome-binding periplasmic protein precursor	X	
4,105,568	4,106,518	Ferrichrome ABC transporter substrate binding protein		X
4,193,280	4,194,575	Arsenic efflux pump protein	X	X
4,233,352	4,234,161	Zinc transporter		X
4,254,132	4,254,503	Cadmium efflux system accessory protein	X	
4,254,484	4,256,607	Lead, cadmium, zinc and mercury transporting ATPase	X	
4,254,484	4,256,607	Cadmium transporter		X

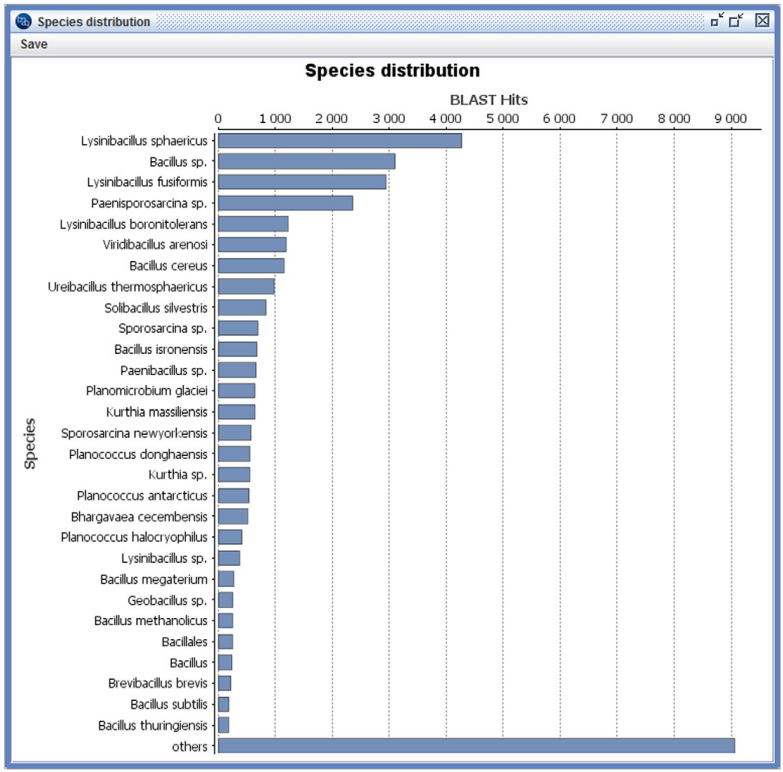

Fig. 5. Schematic representation of species distributions for the homologous proteins found by BlastP in the Blast2GO annotation process.

of predicted tRNA genes in *L. sphaericus* B1-CDA was 77, which was similar to that (83) predicted in the genome of *L. sphaericus* C3-41.

The rRNA prediction in RAST resulted in 11 rRNA genes, including seven 5S, one 16S and three 23S genes, whereas another related strain *L. sphaericus* C3-41 contains 31 rRNA genes, including eleven 5S, ten 16S and ten 23S genes. Due to the surprisingly low number of 16S and 23S genes, RNAmmer [41] scans were performed on the genomes of *L. sphaericus* B1-CDA as well as two unrelated bacteria (*Enterobacter cloacae* and *Salmonella bongori*). The results of these scans were compared to each other prior to making any conclusion. These results confirmed that the *L. sphaericus* B1-CDA genome seems to contain approximately the same number of 5S rRNA genes as the other bacteria, but substantially fewer 16S and 23S rRNA genes. Previously, Pei et al. [48] have shown that 143 bacterial species contain only a single 16S rRNA whereas Pei et al. [49] have shown that 184 genomes had a median of 4.57 23S rRNA genes/genome (range 1 to 15). Therefore, the lower number of 16S and 23S rRNA is not an uncommon feature of bacterial genome.

For prediction of the protein coding genes, RAST uses the GLIMMER algorithm [38]. A total of 4513 protein coding genes were predicted using GLIMMER algorithm), of which 2671 could be annotated by RAST's automated homology analysis procedure and assigned to functional categories (Fig. 4). For confirmation of the number of protein

Table 3
Comparison of some B1-CDA genes with genes of other Lysinobacter species as well as other closely related species exhibiting resistance to arsenics.

ID	Species with closest homolog	Cover	Identity	Gene	InterPro match (selected)	Acc. nr.
Gene 22	*Lysinibacillus borointolerans*	100%	98%	*arsR*	HTH ArsR-type DNA-binding domain	IPR001845
Gene 548	*Lysinibacillus sphaericus* C3-41	99%	88%	*arsC*-like	Arsenate reductase-like	IPR006660
Gene 1254	*Lysinibacillus sphaericus* C3-41	100%	100%	*arsC* (Spx)	Arsenate reductase regulatory protein Spx	IPR006660
Gene 2889	*Lysinibacillus fusiformis*	100%	97%	*arsC*	Arsenate reductase ArsC	IPR014064
Gene 2890	*Lysinibacillus fusiformis*	100%	98%	*arsB*	Arsenical-resistance protein Acr3	IPR004706
Gene 2891	*Lysinibacillus fusiformis*	100%	98%	*arsR*	HTH ArsR-type DNA-binding domain	IPR001845
Gene 4251	*Lysinibacillus fusiformis*	100%	98%	*arsB*	Arsenical pump membrane protein, ArsB	IPR000802

coding genes, the GeneMark [39] and FGenesB [40] algorithms were also applied, yielding 4562 and 4323 genes, respectively. We observed that *L. sphaericus* B1-CDA contains many specific metal resistant genes, such as arsenic, nickel, cobalt, iron, manganese, chromium, cadmium, lead and zinc (Table 2). Further, the functional annotation carried out by the Blast2GO pipeline also indicates that B1-CDA contains many genes which are responsive to specific metal ions like arsenic, cobalt, copper, iron, nickel, potassium, manganese and zinc. (Table 2). The annotations by RAST and Blast2GO remind in agreement. Prediction by RAST and Blast2GO (Supplementary Table 1) revealed that the B1-CDA genome contains additionally a total of 123 proteins which are involved in binding and transport of metal ions. This prediction also indicated that B1-CDA contains many other proteins (approximately 30) that catalyze binding and transport of the metal ions such as metalloendopeptidase, metalloexopeptidase, metallopeptidase, metallocarboxypeptidase and metallochaperone (Supplementary Table 2). Overall statistics of the Blast hits in the Blast2GO annotation process confirmed assignment of the new bacterium as *L. sphaericus*, since this was the most frequent species in the overall list of protein homologs (Fig. 5). The functional assignment of genes into subsystem categories by RAST was compared between B1-CDA and C3-41 (Fig. 5). The large categories of "housekeeping" genes, such as those coding for amino acids, carbohydrates, RNA metabolism, generally contained very similar numbers of genes in the two genomes.

By using InterPro [44] the arsenic responsive genes of B1-CDA genome were compared with the genomes of validly named and sequenced species of Lysinobacter as well as with other closely related arsenic tolerant or resistant species. These results are presented in Table 3. All seven analyzed genes of B1-CDA showed very high similarity with the genes of other Lysinibacillus species. The minimum identity level (97%) was observed in the *arsC* gene (arsenic reductase) of *Lysinibacillus fusiformis*, whereas the highest similarity (100%), in the *arsC* gene (arsenate reductase regulatory protein Spx) of *L. sphaericus* C3-41.

The origin of replication was estimated to be located in the region between 4.3 and 4.4 Mbp, based on homology search in the DoriC database ver. 5.0 [50]. There were significant hits to both *L. sphaericus* oriC regions on scaffold 7. The first covers 772 of the 972 nucleotides of ORI92310378, with 94% identities (and 105 of the remaining nucleotides also match with 94% id 84 bp further downstream), while the second covers 167 of the 170 nucleotides of ORI92310377, again with 94% identities. The corresponding region in the full sequence of the ordered contigs is 4,303,598–4,302,608 bp. In the prediction and annotation of genes, RAST predicted the chromosomal replication initiator protein DnaA at location 4,303,961–4,302,612. Several other replication-related genes were predicted in the near vicinity, such as DNA gyrase subunit A (at bp 4,297,795–4 295,330) and subunit B (at bp 4299,7554–4,297,821), as well as the DNA recombination and repair protein RecF (at bp 4,300,964–4299,849).

4. Conclusions

The native strain *L. sphaericus* B1-CDA, isolated from a cultivated land, was characterized and found to be a metal including arsenic resistant bacterium. A comparison of the genomic sequences of strains B1-CDA with *L. sphaericus* C3-41 and *L. sphaericus* OT4B.31 demonstrated the presence of only a few similar regions with syntenial rearrangements. By using RAST and Blast2GO analyses we have found genes responsive to several metals such as arsenic, nickel, cadmium, iron, manganese, chromium, cadmium, lead, cobalt, zinc, silver and mercury. Therefore, our findings in this study may be useful in bioremediation of toxic metals like arsenic, nickel, cadmium, iron, manganese, chromium, cadmium, lead, cobalt, zinc, and silver mercury in polluted environments. In conclusion, our study demonstrates that it is possible to speed up molecular biology research by using bioinformatics tools.

Acknowledgements

This research has been funded primarily by the Swedish International Development Cooperation Agency (SIDA, grant number: AKT-2010-018) and partly by the Swedish Research Council for Environment, Agricultural Sciences and Spatial Planning (FORMAS, grant number: 229-2007-217). We also acknowledge Nilsson-Ehle (The Royal Physiographic Society in Lund) foundation in Sweden for a mini grant.

Appendix A. Supplementary data

Supplementary data to this article can be found online at http://dx.doi.org/10.1016/j.ygeno.2015.09.006.

References

[1] Y. Chen, F. Parvez, M. Gamble, T. Islam, A. Ahmed, M. Argos, J.H. Graziano, H. Ahsan, Toxicol. Appl. Pharmacol. 239 (2009) 184–192.
[2] F.J. Zhao, S.P. McGrath, A.A. Meharg, Arsenic as a food chain contaminant: mechanisms of plant uptake and metabolism and mitigation strategies, Annu. Rev. Plant Biol. 61 (2010) 535–559, http://dx.doi.org/10.1146/annurev-arplant-042809-112152.
[3] J. Bundschuh, B. Nath, P. Bhattacharya, C.W. Liu, M.A. Armienta, M.V. Moreno Lopez, D.L. Lopez, J.S. Jean, L. Cornejo, L.F. Lauer Macedo, A.T. Filho, Arsenic in the human food chain: the Latin American perspective, Sci. Total Environ. 429 (2012) 92–106.
[4] D. Halder, S. Bhowmick, A. Biswas, U. Mandal, J. Nriagu, D.N. Guha Mazumder, D. Chatterjee, P. Bhattacharya, Consumption of brown rice: a potential pathway for arsenic exposure in rural Bengal, Environ. Sci. Technol. 46 (2012) 4142–4148.
[5] H. Neidhardt, S. Norra, X. Tang, H. Guo, D. Stuben, Impact of irrigation with high arsenic burden groundwater on the soil–plant system: result from a case study in the Inner Mongolia, China, Environ. Pollut. 163 (2012) 8–13.
[6] J. Abedin, J. Feldman, A. Meharg, Uptake kinetics of arsenic species in rice plants, Plant Physiol. 128 (2002) 1120–1128.
[7] M. Valls, V. de Lorenzo, Exploiting the genetic and biochemical capacities of bacteria for the remediation of heavy metal pollution, FEMS Microbiol. Rev. 26 (4) (2002) 327–338.
[8] D.D. Simeonova, K. Micheva, D.A. Muller, F. Lagarde, M.C. Lett, V.I. Groudeva, D. Lievremont, Arsenite oxidation in batch reactors with alginate-immobilized ULPAs1 strain, Biotechnol. Bioeng. 91 (4) (2005) 441–446.
[9] V.H.C. Liao, Y.J. Chu, Y.C. Su, S.Y. Hsiao, C.C. Wei, C.W. Liu, C.M. Liao, W.C. Shen, F.J. Chang, Arsenite-oxidizing and arsenate-reducing bacteria associated with arsenic-rich groundwater in Taiwan, J. Contam. Hydrol. 123 (2011) 20–29, http://dx.doi.org/10.1016/j.jconhyd.2010.12.003.
[10] J.B. Owolabi, B.P. Rosen, Differential mRNA stability controls relative gene expression within the plasmid-encoded arsenical resistance operon, J. Bacteriol. 172 (1990) 2367–2371.
[11] C. Diorio, J. Cai, J. Marmor, R. Shinder, M.S. DuBow, An Escherichia coli chromosomal ars operon homolog is functional in arsenic detoxification and is conserved in Gram-negative bacteria, J. Bacteriol. 177 (1995) 2050–2056.
[12] A.R. Achour, P. Bauda, P. Billard, Diversity of arsenite transporter genes from arsenic-resistant soil bacteria, Res. Microbiol. 158 (2007) 128–137.
[13] S. Silver, L.T. Phung, Genes and enzymes involved in bacterial oxidation and reduction of inorganic arsenic, Appl. Environ. Microbiol. 71 (2005) 599–608.
[14] Y. Sun, E.A. Polishchuk, U. Radoja, W.R. Cullen, Identification and quantification of arsC genes in environmental samples by using real-time PCR, J. Microbiol. Methods 58 (2004) 335–339.
[15] D. Malasarn, C.W. Saltikov, K.M. Campbell, J.M. Santini, J.G. Hering, D.K. Newman, arrA is a reliable marker for As(V) respiration, Science 306 (2004) 455.
[16] T.R. Kulp, S. Han, C.W. Saltikov, B.D. Lanoil, K. Zargar, R.S. Oremland, Effects of imposed salinity gradients on dissimilatory arsenate reduction, sulfate reduction, and other microbial processes in sediments from two California soda lakes, Appl. Environ. Microbiol. 73 (2007) 5130–5137.
[17] B. Song, E. Chyun, P.R. Jaffé, B.B. Ward, Molecular methods to detect and monitor dissimilatory arsenate-respiring bacteria (DARB) in sediments, FEMS Microbiol. Ecol. 68 (2009) 108–117.
[18] E.D. Rhine, S.M. Ní Chadhain, G.J. Zylstra, L.Y. Young, The arsenite oxidase genes (aroAB) in novel chemoautotrophic arsenite oxidizers, Biochem. Biophys. Res. Commun. 354 (2007) 662–667.
[19] N. Hamamura, R.E. Macur, S. Korf, G. Ackerman, W.P. Taylor, M. Kozubal, A.L. Reysenbach, W.P. Inskeep, Linking microbial oxidation of arsenic with detection and phylogenetic analysis of arsenite oxidase genes in diverse geothermal environments, Environ. Microbiol. 11 (2009) 421–431.
[20] T.R. Kulp, S.E. Hoeft, M. Asao, M.T. Madigan, J.T. Hollibaugh, J.C. Fisher, J.F. Stolz, C.W. Culbertson, L.G. Miller, R.S. Oremland, Arsenic(III) fuels anoxygenic photosynthesis in hot spring biofilms from Mono Lake, California, Science 321 (2008) 967–970.
[21] K.M. Handley, M. Héry, J.R. Lloyd, Redox cycling of arsenic by the hydrothermal marine bacterium *Marinobacter santoriniensis*, Environ. Microbiol. 11 (2009) 1601–1611.
[22] A. Rahman, N. Nahar, N.N. Nawani, J. Jass, P. Desale, B.P. Kapadnis, K. Hossain, A.K. Saha, S. Ghosh, B. Olsson, A. Mandal, Isolation of a *Lysinibacillus* strain B1-CDA

PAPER IV

showing potentials for arsenic bioremediation, J. Environ. Sci. Health A 49 (2014) 1349–1360.
[23] R.J. Reece, Analysis of Genes and Genomes, John Willey and Sons Ltd, The Atrium, Southern Gate, Chichester, West Sussex PO19 8SQ, England, 2004.
[24] M.A. Larkin, G. Blackshields, N.P. Brown, R. Chenna, P.A. McGettigan, H. McWilliam, F. Valentin, I.M. Wallace, A. Wilm, R. Lopez, J.D. Thompson, T.J. Gibson, D.G. Higgins, Clustal W and clustal X version 2.0, Bioinformatics 23 (2007) 2947–2948.
[25] A. Untergasser, H. Nijveen, X. Rao, T. Bisseling, R. Geurts, A.M. Jack, Leunissen: Primer3Plus, an enhanced web interface to Primer3, Nucleic Acids Res. 35 (2007) W71–W74.
[26] S. Andrews, FastQC: a quality control tool for high throughput sequence dataAvailable online at: http://www.bioinformatics.babraham.ac.uk/projects/fastqc2010.
[27] D.R. Kelley, M.C. Schatz, S.L. Salzberg, Quake: quality-aware detection and correction of sequencing errors, Genome Biol. 11 (11) (2010) R116 (Epub 2010 Nov 29).
[28] R. Li, H. Zhu, J. Ruan, W. Qian, X. Fang, Z. Shi, Y. Li, S. Li, G. Shan, K. Kristiansen, S. Li, H. Yang, J. Wang, J. Wang, De novo assembly of human genomes with massively parallel short read sequencing, Genome Res. 20 (2) (2010) 265–272.
[29] T.D. Peña-Montenegro, J. Dussán, Genome sequence and description of the heavy metal tolerant bacterium *Lysinibacillus sphaericus* strain OT4b.31, Stand. Genomic Sci. 9 (2013) 42–56, http://dx.doi.org/10.4056/sigs.4227894.
[30] N. Saitou, M. Nei, The neighbor-joining method: a new method for reconstructing phylogenetic trees, Mol. Biol. Evol. 4 (1987) 406–425.
[31] K. Tamura, G. Stecher, D. Peterson, A. Filipski, S. Kumar, MEGA6: Molecular Evolutionary Genetics Analysis version 6.0, Mol. Biol. Evol. 30 (2013) 2725–2729.
[32] M. Kimura, A simple method for estimating evolutionary rate of base substitutions through comparative studies of nucleotide sequences, J. Mol. Evol. 16 (1980) 111–120.
[33] A.E. Darling, B. Mau, N.T. Perna, ProgressiveMauve: multiple genome alignment with gene gain, loss and rearrangement, PLoS ONE 5 (2010), e11147.
[34] J. Krumsiek, R. Arnold, T. Rattei, Gepard: a rapid and sensitive tool for creating dot plots on genome scale, Bioinformatics 23 (8) (2007) 1026–1028.
[35] T. Carver, N. Thomson, A. Bleasby, M. Berriman, J. Parkhill, DNAPlotter: circular and linear interactive genome visualization, Bioinformatics 25 (1) (2009) 119–120.
[36] R.K. Aziz, D. Bartels, A.A. Best, M. DeJongh, T. Disz, R.A. Edwards, K. Formsma, S. Gerdes, E.M. Glass, M. Kubal, F. Meyer, G.J. Olsen, R. Olson, A.L. Osterman, R.A. Overbeek, L.K. McNeil, D. Paarmann, T. Paczian, B. Parrello, G.D. Pusch, C. Reich, R. Stevens, O. Vassieva, V. Vonstein, A. Wilke, O. Zagnitko, The RAST Server: rapid annotations using subsystems technology, BMC Genomics 9 (2008) 75, http://dx.doi.org/10.1186/1471-2164-9-75.
[37] T.M. Lowe, S.R. Eddy, tRNAscan-SE: a program for improved detection of transfer RNA genes in genomic sequence, Nucleic Acids Res. 25 (5) (1997) 955–964.
[38] S.L. Salzberg, A.L. Delcher, S. Kasif, O. White, Microbial gene identification using interpolated Markov models, Nucleic Acids Res. 26 (2) (1998) 544–548.
[39] M. Borodovsky, J. McIninch, GeneMark: parallel gene recognition for both DNA strands, Comput. Chem. 17 (1993) 123–133.
[40] A.A. Salamov, V.V. Solovyev, Ab initio gene finding in drosophila genomic DNA, Genome Res. 10 (2000) 516–522.
[41] K. Lagesen, P. Hallin, E.A. Rødland, H.H. Stærfeldt, T. Rognes, D.W. Ussery, RNAmmer: consistent and rapid annotation of ribosomal RNA genes, Nucleic Acids Res. 35 (9) (2007) 3100–3108, http://dx.doi.org/10.1093/nar/gkm160.
[42] S. Götz, J.M. García-Gómez, J. Terol, T.D. Williams, S.H. Nagaraj, M.J. Nueda, M. Robles, M. Talón, J. Dopazo, A. Conesa, High-throughput functional annotation and data mining with the Blast2GO suite, Nucleic Acids Res. 36 (2008) 3420–3435.
[43] M. Ashburner, C.A. Ball, J.A. Blake, D. Botstein, H. Butler, J.M. Cherry, A.P. Davis, K. Dolinski, S.S. Dwight, J.T. Eppig, M.A. Harris, D.P. Hill, L.I. Tarver, A. Kasarskis, S. Lewis, J.C. Matese, J.E. Richardson, M. Ringwald, G.M. Rubin, G. Sherlock, Gene Ontology: tool for the unification of biology. The Gene Ontology Consortium, Nat. Genet. 25 (1) (2000) 25–29.
[44] E.M. Zdobnov, R. Apweiler, InterProScan—an integration platform for the signature-recognition methods in InterPro, Bioinformatics 17 (9) (2001) 847–848.
[45] J. Qin, B.P. Rosen, Y. Zhang, G. Wang, S. Franke, C. Rensing, Arsenic detoxification and evolution of trimethylarsine gas by a microbial arsenite S-adenosylmethionine methyltransferase, Proc. Natl. Acad. Sci. U. S. A. 103 (2006) 2075–2080.
[46] L.K. Nakamura, Phylogeny of *Bacillus sphaericus*-like organisms, Int. J. Syst. Evol. Microbiol. 50 (2000) 1715–1722.
[47] D. Laslett, B. Canback, ARAGORN, a program to detect tRNA genes and tmRNA genes in nucleotide sequences, Nucleic Acids Res. 32 (1) (2007) 11–16.
[48] A.Y. Pei, W.E. Oberdorf, C.W. Nossa, A. Agarwal, P. Chokshi, E.A. Gerz, Z. Jin, P. Lee, L. Yang, M. Poles, S.M. Brown, S. Sotero, T. DeSantis, E. Brodie, K. Nelson, Z. Pei, Diversity of 16S rRNA genes within individual prokaryotic genomes, Appl. Environ. Microbiol. 76 (12) (2010) 3886–3897.
[49] A. Pei, C.W. Nossa, P. Chokshi, M.J. Blaser, L. Yang, D.M. Rosmarin, Z. Pei, Diversity of 23S rRNA genes within individual prokaryotic genomes, PLoS One 4 (5) (2009), e5437http://dx.doi.org/10.1371/journal.pone.0005437.
[50] F. Gao, H. Luo, C.T. Zhang, DoriC 5.0: an updated database of *oriC* regions in both bacterial and archaeal genomes, Nucleic Acids Res. 41 (2013) 90–93.

Genome analysis of *Enterobacter cloacae* B2-DHA – A bacterium resistant to chromium and/or other heavy metals

Aminur Rahman[1,2], Noor Nahar[1], Björn Olsson[1], Jana Jass[2], Neelu N. Nawani[3], Sibdas Ghosh[4], Ananda K. Saha[5], Khaled Hossain[6] and Abul Mandal[1]

[1]Systems Biology Research Center, School of Bioscience, University of Skövde, P.O. Box 408, SE-541 28 Skövde, Sweden
[2]The Life Science Center, School of Science and Technology, Örebro University, SE-701 82 Örebro, Sweden
[3]Dr. D. Y. Patil Biotechnology and Bioinformatics Institute, Dr. D. Y. Patil Vidyapeeth, Tathawade, Pune-411033, India
[4]School of Arts and Science, Iona College, New Rochelle, NY 10801, USA
[5]Department of Zoology, University of Rajshahi, Rajshahi 6205, Bangladesh
[6]Department of Biochemistry & Molecular Biology, University of Rajshahi, 6205 Bangladesh

Address correspondence to Abul Mandal, System Biology Research Center
School of Bioscience, University of Skövde, P. O. Box 408, SE-541 28 Skövde, Sweden
Phones +46-500448608 (direct), +46-739-876839 (mobile)
E-mail: abul.mandal@his.se

Abstract

Previously we have described a chromium resistant bacterium, *Enterobacter cloacae* B2-DHA, isolated from the landfills of leather manufacturing tannery industries in Bangladesh. This article reports the entire genetic composition of this bacterium probed by massive parallel sequencing and comparative analysis with other known *Enterobacter* genomes. The genome size of B2-DHA and the number of genes in the bacterium are predicted to be about 4.21 Mb and 3955 respectively. All predicted genes of B2-DHA are found to be involved in binding, transport, and catabolism of ions as well as efflux of inorganic and organic compounds. Furthermore, we have identified genes, verified by PCR under *in vitro* conditions, resistance to chromium. The set of ordered contigs have abundant regions similar to those of other *Enterobacter* genomes indicating genome rearrangements. The outcome of this research highlights the significance of this bacterium in removing chromium and other toxic metals from the contaminated sources.

Keywords: Bioremediation; Heavy/Toxic metals; *Enterobacter cloacae;* Genome sequencing; *de novo* assembly; Gene annotation.

Introduction

The globalization through urbanization and industrialization creates pollution including heavy metal toxicity. In particular, chromium toxicity, generated through widespread anthropogenic inputs via leather processing, steel production, wood preservation, chromium/electroplating, metal processing, alloy formation, textiles, ceramics and thermonuclear weapons manufacturing, and agronomic practices including the use of organic biomass (sewage sludge or fertilizers) continues to be a major threat to each segment of environment [1–5]. Furthermore, chromium exerts damage directly on human health through toxic and mutagenic effects causing severe DNA damage [6]. Therefore, it is indeed a matter of concern to everybody as it has direct effect on human and environmental health [7]. Microorganisms have developed various devices to survive chromium toxicity through several mechanisms: (i) the transmembrane efflux of chromate [8] (ii) the chrR transport system [9], (iii) the reduction of chromate [10], (iv) the protection against oxidative stress [11-13] and (v) the DNA repair systems [3,14]. The abilities of microorganisms to survive in these environments and to detoxify chromate require the presence of specific resistance systems. In addition, chromate resistance is attributed to the functions of a series of chromosomal or plasmid encoded genes [8] including chromium resistance (chr) operon comprising either *chrBAC* [15] or *chrBACF* [16] in bacteria. The chrA protein, a member of the CHR superfamily of transporters [17] appears to be active in efflux of chromate driven by the membrane potential [18] whereas the *chrB* gene encodes a membrane bound protein necessary for the regulation of chromate resistance [19]. The *chrC* gene encodes a protein almost similar to iron-containing superoxide dismutase, while the *chrE* gene encodes a gene product resembling a rhodanese type enzyme in *Orthrobacterium tritici* 5bvI1 [19]. The *chrF* gene encodes most probably a repressor for chromate-dependent induction [17] whereas ChrR catalyzes one-electron shuttle followed by a two-electron transfer to Cr^{6+} [20].

Previously, we have characterized *E. cloacae* B2-DHA, a soil-borne bacterium, that can survive and grow on medium containing up to 1000 µg/mL potassium chromate and thereby reducing chromium contents in the contaminated source by 81% [5]. However, the mechanisms by which this chromium-adapted B2-DHA survives were not elucidated. Thus, the present study is aimed to demonstrate, whether the strain B2-DHA harbored the genes in its genome responsible for chromium and, or other metal resistance. Previously, all the genes involved in metal binding activity and reduction of metal by the *E. cloacae* B2-DHA strain, predicted by RAST [21] and/or Blast2GO [22]. In this study, we have performed massively parallel genome sequencing of *E. cloacae* B2-DHA to investigate the metal responsive genes. Furthermore, we have

conducted comparative genome analyses of *E. cloacae* B2-DHA with other known *Enterobacter* genome sequences, and characterized the genetic rearrangements among the various lineages to understand the evolutionary processes involved in shaping the genomes.

Materials and Methods

Strain isolation

The soil samples used for isolation of chromium resistant bacteria were collected from the landfills of about 90-95 percent leather manufacturing tannery industries located in the Hazaribagh in Dhaka, the capital of Bangladesh. The soil surface at 0–15 cm in depth was collected and reserved in plastic bags, and saved at 4ºC until further analysis. The characterization including the content of metal ions in the soil samples has been described previously by Rahman et al [5].

Extraction of genomic DNA

Genomic DNA was extracted from the isolate, *E. cloacae* B2-DHA using DNeasy Blood & Tissue Kit (Qiagen, Cat No 69506) with following modifications: (i) bacteria were cultured in Luria Bertani (LB) medium and pellets were collected from 1.0 ml of bacterial cultures by centrifugation at 8000 rpm for 10 min; and (ii) the pellets were resuspended in TE buffer (10 mM Tris- HCl, 1 mM EDTA [pH 8.0]) containing RNase (50 mg/ml) and lysozyme (50 mg/ml) and incubated at 37°C for 2 h instead of using ALT. The purity and concentration of extracted DNA were measured by using Nanodrop® ND-1000 Spectrophotometer (Saveen Werner, USA). The clear band giving DNA sample was selected on agarose via electrophoresis for whole genome sequencing.

Genome sequencing

The entire genome sequencing of *E. cloacae* B2-DHA was assisted by the Otogenetics Corporation (GA, USA) as follows: (i) Purified 0.5-1.0 µg of genomic DNA sample was clipped into smaller fragments with a Covaris E210 ultrasonicator as described earlier by Rahman et al [23]; (ii) The library of genomic DNA was prepared as per the standard protocol of the NEB library preparation kit (New England Biolabs) for the Illumina sequencer with a single sequencing index; (iii) The sequencing was accomplished with the Illumina HiSeq2500 PE106 (106bp paired-end) read format; (iv) Properly paired reads (≥30bp) were separated from the

corrected read pool and the remaining singleton reads were combined as single-end reads; and (v) Both of the single-end reads and corrected paired-end reads were used in the subsequent *de novo* assembly as described previously [24].

De novo assembly

The *de novo* assembly started with Illumina 106-bp paired-end reads of genomic DNA with insert length 300 bp and the read quality was measured with FastQC, version 1.10.1 [25]. Adapter and quality trimming on raw reads were conducted with cutAdapt [26], and K-mer error correction is performed on the adapter-free reads using Quake, version 0.3.5 [27]. The paired reads were extracted from the corrected read pool and the remaining singleton reads were listed as single-end reads. Both corrected paired-end and single-end reads were used in the k-mer-based *de novo* assembly. SOAPDenovo, version 2.04 [28], was utilized to perform *de novo* assembly optimization with the error corrected reads. A wide range of K-mers (29 - 99) was used to identify the scaffold sequences with the largest N50. The optimal scaffold sequences were further subjected to gap closing by utilizing the corrected paired-end reads, and the resulting scaffolds of length ≥300 bp were chosen as the final assembly. The largest N50 of 492970 bp was produced at the kmer 97. All the scaffolds were ordered by finding the location of the best Blastn hit for each scaffold on the reference genome E. *cloacae* ECNIH2 [NCBI accession number CP008823]. A total of 13 scaffolds were used for prediction of the genome size performed by following the Mauve Contigs Mover (http://darlinglab.org/mauve/user-guide/reordering.html).

Comparative analysis with other Enterbacter genomes

The Whole Genome Shotgun project has been deposited at DDBJ/EMBL/GenBank under the GenBank accession LFJA00000000 [29]. The progressive MAUVE algorithm in the MAUVE genome alignment software, version 2.3.1 [30], was used to study genome rearrangements in *E. cloacae* B2-DHA and related bacteria. Furthermore, another nucleotide-based dot plot analysis was performed with the Gepard software [31] to (i) compare the 4.21 Mbp chromosomal scaffolds of *E. cloacae* B2-DHA with that of 4.85 Mbp chromosome in *E. cloacae* ECNIH2, and (ii) investigate the possible genome rearrangements in these strains.

Prediction and annotation of metal responsive genes

The prediction of all genes in B2-DHA genome was carried out using GeneMark [32] and FGenesB [33]. We have applied Blast2GO [22] pipeline using all translated protein coding sequences resulting from the FGenesB to execute all functional annotation analyses. In Blast2GO, the BlastP option was chosen to find the closest homologs in the non-redundant protein databases (nr), followed by employment of Gene Ontology (GO) annotation terms to each gene [34]. An InterPro scan [35] was then performed through the Blast2GO interface with the InterPro IDs for obtaining integrated annotation results. Annotation of all putative metal responsive genes was manually curated. The assembled genome sequence was annotated with Rapid Annotations using Subsystems Technology, RAST [21] which uses (i) the GLIMMER algorithm to predict protein-coding genes [36], (ii) the tRNAscan-SE to predict tRNA genes [37], (iii) an internal script for identification of rRNA genes [21], and (iv) the RNAmmer prediction server version 1.2, to identify rRNA genes [38]. Furthermore, RAST (i) infers putative function(s) of the protein coding genes based on homology with known protein families in phylogenetic neighbor species, and (ii) detects subsystems represented in the genome, and helps reconstruct the metabolic networks. RAST results obtained in prediction of protein coding genes were compared with the GeneMark and the FGenesB algorithms. Circular plot of ordered contigs of B2-DHA was generated with DNAPlotter [39] to predict the graphical map of the genome.

PCR amplification of chromium-responsive genes

Primers for the gene *chrR* and *chrA* were designed by using the Primer3Plus web tool [40]. The two primer pairs, *chrR*-F/ *chrR*-R (5'-ATGTCTGATACGTTGAAAGTTGTTA-3'/ 5'-CAGGCCTTCACCCGCTTA-3') and *chrA*-F/ *chrA*-R (5'-TGAAAAGCTGTTTACCCCACT-3'/ 5'- TTACAGTGAAGGGTAGTCGGTATAA-3') were selected for the detection of *chrR* and *chrA* genes, respectively. PCR amplification of chromium-related marker genes was performed using bacterial genomic DNA as a template in a piko thermal cycler (Finzymes) under the following cycling conditions: 5 min of denaturation at 95°C followed by 30 cycles of 1 min of denaturation at 95°C, 45 s of annealing at 54.5°C, and primer extension at 72°C for 1 min of each Kb product size. All PCR reaction mixtures contained approximately 50 ng DNA template, 0.2 mM of each deoxyribonucleoside triphosphate, 1X PCR buffer, 0.5 mM of each primer, and 1 U Taq DNA polymerase in a final volume of 50 µl. The final extension reaction was conducted at 72°C for 15 min. PCR products were purified with a QIAquick PCR Purification Kit (Qiagen, Cat No 28104).

Results and discussion

Sequencing and de novo genome assembly

Illumina deep sequencing analysis revealed a total of 1,756,877,072 bases containing 16,574,312 pairs of reads with an overall GC content of 55% in the genome. After quality trimming error correction followed by removal of the TruSeq adaptor sequence 15,708,650 read pairs (94.78%) and 331,106 single end sequences remained for further analysis. Analysis of the raw reads with FastQC showed that the mean score per base Phred and per sequence Phred was ≥36 and 36 respectively for all positions [29]. The set of scaffold sequences with maximal N50 (492,970 bp) was detected at k-mer 97. The corresponding scaffold sequences were subjected to gap closure using the corrected paired-end reads and the resulting scaffolds (≥24300 bp) were defined as the final assembly. The genome summary including the nucleotide contents and gene counts are posted in Table 1. The scaffolds were ordered by finding the location of the best Blastn hit for each scaffold on the reference genome *Enterobacter cloacae* ECNIH2. The final assembly of 4,218,945 bp was comprised of 13 scaffolds ranging from 72,208 to 777,700 bp.

Comparative genome analysis

The chromosomal arrangement of *E. cloacae* B2-DHA is compared with that of the *E. cloacae* ECNIH2 by employing the progressive Mauve from the Mauve software [30] and Gepard dot plot software [31]. While the alignment remains approximately identical in chromosomal rearrangement, but the progressive Mauve analysis reveals several inversions in scaffolds of *E. cloacae* B2-DHA compared to that in *E. cloacae* ECNIH2 (Figure 1A). The dot plot performed with *E. cloacae* B2-DHA and *E. cloacae* ECNIH2 depicts a similar observation of inversions in scaffolds of *E. cloacae* B2-DHA (Figure 1B). Furthermore, there are large segments of high similarity when most parts of the chromosomes of *E. cloacae* B2-DHA and *E. cloacae* ECNIH2 are mapped onto each other (Figure 1B).

Gene predictions

The goal of gene prediction was to catalogue all the genes encoded within the *E. cloacae* genome to help us better understand the mechanisms involved in becoming resistant to chromium and other toxic metals. The genome and the locations of all predicted genes through RAST server are shown via a circular plot in Figure 2. The prediction of rRNA coding genes

performed through RAST server revealed 22 rRNA genes including four LSU, four SSU, eight 16S and six 23S genes (Figure 2) in *E. cloacae* B2-DHA compared to that of *Enterobacter cloacae* ECNIH2 strain containing 25 (5S, 16S, 23S) rRNA genes [http://www.ncbi.nlm.nih.gov/nuccore/CP008823]. ARAGORN, version 1.2.36 [41], employed to predict tRNA genes, revealed 66 tRNA genes with a GC content ranging from 48.0% to 67.5% in *E. cloacae* B2-DHA compared to 87 tRNA genes previously described for *Enterobacter cloacae* ECNIH2 strain [http://www.ncbi.nlm.nih.gov/nuccore/CP008823]. The difference in the number of tRNAs is found to be a common feature of bacterial and archaea genomes [42]. However, the bacteria which have the highest number of 16S rRNA genes are reported to have also the highest number of total tRNA genes [43]. Overall, the genome of *E. cloacae* B2-DHA is very similar in size, number of predicted genes, and nucleotide composition to *E. cloacae* ECNIH2.

RAST analysis using the GLIMMER algorithm [36] predicted a total of 3958 protein coding genes of which 3401 could be annotated by RAST's automated homology analysis procedure and assigned to functional categories (Figure 3). For confirmation of the number of protein coding genes, the GeneMark [32] and the FGenesB [33] algorithms were also applied, yielding 3764 and 3955 genes, respectively. This difference in number of protein coding gene in a bacterial strain can be attributed to a common phenomenon as previously reported for a Gram-positive bacterium, *Lysinibacillus sphaericus* B1-CDA, harboring different number of protein coding genes analyzed by different web tools [23]. RAST analysis predicted that the strain *E. cloacae* B2-DHA contains a large number of genes involved in the ion binding, transport, catabolism and efflux of inorganic as well as organic compounds. More specifically, B2-DHA strain contains many predicted specific toxic metal resistant genes, such as arsenic, chromium, cadmium, cobalt, lead and nickel (Table 2). The Blast2GO pipeline analysis also indicates that B2-DHA contains many genes that are responsive directly to toxic metal ions like arsenic, chromium, cadmium, cobalt, lead and nickel (Table 2). Hence, the annotations performed by RAST and Blast2GO remain in agreement. Recently, Rahman et al [23] discovered an arsenic resistant bacterial isolate that is also contains cobalt, copper, iron, nickel, potassium, manganese and zinc resistant proteins. RAST and/or Blast2GO predicted that B2-DHA strain possess many trace elements (manganese, molybdenum and tellurite) binding and/or transporter proteins (Table 3). Also, a large number of zinc ion binding and/or transporter proteins as well as many calcium, copper, iron, magnesium, potassium and sodium ion binding/transport proteins are retained in B2-DHA predicted by RAST and/or Blast2GO (data not shown). The RAST and

Blast2GO analyses revealed that the B2-DHA genome contains additionally a total of 104 proteins involved in binding and transport of metal ions and many other proteins that catalyze binding and transport of the metal ions such as metalloendopeptidase, metalloexopeptidase, metallopeptidase, metallocarboxypeptidase and metallochaperone as well as this strain owns some metallocenter assembly protein such as HypA, HypB, HypC, HypD, HypE and HypF (data not shown). However, several polymyxin resistance proteins such as PmrM, PmrL, PmrJ and ArnC are present in B2-DHA predicted by RAST and/or Blast2GO (Table 4). Polymyxin resistance proteins are polycationic antimicrobial peptides that are presently serve as antibiotics for the treatment of multidrug-resistant, Gram-negative bacterial infections. Several bacteria such as *Serratia* sp., *Burkholderia* sp., and *Proteus* sp., are naturally resistant to these antibiotics whereas other bacteria such as *Pseudomonas aeruginosa*, *Acinetobacter baumannii* and *Klebsiella pneumoniae* develop resistance to polymyxins in a process as acquired resistance [44]. RAST analysis also enabled us to detect several multidrug transporter proteins like MdtA, MdtB, MdtC and MdtD in B2-DHA strain (Table 4). This strain also contains universal stress protein A, B, C, E and G as well as it harbors several multiple antibiotic resistance protein like MarA, MarB, MarC and MarR (Table 4). All of these proteins are present in both Gram positive and Gram-negative bacteria and archaea [42, 45]. These proteins contain many possible metal-binding residues, which may bind to several metal ions, mostly with nickel ion [45]. The strain B2-DHA owns many metalloproteinase or metalloprotease enzymes. These protease enzymes having catalytic mechanism involves metal binding ion [46]. Among several means to protect themselves from adverse environmental stimuli, including exposure to stress factor, cationic antimicrobial peptides, and toxic metals [44], bacteria various strategies containing alterations of their lipopolysaccharides (LPSs) in their cell walls, which have overall negative charges and are the initial targets of polymyxins [47]. Other strategies comprise the employment of an efflux pump and capsule formation [48-49]. Thus, the strain B2-DHA, isolated from a highly chromium contaminated tannery industries areas, might have developed similar mechanisms to survive in adverse conditions.

Statistical analyses of the Blast top hits in the Blast2GO annotation revealed several bacterial species with the highest similarity based on the best/first sequence alignment for a given Blast, however, confirmed assignment of the bacterium as *E. cloacae*, since this was the most frequent species in the overall list of protein homologs (Figure 4). The best alignment is the one with the lowest e-value.

Detection of chromium marker genes

Several researchers have studied genetic markers to detect chromium transformation mechanisms [16-17, 19-20, 50]. In this article, we present a genetic mechanism for chromium resistance and chromium transformation along with other toxic metals in the bacterial strain B2-DHA. The presence of chromium reductase genes was verified by laboratory based PCR amplification and found B2-DHA strain to harbor *chrR* and *chrA* chromium marker genes (data not shown). The chrA protein appears to be active in efflux of chromate driven by the membrane potential [18]. The ChrR catalyzes an initially one-electron shuttle followed by a two-electron transfer to Cr6+ with the formation of intermediate(s) Cr^{5+} and/or Cr^{4+}before further reduction to Cr^{3+} [20], a critical process involved in detoxification of chromium. Therefore, these genetic mechanisms of the isolate could be used to cope with chromium toxicity.

Conclusions

In this article we report the strain, *E. cloacae* B2-DHA isolated from a landfill containing effluents disposed from leather manufacturing tannery industries, contains characteristics of a heavy metal including chromium resistant bacterium. Furthermore, using RAST and Blast2GO analyses we predicted the presence of genes in this strain responsive to several metals such as arsenic, cadmium, cobalt, iron, lead, manganese, mercury, nickel, silver and zinc. These findings can be employed in bioremediation of these toxic metals in polluted environments. In a long-term perspective, millions of people worldwide, in turn, can avoid many lethal diseases caused by chronic exposure of toxic metal poisoning. Therefore, our discoveries have a great potential through further investigations in contributing to a significant positive impact on the socioeconomic status of the people particularly in the developing world.

Acknowledgements

This research was supported by a major grant (no. AKT-2010-018) from the Swedish International Development Cooperation Agency (SIDA), and partly by a small grant from the Nilsson-Ehle (The Royal Physiographic Society in Lund) foundation in Sweden.

References

[1]. Rahman A., Nahar N., Nawani N.N., Jass J., Desale P., Kapadnis B.P., Hossain K., Saha A.K., Ghosh S., Olsson B., Mandal A. (2014) Isolation of a *Lysinibacillus* strain B1-CDA showing potentials for arsenic bioremediation. J. Environ. Sci. and Health, Part A. 49, 1349–1360.

[2]. Viti C., Pace A., Giovannetti L. (2003) Characterization of Cr (VI)-resistant bacteria isolated from chromium-contaminated soil by tannery activity. Curr. Microbiol. 46: 1–5.

[3]. Chourey K., Thompson M.R., Morrell-Falvey J., VerBerkmoes N.C., Brown S.D., Shah M., Zhou J., Doktycz M., Hettich R.L., Thompson D.K. (2006) Global molecular and morphological effects of 24-hour chromium(vi) exposure on *Shewanella oneidensis* MR-1. Appl. Environ. Microbiol. 72: 6331–6344. doi:10.1128/AEM.00813-06

[4]. Saha R., Nandi R., Saha B. (2011) Sources and toxicity of hexavalent chromium, a review. Journal of Coordination Chemistry. 64(10): 1782-1806. doi:10.1080/00958972.2011.583646.

[5]. Rahman A., Nahar N., Nawani N.N., Jass J., Hossain K., Alam Z.A., Saha A.K., Ghosh S., Olsson B., Mandal A. (2015) Bioremediation of hexavalent chromium (VI) by a soil borne bacterium, *Enterobacter cloacae* B2-DHA. J. Environ. Sci. and Health, Part A. 50:11, 1136-1147.

[6]. Hailer M.K., Slade P.G., Martin B.D., Sugden K.D. (2005) Nei deficient *Escherichia coli* are sensitive to chromate and accumulate the oxidized guanine lesion spiroiminodihydantoin. Chem. Res. Toxicol. 18:1378–1383. doi:10.1021/tx0501379

[7]. Hogan C.M. (2012) *Heavy metal*. In: Encyclopedia of Earth. Eds. Cutler J. Cleveland (Washington, D.C.: Environmental Information Coalition, National Council for Science and the Environment).

[8]. Ramirez-Diaz M., Diaz-Perez C., Vargas E., Riveros-Rosas H., Campos-Garcia J., Cervantes C. (2008) Mechanisms of bacterial resistance to chromium compounds. Biometals. 21: 321–332.

[9]. Saier M.H. Jr. (2003) Tracing pathways of transport protein evolution. Mol. Microbiol. 48: 1145 - 1156. doi:10.1046/j.1365-2958.2003.03499.x

[10]. Cervantes C., Campos-Garcia J. (2007) Reduction and efflux of chromate by bacteria. In: Nies, D. H., Silver S. (Eds.). *Molecular Microbiology of Heavy Metals*. Springer-Verlag, Berlin, 407 - 420.

[11]. Ackerley D.F., Barak Y., Lynch S.V., Curtin J., Matin A. (2006) Effect of Chromate Stress on *Escherichia coli* K-12. J. Bact. 188 (9): 3371 - 3381. doi:10.1128/JB.188.9.3371–3381.2006

[12]. Brown S.D., Thompson M.R., Verberkmoes N.C., Chourey K., Shah M., Zhou J., Hettich R.L., Thompson D.K. (2006) Molecular dynamics of the *Shewanella oneidensis* response to chromate stress. Mol. Cell. Proteom. 5: 1054 - 1071. doi:10.1074/mcp.M500394-MCP200

[13]. Henne K.L., Nakatsu C.H., Thompson D.K., Konopka A.E. (2009) High-level chromate resistance in *Arthrobacter* sp. strain FB24 requires previously uncharacterized accessory genes. BMC Microbiol. 9: 199. doi:10.1186/1471-2180-9-199

[14]. Miranda A.T., González M.V., González E.G., Vargas E., Campos-García J., Cervantes C. (2005) Involvement of DNA helicases in chromate resistance by *Pseudomonas aeruginosa* PAO1. Mutat. Res. 578: 202 - 209. doi:10.1016/j.mrfmmm.2005.05.018

[15]. Nies A., Nies D.H., Silver S. (1990) Nucleotide sequence and expression of a plasmid encoded chromate resistance determinant from *Alcaligens eutrophus*. J. Biol. Chem. 265: 5648–5653.

[16]. Branco R., Chung A.P., Johnston T., Gurel V., Morais P., Zhitkovich A. (2008) The Chromate-Inducible *chrBACF* Operon from the Transposable Element Tn*OtChr* Confers Resistance to Chromium(VI) and Superoxide. Journal of Bacteriology. 190(21): 6996–7003.

[17]. Diaz-Perez C., Cervantes C., Campos-Garcia J., Julian-Sanchez A., Riveros-Rosas H. (2007) Phylogenetic analysis of the chromate ion transporter (CHR) superfamily. FEBS J. 274: 6215–6227.

[18]. Pimentel B.E., Sa´nchez R.M., Cervantes C. (2002) Efflux of chromate by Pseudomonas aeruginosa cells expressing the ChrA protein. FEMS Microbiology Letters. 212: 249-254.

[19]. Branco R., Morais P. (2013) Identification and characterization of the transcriptional regulator *ChrB* in the chromate resistance determinant of *Ochrobactrum tritici* 5bvl1. PLoS ONE. 8: e77987.

[20]. Cheung K.H., Ji-Dong G. (2007) Mechanism of hexavalent chromium detoxification by microorganisms and bioremediation application potential: A review. International Biodeterioration & Biodegradation. 59: 8–15. doi:10.1016/j.ibiod.2006.05.002

[21]. Aziz R.K., Bartels D., Best A.A., DeJongh M., Disz T., Edwards R.A., Formsma K., Gerdes S., Glass E.M., Kubal M., Meyer F., Olsen G.J., Olson R., Osterman A.L., Overbeek R.A., McNeil .LK., Paarmann D., Paczian T., Parrello B., Pusch G.D., Reich C., Stevens R., Vassieva O., Vonstein V., Wilke A., Zagnitko O. (2008) The RAST Server: Rapid Annotations using Subsystems Technology BMC Genomics. 9:75. doi:10.1186/1471-2164-9-75.

[22]. Götz S., García-Gómez J.M., Terol J., Williams T.D., Nagaraj S.H., Nueda M.J., Robles M., Talón M., Dopazo J., Conesa A. (2008) High-throughput functional annotation and data mining with the Blast2GO suite. Nucleic Acids Res. 36:3420-3435. doi:10.1093/nar/gkn176

[23]. Rahman A., Nahar N., Nawani N.N., Jass J., Ghosh S., Olsson B., Mandal A. (2015) Comparative genome analysis of *Lysinibacillus* B1-CDA, a bacterium that accumulates arsenics. Genomics. 106: 384-392. doi:10.1016/j.ygeno.2015.09.006

[24]. Rahman A., Nahar N., Jass J., Olsson B., Mandal A. (2016) Complete genome sequence of *Lysinibacillus sphaericus* B1-CDA, a bacterium that accumulates arsenic. Genome Announce 4(1):e00999-15. doi:10.1128/genomeA.00999-15

[25]. Andrews S. (2010) FastQC: a quality control tool for high throughput sequence data. Available online at: http://www.bioinformatics.babraham.ac.uk/projects/fastqc.

[26]. Martin M. (2011) Cutadapt removes adapter sequences from high-throughput sequencing reads. EMBnet.journal, 17(1):10-12. doi:http://dx.doi.org/10.14806/ej.17.1.200

[27]. Kelley D.R., Schatz M.C., Salzberg S.L. (2010) Quake: quality-aware detection and correction of sequencing errors. Genome Biology. 11: R116. doi:10.1186/gb-2010-11-11-r116

[28]. Luo R., Liu B., Xie Y., Li Z., Huang W., Yuan J., He G., Chen Y., Pan Q., Liu Y., Tang J., Wu G., Zhang H., Shi Y., Liu Y., Yu C., Wang B., Lu Y., Han C., Cheung D.W., Yiu S.M., Peng S., Xiaoqian Z., Liu G., Liao X., Li Y., Yang H., Wang J., Lam T.W., Wang J. (2012) SOAPdenovo2: an empirically improved memory-efficient short-read de novo assembler. GigaScience. 1: 18.

[29]. Rahman A., Nahar N., Olsson B., Mandal A. (2016) Complete genome sequence of Enterobacter cloacae B2-DHA, a chromium resistant bacterium. Genome Announce. 4(3): e00483-16.

[30]. Darling A.E., Mau B., Perna N.T. (2010) ProgressiveMauve: multiple genome alignment with gene gain, loss and rearrangement. PLoS ONE. 5: e11147.

[31]. Krumsiek J., Arnold R., Rattei T. (2007) Gepard: A rapid and sensitive tool for creating dot plots on genome scale. Bioinformatics. 23(8):1026-1028. doi:10.1093/bioinformatics/btm039

[32]. Borodovsky M., McIninch J. (1993) GeneMark: parallel gene recognition for both DNA strands. Comput Chem. 17: 123-133. doi:10.1016/0097-8485(93)85004-V

[33]. Salamov A.A., Solovyev V.V. (2000) Ab initio gene finding in Drosophila genomic DNA. Genome Res. 10:516–522. doi:10.1101/gr.10.4.516

[34]. Ashburner M., Ball C.A., Blake J.A., Botstein D., Butler H., Cherry J.M., Davis A.P., Dolinski K., Dwight S.S., Eppig J.T., Harris M.A., Hill D.P., Tarver L.I., Kasarskis A., Lewis S., Matese J.C., Richardson J.E., Ringwald M., Rubin G.M., Sherlock G. (2000) Gene Ontology: tool for the unification of biology. The Gene Ontology Consortium. Nature Genetics. 25(1): 25–29. doi:10.1038/75556

[35]. Zdobnov E.M., Apweiler R. (2001) InterProScan—an integration platform for the signature-recognition methods in InterPro. Bioinformatics. 17(9): 847–848. doi:10.1093/bioinformatics/17.9.847

[36]. Salzberg S.L., Delcher A.L., Kasif S., White O. (1998) Microbial gene identification using interpolated Markov models. Nucleic acids Res. 26(2): 544–548. doi:10.1093/nar/26.2.544

[37]. Lowe T.M., Eddy S.R. (1997) tRNAscan-SE: a program for improved detection of transfer RNA genes in genomic sequence. Nucleic Acids Res. 25(5): 955-964. doi:10.1093/nar/25.5.0955

[38]. Lagesen K., Hallin P., Rødland E.A., Stærfeldt H.H., Rognes T., Ussery D.W. (2007) RNAmmer: consistent and rapid annotation of ribosomal RNA genes. Nucleic Acids Research. 35 (9):3100–3108.

[39]. Carver T., Thomson N., Bleasby A., Berriman M., Parkhill J. (2009) DNAPlotter: circular and linear interactive genome visualization. Bioinformatics (Oxford, England). 25(1):119-120.

[40]. Untergasser A., Nijveen H., Rao X., Bisseling T., Geurts R., Jack A.M. (2007) Leunissen: Primer3Plus, an enhanced web interface to Primer3. Nucleic Acids Res. 35:W71-W74.

[41]. Laslett D., Canback B. (2004) ARAGORN, a program to detect tRNA genes and tmRNA genes in nucleotide sequences. Nucleic Acids Research. 32(1):11-16. doi:10.1093/nar/gkh152

[42]. Lee Z.M.P., Bussema C., Schmidt T.M. (2009) rrnDB: documenting the number of rRNA and tRNA genes in bacteria and archaea. Nucleic Acids Research. 37: D489–D493. doi:10.1093/nar/gkn689

[43]. Vezzi A., Campanaro S., D'Angelo M., Simonato F., Vitulo N., Lauro F.M., Cestaro A., Malacrida G., Simionati B., Cannata N., Romualdi C., Bartlett D.H., Valle G. (2005) Life at depth: Photobacterium profundum genome sequence and expression analysis. Science. 307: 1459–1461.

[44]. Olaitan A.O., Morand S., Rolain J.M. (2014) Mechanisms of polymyxin resistance: acquired and intrinsic resistance in bacteria. A review article. Frontiers in microbiology. 5(643), 1-18.

[45]. Paschos A., Bauer A., Zimmermann A., Zehelein E., Böck A. (2002) HypF, a carbamoyl phosphate-converting enzyme involved in [NiFe] hydrogenase maturation. J. Biol. Chem. 277(51): 49945-51.

[46]. Rahman A., Nahar N., Nawani N.N., Jass J., Ghosh S., Olsson B., Mandal A. (2015) Data in support of the comparative genome analysis of Lysinibacillus B1-CDA, a bacterium that accumulates arsenics. Data in Brief. 5: 579–585. doi:10.1016/j.dib.2015.09.040

[47]. Moffatt J.H., Harper M., Harrison P., Hale J.D., Vinogradov E., Seemann T., et al. (2010) Colistin resistance in *Acinetobacter baumannii* is mediated by complete loss of lipopolysaccharide production. Antimicrob. Agents Chemother. 54: 4971–4977. doi:10.1128/AAC.00834-10.

[48]. Campos M.A., Vargas M.A., Regueiro V., Llompart C.M., Alberti S., Bengoechea J.A. (2004) Capsule polysaccharide mediates bacterial resistance to antimicrobial peptides. Infect. Immun. 72: 7107–7114. doi:10.1128/IAI.72.12.7107-7114.2004

[49]. Padilla E., Llobet E., Domenech-Sanchez A., Martinez-Martinez L., Bengoechea J.A., Alberti S. (2010) Klebsiella pneumoniae AcrAB efflux pump contributes to antimicrobial resistance and virulence. Antimicrob. Agents Chemother. 54: 177–183. doi:10.1128/AAC.00715-09

[50]. Kamika I., Momba M. (2013) Assessing the resistance and bioremediation ability of selected bacterial and protozoan species to heavy metals in metal-rich industrial wastewater. BMC Microbiol. 13: 28. doi:10.1186/1471-2180-13-28

Tables

Table 1. Summary of the genome of B2-DHA with nucleotide content and gene count

Attribute	**Value**	**% of total**
Genome size (bp)	4 218 945	100
DNA GC content (bp)	2 353 515	55
DNA coding region (bp)	3 768779	89,33
Number of replicons	1	
Total scaffolds	13	100
Total genes	4043	100
rRNA genes	22	0,54
tRNA genes	66	1,63
Protein coding genes	3955	97,82
Genes assigned to RAST functional categories	3954	97,79
Genes assigned Gene Ontology terms by Blast2GO	3159	79,87
Largest N50*	492970	
Largest N90*	111054	

Table 2. Heavy metals responsive proteins in B2-DHA predicted by RAST and/or Blast2GO

			Predicted by	
Start (bp)	**End (bp)**	**Predicted function**	**RAST**	**Blast2GO**
36960	37526	Chromate reductase	X	X
242454	243404	Magnesium and cobalt transport protein CorA	X	X
495488	496147	ArsR family	X	
615926	616912	Cobalt, zinc, magnesium ion binding		X
964298	965137	Nickel, Cobalt cation transporter activity		X
997848	1000430	Copper, lead, cadmium, zinc, mercury transporting ATPase	X	X
1100748	1099984	Ferric enterobactin transport protein FepC	X	X
1101770	1100781	Ferric enterobactin transport protein FepG	X	X
1102774	1101770	Ferric enterobactin transport protein FepD	X	X
1105147	1104188	Ferric enterobactin transport protein FepB	X	X
1251060	1252157	Chromate reductase	X	X
1510555	1509272	Ferrous iron transport peroxidase EfeB	X	X
1511686	1510559	Ferrous iron transport periplasmic protein EfeO,	X	
1512560	1511727	Ferrous iron transport permease EfeU	X	X
1703726	1704046	Arsenite resistance operon repressor	X	X
1704087	1705376	Arsenite efflux pump protein	X	X
1705389	1705820	Arsenate reductase	X	X
1834407	1835345	Cobalt-zinc-cadmium resistance, Zinc transporter ZitB	X	X
1919484	1921043	Magnesium and cobalt efflux protein CorC	X	
2058555	2059283	Ferric siderophore transport protein TonB	X	
2216754	2216455	Transcriptional regulator, ArsR family	X	
2304506	2303766	Cobalt-zinc-cadmium resistance	X	
2591739	2592824	Cobalt-zinc-cadmium resistance	X	
2592824	2595886	Cobalt-zinc-cadmium resistance protein CzcA	X	
2735411	2736391	Nickel, Cobalt cation transporter activity		X
2810083	2809727	Arsenate reductase	X	X
3168971	3169588	Nickel cation binding		X
3169598	3170242	Nickel cation binding		X
3170821	3171285	Nickel cation binding		X
3171295	3172998	Nickel cation binding		X
3173316	3173618	Nickel cation binding		X
3173629	3174456	Nickel cation binding		X
3170811	3170272	Transport of Nickel and Cobalt, Urea decomposition	X	
3500732	3499869	Nickel incorporation-associated protein HypB	X	X
3505195	3506904	Nickel cation binding		X
3501086	3500736	Nickel incorporation protein HypA	X	X
3516192	3517214	Nickel/cobalt transporter	X	X
3892272	3892499	Ferrous iron transport protein A	X	X
3892530	3894848	Ferrous iron transport protein B	X	
3951655	3953826	Copper, lead, cadmium, zinc, mercury transporting ATPase	X	X
4172744	4173628	Cobalt-zinc-cadmium resistance protein	X	X
4176907	4178211	Arsenic efflux pump protein	X	

Table 3. Manganese, molybdenum and tellurite resistant proteins in B2-DHA predicted by RAST and/or Blast2GO

Gene	Start	End	Term
Gene 802	858022	859119	manganese ion binding
Gene 196	202800	204344	manganese ion binding
Gene 209	215336	216379	manganese ion binding
Gene 271	277278	279605	molybdenum ion binding
Gene 597	628652	630154	manganese ion binding
Gene 626	664374	665294	manganese ion binding
Gene 720	771440	772036	manganese ion binding
Gene 861	919680	921458	manganese ion binding
Gene 1016	1088133	1089044	Manganese transporter protein SitA
Gene 1017	1089047	1089853	Manganese transporter protein SitB
Gene 1018	1089850	1090701	Manganese transporter protein SitC
Gene 1019	1090695	1091534	Manganese transporter protein SitD
Gene 1049	1125413	1124667	Molybdenum transport protein ModB
Gene 1071	1148010	1150448	molybdenum ion binding
Gene 1223	1294800	1296950	molybdenum ion binding
Gene 1504	1570809	1571876	molybdenum ion binding
Gene 1548	1623197	1625641	molybdenum ion binding
Gene 1610	1694840	1695742	manganese ion binding
Gene 1725	1822796	1821738	Molybdenum transport protein ModC
Gene 1726	1823488	1822796	Molybdenum transport protein ModB
Gene 1727	1824261	1823485	Molybdenum-binding protein ModA
Gene 1729	1824720	1825508	molybdate ion transport
Gene 1756	1853924	1855090	manganese ion binding
Gene 1818	1924327	1924905	manganese ion binding
Gene 1903	2021204	2023633	molybdenum ion binding
Gene 1908	2029753	2033496	molybdenum ion binding
Gene 2091	2224133	2227873	molybdenum ion binding
Gene 2098	2235200	2237611	molybdenum ion binding
Gene 2209	2348836	2349429	Tellurite resistance protein TehB
Gene 2210	2349429	2350424	Tellurite resistance protein TehA
Gene 2610	2758489	2760867	molybdenum ion binding
Gene 2650	2805061	2806479	manganese ion binding
Gene 2682	2845329	2847608	manganese ion binding
Gene 2713	2876204	2877379	Manganese transport protein MntH
Gene 2785	2950966	2953689	molybdenum ion binding
Gene 3085	3280624	3281571	manganese ion binding
Gene 3130	3326886	3328205	manganese ion binding
Gene 3151	3347474	3349207	manganese ion binding
Gene 3540	3756054	3757565	manganese ion binding
Gene 3885	4139417	4141831	molybdenum ion binding
Gene 3886	4141880	4142467	molybdenum ion binding

Table 4. Universal stress proteins, multiple antibiotic resistant proteins, multidrug resistance proteins and polymyxin resistance protein in B2-DHA predicted by RAST and/or Blast2GO

Seq. Name	Start	End	Predicted function
Gene- 1057	1135310	1134879	Universal stress protein G
Gene- 1121	1198337	1199287	Universal stress protein E
Gene- 2184	2325505	2324840	Multiple antibiotic resistance protein MarC
Gene- 2185	2325818	2326195	Multiple antibiotic resistance protein MarR
Gene- 2186	2326216	2326596	Multiple antibiotic resistance protein MarA
Gene- 2187	2326629	2326844	Multiple antibiotic resistance protein MarB
Gene- 2364	2487111	2487539	Universal stress protein C
Gene- 2463	2591265	2590834	Universal stress protein G
Gene- 2531	2669613	2672735	Multidrug resistance MdtB
Gene- 2533	2672736	2675813	Multidrug resistance MdtC
Gene- 2534	2675814	2677229	Multidrug resistance MdtD
Gene- 3334	3544616	3543069	Multidrug resistance MdtB
Gene- 3335	3545805	3544633	Multidrug resistance MdtA
Gene- 3746	3974324	3973941	Polymyxin resistance protein PmrM
Gene- 3747	3974644	3974321	Polymyxin resistance protein PmrL,
Gene- 3749	3977186	3976284	Polymyxin resistance protein PmrJ
Gene- 3751	3980145	3979162	Polymyxin resistance protein ArnC
Gene- 3760	3989137	3988850	Universal stress protein B
Gene- 3761	3989469	3989906	Universal stress protein A

Figure legends

Figure 1. (A) Nucleotide-based alignment of a 4.21Mbp chromosomal assembly of *E. cloacae* B2-DHA (upper) and 4.85 Mbp chromosome of *E. cloacae* ECNIH2 (lower). A total of 12 homologous blocks are shown as identically colored regions and linked across the sequences. Regions that are inverted relative to *E. cloacae* B2-DHA are shifted to the right of center axis of the sequence. (B) Dot plot of nucleotide sequences of *E. cloacae* B2-DHA (X-axis) and *E. cloacae* ECNIH2 (Y-axis). Aligned segments are represented as dots, with regions of conservation appearing as lines.

Figure 2. Circular plot of ordered contigs, generated with DNAPlotter. Tracks indicate (from outside inwards) Protein coding genes in forward direction (blue) and Protein coding genes in reverse direction (green), tRNA genes (red), rRNA genes (dark blue), metal responsive genes (black), GC ratio and GC skew.

Figure 3. RAST analysis of genes connected to subsystems and their distribution in different functional categories.

Figure 4. Species distributions for the homologous proteins found by BlastP in the Blast2GO annotation process.

Figures

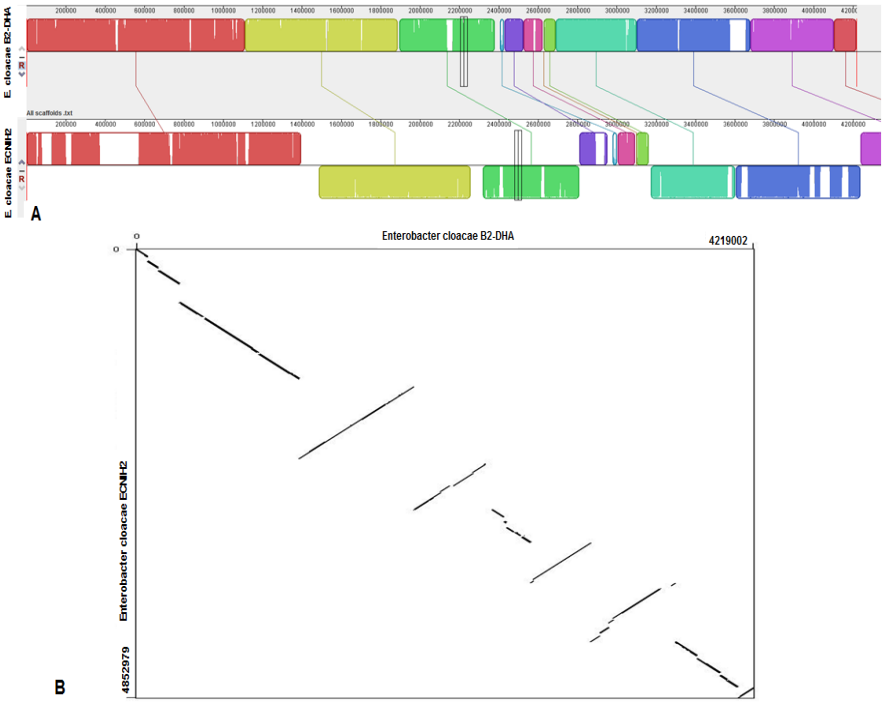

Figure 1.

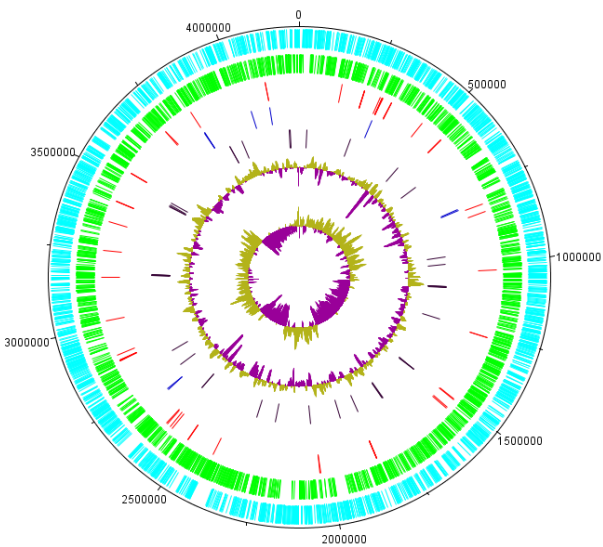

Figure 2.

PAPER V

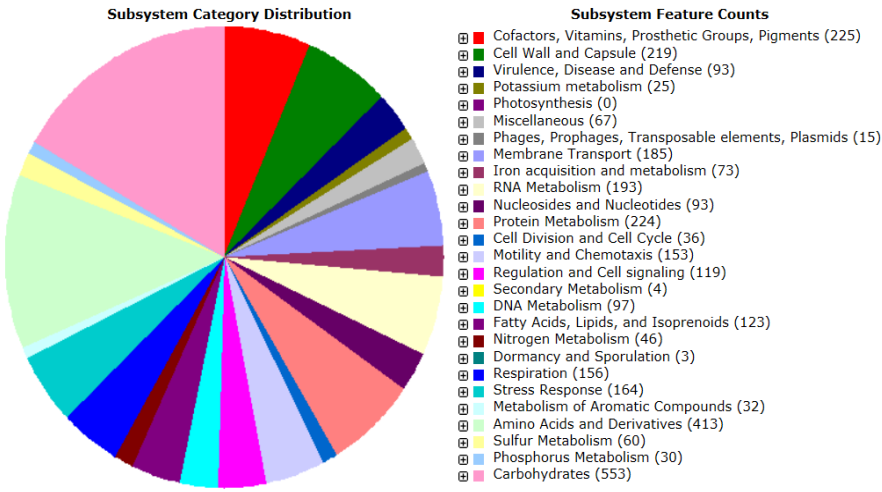

Figure 3.

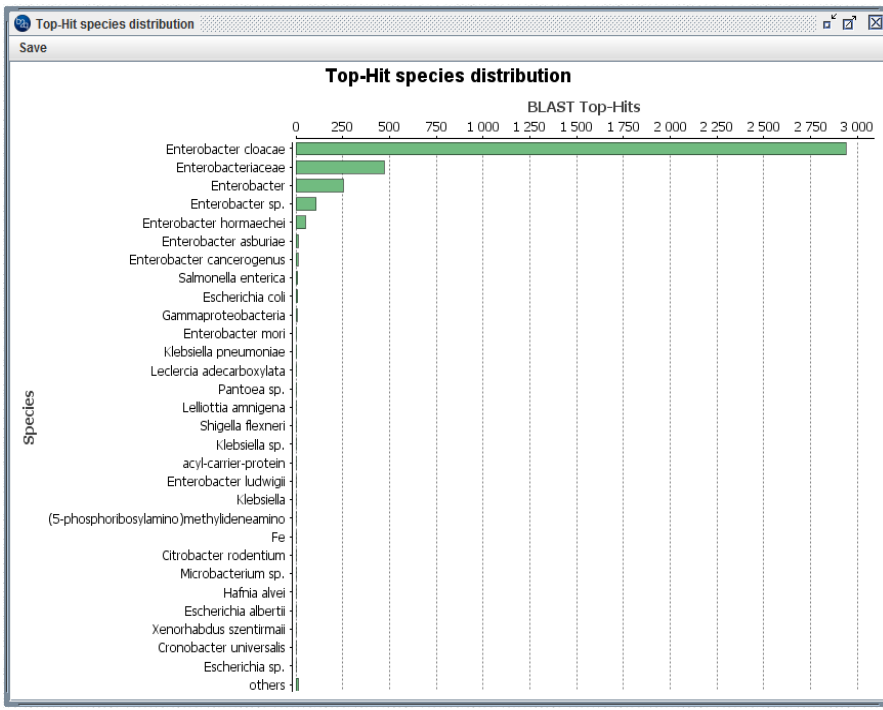

Figure 4.

Publications *in the series*
Örebro Studies in Life Science

1. Kalbina, Irina (2005). *The molecular mechanisms behind perception and signal transduction of UV-B irradiation in Arabidopsis thaliana.*
2. Scherbak, Nikolai (2005). *Characterization of stress-inducible short-chain dehydrogenases/reductases (SDR) in plants. Study of a novel small protein family from Pisum sativum (pea).*
3. Ristilä, Mikael (2006). *Vitamin B_6 as a potential antioxidant. A study emanating from UV-B-stressed plants.*
4. Musa, Klefah A. K. (2009). *Computational studies of photodynamic drugs, phototoxic reactions and drug design.*
5. Larsson, Anders (2010). *Androgen Receptors and Endocrine Disrupting Substances.*
6. Erdtman, Edvin (2010). *5-Aminolevulinic acid and derivatives thereof. Properties, lipid permeability and enzymatic reactions.*
7. Khalaf, Hazem (2010). *Characterization and environmental influences on inflammatory and physiological responses.*
8. Lindh, Ingrid (2011). *Plant-produced STI vaccine antigens with special emphasis on HIV-1 p24.*
9. El Marghani, Ahmed (2011). *Regulatory aspects of innate immune responses.*
10. Karlsson, Mattias (2012). *Modulation of cellular innate immune responses by lactobacilli.*
11. Pradhan, Ajay (2015). *Molecular mechanisms of zebrafish sex differentiation and sexual behavior.*
12. Asnake, Solomon (2015). *Interaction of brominated flame retardants with the chicken and zebrafish androgen receptors.*
13. Banjop Kharlyngdoh, Joubert (2015). *Modulation of Androgen Receptor Function by Brominated Flame Retardants.*
14. Stighäll, Kristoffer (2015). *Habitat composition and restocking for conservation of the white-backed woodpecker in Sweden.*
15. Rahman, Aminur (2016). *Bioremediation of Toxic Metals for Protecting Human Health and the Ecosystem.*